



Extraction and Determination of Valuable Components from Lupin Beans

Von der Fakultät für Mathematik und Naturwissenschaften der Carl von Ossietzky
Universität Oldenburg zur Erlangung des akademischen Grades und Titels

Doktor der Naturwissenschaften

– Dr. rer. nat. –

angenommene Dissertation

von Herrn Kai Kniepkamp
geboren am 27.12.1992 in Bremen

Gutachter:

1. Prof. Dr. Michael Wark
2. Prof. Dr. Heinz Wilkes

Tag der Disputation: 10.10.2024

Abstract

One of the grand challenges of the 21st century is the ongoing climate change and its threat to human well-being. It is caused by the excessive emission of greenhouse gases such as methane and CO₂ and results in a long-term temperature shift. To tackle this issue, new materials and processes are developed with smaller emissions of greenhouse gases. One example is the switch from imported to locally grown and processed food products with reduced environmental impact through shorter transport distances.

To discover new local applicable possibilities, the here-presented research focuses on the exploration of Lupin beans and the analysis and extraction of its valuable components. Lupin beans are produced by the crop *Lupinus*, a genus of a plant in the family of Fabaceae/legumes. Lupin crops can grow on marginal lands in cold regions of Europe and can therefore be grown locally. The here-extensively tested beans of the *Lupinus mutabilis branco* species (Peru) had a determined protein content of 49.1 ± 0.8 g (N \times 6.25), lipid content of 21.8 ± 0.8 g, and dietary fiber content of 23.2 ± 0.2 g per 100 g dry weight (DW). Those nutritional values put the Lupin seeds into direct competition with soybeans, which are mostly imported and therefore often considered less sustainable. Despite their promising nutritional value, lupin beans contain toxic quinolizidine alkaloids in a wide range of concentrations. For example, the here-tested *Lupinus mutabilis branco* beans contained 4424.9 mg/100 g DW (Randall extraction), while another tested lupin variety (*Lupinus albus*) species contained only 151.0 mg/100 g DW. An often safe-to-consume threshold is estimated at 20 mg/100 g DW, which is exceeded by both varieties. Quinolizidine alkaloids are harmful to human consumption, so correct concentration determination needs consideration. According to the literature, the most common method is the extraction via acid-base mechanism followed by solid phase extraction (SPE) or liquid-liquid extraction (LLE). Although the here-carried-out experiments showed low limit of detection (LOD) values for those methods, an unreported discrimination of polar alkaloids was observed. In comparison to other extraction methods, dihydroxylupanine (Di-OH) was only extracted for 15 % with SPE and 5 % with LLE. It was found that the quantification via Soxhlet and Randall extraction did not discriminate certain alkaloids and resulted therefore in the highest quantification yields but had the drawback of higher LOD values. This problem was solved by using GC-MS in selected ion monitoring (SIM) mode. Since Randall extraction (2 h) was more time efficient than Soxhlet extraction (5 h), it was chosen for the quantification of alkaloids from lupin bean samples which were provided by the Lisbon seed bank. Out of 76 samples, 16 had an alkaloid content below the threshold of 20 mg/100 g DW. In addition to the quantification, isolation of lupanine, 3 β -hydroxylupanine, 13 α -hydroxylupanine, and 3 β ,13 α -dihydroxylupanine was carried out successfully.

Proteins are another valuable fraction of lupin beans. Extraction methods that involve precipitation by ionic strength and pH were tested. The highest yield was gained by isoelectric point precipitation. The parameters affecting the yields were analyzed, and it was found that the use of CO₂ as a precipitation agent instead of the more commonly used HCl had no drawback in terms of yield but could help to increase the process sustainability. A process design that applies only CO₂ and water as extraction agents was developed and extensively tested. However, none of the tested parameters dissolved the proteins from the lupin matrix successfully.

The extraction of lipids from lupin beans was performed with different methods and on two different matrices (lupin beans and cherry stones). The extractions from lupin beans were performed via supercritical carbon dioxide (scCO₂) on small and large scales and its economic potential was analyzed. Soxhlet extraction led to ca. 16 % higher lipid yields than scCO₂ extraction. However, the scCO₂ extraction offers a sustainable extraction method, which showed a high economic potential. The results are published in the Journal of Food Process Engineering (DOI: 10.1111/jfpe.14289).

A more detailed analysis of lipid extraction parameters was performed with cherry stones. The influence of matrix separation (kernel/shell), moisture content, pressure (only scCO₂), and temperature (only scCO₂) on the lipid content was investigated. A comparison between Randall, Soxhlet, and scCO₂ has shown that the scCO₂ extraction showed lower yields in all tested cases compared to the two other methods. The highest yield was gained via Soxhlet extraction of the driest sample when the kernel and shell were separated. The results are published in the Journal of Chemical Technology & Biotechnology (DOI: 10.1002/jctb.7581). Furthermore, the lupin bean was also analyzed in terms of ash, moisture, and carbohydrate content. It was found that the carbohydrate fraction of lupin beans mainly consists of dietary fiber (23.2 g/100 g DW), giving another good argument for food applications.

Comprehensively, this thesis shows the huge potential of lupin beans regarding their valuable components and their ability to be grown and produced locally. The discussion of the different extraction methods and corresponding parameters supports future researchers to develop industrial processes with higher efficiency and less environmental impact, which contributes on the way to tackle climate change.

Zusammenfassung

Eine der großen Herausforderungen des 21. Jahrhunderts ist der fortschreitende Klimawandel und seine Bedrohung für das menschliche Wohlergehen. Er wird durch die übermäßige Emission von Treibhausgasen wie Methan und CO₂ verursacht und führt zu einer langfristigen Temperaturverschiebung. Um diesem Problem zu begegnen, werden neue Materialien und Verfahren mit reduzierten Treibhausgasemissionen entwickelt. Ein Beispiel dafür ist die Umstellung von importierten auf lokal angebaute und verarbeitete Lebensmittel, welche durch kürzere Transportwege die Umwelt weniger belasten. Um neue lokal anwendbare Möglichkeiten zu ermitteln, widmet sich die hier vorgestellte Arbeit auf die Erforschung von Lupinenbohnen und die Analyse und Extraktion ihrer wertvollen Bestandteile. Lupinenbohnen werden von der Pflanze *Lupinus* produziert, einer Pflanzengattung aus der Familie der Hülsenfrüchte (Fabaceae/Leguminosen). Lupinenkulturen können auf marginalen Böden (Grenzstandorten) und in kalten Regionen Europas wachsen, wodurch sie lokal angebaut werden können. Die hier ausgiebig getesteten Bohnen der Art *Lupinus mutabilis branco* (Peru) hatten einen ermittelten Proteingehalt von 49.1 ± 0.8 g (N \times 6.25), einen Lipidgehalt von 21.8 ± 0.8 g und einen Ballaststoffgehalt von 23.2 ± 0.2 g pro 100 g Trockengewicht (DW). Mit diesen Nährwerten stehen die Lupinenbohnen in direkter Konkurrenz zu Sojabohnen, welche meist importiert werden und daher als weniger nachhaltig gelten. Trotz ihres vielversprechenden Nährwerts enthalten Lupinenbohnen giftige Chinolizidin-Alkaloide in unterschiedlichen Konzentrationen. So enthielten die hier getesteten *Lupinus mutabilis branco* Bohnen 4424.9 mg/100 g DW (Randall-Extraktion), während eine andere getestete Lupinensorte (*Lupinus albus*) nur 151.0 mg/100 g DW enthielt. Der Grenzwert für die Unbedenklichkeit des Verzehrs wird häufig auf 20 mg/100 g DW geschätzt, welcher von beiden Sorten überschritten wird. Da Chinolizidin-Alkaloide für den menschlichen Verzehr schädlich sind, ist eine korrekte Konzentrationsbestimmung unabdingbar. Laut Literatur ist die gebräuchlichste Methode die Extraktion mittels Säure-Base-Mechanismus und anschließender Festphasenextraktion (SPE) oder Flüssig-Flüssig-Extraktion (LLE). Obwohl die hier durchgeführten Experimente eine niedrige Nachweisgrenzen (LOD) für diese Methoden ergaben, wurde eine bisher noch nicht bekannte Diskriminierung polarer Alkaloide beobachtet. Im Vergleich zu anderen Extraktionsmethoden wurde Dihydroxylupanin (Di-OH) mit SPE nur zu 15 % extrahiert und mittels LLE zu 5 %. Im Gegensatz dazu wurden bei der Extraktion mittel Soxhlet- und Randall-Verfahren keine Diskriminierung festgestellt, wodurch diese Methoden zu einem höheren Gesamtalkaloidgehalt führen, allerdings mit dem Nachteil höherer Nachweisgrenzen. Dieses Problem wurde durch die Verwendung von GC-MS im selected ion monitoring (SIM) Modus gelöst. Da die Randall-Extraktion (2 Stunden) zeitsparender war als die Soxhlet-Extraktion (5 Stunden), wurde sie für die Quantifizierung

von Alkaloiden aus Lupinenproben gewählt, welche von der Saatgutbank aus Lissabon zur Verfügung gestellt wurden. Von 76 Proben wiesen 16 einen Alkaloidgehalt unterhalb des Grenzwerts von 20 mg/100 g DW auf. Des Weiteren wurde, neben der Quantifizierung, auch eine Isolierung von Lupanin, 3β -Hydroxylupanin, 13α -Hydroxylupanin und $3\beta,13\alpha$ -Dihydroxylupanin erfolgreich durchgeführt.

Proteine sind ein weiterer wertvoller Bestandteil der Lupinenbohne. Es wurden Extraktionsmethoden getestet, die eine Ausfällung durch Ionenstärke und pH-Wert verwendeten. Dabei wurde die höchste Ausbeute durch Beeinflussung des pH-Werts und der Fällung am isoelektrischen Punkt erzielt. Die Parameter, die sich auf die Ausbeute auswirken, wurden analysiert. Es wurde festgestellt, dass die Verwendung von CO_2 als Fällungsmittel anstelle der üblicherweise verwendeten Salzsäure keine Nachteile auf die Ausbeute hat, aber dazu beitragen kann, die Nachhaltigkeit des Verfahrens zu erhöhen. Es wurde ein Prozessdesign entwickelt und ausgiebig getestet, bei dem nur CO_2 und Wasser als Extraktionsmittel verwendet werden. Dabei erwiesen sich keine der hier getesteten Parameter als geeignet, um Proteine erfolgreich aus der Lupinenmatrix herauszulösen.

Die Extraktion von Lipiden aus Lupinenbohnen wurde mit verschiedenen Methoden und mittels zwei verschiedener Matrizen (Lupinenbohnen und Kirschkerne) getestet. Die Extraktionen aus Lupinenbohnen wurden in kleinem und großem Maßstab mit überkritischem Kohlendioxid (scCO_2) durchgeführt und ihr wirtschaftliches Potenzial dabei untersucht. Dabei ergab die Soxhlet-Extraktion eine ca. 16 % höhere Lipidausbeute als die scCO_2 -Extraktion. Allerdings bietet die scCO_2 -Extraktion eine nachhaltige Methode mit einem hohen wirtschaftlichen Potenzial. Die Ergebnisse sind im Journal of Food Process Engineering veröffentlicht (DOI: 10.1111/jfpe.14289).

Eine detailliertere Analyse der Lipidextraktionsparameter wurde mit Kirschkernen durchgeführt. Untersucht wurde der Einfluss von Matrix-Trennung (Kern/Schale), Feuchtigkeitsgehalt, Druck (nur scCO_2) und Temperatur (nur scCO_2) auf den Lipidgehalt. Ein Vergleich zwischen Randall-, Soxhlet- und scCO_2 -Extraktion zeigte, dass die scCO_2 -Extraktion in allen untersuchten Fällen eine geringere Ausbeute als die beiden anderen Methoden ergab. Die höchste Ausbeute wurde mittels Soxhlet-Extraktion der trockensten Probe erzielt, wobei Kern und Schale getrennt waren. Die Ergebnisse sind im Journal of Chemical Technology & Biotechnology veröffentlicht (DOI: 10.1002/jctb.7581).

Darüber hinaus wurde die Lupine auch auf ihren Asche-, Feuchtigkeits- und Kohlenhydratgehalt hin untersucht. Dabei wurde festgestellt, dass die Kohlenhydratfraktion der *Lupinus mutabilis* Bohne hauptsächlich aus Ballaststoffen besteht (23.2 g/100 g DW), was ein weiteres Argument für die Verwendung als Lebensmittel darstellt.

Insgesamt verdeutlichen die hier gezeigten Ergebnisse das große Potenzial der Lupinenbohne hinsichtlich ihrer wertvollen Inhaltsstoffe und ihrer Fähigkeit, lokal angebaut

und produziert zu werden. Dabei helfen die hier herausgearbeiteten Extraktionsparameter zukünftigen Forschern bei der Entwicklung von industriellen Prozessen mit höherer Effizienz und geringerer Umweltbelastung, was ein weiterer Schritt zur Bewältigung des Klimawandels sein kann.

Acknowledgment

My greatest appreciation goes to my beloved wife Sophie Kniepkamp, who has enriched and supported me in all areas of my life, making this work possible in the first place. Thank you!

I also express my gratitude to my parents Barbara and Jens Kniepkamp, for always believing in me and giving me the freedom I needed. Also, I am thankful for my friends, who have always been there for me.

Furthermore, I would like to thank Prof. Dr. Michael Wark for the opportunity to carry out this work in this setting and for the trust he has placed in me. Moreover, I thank Prof. Dr. Rob van Haren, who gave me much support and autonomy, always sharing his enthusiasm for the topics, and enabling new ideas and projects. I also express my gratitude to Prof. Dr. Heinz Wilkes for the uncomplicated communication and for accepting the position as second assessor. I would also like to acknowledge the financial support from project “*Libbio*” and “*Circular BIOMass CAScade to 100%*”.

I also thank Dr. Massimiliano Errico from the University of Southern Denmark and Prof. Dr. João Neves Martins from University of Lisbon for the cooperation and the sent samples. Moreover, I would like to underline the fruitful discussion and close collaboration with Jan Pieter Thie, Miao Yu, and Manon Kuipers which were always helpful and appreciated. Finally, I would like to state, that it was always a pleasure for me to work at the Hanze University of Applied Sciences Groningen and I am deeply grateful for the created opportunities. I would also like to thank their students, explicitly Sijtze van der Meer, Jelle-Geerts Eilers, and Melvin Voorhorst, who conducted a lot of work and familiarized me with the Dutch culture.

Table of content

1	Introduction	1
2	Basics	2
2.1	Lupin beans	2
2.2	Quinolizidine alkaloids	3
2.2.1	Debittering	4
2.2.2	Quantification	4
2.3	Proteins	7
2.3.1	Amino acids	7
2.3.2	Protein determination	8
2.3.3	Protein fractions	9
2.3.4	Isoelectric point	10
2.3.5	Ionic strength	11
2.3.6	Protein extraction strategies	11
2.4	Lipids	15
2.4.1	Lipids from lupin beans	16
2.4.2	Lipids from sour cherry stones	16
2.4.3	Extraction strategy for lipids	17
2.4.4	Fatty acid methyl ester (FAME)	17
2.5	Carbohydrates	17
2.6	Extraction techniques	18
2.6.1	Solid-liquid extraction mechanism	19
2.6.2	One step extraction	20
2.6.3	Multi-step extraction	20
2.6.4	Soxhlet extraction	20
2.6.5	Randall extraction	21
2.6.6	Liquid-liquid extraction	22
2.6.7	Supercritical fluid extraction	22
2.6.8	Chromatography	25
2.7	Carbon dioxide as volatile acid	26
3	Materials and methods	28
3.1	Materials	28
3.1.1	Lupin beans	28
3.1.2	Cherry stones	28
3.2	Experimental design	29
3.2.1	Analytical alkaloid extraction	29

3.2.2	Isolation of alkaloids from <i>Lupinus mutabilis</i> branco.....	31
3.2.3	Lipid extraction.....	34
3.2.4	Protein extraction.....	36
3.3	Analytical methods.....	39
3.3.1	Moisture determination.....	39
3.3.2	Ash determination.....	39
3.3.3	Alkaloid analysis.....	39
3.3.4	Protein determination.....	42
3.3.5	Dietary fiber analysis.....	42
3.3.6	Lipid analysis.....	43
3.4	Calculations.....	44
3.4.1	Variance and standard deviation.....	44
3.4.2	Student's t-test.....	44
3.4.3	Graphical processing.....	45
3.4.4	Recovery rate.....	45
3.4.5	Internal standard.....	45
3.4.6	Simple accumulated area calculation.....	47
3.4.7	Limit of detection (LOD) and limit of quantification (LOQ) determination.....	47
3.4.8	Solvent-to-feed ratio.....	48
3.4.9	Moisture content.....	48
3.4.10	Ash content.....	48
3.4.11	Proteins.....	49
3.4.12	Carbohydrates.....	50
4	Results and discussion.....	51
4.1	Overview.....	51
4.2	Moisture content.....	52
4.3	Ash content.....	52
4.4	Quinolizidine alkaloids in lupin beans.....	53
4.4.1	Grinding of lupin samples.....	54
4.4.2	Identification of alkaloids.....	54
4.4.3	Quantification of alkaloids.....	55
4.4.4	Soxhlet extraction of alkaloids.....	57
4.4.5	Randall extraction of alkaloids.....	66
4.4.6	Extraction of alkaloids via acid-base mechanism.....	67
4.4.7	Method comparison.....	76
4.4.8	Final evaluation.....	81
4.4.9	Reasons for the insufficient alkaloid extraction via acid base extraction.....	82

4.4.10	Ranking unknown <i>Lupinus mutabilis</i> samples from Lisbon seed bank	83
4.4.11	Chromatographic behavior of alkaloids from <i>Lupinus mutabilis</i> branco	84
4.4.12	Isolation of quinolizidine alkaloids from <i>Lupinus mutabilis</i> branco	84
4.4.13	Alkaloid extraction via scCO ₂	89
4.5	Protein extraction of lupin beans	90
4.5.1	Choice of protein determination method	90
4.5.2	Protein content of <i>Lupinus mutabilis</i> beans	91
4.5.3	Method comparison	91
4.5.4	Influence of pH on the protein solvation	93
4.5.5	Influence of extraction time on the protein solvation.....	98
4.5.6	Parameters influencing the protein precipitation step in the IEPP-CO ₂ process....	99
4.5.7	Concept CO ₂ -only protein extraction	104
4.5.8	Protein extraction evaluation	108
4.6	Lipids.....	108
4.6.1	Lipid extraction and analysis of lupin beans.....	109
4.6.2	Lipid extraction and analysis of cherry stones	109
4.7	Carbohydrates and dietary fiber in lupin beans.....	110
5	Conclusion and outlook.....	114
6	Literature.....	116
7	Appendix.....	122
7.1	Detailed alkaloid quantification results	122
7.2	Alkaloid analysis of seed bank samples.....	124
7.3	Results nitrogen solvation experiment	127
7.4	Regression data.....	128
7.5	Lupin oil extraction	130
7.6	Lipid extraction from cherry stones	149
8	List of publications	159
9	Erklärung	160

List of figures

Figure 1: Lupin plant and lupin beans.	2
Figure 2: Acid-base behavior of alkaloids.	5
Figure 3: Amino acids and its ampholytic character.	7
Figure 4: Amino acid behavior in acidic, neutral, and basic milieu.	10
Figure 5: Process overview of the protein extraction process.	11
Figure 6: Nitrogen solubility of <i>Lupinus angustifolius</i> reported by Ruiz and Hove ⁵⁰	12
Figure 7: IEPP-CO ₂ setup according to Hofland et al. ⁵²	13
Figure 8: Nitrogen solubility of <i>Lupinus mutabilis</i> branco flour.	14
Figure 9: Triglyceride molecule.	15
Figure 10: Different oligosaccharides and their molecular structure.	18
Figure 11: Soxhlet operation as reported by Kou and Somenath ⁷²	21
Figure 12: Different states of a Randall equipment during an extraction.	21
Figure 13: Phase diagram of carbon dioxide adapted from Witkowski et al. ⁷⁸	23
Figure 14: Scheme of a SFE unit without recycling as reported by Brunner ⁸¹	24
Figure 15: Overview about the phases of CO ₂ during extraction in SuperPro Designer.	25
Figure 16: Solubility of carbon dioxide in water.....	26
Figure 17: Overview about alkaloid isolation process.	32
Figure 18: Supercritical extraction unit SFE 500 unit.....	35
Figure 19: Supercritical extraction unit SFT-NPX-10.....	36
Figure 20: Sample after depressurization inside extraction vessel.	37
Figure 21: Theoretical setup for the solvation and precipitation with CO ₂	38
Figure 22: Setup for two parallel solvation experiments.	38
Figure 23: Example of plotted calibration curves.	40
Figure 24: Chromatogram of the soluble dietary fiber fraction.	43
Figure 25: GC-FID and GC-MS chromatogram of <i>Lupinus mutabilis</i> Soxhlet extract.....	54
Figure 26: Linearity of the internal standard (caffeine).	56
Figure 27: Soxhlet alkaloid extraction progress of <i>Lupinus mutabilis</i> branco beans.	57
Figure 28: GC-FID chromatogram of Soxhlet extracts from two different species.....	60
Figure 29: Detailed GC-FID chromatogram comparison of 13-OH from two lupin species. ...	60
Figure 30: Detailed 13-OH chromatogram via splitless injection.....	61
Figure 31: Detailed GC-MS chromatogram comparison of the 13-OH peak.....	64
Figure 32: Process overview of the acid-base mechanism.	68
Figure 33: Emulsion during LLE of <i>Lupinus mutabilis</i> beans.....	70
Figure 34: GC-FID chromatogram of <i>Lupinus mutabilis</i> extract via SPE (Extrelut).	72
Figure 35: Extraction progress of SPE(Extrelut) from <i>Lupinus mutabilis</i> branco beans.	73

Figure 36: LOD and LOQ values for acid-base extraction via GC-MS quantification.	74
Figure 37: Effect of extraction parameter on the elution of 13-OH and Di-OH via SPE.....	75
Figure 38: GC-FID chromatograms comparison of different extraction methods.....	76
Figure 39: Schematic drawing of the lupanine family structure.	82
Figure 40: Picture of the samples from the seed bank of Portugal.....	83
Figure 41: Steward chart of the average recovery rate.	83
Figure 42: Alkaloid column elution profile for normal phase (NP).	85
Figure 43: Resonance stability of an N,N-dialkylamide.	87
Figure 44: Solvation behavior of 13-OH and Di-OH during LLE.....	88
Figure 45: GC-FID analysis of purified alkaloid fractions in MeOH.	88
Figure 46: Picture of freeze-dried supernatant I fraction after pH treatment.....	94
Figure 47: Influence of pH on the mass fraction (after drying).	94
Figure 48: Influence of pH on the nitrogen concentration.....	95
Figure 49: Influence of pH on the nitrogen yield.	96
Figure 50: pH-dependent calculated recovery rate for individual alkaloids in supernatant....	97
Figure 51: Influence of time on the nitrogen yield.	98
Figure 52: Precipitated nitrogen for different pressure and temperature values.	100
Figure 53: Influence of time on the nitrogen precipitation yield in the IEPP-CO ₂ process...	102
Figure 54: Process design for CO ₂ -only protein precipitation.....	105
Figure 55: Filter cascade as used in protein solvation via CO ₂ experiments.....	106

List of tables

Table 1: Raw and end-products of the alkaloid biosynthesis in lupin crops.	3
Table 2: Main alkaloids in <i>Lupinus mutabilis branco</i> beans based on Soxhlet extraction.	4
Table 3: Reported extraction and quantification methods of alkaloids from lupin beans.	6
Table 4: Solubility of different Osborne fractions.	9
Table 5: Overview about the protein fractions in different food sources.	9
Table 6: Examples of different carbohydrate fractions.	17
Table 7: Separated fractions and its dominating alkaloid.	33
Table 8: Retention time of alkaloids on the preparative C18 column.	34
Table 9: SIM table for GC-MS quantification.	41
Table 10: Retention factor of alkaloids in the TLC experiment.	42
Table 11: Retention time of the components in the soluble dietary fiber fraction.	43
Table 12: Applied parameters for the alkaloid LOD/LOQ values calculation.	48
Table 13: Overview of the components in <i>Lupinus mutabilis branco</i> beans.	51
Table 14: Result-overview of extractions from <i>Lupinus mutabilis branco</i> beans.	52
Table 15: Moisture content of the two tested lupin species.	52
Table 16: Ash content of the two tested lupin species.	53
Table 17: Detected alkaloid species in <i>Lup. mut. branco</i> samples.	55
Table 18: Alkaloid distribution in <i>Lupinus mutabilis branco</i> beans.	56
Table 19: GC-FID quantification of <i>Lupinus mutabilis</i> Soxhlet extraction experiment.	58
Table 20: GC-FID quantification of <i>Lupinus albus</i> Soxhlet extraction experiment.	59
Table 21: LOD and LOQ values for Soxhlet extraction and GC-FID quantification.	59
Table 22: LOD and LOQ values for Soxhlet and Randall extraction via GC-MS.	65
Table 23: GC-MS quantification of <i>Lupinus albus</i> Soxhlet extraction experiment.	65
Table 24: GC-FID quantification of <i>Lupinus mutabilis</i> Randall extraction experiment.	66
Table 25: GC-MS quantification of <i>Lupinus albus</i> Randall extraction experiment.	67
Table 26: LOD and LOQ values for acid-base extraction via GC-FID quantification.	69
Table 27: GC-FID quantification of <i>Lupinus mutabilis</i> LLE experiment.	69
Table 28: GC-FID quantification of <i>Lupinus albus</i> LLE extraction experiment.	69
Table 29: GC-FID quantification of <i>Lupinus mutabilis</i> SPE extraction experiment.	71
Table 30: GC-MS quantification of <i>Lupinus albus</i> SPE (Extrelut) extraction experiment.	74
Table 31: Recovery rate comparison of different alkaloid extraction methods.	77
Table 32: LOD/LOQ value comparison for different methods.	77
Table 33: Average <i>Lupinus mutabilis</i> alkaloid extraction method yield.	78
Table 34: Maximum yield comparison between the methods for <i>Lupinus mutabilis branco</i> .	78
Table 35: <i>Lupinus albus</i> alkaloid extraction comparison quantified via GC-MS.	79

Table 36: Maximum mass concentration of <i>Lupinus albus</i> quantified via GC-MS.....	79
Table 37: Standard deviation for <i>Lupinus mutabilis</i> extractions via GC-FID.....	79
Table 38: Standard deviation for six <i>Lupinus albus</i> extractions via GC-MS.	80
Table 39: Summary of non-analytical extraction method comparison criteria.....	80
Table 40: Extracted mass and recovery rate for the purification.	89
Table 41: Calculated protein content of <i>Lupinus mutabilis</i> flour with different properties.....	91
Table 42: Overview of protein extraction process parameters and results.	92
Table 43: Time-dependent optical change after pressurization at 60 bar.	99
Table 44: Physical state of CO ₂ for different temperature and pressure values.	101
Table 45: Valve regulation during a CO ₂ -only protein extraction.....	105
Table 46: Analysis of weight and protein content of the only-CO ₂ process.....	106
Table 47: Original reported normalized <i>Lupinus mutabilis</i> FAME composition.....	109
Table 48: FAME composition of <i>Lupinus mutabilis</i>	109
Table 49: Lipid yield and recovery rate.	110
Table 50: Total carbohydrates in <i>Lupinus mutabilis</i>	110
Table 51: Total dietary fiber and its composition.	111
Table 52: HPLC analysis of the total oligosaccharide fractions.....	111
Table 53: Total weight distribution of dietary fiber fraction.	112
Table 54: Detailed GC-FID results of <i>Lupinus mutabilis</i> extraction experiments.....	122
Table 55: Detailed GC-FID results of <i>Lupinus albus</i> extraction experiments.....	123
Table 56: Detailed GC-MS results of <i>Lupinus albus</i> extraction experiment.....	123
Table 57: Seed bank samples analyzed via GC-FID.....	124
Table 58: Low alkaloid-containing seed bank samples analyzed via GC-MS method.....	126
Table 59: Protein solvation experiment of <i>Lupinus mutabilis</i> beans at different pH values.	127
Table 60: Four parameter regression data for Figure 27.....	128
Table 61: Four parameter regression data for Figure 35.....	128
Table 62: Four parameter regression data for Figure 37.....	128
Table 63: Four parameter regression data for Figure 52.....	128
Table 64: Four parameter regression data for Figure 53.....	129

1 Introduction

Chemistry is a natural science concerned with the study of properties, reactions, and transformation of different materials and influences everyone's lives. Not only do the resulting products have a huge impact on our daily lives, but the created by and waste products as well. It has been observed that the earth's surface temperature increased in recent decades. In addition to natural global warming, climate gases emitted by humans have emerged as the main drivers for this phenomenon. The so-called greenhouse gasses absorb the rays from the sun and the reflected rays from the earth's surface, which results in higher temperatures on Earth and leads to the anthropogenic climate change. The main responsible gas for this greenhouse gas effect is carbon dioxide (CO₂). It appears as a waste product when fossil fuel is burned and is mostly emitted by the energy, industry, and transportation sector ¹. The second largest contributing greenhouse gas is methane (CH₄), which is emitted by fossil fuel and agriculture/livestock activities ¹.

Since the 1950s the world population has been growing ², which multiplies the effect of climate change by intense usage of fossil fuels. The growth results also in an increasing demand for food, especially a protein-rich diet. To tackle these challenges, the United Nations stated seventeen sustainable development goals (SDGs) as a call of action to "end poverty, protect the planet, and ensure that by 2030 all people enjoy peace and prosperity" ³. To reach these SDGs, research into the development of sustainable food resources is needed, and the expertise of many disciplines is asked for ⁴. This led to a change, where researchers and industries are continuously developing new pathways of production to not only increase the economic output but also minimize the negative ecological impact.

Lupin beans are one opportunity to challenge these problems. Lupin beans are produced by the lupin crop, which can grow on marginal land in cold regions of Europe. Lupin beans are rich in protein, but also in lipid and dietary fiber content. It puts the plant into direct competition with soy, which is often imported to Europe ⁵, hence causing environmental pollution through transport. Furthermore, the locally grown lupin beans might not only replace soy but also reduce meat production by being processed into meat substitutes. Since a high in plant protein and low in meat dairy is significant connected to a lower emission of greenhouse gases ¹, the exploration of lupin beans can help to reduce the environmental impact even further. However, lupin beans also contain alkaloids which are toxic for human consumption. Subsequently, this thesis focuses on the exploration of extraction methods for valuable components from lupin beans and analyzes the influence of various parameters.

2 Basics

All used biomaterials are food related and serve the purpose of developing new pathways to utilize resources. Lupin beans were extracted for several components, namely alkaloids, carbohydrates, lipids, and proteins. However, the identification of influencing parameter for the lipid extraction was carried out with cherry stones, in respect to its increased complexity.

2.1 Lupin beans

Lupin beans are the seeds of the plant *Lupinus*, which belongs to the family of Fabaceae. More than 280 Lupin species are known. Four of them have agricultural importance, namely *Lupinus albus*, *Lupinus angustifolius*, *Lupinus luteus*, which have their origin in the Mediterranean region, and *Lupinus mutabilis*, which has its origin in the Andean region ⁶. Many Lupin species can be grown in Europe, however great emphasis is taken to cultivate Andean species like *Lupinus mutabilis* in Europe, in respect to its high protein and oil yield ^{6,7}.



Figure 1: Lupin plant and lupin beans.

Wild growing Lupin crop (left) and *Lupinus mutabilis* branco beans (right). Photo was taken in Cusco, Peru.

Lupin beans can be a great source of protein and oil. The seeds can have a protein content of up to half its own weight, which initialized the discussion about the substitution of imported soy with lupin beans ⁷. This work focuses on *Lupinus mutabilis* because of its high protein yield and the advantage to grow on marginal lands, allowing colder climates and lower agriculture input in comparison to soy ⁷. Therefore, *Lupinus mutabilis* can grow on non-utilized lands in Europe reducing the carbon dioxide footprint due to transportation of soy and allowing a new source of income.

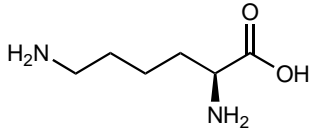
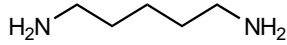
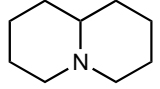
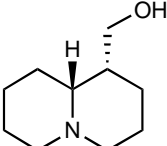
Lupinus mutabilis has its origin of domestication presumable in the Cajamarca region 500 to 1000 AD ⁶. The beans contain approximately 44 % proteins, 33 % carbohydrates, 19 % lipids, and 4 % alkaloids, which brings the plant to a very auspicious position ^{8,9}. However, the lupin beans are not ready to consume because of their toxicity for humans through alkaloids ¹⁰. To avoid this problem three different approaches can be taken.

At first, cultivars of *Lupinus mutabilis* species with lower alkaloid content can be identified and cultivated. This avoids a separation process and allows the direct consumption. For this approach, several different analytical techniques to extract and quantify alkaloids were introduced and tested in this thesis. Secondly, single component classes can be extracted. This is shown and tested for proteins, dietary fiber and lipids. The last approach focuses on the extraction of alkaloids prior food processing, also called debittering. This can be conducted by traditional aqueous water extraction or solvent extraction like scCO₂ and was beyond the scope of this thesis.

2.2 Quinolizidine alkaloids

Alkaloids are secondary plant metabolites and can be biosynthesized from amino acids. They can help the plant to defend itself against different predators, herbivores, and microorganism^{11, 12}. In the case of lupin plants, the biosynthesis is based on the essential amino acid L-Lysine, which is converted by the enzyme lysine decarboxylase to cadaverine¹². The cyclization of two cadaverine molecules will lead to bicyclic alkaloids (quinolizidine, lupinine), while the cyclization of three or more cadaverine molecules results in the tetracyclic alkaloids (sparteine, lupanine, etc.). The variety of alkaloids in lupin beans is created by modification of the alkaloids via different enzymes.

Table 1: Raw and end-products of the alkaloid biosynthesis in lupin crops.

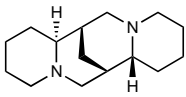
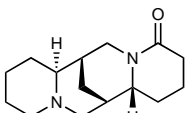
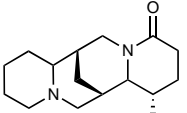
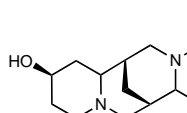
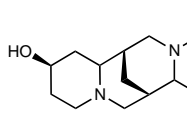
L-Lysine	Cadaverine	Quinolizidine	Lupinine
			
C ₆ H ₁₄ N ₂ O ₂	C ₅ H ₁₄ N ₂	C ₉ H ₁₇ N	C ₁₀ H ₁₉ NO

Quinolizidine alkaloids are toxic to humans and can cause several diseases⁹. Incidents of intoxications are reported for animals and humans of which some were mortal^{9, 13}. It is therefore important to know the exact alkaloid content in lupin products and the safe-to-consume threshold. The British government suggested 1996 a threshold of 20 mg/100 g (0.02 %) alkaloids in lupin beans and their products for safe consumption, which is still widely accepted^{9, 13, 14}.

Lupinus mutabilis is a cultivar of lupin crops, which was extensively used in this thesis as *Lupinus mutabilis* Branco. It is reported to contain several different tetracyclic alkaloids from the quinolizidine family, most abundant being lupanine followed by sparteine, 13 α -hydroxylupanine (13-OH), and 3 β -hydroxylupanine (3b-OH)⁸. Other alkaloids as 3 β ,13 α -dihydroxylupanine (Di-OH), tetrahydrorhombifoline, α -isolupanine, are reported to be

less present and are therefore considered as minor alkaloids ^{8, 13, 15, 16}. Other lupin cultivars also contain alkaloids, but the ratio and total alkaloid content might differ strongly.

Table 2: Main alkaloids in *Lupinus mutabilis branco* beans based on Soxhlet extraction.

Sparteine	Lupanine	3 β Hydroxy-lupanine (3 β -OH)	13 α Hydroxy-lupanine (13-OH)	3 β ,13 α Dihydroxy-lupanine (Di-OH)
				
C ₁₅ H ₂₆ N ₂	C ₁₅ H ₂₄ N ₂ O	C ₁₅ H ₂₄ N ₂ O ₂	C ₁₅ H ₂₄ N ₂ O ₂	C ₁₅ H ₂₄ N ₂ O ₃
234.38 g/mol	248.36 g/mol	264.36 g/mol	264.36 g/mol	280.36 g/mol
pK _a 12 ¹⁷	pK _a : 9.4 ¹⁷ pK _a : 9.1 ¹⁸		pK _a : 8.8 ¹⁷	

The alkaloids are sorted by appearance in the GC-chromatogram.

2.2.1 Debittering

An extraction can be either carried out in a destructive or nondestructive way. Destructive ways are mostly applied when the alkaloids themselves are of interest. This is the case for analytical quantification or purification steps. The remaining matrix is then often contaminated with harmful chemicals, making it unsuitable for food purposes. A non-destructive way is considered whenever the remaining matrix is of interest. This is the case when the lupin bean's main components (everything except alkaloids) are of interest. This process is called debittering because most quinolizidine alkaloids are bitter and therefore debittering refers to the removal of alkaloids from the matrix.

One possibility is leaching with an excessive amount of water (i.e. in a river). This is rather a traditional way which was also practiced in the Mediterranean and Andean regions for more than a thousand years ¹⁹. The debittering is related to the water-solubility and polarity of the quinolizidine alkaloids. For example, lupanine has a calculated solubility of 8.1 g/l ¹⁷.

Another method is debittering via cold and warm aqueous processing, where the lupin beans get treated with hot water before the alkaloids are leached with cold water ⁸. Also, industrial applications are known in which the lupin beans are hydrated, swollen, cooked, and rinsed with water until the bitterness is gone ^{20, 21}.

2.2.2 Quantification

In the case of quantification, not the matrix but the alkaloids themselves are of interest. Therefore, three different approaches are reported, namely titrimetric determination, acid-base extraction, and solvent extraction. All have in common that, prior quantification, an extraction step needs to be carried out. In contrast to debittering, which is often executed with intact or split lupin beans, these extractions require fine powder.

Solvent extraction with titrimetric determination: A rapid quantification is based on a simple extraction and titration of the alkaloids. Baer et al.²² suggest the extraction by mixing chloroform with lupin flour, followed by sonification and addition of an aqueous base. Basic aluminum oxide is added to soak the aqueous layer before it is removed by filtration together with the remaining matrix. The extracted alkaloids in chloroform are then titrated with p-toluenesulfonic acid (in chloroform) with a tetrabromophenolphthaleine ethyl ester as indicator²³. This method allows a quick but rough determination of the total alkaloid content in the sample. It lacks in sensitivity and accuracy for the low alkaloid-containing samples.

Solvent extraction and chromatographic determination: The solvent extraction followed by a chromatographic determination is another method for the quantification of alkaloids in lupin beans. For this either a solvent extraction as shown for the titrimetric determination or more advanced processes as Soxhlet or Randall extraction can be applied. To analyze the extract, gas chromatography (GC) coupled to a flame ionization detector (FID), mass spectrometer (MS), or phosphor-nitrogen detector can be applied. Caffeine can be used as internal standard (IS)^{16,24}. Other chromatographic determinations might involve high-performance liquid chromatography (HPLC) with MS/MS detector²⁵.

Soxhlet extraction of quinolizidine alkaloids from lupin beans is a rather uncommon extraction method because co-extraction of other materials i.e. crude fats can take place and disturb the chromatogram and quantification¹⁵. However, methanol has the advantage that it can dissolve the protonated and non-protonated form of alkaloids and is therefore prone for the use as a solvent in Soxhlet operation¹⁵.

Acid-base extraction and chromatographic determination: The most common method is the extraction via acid-base reaction. Lupin flour is mixed with an acidic solution, for example HCl²⁶⁻²⁸ or trichloroacetic acid (TCA)²⁹⁻³¹. During this step, the alkaloids become protonated which enhances the water solubility and salt character. The alkaloid-containing aqueous phase can then be separated by filtration or centrifuging. The following alkalization converts the protonated alkaloids into their non-protonated form. In the following, the non-protonated form is often referred as the non-polar form and the protonated form is often referred as the polar form. The non-polar form is reported to favor organic solvents, while the polar form prefers aqueous solutions¹⁵.

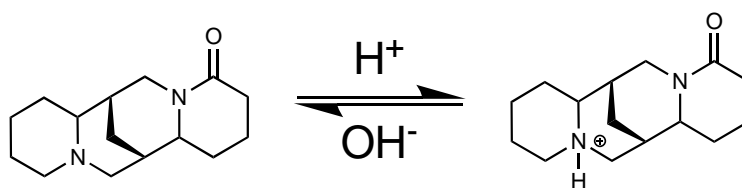


Figure 2: Acid-base behavior of alkaloids.
Non-polar/deprotonated form (left) and polar/protonated form of lupanine (right).

The alkaloids from the basic aqueous solution can then be either separated by a standard liquid-liquid extraction (LLE) or a supported liquid-liquid extraction. The latter one is often referred to as solid phase extraction (SPE) and helps to overcome formation of emulsions ¹². The stationary phase of the SPE is diatomaceous earth (mostly Extrelut from Merck) and it adsorbs the alkaline aqueous solution. In the following step, the non-polar alkaloids are eluted via an organic solvent, e.g. dichloromethane (DCM). The gained extract can be used directly or evaporated and resolved for lower quantification and detection limits. Chromatographic determination is carried out as described above.

An overview about the reported methods and its chromatographically application is given in Table 3.

Table 3: Reported extraction and quantification methods of alkaloids from lupin beans.

Year	Extraction and quantification	Ref.
1979	Solvent, Titration: -CHCl ₃ , 1 mL 15 % KOH, Al ₂ O ₃	22
1983	Acid-base (SPE), GC: -2 M HCl, NH ₃ (25 %), Extrelut CH ₂ Cl ₂	32
1988	Acid-base (SPE): -1.0 g, 15 mL 0.5 M HCl, 4 M NaOH, Extrelut CH ₂ Cl ₂	26
1992	Solvent, GC: -Soxhlet MeOH	15
1992	Acid-base (SPE), GC: -0.5 g, 15 mL 0.5 M HCl, NH ₃ /NaOH pH 12, 3 × 20 mL CH ₂ Cl ₂ Extrelut	15
1994	Acid-base (LLE), GC-PND: -0.5 g, 3 × 5 mL TCA, 1 mL 10 M NaOH, 3 × 5 mL CH ₂ Cl ₂	33
1995	Acid-base (SPE), GC-MS: -0.5 M HCl, 2 M NaOH (or NH ₃), Extrelut CH ₂ Cl ₂	31
2000	Acid-base (SPE and LLE), GC-FID/GC-MS: -1.0 g, Agitation, NaOH (pH > 11), 4 × 25 mL Extrelut CH ₂ Cl ₂	34
2001	Acid-base (SPE), GC-MS: -0.5 g, 20 mL 1 M HCl, 6 M NaOH (pH 12), Extrelut CH ₂ Cl ₂	27
2008	Acid-base (SPE), GC-MS: -0.5 g, 8 mL 0.1 M HCl, 5 % NH ₃ (pH 10-11), 4 × 20 mL CH ₂ Cl ₂ Extrelut	28
2016	Acid-base (LLE), GC: -0.5 g, 3 × 5 mL 5 % TCA, 1 mL 10 M NaOH, 3 × 15 mL CH ₂ Cl ₂	29
2019	Acid-base (LLE), GC-FID: -0.5 g, 3 × 5 mL 5 % TCA, 25 % NH ₃ pH 10, 3 × 20 mL CH ₂ Cl ₂ Extrelut	30
2020	Acid-base (LLE), GC-FID: -0.1 g, 3 × 5 mL 5 % TCA, 0.8 mL 10 M NaOH	24

Although the table does not claim completeness, all experiments were conducted with an initial lupin material between 0.1 and 1.0 g. A trend is emerging in which extractions are based less

on solvent extraction and more on acid-base extraction. If an acid-base extraction was chosen, DCM was applied either as an organic phase for the LLE or as an eluent for the SPE. For the latter one Extrelut column material was preferred. In general, it can be said, that acid-base extraction is therefore the most common extraction method for quinolizidine alkaloid extraction from lupin material either with LLE or SPE.

2.3 Proteins

The protein content of lupin beans is one of its biggest advantages among other crops. It can reach up to 50 % of the lupin bean weight bringing it to a superior position ⁸. In this thesis, a few widely known protein extraction methods were tested and its parameters influencing the protein yield were analyzed. This also includes the substitution of conventional reagent agents by CO₂ to increase the sustainability of the process.

2.3.1 Amino acids

Proteins can consist of 20 different proteinogenic amino acids (without selenocysteine and pyrrolysine, see ³⁵), which are linked via peptide bonds to build a large macromolecule ³⁶. Proteinogenic amino acids are used in living cells which are only a small part of all constitutionally possible amino acids. However, all the proteogenic amino acids consist of a carboxylic group (-COOH, green Figure 3) and an amino group (-NH₂, blue Figure 3) in α -position and have at least one chiral carbon atom (except glycine with R=H) ³⁷. Both functional groups have an acid/base character and can be protonated or deprotonated, which is influenced by the pH of the surrounding solution. Amino acids are ampholytes because they have an acidic and a basic functional group. At neutral pH, the carbonic acid of most amino acids is deprotonated while the amino group is protonated (see Figure 3).

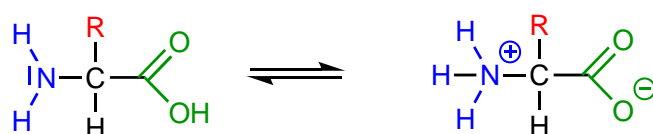


Figure 3: Amino acids and its ampholytic character.

Amino acids can be distinguished via their functionality on their side group (R). They can be divided into subgroups, e.g. based on their chemical properties (hydrophobic, hydrophilic, electrically charged) or biosynthesize (essential/non-essential) ³⁶. The side chain has also influence on different parameters of the protein characteristics, i.e. is the solubility largely affected by the chemical side structure.

2.3.2 Protein determination

The nitrogen factor or Kjeldahl factor is also dependent on the acid composition/side chains of the proteins. The nitrogen factor describes the relation between the total weight fraction of the amino acids to the measured nitrogen. It is calculated by the total weight of the amino acids divided by the specific nitrogen content of the amino acid and is also referred to as the Kjeldahl factor (K_F , see Equation 1). For example, β -alanine has a conversion factor of 6.36. This can be calculated by using the molecular weight of β -alanine (Mw: 89.10 g/mol) and nitrogen content of the β -alanine (14.01 g/mol). The calculation can be seen below and was calculated for one mol.

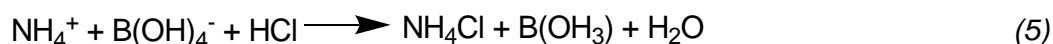
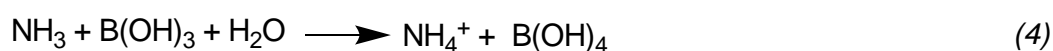
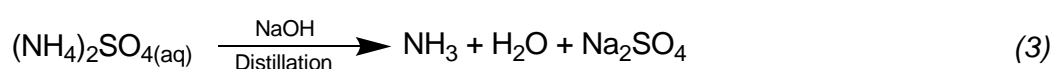
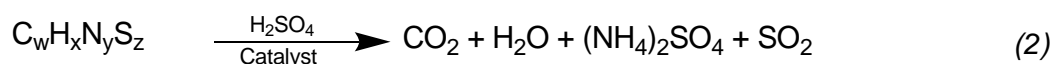
$$K_F = \frac{m_{total}}{m_{nitrogen}} = \frac{89.10 \text{ g}}{14.01 \text{ g}} = 6.36 \quad (1)$$

K_F : Kjeldahl factor,

m_{total} : Mass of total protein/amino acid (g),

$m_{nitrogen}$: Mass of nitrogen in the protein/amino acid (g).

In 1883 Johan Kjeldahl described a method to analyze the nitrogen content in organic matrices³⁸. It is based on the destruction of the organic matrix by sulfuric acid and the simultaneous conversion of nitrogen to ammonium sulfate (Equation 2). The ammonium sulfate can be purified in a second step by base-induced steam distillation (Equation 3). The so-formed ammonia is then captured by a boric acid solution (Equation 4). The acid consumption during the following titration step refers to the amount of nitrogen in the sample (Equation 5).



Kjeldahl nitrogen determinations are used, whenever the determination of amino acids is of no significance. This can be the case when the samples contain roughly similar amino acid compositions and only the total protein content is of interest. In those cases a standard Kjeldahl conversion factor for unknown proteins in legumes of 6.25³⁹ can be applied (for comparison: dairy products is 6.38⁴⁰). Although the Kjeldahl determination factor is widely accepted, there are doubts if the calculated protein content is in line with the real protein content. In the case of lupin beans, the alkaloids themselves might also affect the total protein content since they also contain nitrogen.

Another method to determine the protein concentration is the bicinchoninic acid (BCA) method, which was developed by Smith et al. ⁴¹. It is based on the reduction of Cu²⁺ to Cu⁺ through peptide bonds and is therefore in linear relation to the abundance of peptide bonds. The BCA builds a violet-colored complex with Cu⁺ ions and its absorption can be measured via UV/VIS. According to the Beer-Lambert law is the measured absorbance linear related to the peptide bond concentration. However, in this thesis, in almost all cases (except for the CO₂-only process) the Kjeldahl nitrogen determination was preferred over the BCA protein determination since it is independent of the solubility of proteins.

2.3.3 Protein fractions

For the extraction of proteins from a complex biomatrix, parameters that influence the solubility of the protein are important. A method which classifies the proteins in terms of solubility was developed by Osborne and Harris ⁴². Following the method and its further development, proteins can be classified into four different classes: albumins, globulins, glutelins, and prolamins. An overview of the solubility properties of each group can be seen in Table 4.

Table 4: Solubility of different Osborne fractions.

	H ₂ O	NaCl	OH ⁻	H ⁺	EtOH
Albumins	+	+	-	-	-
Globulins	-	+	+	+	-
Glutelins	-	-	+	+	-
Prolamins	-	-	-	-	+

Data are obtained from Muranyi ⁴³. Suitable solvation relations are indicated via +.

Albumins are soluble in water, globulins are soluble through ionic strength, glutelins are soluble in dilute acids and alkaline solutions, and prolamins are soluble in mixtures of water with ethanol (EtOH) ^{44, 45}.

The major protein fraction for most legume seeds is globulin, followed by albumins ⁸. An overview of different plant-based proteins is given in Table 5.

Table 5: Overview about the protein fractions in different food sources.

	Bean	Lupin	Pea	Soybean
Albumins	28 - 37 %	11 %	21 %	10 %
Globulins	35 - 39 %	72 %	66 %	90 %
Glutelins	0 %	6 %	12 %	0 %
Prolamins	0 %	1 %	0 %	0 %

Data is obtained from Sanchez-Chino et al. ⁴⁶.

Globulins are the major protein class in lupin beans (see Table 5). The distribution differs between the different varieties. The here-used variety *Lupinus mutabilis*, has a weight fraction

of around 91 to 94 % globulins according to Carvajal-Larenas et al. ⁸. The globulin fraction in lupin beans contains the storage proteins α -, β -, γ -, δ -conglutin, as well as legumine-like proteins. They are not soluble in pure water but in salt solutions, diluted acid, and lye solutions (see Table 4). Since globulins are by far the biggest fraction of all proteins, an extraction strategy especially focused on this fraction is needed. The strategy can be either focus on the isoelectric point or the ionic strength.

2.3.4 Isoelectric point

The isoelectric point describes the pH value where the amino acid or protein is net-charged zero. At this point many proteins are not soluble in water anymore and start to precipitate. Therefore, this phenomenon can be used to separate the proteins from the matrix.

Every amino acid/protein has its own isoelectric point, which depends on the amount and charge of the acidic and basic groups from the amino acids. Figure 4 describes the behavior of the carbonic acid and amino group of an amino acid at low, neutral, and high pH media.

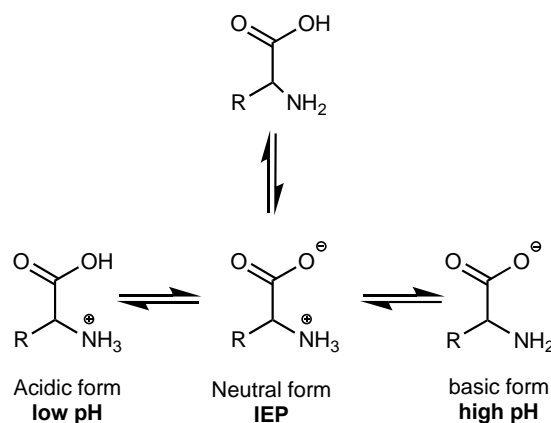


Figure 4: Amino acid behavior in acidic, neutral, and basic milieu.

In a region of low pH, the carbonic acid and the amino group of the amino acid are protonated. This means that the carbonic acid group is charged neutral, while the amino group is charged positively (here shown on the left side of Figure 4), hence increasing its water solubility.

In an alkaline media (see right side of Figure 4), the opposite reaction will occur. The deprotonated carbonic acid is charged negatively, which increases the water solubility, while the amino group is not charged. The solubility of the amino acid at low and high pH media is therefore increased in comparison to the neutral form.

At neutral pH, the protein is at its isoelectric point (IEP), where the net-charge is zero. This means that the charged amino and carbonic acid groups are in equilibrium with the non-charged form, which results in lower solubility of the protein in aqueous solutions ⁴⁷.

2.3.5 Ionic strength

Proteins are relatively sensitive to all kind of changes inside a system. Ionic strength can be used to dissolve and precipitate proteins. In case of a very low ionic strength, the proteins will bind to themselves and build agglomerates⁴⁸. If the salt content increases, the solubility of the proteins will mostly become higher. The salts can attach to some functional groups of the protein and form solvation shells with water. However, if the salt content is further increased, the protein solubility will decrease again. This is due to the formation of a very polar solution, which can force the protein to interact with itself and leads to agglomerates. Therefore, the protein solubility is not only depending on the pH, it is also dependent on the amount and type of salt.

2.3.6 Protein extraction strategies

Several different protein principles are known for the extraction of lupin proteins from their biomatrix. All here-discussed principles and methods are based on wet processing, with the principle of solvation and precipitation. Although dry protein separation processes exist, they are still under development and lack through low yield⁴⁹. A general scheme about the wet extraction principle is shown in Figure 5.

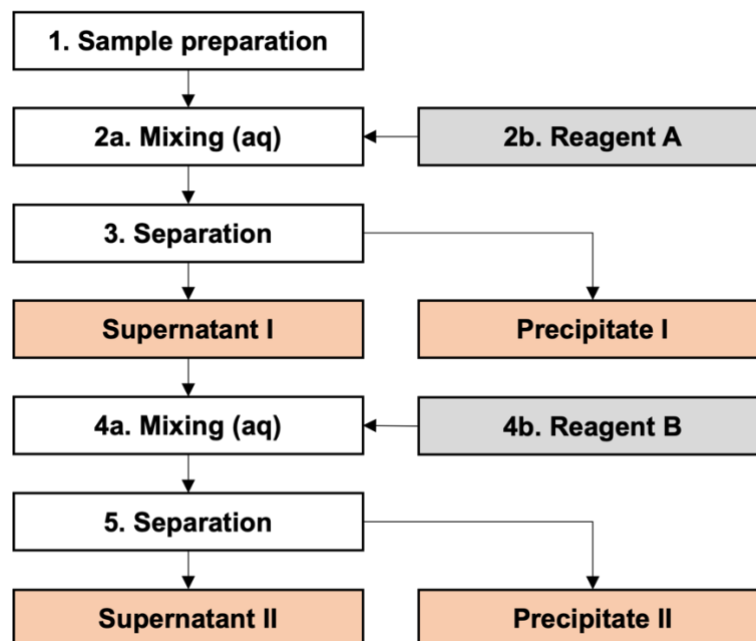


Figure 5: Process overview of the protein extraction process.

All applied methods have in common that the lupin beans are converted into a smaller matrix (1). Water and a solvation reagent are added (2b) and mixed with the sample (2a) to dissolve the proteins into the aqueous phase. With respect to the high globulin content in *Lupinus mutabilis*, an extraction with salt, alkaline, or acidic solution could be considered (see Table 4). After the solvation of proteins in the aqueous solution, a separation step (3) is

conducted. The separation mostly involves centrifuging, where the dissolved protein solution (supernatant I) is separated from the precipitated insoluble matrix (precipitate I). The now separated solution (supernatant I) contains protein and other under this condition soluble materials, i.e. small carbohydrates. In the next step, a precipitation agent is added (**4b**) to the supernatant I and mixed (**4a**) before precipitation of the protein occurs. Another separation step (**5**) splits the precipitated proteins from the remaining soluble solution, i.e. by centrifuging.

Isoelectric point precipitation (IEPP): The isoelectric point precipitation (IEPP) uses the isoelectric point (IEP) of the proteins to separate them from their surrounding biomatrix.

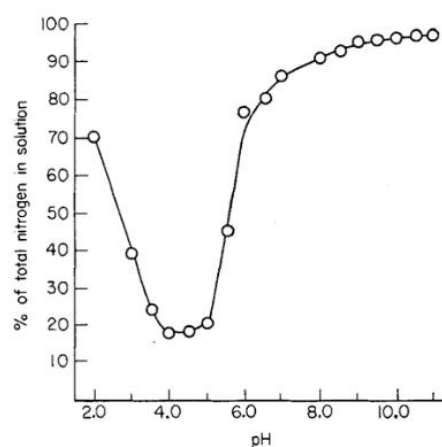
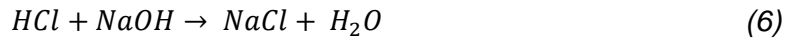


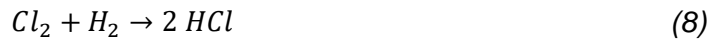
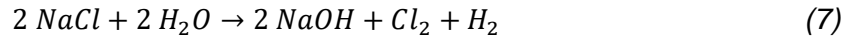
Figure 6: Nitrogen solubility of *Lupinus angustifolius* reported by Ruiz and Hove⁵⁰.

The nitrogen solubility behavior refers to the protein content (see Section 2.3.2) and is described in Figure 6. At high and low pH, the solubility seems to increase. At pH 4-5 the solubility has its lowest value, which refers to the IEP. A common extraction strategy is the solvation at high pH (8 or higher), followed by a separation. Afterwards, the pH of the dissolved protein fraction is adjusted to the IEP value (pH 4.5) and another separation step is conducted. Hove and Ruiz⁵⁰ analyzed the protein extraction of *Lupinus angustifolius* beans. They mixed defatted flour in a ratio of 1:10 with water and adjusted the pH to 8.5 for 30 minutes (min). After separation of the supernatant I by centrifuging, the pH was adjusted to pH 4.8 (IEP value), before another separation took place. The collected precipitate II was washed, dried, and analyzed via Kjeldahl-method. The total nitrogen yield was ca. 52 %, with a concentration of 89,4 % for whole flour and 92,5 % for defatted flour ($N \times 6,25$). This method was also carried out by King, Aguirre and Pablo with similar results⁵¹.

The IEPP allows the isolation of proteins from the remaining matrix via a simple wet process. Nevertheless, this process consumes a strong lye and a strong acid, which will form salts. In case of Ruiz and Hove HCl and NaOH were used, which produce NaCl as a waste product (see Equation 6).



The use of NaOH and HCl for neutralization is questionable, in view of the high energy consumption for the industrial production of those chemicals from sodium chloride (NaCl) via chlor-alkali electrolysis (see Equation 7 and 8).



IEPP-CO₂: An alternative is shown by Hofland et al.⁵² for soybeans, where the addition of HCl was substituted by carbon dioxide. The first steps were carried out similarly to the IEPP as shown in Section 2.3.6. Shortly, defatted soy flour was dissolved in demineralized water (1:10) and 1 M NaOH solution was added until a pH of 9 was reached. After 30 min the solution was centrifuged, and the supernatant was transferred into a pressure vessel as shown in Figure 7.

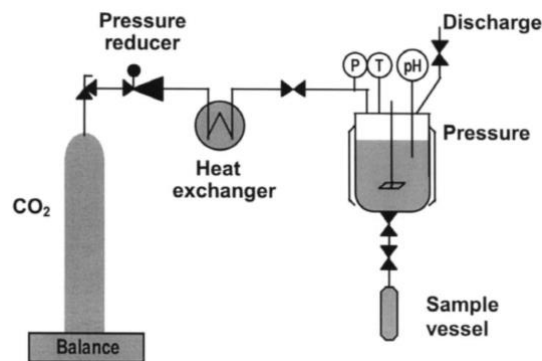


Figure 7: IEPP-CO₂ setup according to Hofland et al.⁵².

At 25 °C the variation of stirring rate 50, 300, and 800 revolutions per minute (RPM), variation of pressure (0 to 50 bar), and variation of time and composition were tested for the precipitation of the proteins⁵². The results from their CO₂ precipitation showed comparable results in terms of protein yield but offered an improved particle morphology.

Although this process might be more sustainable than the use of HCl, it still requires a lye solution (here NaOH) to dissolve the proteins.

IEPP - Only CO₂: To further increase the sustainability of the protein extraction process, an advanced process was developed in this thesis. The focus of the new concept is laying on the replacement of the alkalinization step for the solvation of proteins (step 2, Figure 5) through an acidification step. As shown in Figure 6, the nitrogen/protein solubility increases with higher and lower pH values. This means that the CO₂ might not only replace the acid for the precipitation step, but also the lye in the solvation step. The method of dissolving proteins through acid is less common, because the highest nitrogen solubility is at a pH of 8 and higher (see Figure 6 and Figure 8), hence a lower protein extraction yield will be expected.

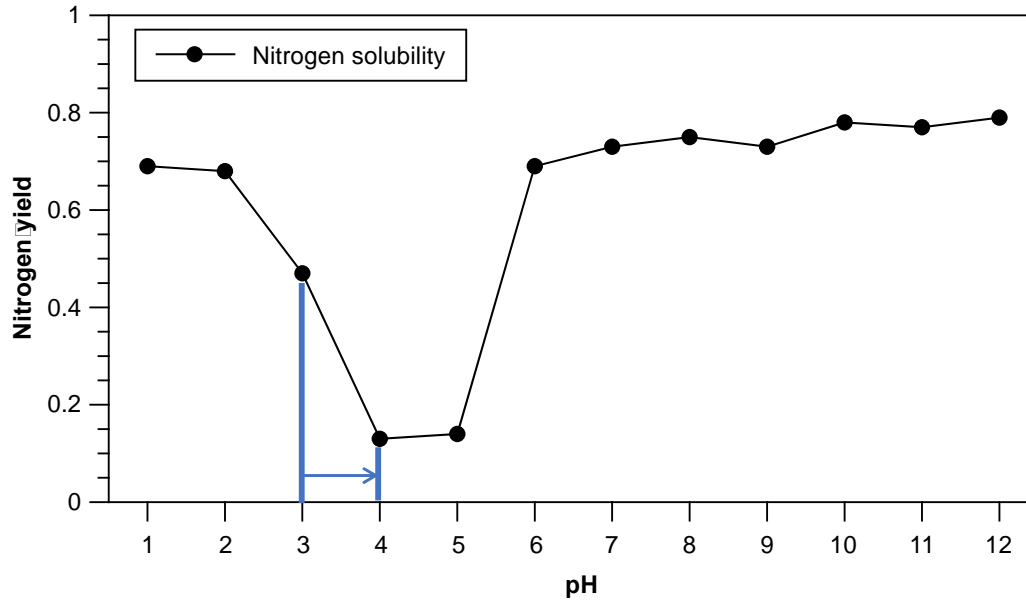


Figure 8: Nitrogen solubility of *Lupinus mutabilis branco* flour.
The theoretical applied pH values of the CO₂-only process are indicated in blue.

To utilize CO₂ as a volatile acid, a pH of 3 or lower needs to be reached to dissolve the proteins (step 2, Figure 5). The pH and solubility of CO₂ are greatly influenced by temperature and pressure (see later in Figure 16). A lower temperature and higher pressure mean more dissolved CO₂ which ultimately lead to lower pH values and higher protein solubility. For the solvation of proteins, cold temperature and high pressure parameters should be chosen. The following protein precipitation can be either carried out as described from Hofland⁵² for soy or as shown below for lupin beans.

Salt-induced precipitation: Not only the proteins behavior at their IEP can be an extraction strategy, but also their behavior at different ionic strengths. Ionic strength can be either applied as salting in or as salting process. Both approaches start identically, by using salt and water to dissolve the proteins. After the proteins become soluble, a separation is conducted and the newly gained supernatant I will be either diluted with demineralized water (salting-in) or more salt is added, forcing the proteins to precipitate out (salting-out). Ammonium sulfate is one of the most common salts, but others may have similar effects⁴⁸.

Sussmann et al.⁵³ investigated the effect of several parameters on the extraction of proteins from *Lupinus angustifolius*. Instead of the often-used ammonium sulfate, 0.5 M sodium chloride solution was used to dissolve the proteins. After solvation and separation, the proteins got precipitated by using demineralized water. A protein yield of 35.8 % was reported for their optimized protein extraction method.

This approach has the benefit of using no acid or lye. In contrast, a lot of water is used, and the protein extraction yield is lower than shown for the IEPPs.

2.4 Lipids

The extraction of lipids from lupin beans⁵⁴ and from cherry stones⁵⁵ are extensively discussed in two publications (see Section 7.5 and Section 7.6), and are therefore only briefly introduced. Lipids are defined as molecules that dissolve in non-polar solvents. This broad category can be divided into subgroups such as fats, phospholipids, and steroids. Fats are the major fraction of legumes and are used as energy storage by humans and plants³⁶. Fats consist of triglycerides and have a non-polymer character. A triglyceride is based on a glycerol molecule which is linked via ester bonds to fatty acids. Up to three different fatty acids can be linked to the glycerol molecule (see Figure 9) and they can consist of various chain length with even carbon atom numbers.

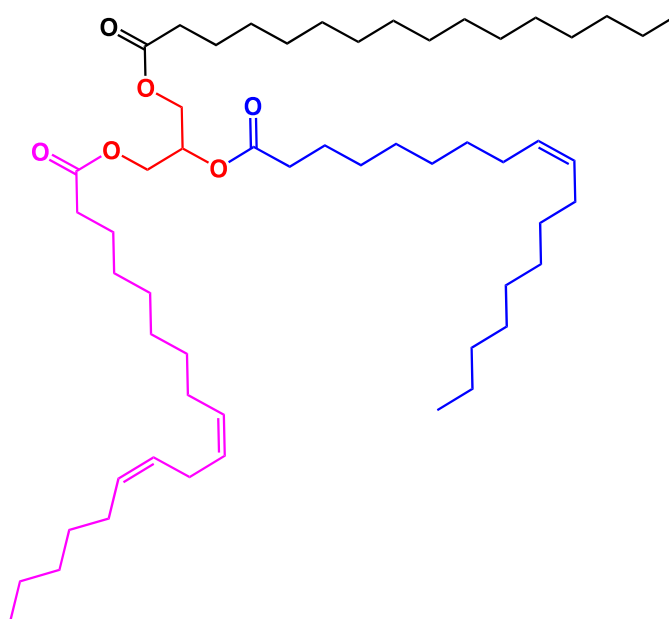


Figure 9: Triglyceride molecule.

Triglyceride molecule contains glycerol (red) connected via ester bond to palmitic acid (black), oleic acid (blue) and linoleic acid (purple).

The fatty acid can not only be distinguished by carbon atom chain lengths but also by the position of C-C double bonds. The number and position of the C-C double bond have a great influence on the fatty acid behavior. The so-called saturated fatty acids do not contain any double bonds. Palmitic acid (C16:0, see Figure 9) and stearic acid (C18:0) are saturated fatty acids. Through the lack of double bonds, triglycerides with saturated fatty acids have mostly a lower melting point than triglycerides with unsaturated fatty acids, which can be explained by their denser packing (see Figure 9)⁵⁶. A monounsaturated fatty acid consists of one C-C double bond, which can be at various positions. Oleic acid (C18:1) is a common fatty acid and has a cis C-C double bond at position 9 (see Figure 9).

Most natural fatty acids have cis C-C double bonds, especially from plant-based origin. Fats with trans C-C double bonds can be found in animal products, partly hydrolyzed fats, and after high-temperature treatment of fats. Trans fats are suspected of promoting cardiovascular problems, which is why there are official recommendations to lower the uptake in the human diet ^{57, 58}.

Polyunsaturated fatty acids contain more than one C-C double bond. A prominent polyunsaturated fatty acid is linoleic acid (C18:2). The linoleic acid molecule has a C-C double bond in positions 9 and 12 (see Figure 9) and is an essential fatty acid. The ratio of saturated fatty acid to unsaturated fatty acid is important with respect to specific health claims. A low saturated fatty acid content and the elimination of trans fatty acids might decrease the risk of cardiovascular problems and is considered healthy ^{57, 58}.

2.4.1 Lipids from lupin beans

Carvajal-Larenas et al. ⁸ summarized that *Lupinus mutabilis* beans contain between 13.0 and 24.6 g lipids per 100 g dry weight (DW) with 80 % unsaturated fatty acids. The fatty composition was reported in following order of abundance: ca. 50 % oleic acid (C18:1), 35 % linoleic acid (C18:2), 15 % palmitoleic acid (C16:1), 10 % palmitic acid (C16:0), 10 % stearic acid (C18:0), and 5 % minor fatty acids as Linolenic acid (C18:3).

Bhardwaj, Hamama, and van Santen ⁵⁹ extracted oil from *Lupinus albus* seeds via a multi-step extraction with a hexane/isopropanol mixture. An oil extraction yield of 7.2 to 8.2 % was reported and the fatty acids are present in following order 18:1 > 18:2 > 18:3 > 16:0 > 20:1 > 22:1 > 22:0 > 18:0 > 24:0 > 20:0, which shows a similar fatty acid abundance.

2.4.2 Lipids from sour cherry stones

Cherries belong to the botanical family of roses, namely Rosaceae. Sour cherries can, similar to lupin beans, grow in cold European regions and are commercially available. The sour cherry consists of skin, flesh, seed (shell + kernel) and stem ⁶⁰. For sour cherry products, commonly the juice of the cherry is needed. To produce sour cherry juice, the fresh sour cherry gets pressed, and the desired liquid fraction is obtained. The remaining fraction consists of skins, stems, flesh leftovers, and seeds and is considered as waste material ⁶⁰.

In this thesis the stones from the sour cherry (*Prunus cerasus*) are used to analyze the effect of extraction method, moisture content and pre-treatment on the extraction yield of lipids. In contrast to lupin beans, they offer a more complex matrix and are therefore better suitable for the detailed analyzes of parameter influence.

2.4.3 Extraction strategy for lipids

Lipids can be extracted by either mechanical pressing of the matrix or solvation through a non-polar solvent^{56,61}. For the solvation, hexane or heptane can be used as an extraction agent in a simple rinsing/mixing process. In lab scale more advanced processes e.g. Soxhlet or Randall can be applied. Another possibility of solvent extraction is the use of supercritical CO₂ (scCO₂), which offers unique benefits as safe-to-consume products but requires special high-pressure equipment.

2.4.4 Fatty acid methyl ester (FAME)

The determination and analysis of fats can be carried out with different techniques. One possibility is the analysis of fatty acids in form of fatty acid methyl esters (FAME). FAME determination and quantification can be used to characterize a lipid fraction. The major component of the lipid fraction for lupin beans as well as cherry stones are triglycerides. Since the determination of intact triglycerides is time consuming and hard to achieve, most often the triglycerides undergo a derivatization step (here: acid catalyzed transesterification). The derivatization step converts the polar and low volatile triglyceride into non-polar and volatile FAMES, which can be separated by gas chromatography (GC)^{62,63}.

2.5 Carbohydrates

Carbohydrates consist of multiple of CH₂O and are the fuel and building material of living cells³⁶. They are considered as major fractions of biomass and can be divided by their type of monomer, degree of Polymerization (DP), and type of linkage (α or β)⁶⁴. The following table (Table 6) gives a general overview about the difference in carbohydrate classes.

Table 6: Examples of different carbohydrate fractions.

Class (DP)	Subgroup	Principal components
Sugars (1-2)	Monosaccharides	Glucose, fructose
	Disaccharides	Sucrose, lactose
	Sugar alcohols	Sorbitol, mannitol
Oligosaccharides (3-9)	α -glucan	Maltodextrins
	Non- α -glucans	Raffinose, stachyose
Polysaccharides (≥ 10)	Starch	Amylose, amylopectin
	Non-starch polymers (NSP)	Cellulose, hemicellulose

Original data were reported by Cummings and Stephen⁶⁴.

The role of carbohydrates in human nutrition is related to their digestibility and resorption in the human body. It is based on the chemical structure and breakdown by enzymes in the human body⁶⁵. Sucrose (table sugar) will be broken down to glucose and fructose, which is used as an energy resource and will be resorbed by the intestine and will increase the glycemic index. Also, starch will be broken down to Glucose, where it can be used as an

energy resource. In contrast to Glucose and starch, other carbohydrates cannot be broken down and resorbed due to their glycosidic bonding. This is the case for oligosaccharides (DP 3-9) like raffinose (DP=3), stachyose (DP=4), and verbascose (DP=5), but also for non-starch polysaccharides (NSP), like cellulose, hemicellulose and pectin^{64,65}. They will not increase the glycaemic index but will have other properties. For example, NSPs increase satiety and stool output, while oligosaccharides are a nutrient for the bacteria inside the intestine and will lead to a balanced flora^{64,66}.

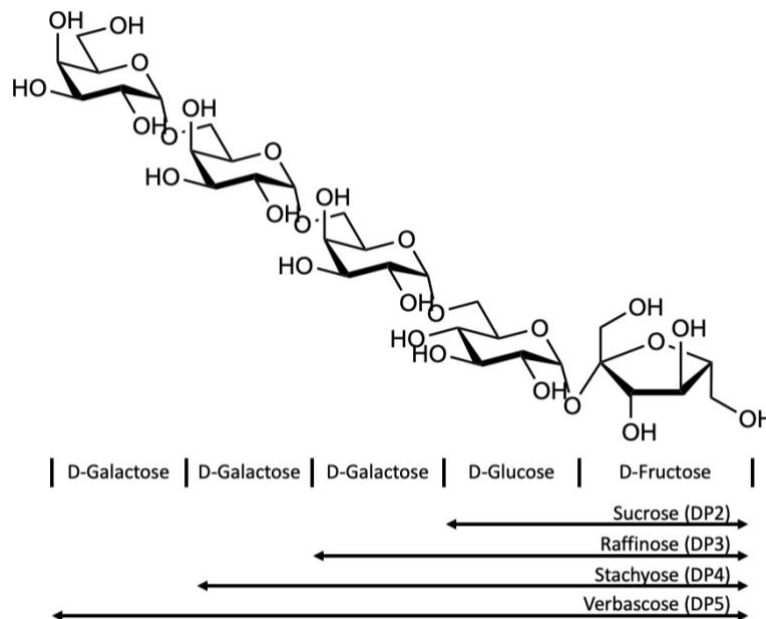


Figure 10: Different oligosaccharides and their molecular structure.

The definition of dietary fiber differs widely. In this thesis, dietary fiber is defined as non-digestible soluble and insoluble carbohydrates (and lignin) with 3 or more monomeric units⁶⁷. According to this definition, dietary fiber consists mostly of non- α -glucan oligosaccharides and NSPs (see Table 6).

A lab-scale carbohydrate extraction can be carried out via ethanolic solutions of defatted flour. Proteins are not soluble in the ethanolic solution, hence only low molecular weight carbohydrates will be extracted. However, the extraction of carbohydrates is already widely applied on an industrial scale. Large-scale carbohydrate/sugar extraction requires a designated feedstock (sugar cane, sugar beets, etc.) in a refinery-like process, where the juice from the feedstock is extracted via pressing or solvation⁶⁸.

2.6 Extraction techniques

Several different extraction techniques were applied to extract valuable fractions from lupin beans and lipids from cherry stones. The mechanisms and technologies regarding those techniques are discussed below.

2.6.1 Solid-liquid extraction mechanism

Solid-liquid extraction describes a process where a solid matrix is penetrated with a liquid solvent to dissolve, wash, or leach the molecules of interest⁶⁹. It is used as a purification method and can be applied to various samples. The extracted molecules are called solute or analyte, while the solvent containing the molecules of interest is called extract. This extraction method requires solubility of the targeted molecules in the chosen solvent and often involves another purification step to separate the solute from the solvent.

The mechanism of solid-liquid extraction involves the transfer of solvent from the bulk of the solvent to the solid matrix surface (1), the diffusion of the solvent into the solid matrix (2), the dissolution of the solute from the matrix into the solvent (3), transfer of the solute to the matrix surface (4), transportation of the solute from the surface to the bulk of the solvent (5), and separation of the extract from the matrix (6)⁷⁰. The extraction speed is determined by the slowest step, which often is the solvent reaching the solid matrix surface (1) and the diffusion of the solvent into the matrix (2)^{69, 70}. Diffusion is the driving force for solid-liquid extraction and can be mathematically expressed by the first Fick's law⁷¹.

$$J_x = -D \frac{d_c}{d_x} = \frac{N}{A} \quad (9)$$

J_x : Mass flux ($\text{mol} \cdot \text{m}^{-2} \cdot \text{s}^{-1}$),

D : Diffusion coefficient ($\text{m}^2 \cdot \text{s}^{-1}$),

$\frac{d_c}{d_x}$: concentration gradient along the x-axis ($\text{mol} \cdot \text{m}^{-4}$),

N : dissolution rate of solute into the solvent ($\text{mol} \cdot \text{s}^{-1}$),

A : Area in the solid liquid interface (m^2).

With this expression a few phenomena can be explained. If the concentration gradient is zero, the diffusion stops (see Equation 9). The concentration gradient can be zero, when either no targeted molecules are inside the solid matrix or the concentration of solute in the extract is as high as the concentration inside the solid matrix. This means that the solute can never have a higher concentration than the sample itself.

Furthermore, an increased area of penetration (A) results in a higher dissolution rate (N) by similar mass flux, meaning more solute can be dissolved per time. This means, that the particle size has often a huge effect on the extraction speed and should therefore be chosen as small as possible.

Moreover, the choice of solvent offers an easy way to decrease the total extraction time through increased dissolution rates (N). Hence, a solvent with a great solubility for the targeted molecule and decreased solubility for by-products should be chosen. But the dissolution rate can also be influenced by other parameters as temperature or pressure. A higher extraction

temperature leads to lower viscosity and therefore to a better penetration of the sample matrix and increased dissolution rate.

Lastly, the implementation of pretreatment steps can be considered, e.g. drying or defatting. This decreases the sample weight and increases the concentration of the analyte.

2.6.2 One step extraction

The easiest way to achieve a solid-liquid extraction can be performed by mixing a fine powder solid matrix with a solvent. In this way, the diffusion takes place until the solvent has the same concentration as the solid matrix. The higher the volume of the solvent, the lower the remaining concentration in the solid matrix and the lower the extract concentration. This method can be accelerated by ultra-sonification or microwave-assisted extraction ⁷².

2.6.3 Multi-step extraction

To increase the mass of the extracted analyte multiple extractions can be performed with the same matrix. This involves a separation step after each extraction and the addition of fresh solvent to achieve a new equilibrium between the matrix and extract. In theory, this step must be continued for an infinite number of times to achieve a total extraction of every component. In practice, three to five steps are often sufficient to get the majority of solute out.

2.6.4 Soxhlet extraction

Soxhlet extraction is a multi-step extraction and applies heat to regain the solvent for each new extraction cycle ⁷². To perform a Soxhlet extraction, the solid matrix is loaded into a porous thimble made of cotton or glass and placed into the Soxhlet extractor. The round bottom flask is filled with the solvent, and a few boiling stones and placed into a heating mantle. The Soxhlet extractor is positioned on top of the round bottom flask before a condenser is placed above.

The heating of the round bottom flasks allows the solvent to evaporate and condense at the condenser. The solvent is dripping into the thimble and extracting the analyte. After the solvent/extract level reaches the highest point of the siphon, the extract is drained back into a round bottom flask. The extract will start boiling again and only fresh solvent is evaporated to the condenser. This cycle will be repeated for several hours allowing a fresh equilibrium for every cycle. This process can only be quantitative if the solute has a higher boiling point than the solvent and can be sufficiently extracted by the chosen solvent ⁷²

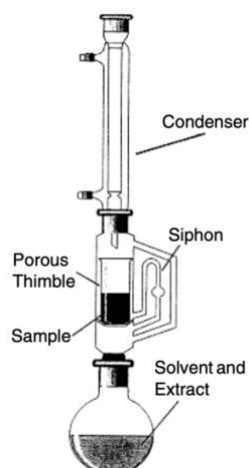


Figure 11: Soxhlet operation as reported by Kou and Somenath ⁷²

Soxhlet extraction is mostly performed as benchmark for other extraction techniques and has limited industrial purposes. Extractions can be performed in scales of a few mL to about 5 L ⁷³.

2.6.5 Randall extraction

Randall extraction is a similar process but applies an additional cooking step prior to the rinsing step.

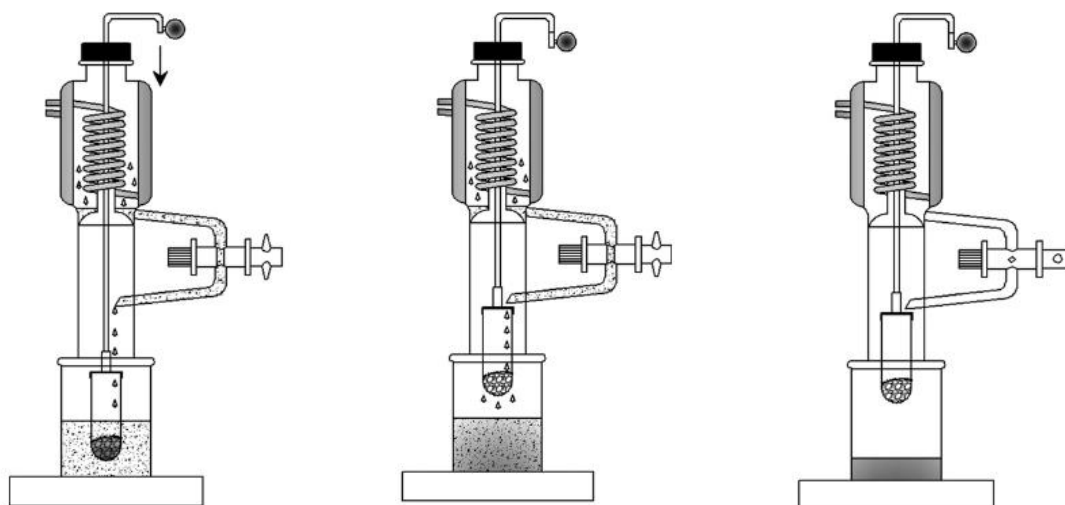


Figure 12: Different states of a Randall equipment during an extraction.

Left: cooking, middle: rinsing, right: solvent recovery as shown from Zyglar et al. ⁷⁴.

To conduct a Randall extraction, the sample is placed into a thimble. The thimble is connected to an adjustable holder to allow different positions during the extraction. Below the thimble, an extraction cup is placed and filled with a solvent. Above the thimble, a condenser is located. To start the extraction (Figure 12, left), the solvent-filled cup is pressed onto the heating plate and is heated above its boiling point. During this phase, the adjustable holder is in the lowest position, allowing the cooking of the solid matrix inside the solvent. The evaporating solvent is condensed at the condenser and guided back into the cup.

In the next step (Figure 12, middle), the adjustable holder lifts the thimble out of the cooking solvent allowing the rinsing procedure to start. In this step, the still-heated solvent is evaporated, condensed, and dripped back into the thimble, allowing sufficient washing.

Afterwards, a solvent recovery step can be performed (Figure 12, right). This is done by closing the valve, which guides the solvent from the condenser back into the thimble or cup, while the cup is still pressed on the hot plate. In this step, the solvent is still evaporating from the cup, but is collected into a solvent recovery storage and can be used for other extractions ^{72, 74, 75}.

2.6.6 Liquid-liquid extraction

Liquid-liquid extraction is a commonly applied method to separate the analyte from other parts of the matrix via two immiscible liquids. It is used whenever the analyte has a higher affinity towards a phase, which is not preferred by other components of the sample. Typically, liquid-liquid extractions consist of an organic and aqueous phase. The affinity of each component can be mathematically described by the distribution coefficient (K_D) ⁷⁶.

$$K_D = \frac{c_1}{c_2} \quad (10)$$

K_D : Distribution coefficient,

c_1 : concentration of the analyte in phase 1 (mostly organic phase),

c_2 : concentration of the analyte in phase 2 (typically aqueous phase).

2.6.7 Supercritical fluid extraction

A supercritical fluid extraction (SFE) describes the process, where a fluid is pressurized above its critical pressure and heated above its critical temperature to extract components from a complex matrix. It is often used for highly valuable extracts from solid matrices, with low-volume products. A typical application is the extraction of secondary plant metabolites from a solid plant matrix ⁷⁷.

The supercritical state is reached when the pressure and temperature are above their critical value, hence exceeding the critical point (see phase diagram in Figure 13). The supercritical state has therefore properties in between liquid and gaseous state.

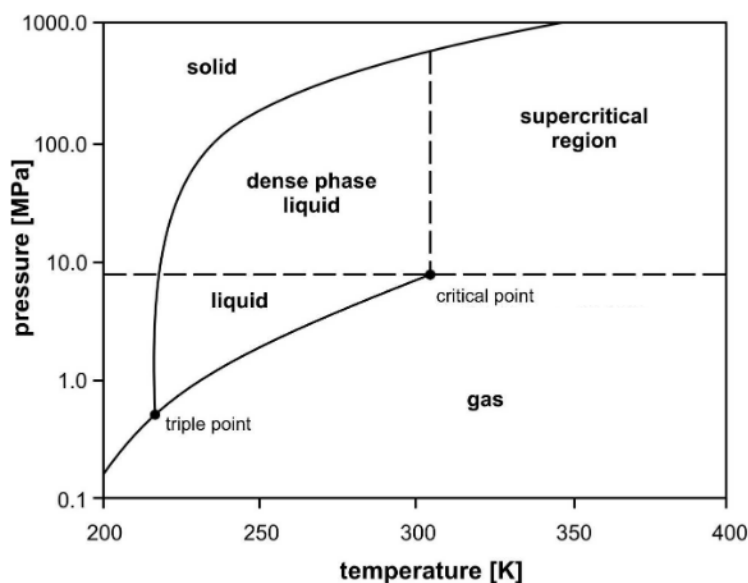


Figure 13: Phase diagram of carbon dioxide adapted from Witkowski et al. ⁷⁸.

There are many factors influencing the solvation power of a fluid.

One important factor is the density. In general, the higher the density, the greater the solvation power. Liquid fluids have a higher density than gaseous fluids, hence allowing a higher solvation power. However, the mass transport is limited by the diffusivity and viscosity of the fluid. The higher the diffusivity and the lower the viscosity, the better a matrix can be penetrated with the fluid ⁷⁹. Solvents in liquid state have lower diffusivity and higher viscosity than in gaseous state, reducing the penetration rate.

The supercritical state allows the combination of both contrary working abilities. The densities can be adjusted nearly as high as liquid state properties, but with a much higher diffusivity and lower viscosity than the liquid state ^{79,80}, enabling better penetration of the sample.

Many different fluids can be used as solvents for the SFE, but CO₂ is the most common. Supercritical CO₂ has a critical pressure of 73.8 bar ⁷⁹, a critical temperature of 31 °C ⁷⁹, is non-toxic, easy to separate, non-flammable, easy to acquire, and has often no degradation effect with respect to its low critical temperature ⁷⁷. An example for industrial usage is the extraction of caffeine from coffee beans ⁷⁷. The mechanism of the SFE is similar to the solid-liquid extraction (see Section 2.6.1).

To carry out an SFE special apparatus are needed. Figure 14 shows the basic principle of such apparatus.

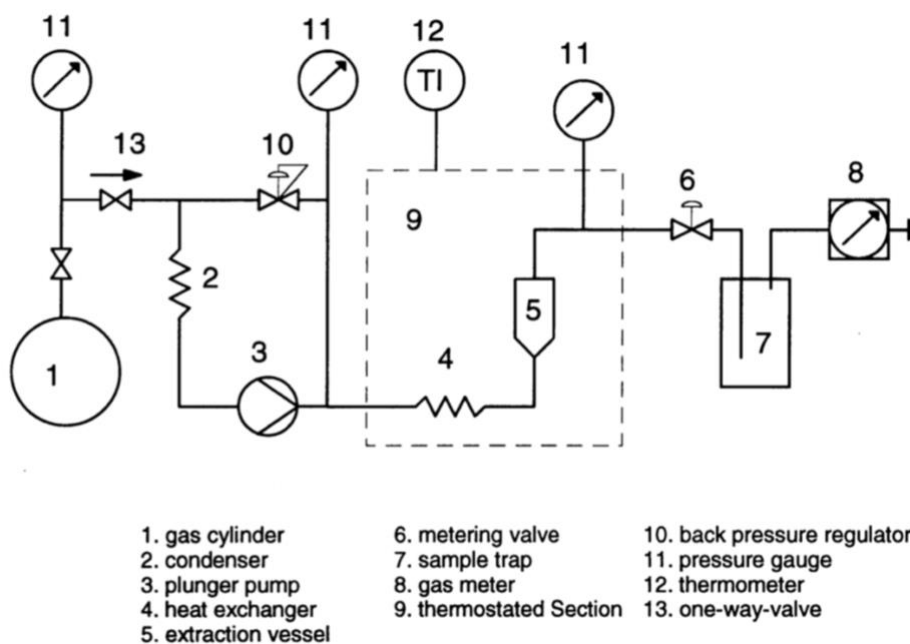


Figure 14: Scheme of a SFE unit without recycling as reported by Brunner⁸¹

The gas/liquid from the cylinder (1) is condensed (2) and supplies the pump (3) with liquified fluid. The pump increases the pressure of the liquified fluid above its critical pressure and guides it to the heat exchanger (4) where the temperature is increased above the critical temperature, allowing a supercritical state. The stream is then guided to the extraction vessel (5) filled with the solid matrix. The fluid is adsorbed by the solid matrix, dissolving the molecules of interest, and diffuses back to the bulk phase of the solvent. This bulk phase is led through a metering valve, therefore lowering the pressure and reaching a subcritical state. During this phase, the solute becomes less soluble in the subcritical fluid stream and a separation of solute and fluid takes place inside the sample trap/collection vessel (7). The pressure on the high-pressure side can be adjusted by the pump (3) or the backpressure regulator (10), while the pressure on the subcritical side can be adjusted by the metering valve (6) and the outlet (8). Temperature and pressure can be adjusted, to yield in optimized parameters for an extraction.

Since most fluids are potentially dangerous or have an impact on the environment a recycling of the fluid stream can be considered. Figure 15 shows a color-coded SFE flow diagram with supercritical carbon dioxide as it is used in this thesis.

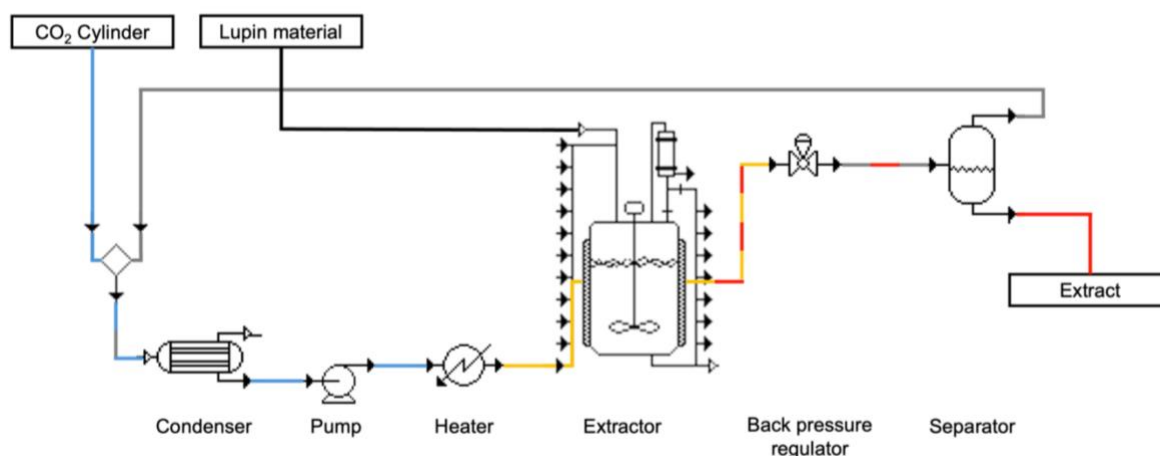


Figure 15: Overview about the phases of CO₂ during extraction in SuperPro Designer.

Colors are used as following: liquified CO₂ (blue), supercritical CO₂ (yellow), gaseous CO₂ (grey), raw material (black), solute (red).

The process is similar to the above-shown flow diagram (Figure 14) but has an additional recycling loop. After the separation (Separator, 7 in Figure 14), the gaseous CO₂ is guided back to the condenser, where the CO₂ will be liquefied and reused in a continuous process. In this way, the CO₂ can be reused multiple times.

2.6.8 Chromatography

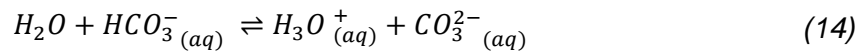
Chromatography is a widely applied separation technique. It is used for the isolation of single components from a complex mixture. The technique was initially invented by Mikhail Tsvet to separate pigments from plants and involves a non-moving material, the stationary phase, and a moving material, the mobile phase⁸². The latter one is used to create a continuous flow through the stationary phase. Both phases are immiscible and can have various states. For example, do most high-performance liquid chromatography (HPLC) separations apply a solid stationary phase (column) and a liquid mobile phase (eluent). However, HPLC is not limited to solid stationary phases. Nowadays, chromatography is used in GC, HPLC, flash chromatography, thin layer chromatography (TLC), and many other applications.

The separation occurs through the different affinity of the analyte towards the stationary and mobile phases. A component with high affinity towards the mobile phase will barely interact with the stationary phase and therefore be quickly released from the column. Contrary, a component with high affinity towards the stationary phase and low affinity towards the mobile phase, will interact with the column and not be released quickly⁸³. This principle is also often used for solid-phase extraction (SPE), where the analyte is strongly retained by the column material during washing steps and later eluted via a solvent with a high affinity to the analyte. The here-used Extrelut column is a wide pore and highly pure diatomaceous-earth-based solid

phase. It is suitable for the extraction of lipophilic compounds from an aqueous solution and works as a support for liquid-liquid extractions, where emulsion can be formed, or poor phase separation is encountered ⁸⁴. In this thesis, the supported liquid-liquid extraction is here-referred to as SPE.

2.7 Carbon dioxide as volatile acid

Carbon dioxide can be dissolved in water and influence its pH value. This phenomenon can be explained by the formation of carbonic acid and its dissolution in water. The mechanism of this reaction is described by following equilibriums ⁸⁵.



In the first step, the CO₂ is dissolved in water (Equation 11). The dissolved CO₂ will react with water to carbonic acid (Equation 12). Carbonic acid is unstable and will react to bicarbonate and dissociate a proton (Equation 13) or will react to water and CO₂ again (Equation 14). The proton will acidify the solution and the pH will drop. Another proton can be dissociated by the reaction of bicarbonate to carbonate. These equilibriums are connected and can be influenced by concentration, pressure, temperature, and volume ⁸⁵.

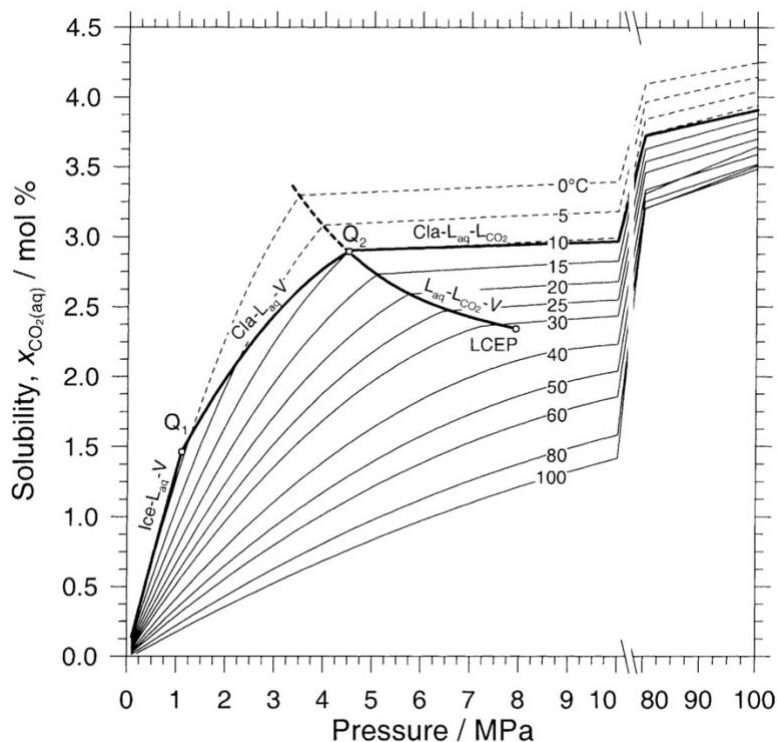


Figure 16: Solubility of carbon dioxide in water.

Influence of pressure and temperature on the CO₂ solubility in water as shown by Diamond and Akinfiyev ⁸⁶.

A detailed curve of the solubility data from carbon dioxide in water is shown in Figure 16. It shows that a lower temperature will lead to a higher concentration of dissolved carbon dioxide and therefore to a lower pH value of the solution. However, the solubility is also influenced by the pressure, the higher the pressure, the more CO₂ is dissolved in water, which also reduces the pH value of the solution. Hence, to reach a low pH a low temperature and high pressure should be applied.

3 Materials and methods

3.1 Materials

3.1.1 Lupin beans

Lupinus mutabilis branco beans (Frijol Chocho) were grown in Peru and harvested in August 2018. After transportation, they were stored dark and dry at room temperature. Already ground (>180 µm) and toasted *Lupinus albus* flour (Fralu-T) was obtained from FRANK food products and used as reference measurements. Potential low alkaloid seed samples were provided by the University of Lisbon from the Portuguese seed bank in a five-to-eight-gram sample size. All samples did contain the shell and kernel fraction.

Sample preparation for alkaloid analysis: All beans were unified to a <1 mm flour by firstly using a ceramic coffee grinder (Hario, Amstelveen, the Netherlands), followed by using a Knife mill (MF10 basic, IKA, Staufen im Breisgau, Germany) in a two-stage grinding process with a 2- and 1-mm sieve. The unified sample was stored in a closed container, well mixed, and kept in the dark at room temperature until further use.

Sample preparation for defatting and bulk protein extraction: The whole beans were milled with a grain mill (Bartscher, Salzkotten, Germany) attached to a KitchenAid machine (Artisan, Benton Harbor, USA). A first grinding was carried out with an adjusted distance of 4 mm, before multiple runs with 2 mm distance were conducted. The so gained flour was sieved (Endecotts, London, England) to reach the desired mesh size of 0.5 mm. The grinding and sieving were repeated until ca. 80 % of the lupin mass input was processed into 0.5 mm lupin flour.

3.1.2 Cherry stones

The cherry pomace used for the experiments was provided by the cherry wine producer Frederiksdal located in the Danish region of Sjælland. The processing of fresh material, including the collection separation (stone/kernel fraction) and drying was done by the Southern Denmark University. The samples were sent with dry ice and were placed immediately into the freezer at -22 °C until further use. More details information regarding the experimental work can be found in Section 7.6.

3.2 Experimental design

3.2.1 Analytical alkaloid extraction

Soxhlet extraction: 1 g of ground alkaloid bean flour was accurately weighted (± 0.1 mg) into a pre-extracted cotton 22 x 80 mm thimble (VWR, Radnor USA). The thimble was covered with cotton and placed into a 70 mL Soxhlet extractor. Pre-extracted boiling stones (3-5 pieces) and 100 mL technical grade methanol (Acros Organics, Geel, Belgium) were transferred into a 100 mL round bottom flask. Next a 2500 $\mu\text{g}/\text{mL}$ caffeine solution (caffeine, 99 %, Mettler Toledo, Columbus, USA) in LC-MS grade methanol (Biosolve, Valkenswaard, the Netherlands) was prepared of which was 1 mL (2.5 mg caffeine) added via a repetitive pipette (VWR, Radnor USA) to the round bottom flask as internal standard (IS). The pipette was continuously monitored and showed no weight/volume inaccuracy. The round bottom flask was connected to the Soxhlet extractor. A heating basket was used to boil the methanol and adjusted to reach a cycling time of 12 min. The extraction was stopped after 4-5 hours (h, 20-25 cycles). After a cooling phase, the extract was filtered through cotton into another round bottom flask. The round bottom flask was then evaporated at 40 °C via rotary evaporator to dryness before 10 mL methanol was added. To reach full solvation, an ultrasonicator (LLG-Unisonic 1, Meckenheim, Germany) was used for 3 min, while the round bottom flask was continuously shaken. The complete extract was transferred into a 15 mL centrifuge tube and centrifuged for 10 min at 4000 RPM (Universal 320, Hettich, Tuttlingen, Germany). Around 1 mL of the supernatant was transferred into a GC-Vial and was ready for analysis.

Soxhlet alkaloid extraction over time: The experimental setup and execution were similar to the shown method above for the Soxhlet extraction, with the difference that a three-neck round bottom flask was used. The flask was filled with 10 mL of IS solution (caffeine 2500 $\mu\text{g}/\text{mL}$, 25 mg caffeine), 90 mL technical grade methanol (250 $\mu\text{g}/\text{mL}$), and 3-5 boiling stones. Two septa were placed above the outer openings before connecting the flask to the Soxhlet extractor. The following samples were collected: At the beginning (only IS), after the first cycle (12 min), second cycles (24 min), 5 cycles (60 min), 10 cycles (120 min), 15 cycles (180 min), 20 cycles (240 min), and 25 cycles (300 min). Each sample contained 1 mL of the extract and was transferred by a syringe. The sample was taken immediately after the extract was drained through the siphon, to reach the internal standard concentration of ca. 250 $\mu\text{g}/\text{mL}$. The exact weight of the extract in the sample was noted, and the cycles were counted. After the first sample, subsequent concentration determinations were corrected for the removed caffeine and alkaloid concentrations. The alkaloid concentration was calculated as described in Section 3.4.5.

Randall extraction: 1 g of ground lupin beans were accurately weighted (± 0.1 mg) into a 26 x 60 mm thimble (Whatmann, Maidstone, England) and closed with pre-extracted cotton. A stainless-steel ring was placed on top and connected via magnetic force to the Soxtec 2050 extractor (Foss, Hillerod, Denmark). Soxtec Aluminum cups were filled with 3-5 boiling stones and 1 mL of internal standard solution (see Soxhlet experiment) was added. The so prepared six cups were put below the thimbles and 100 mL of technical-grade methanol was filled in every extraction chamber via syringe. The extraction was carried out at a heating plate temperature of 240 °C via a cooking step for 40 min, a solvent rinsing step for 80 min, and a solvent collection step for around 3-5 min. The gained extracts were filtered through pre-extracted cotton into a round bottom flask. The cups were rinsed with 3 x 5 mL methanol which was also filtered and collected in the round bottom flask. From this point, the extract in the round bottom flask was treated as shown for the Soxhlet extraction. For the determination of alkaloid content in unknown samples from the Lisbon seed bank, the position inside the extraction unit was tested and found to not influence the extraction yield. However, every extraction from the same sample (analyzed in triplicates) was still carried out in a different position in the Soxtec unit.

Liquid-liquid extraction: The method was carried out as described by Muzquiz et al.³³ and Cortes-Avendano et al.²⁴. Around 0.5 g ground lupin beans were accurately measured and placed in a plastic test tube before 50 μ L of IS solution (125 μ g caffeine) and 5 mL of 5 % TCA solution (w/v, 99 % extra pure, Acros Organics) were added. The mixture was homogenized using a Turrax (IKA T25 digital turrax, Staufen im Breisgau, Germany) for 1 min at 15600 RPM. The test tube was centrifuged for 10 min at 5000 RPM and the supernatant was collected. Afterwards the extraction process of the remaining flour was repeated with 5 % TCA for two more times without the addition of IS. The separated supernatants were combined, and 1 mL of 10 M NaOH (technical grade, VWR, Radnor USA) solution was added before the solution was transferred into a liquid-liquid separatory funnel. The aqueous solution was extracted via 3 x 25 mL dichloromethane (DCM, 99.8 %, Thermo fisher, Massachusetts, USA). The formed emulsion was encountered by placing the separation funnel into freezing conditions at -22 °C for ca. 15 min (no freezing occurred). The organic extracts were combined in a round bottom flask and evaporated to dryness via rotary evaporation at 35 °C. The remains were transferred via MeOH into a GC-vial, left open overnight to dry and re-dissolved in 0.5 mL LC-MS grade MeOH by vortexing and vigorously shaking.

Solid phase extraction/supported liquid/liquid extraction: Lee et al.³⁰ has described a method in which the alkaloid content of lupin beans was determined by the extraction via acid-base reaction. In this thesis, this method was adapted as follows.

0.5 g of ground lupin sample were accurately weighted (± 0.1 mg) and transferred into a 15 mL centrifuge cup and 50 μ L mL of IS solution (125 μ g caffeine) was added. 5 mL of 5 % TCA were added to the test tube, before it got vigorously shaken and placed in an ultra-sound bath for 15 min. After every 3 min the test tube was shaken to ensure a good extraction. The test tube was then centrifuged for 5 min at 5000 RPM and the supernatant was collected in a 50 mL centrifuge tube. The extraction was repeated two more times without and merged. The pH of the extract (1-1.5) was modified with 1.0 mL 24.5 % Ammonia solution to reach a pH of 9.5-10. Afterwards, the solution was adjusted to a volume of 18-20 mL by demineralized water, vigorously shaken, and applied on the Extrelut NT20 column (Merck, Darmstadt, Germany). The tube was rinsed by 0.5 mL of demineralized water and applied to the column. After 15 min soaking time (as suggested by column manufacturer ⁸⁴) the alkaloids were eluted with DCM and collected in a round bottom flask. After one DCM elution (20 mL) a waiting period of 10 min was conducted before the following DCM elution was carried out. A standard experiment is carried out via 3 \times 20 mL DCM and its fractions were collected in the same round bottom flask. However, for some experiments, it was necessary to determine every elution of DCM fractions. Therefore, the internal standard was not added to the flour but to the round bottom flask directly, and the single fractions (20 mL) were collected individually. For both processes, the round bottom flasks were evaporated via rotary evaporation with a water bath at 35 °C to dryness. The remaining alkaloids were transferred via 3 \times 0.5 mL DCM into a GC-vial and left open overnight for weight determination. For the final analysis, the dried GC-vial was filled with 0.5 mL LC-MS grade methanol, vortexed, and shaken vigorously. Furthermore, this method was also carried out with a modification in extraction and alkalinization parameters as shown by Wink et al. ¹⁵. Therefore, the TCA was replaced with 0.5 M HCl, and instead of the ammonia solution 0.5 mL of 10 M NaOH solution was used, which increased the pH from 9.5-10 to 12.

3.2.2 Isolation of alkaloids from *Lupinus mutabilis branco*

Several different steps were required to extract and purify the alkaloids. Following figure gives the reader an overview about the combination of methods described below:

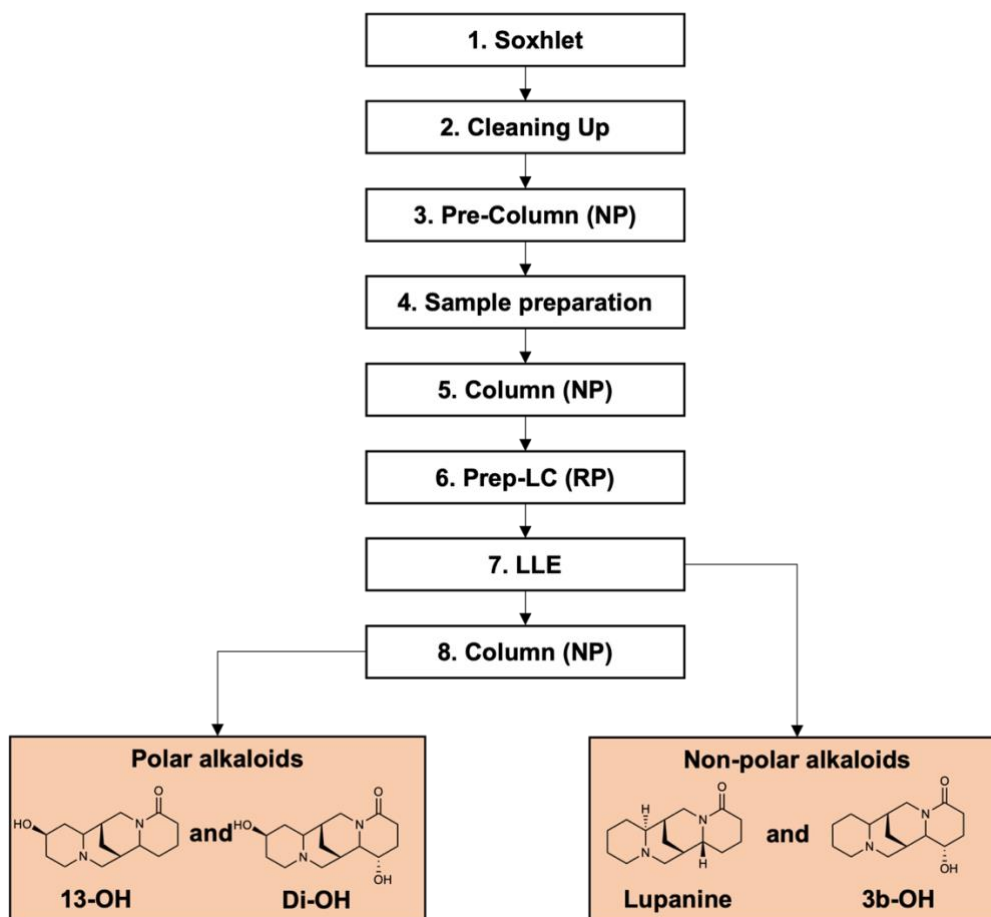


Figure 17: Overview about alkaloid isolation process.

Step 1 (Soxhlet extraction): Circa 90 g to 0.5 mm ground lupin beans were extracted for 24h via MeOH in a 1-liter Soxhlet extractor.

Step 2 (Cleaning up): The extract was cotton filtered, separated via liquid-liquid separation (oil/methanol), and evaporated via rotary evaporation, where 26.40 g of an oily liquid was obtained. After re-dissolving the extract in methanol, a separation via centrifuge (10 min x 5000 RPM) was performed, where the remaining oil layer was separated from the supernatant. The collected supernatant was evaporated and a part which was equal to 68.93 g of initial lupin beans taken for a Pre-column separation.

Step 3 (Pre-column normal phase, NP): The pre-column (\varnothing 25 mm) consisted of 40 g silica gel (60 Å, Supelco, St. Louis, USA) and was conditioned with 5 % MeOH/DCM + 1 % triethylamine (TEA). The sample was dissolved in 20 % MeOH/DCM + 1 % TEA and showed a gel-like precipitation, which would ultimately result in column blockage and reduced separation capability. Therefore ca. 10 % water was added which removed the precipitation and allowed the easy preparation of a thin layer on top of the silica column. The elution was performed via 100 mL 5 % MeOH/DCM + 1 % TEA, 100 mL, 100 mL 10 % MeOH/DCM + 1 % TEA, 100 mL, 100 mL 20 % MeOH/DCM + 1 % TEA and finally 100 mL MeOH + 1 % TEA.

The alkaloids were collected in 20 mL fractions and were all present in fractions 6-15, which correspond to 10 and 20 % MeOH.

Step 4 (Sample preparation): The alkaloid fraction remained difficult to dissolve due to precipitation with non-polar solvents. This problem was avoided by evaporation of the pre-cleaned alkaloid fractions (Fraction 6-15, step 3) and dissolving it in ca. 20 mL 20 % MeOH/DCM + ca. 2 mL demineralized water before adding ca. 7 g silica to the mixture. The silica soaked most of the solution and was then evaporated via rotary evaporation (40 °C) until complete dryness, which resulted in a total weight of 10.5 g.

Step 5 (Column, NP): 3.5 g of the prepared silica (equal to 22.98 g lupin beans) were used for a second 70 g silica column (\varnothing 30 mm) separation. Instead of TEA, Ammonia (NH₃) was used as described for the purification of Di-OH by Murakoshi et al.⁸⁷. The column was conditioned with 5 % MeOH/DCM + 1 % NH₃ (24.5 %), before the silica sample was applied and fraction 1-34 eluted by 1 L of 5 % MeOH/DCM + 1 % NH₃ (24.5 %) and fraction 35-47 eluted by 250 mL of 20 % MeOH/DCM + 1 % NH₃ (24.5 %). The fractions were collected in 20 mL reaction tubes. From all fractions, 1 mL was taken and transferred into a pre-weighted GC-vials, evaporated, weighted, and then filled with 1 mL LC-MS grade MeOH before GC-FID measurements were carried out.

Table 7: Separated fractions and its dominating alkaloid.

Name	Fractions	Name	Fractions
Lupanine	27-36	3b-OH	37-41
13-OH, Di-OH	42,43,44,46	Testing	45

Step 6 (Prep-LC reversed phase, RP): The previously separated fractions were combined according to its dominating alkaloid to form four fractions (see Table 7) and evaporated at 40 °C via rotary evaporation. Afterwards, each residue was re-dissolved in 1 mL MeOH, 1 mL 1 M acetic acid, and 8 mL buffer solution (10 mM acetic acid) and ultra-sonicated. The pH was checked and ensured to be acidic in the range of pH 3-4.

The Preparative LC (Shimadzu LC-20AT) was equipped with a C18 Kinetex 5 μ m 100 Å, 150 x 21.2 mm preparative column and tested with fraction 45 (from step 5) which contained Di-OH and 13-OH. The pre-run has shown that for economic reasons the separation can be performed via a fixed eluent ratio of 9.5 ml/min 10 mM acetic acid and 0.5 ml/min MeOH within the first 20 min.

The prepared 10 mL fractions were injected by a 1000 μ L injection loop and the column output was continuously monitored via a UV detector (200 nm). After a certain threshold of absorption was monitored, the solution was automatically transferred into 14 mL vials (working volume 12 mL) placed in the apparatus. If an unexpected higher slope was detected, the system was adjusted to switch vials. The retention time showed dependency on column loading, which

was then different for every combined 10 mL fraction. The rough retention times are shown in the following table.

Table 8: Retention time of alkaloids on the preparative C18 column.

	Sparteine	Lupanine	3b-OH	13-OH	Di-OH
Retention time (Rt)	15.0 min	9.0 min	6.0 min	4.9 min	3.7 min

Several injections of the same solution were carried out (ca. 10) before the newly isolated alkaloid fractions were combined by analyzing the fraction report and the column was cleaned by 95 % MeOH/water for 20 min at 10 ml/min. It should be noted that the fraction report analyzing had to be carried out manually, since although all parameters stayed similar the number of fractions changed for every injection.

Step 7 (LLE): The now purified and combined alkaloid fractions were combined and basified by adding 100 μ L of 10 M NaOH to every 50 mL solution. It was ensured, that every fraction had a pH of 12 or higher. A liquid-liquid separation was conducted, and the now alkaline solution was extracted via 3 \times 10 mL DCM. The DCM extracts were combined and washed via 3 \times 15 mL Water. The washed DCM layer was evaporated and transferred into a GC-vial before a weight determination and GC analysis was carried out.

Step 8 (Column, NP): For Di-OH and 13-OH the remaining aqueous fractions (from LLE) were evaporated and contained still some salts and other impurities, which is the reason why an additional purification step was conducted. Therefore ca. 6 g silica was conditioned via DCM and 1% TEA to prepare a normal phase column (\varnothing 10 mm). The sample was eluted via 40 mL 5 %MeOH/ DCM + 1 %TEA into 5 mL vials (fraction 1-8) and later 40 mL 10 %MeOH/ DCM + 1 %TEA (Fraction 9-18). This experiment was carried out for both alkaloids (Di-OH and 13-OH) individually. The alkaloid 13-OH could be found in fractions 8-12, while Di-OH was found in 12-14. Although TLC could have been carried out, it was chosen to analyze all fractions via GC-FID. The fractions were combined and evaporated before a final GC-analyses in 1 mL methanol and weight determination took place.

3.2.3 Lipid extraction

Analytical Soxhlet extraction: The details regarding the lipid extraction can be found in Kniepkamp et al. ⁵⁵ (see Section 7.6). Shortly, 2 g of biomass were accurately weighted and extracted with hexane 100 mL (technical grade, Argos Organics, Geel, Belgium) in a 70 mL Soxhlet extractor. The extract was filtered evaporated, and the lipids transferred into a GC-vial, where weight determination of the lipid fraction took place. This extraction was carried out for lupin flour and cherry stones.

Analytical Randall extraction: The details regarding the extraction of lipids via Randall can be found in Kniepkamp et al. ⁵⁵ (see Section 7.6). Shortly, 2 g ground biomass was extracted via hexane with a 40 min cooking step and 80 min rinsing step at 170 °C. After solvent removal, the lipids were transferred into a GC-vial, which was used for weight determination.

Lipid extraction as defatting step: Around 150 g of ground (0.5 mm) lupin flour was weighted into a thimble, closed by pre-extracted cotton, and placed into a 1500 mL Soxhlet extractor. A 2 L round bottom flask was filled with boiling stones (around 10) and weighed, prior to the addition of 2 L of hexane. The temperature was adjusted to reach 3-4 cycles per hour and carried out for 5 to 6 h (15-24 cycles). After extraction, the defatted flour was left open for 24 h in a fume hood to let the remaining hexane evaporate.

ScCO₂ extraction of lipids (500 mL):



Figure 18: Supercritical extraction unit SFE 500 unit.

The details of the lipid extraction via scCO₂ can be found in Yu et al. ⁵⁴ and Kniepkamp et al. ⁵⁵ (see Section 7.5 and Section 7.6). Shortly, an SFE 500 unit (Separex, Champigneulle, France) was used with carbon dioxide (99.7 %, Linde, Schiedam, the Netherlands) to extract 50 g cherry material, respectively 100 g lupin flour over a period of up to 6 h. The extractor had a volume capacity of 500 mL and the introduced CO₂ was recycled during the run. Although different pressure, temperature, and flowrate parameters were used, most experiments were carried out with 350 bar, 40 °C, and 25 g/min CO₂. The lipid yield was determined by weight measurements after separation of the aqueous layer via centrifuging. The apparatus is presented in Figure 18.

Large scale scCO₂ extraction of lipids: Large-scale scCO₂ extractions were only carried out for lupin flour extraction and the details are described in Yu et al. ⁵⁴ (see Section 7.5). Shortly, 5 kg of lupin flour were extracted via the SFT-NPX-10 (Supercritical fluid technologies Inc.,

Newark, USA) at 500 g/min CO₂ flowrate. The extractor had a volume-capacity of 10 L. The apparatus is presented in Figure 19.



Figure 19: Supercritical extraction unit SFT-NPX-10.

3.2.4 Protein extraction

All here-tested protein extraction processes are aqueous processes and consist of five steps with different parameters. An overview of the five steps is given in Figure 5. The first three steps divide the soluble protein fraction from the insoluble matrix. The dissolved proteins are then in two more steps (step 4-5) precipitated and separated from the remaining soluble matrix. The desired proteins can be found in the *Precipitate II* fraction. All extracts were dried via lyophilization for 12-24 hours at 1 mbar (Alpha 2-4 LSCbasic, Christ, Osterode am Harz, Germany), before weight and nitrogen determination (Kjeldahl) took place.

Ionic strength extraction – salting out: The method was adapted from Sussmann et al ⁵³ and refers to the steps shown in Figure 5.

Step 1: The sample preparation was performed as shown above (see Section 3.1.1). Shortly, the flour was defatted and ground to 0.5 mm mesh sieve size.

Step 2a: 4 g of flour was mixed with 32 g of 0.5 M NaCl solution (reagent A, **step 2b**) at 30 °C and stirred (C-Mag HS-7, IKA, Staufen im Breisgau, Germany) for 60 min.

Step 3: The suspension was separated via centrifugation (10 min, 4000RPM) and split by decanting into two fractions, namely *supernatant I* and *precipitate I*.

Step 4a: The *supernatant I* was transferred into a 200 mL beaker and the weight of the solution was determined. Demineralized water (reagent b, **step 4b**) in the weight ratio of 1:3

(supernatant/water) was added before the beaker was placed into an ice bath (1-2 °C) and stirred for 60 mins.

Step 5: The solution was transferred into centrifuge vials and centrifuged (10 min, 4000RPM) before the *supernatant II* was removed via decanting.

Standard isoelectric point precipitation: This method is based on Ruiz and Hove ⁵⁰ and refers to the steps shown in Figure 5.

Step 1: The flour is prepared as shown in Section 3.2.4.

Step 2a: 4 g flour was accurately weighed (± 0.01 g) and dissolved with demineralized water in a weight ratio of 1:10 (weight flour to demineralized water). The solution was stirred for 10 min at room temperature before a 1 M NaOH solution (reagent A, step **2b**) was added dropwise to adjust the pH of 8.5. The prepared suspension was stirred for 60 min while keeping the pH constant.

step 3: The suspension was separated via centrifugation (10 min, 4000RPM) and split by decanting into two fractions, namely *supernatant I* and *precipitate I*.

step 4a: The *supernatant I* was transferred into a new beaker, stirred and the pH was adjusted dropwise to pH 4.5 via 1 M HCl (reagent B, **step 4b**). The stirring was continued for 60 min and the pH was checked and adjusted regularly.

Step 5: Lastly, the suspension was centrifuged again (10 min, 4000RPM) and separated into *supernatant II* and *precipitate II* by decanting.

IEPP-CO₂: **Step 1-3:** The first steps of the isoelectric point precipitation via CO₂ were similar



Figure 20: Sample after depressurization inside extraction vessel.

to the standard IEP procedure (see above), therefore steps 1-3 were carried out as described in Section 3.2.4 and yield in identical *supernatant I* and *precipitate I* fractions.

Step 4a: For the IEPP-CO₂, the *supernatant I* (ca. 35-40 mL) is placed in a 50 mL centrifuge cup and placed inside the SFE500 extraction vessel. The Vessel is closed, connected to the SFE 500 unit, and equilibrated to the desired temperature (standard 20 °C). After 30 min, CO₂ (reagent B, **step 4b**) is introduced to the desired pressure (standard 60 bar). The experiment time

was measured from the moment a constant pressure was present at the desired pressure to the point where the set time was reached, and the system could be depressurized. Care was taken to avoid foaming and loss of solution during the depressurization.

Step 5: After depressurization, the sample cup was immediately centrifuged (10 min, 4000 RPM) before the *supernatant II* and *precipitate II* were separated via decanting.

IEPP-CO₂: View cell: Two droplets of bromthymolblue (pK_a 7.1) and 7 mL demineralized water were mixed and placed into a modified 15 mL centrifuge cup (cut to 10 mL size). The modified centrifuge tube was placed into the view cell (see Table 43, unknown supplier), which was equipped with a sapphire glass to allow observation. The view cell replaced the extraction vessel from the SFE 500 unit and was pressurized with liquid CO₂ at 60 bar at 20 °C.

CO₂-only: The CO₂-only process applies CO₂ for the solvation and precipitation of proteins. Precipitation by using CO₂ is shown in Section 3.2.4, therefore the research regarding the CO₂-only process focuses mostly on the solvation of proteins and the experimental design.



Figure 21: Theoretical setup for the solvation and precipitation with CO₂.



Figure 22: Setup for two parallel solvation experiments.

Step 1: In the first step, the flour is prepared as shown above.

Step 2a: Most experiments were carried out with 4 g of defatted flour dissolved in 40 g water (same ratio as IEPP). After 60 min of stirring, the slurry was divided into 10 mL aliquots. One aliquot was centrifuged before it was analyzed in weight fraction and nitrogen content (BCA). The result was used as a reference measurement. The 3 other aliquots are used in solvation experiments where time, temperature, pressure, flour/water ratio, and filter setup were varied. The remaining aliquots were transferred individually into stainless-steel tubes (0.5 inch unknown supplier), which were surrounded by an outer one inch tube (see Figure 22). The outer tube could be connected to a cooling circuit (MC 600, Lauda, Lauda-Königshofen, Germany) and was able to apply water at 4 °C. A CO₂ bottle with a dip-tube or nitrogen (5.0, Linde, Schiedam, the Netherlands) was connected to a piston pump (260D, Teledyne, Thousand Oaks, USA) and used for pressure adjustments. Most experiments were carried out at 60 bar and 4 °C.

Step 3: The separation of the potential dissolved proteins and the insoluble matrix is carried out via filtration. After depressurization the filtration unit was disassembled, and the filter cake dried via freeze-drying before BCA analysis for the protein content took place.

Step 4-5: The protein precipitation was not part of this experiment design but can be carried out as shown in Section 3.2.4.

3.3 Analytical methods

3.3.1 Moisture determination

Moisture analyses/dry weight determination were carried out by a MB160 moisture analyzer (VWR, Radnor USA). The device applies a halogen lamp at 120 °C and measures continuously the weight. If no weight loss of <0.1 % is determined for 1 min, the measurement is stopped. The calculation is performed automatically and uses the initial weight as fresh weight and the weight when the measurement was stopped as dry weight. For most determination, 2 g of sample were applied in triplicate.

3.3.2 Ash determination

For the ash determination, 0.5 g of sample was accurately measured (± 0.1 mg) and transferred into a pre-ashed and weighed crucible. The crucible was placed into a furnace (4/900 Snol, Utena, Lithuania) and heated at 20 °C/min to 600 °C. This temperature was held for a period of two hours, before being left to cool overnight. After reaching around 100 °C the crucible was transferred into a desiccator and allowed to reach room temperature before weight determination took place.

3.3.3 Alkaloid analysis

For all here-shown quantification methods, either a gas chromatograph coupled to a flame ionization detector (GC-2014, Shimadzu, Kyoto, Japan) or coupled to a mass spectrometer (5973/6890N Agilent, Santa Clara, USA) was used. Both types of apparatus were equipped with a 30 m x 0.25 mm x 0.25 μ m HP5-MS column (Agilent, Santa Clara, USA). For quantification, a stock solution was prepared to contain 850 μ g/ml sparteine ($\geq 98\%$, Sigma-Aldrich, Missouri, USA) 850 μ g/ml lupanine (96 %, BOC science, Shirley, USA), and 250 μ g/ml 13 α -hydroxylupanine (98 %, BOC science, Shirley, USA) in LC-MS grade MeOH. The stock solution was diluted 16 times in a ratio of 1:3 with MeOH. From every prepared standard 0.9 mL was mixed with 0.1 mL of internal standard (250 μ g caffeine). All preparations were carried out via mass measurements (± 0.1 mg).

Quantification with GC-FID: The GC temperature program was adapted from Kamel et al.²⁹ and other parameters were modified as follows: 0.5 μ L was injected at 290 °C with hydrogen (6.0, Linde Schiedam, the Netherlands) as carrier gas. A split ratio of 1:8 with (purge flow of 1 ml/min) in constant linear velocity mode at 37.0 cm/s was applied. The GC-oven was set to

180 °C for 2 min, before increasing to 300 °C with a rate of 6 °C/min and kept for 10 min. The temperature of the FID detector was continuously set at 300 °C. The concentration was calculated via an area-based calibration curve, where the area of alkaloid divided by the area of internal standard was plotted against the concentration of alkaloid standard divided by the concentration of internal standard (see Figure 23).

3b-OH concentrations were determined by assuming similar calibration curve parameters as shown for 13-OH (same molecular mass). Di-OH concentrations were determined by also using the 13-OH calibration curve and correction of the heavier molecular mass. Additionally, the linearity of caffeine was tested by preparing a stock solution of 1000 µg/ml caffeine in MeOH and diluting it into 500, 250, 150, and 100 µg/ml with MeOH using the similar GC-FID method as shown above.

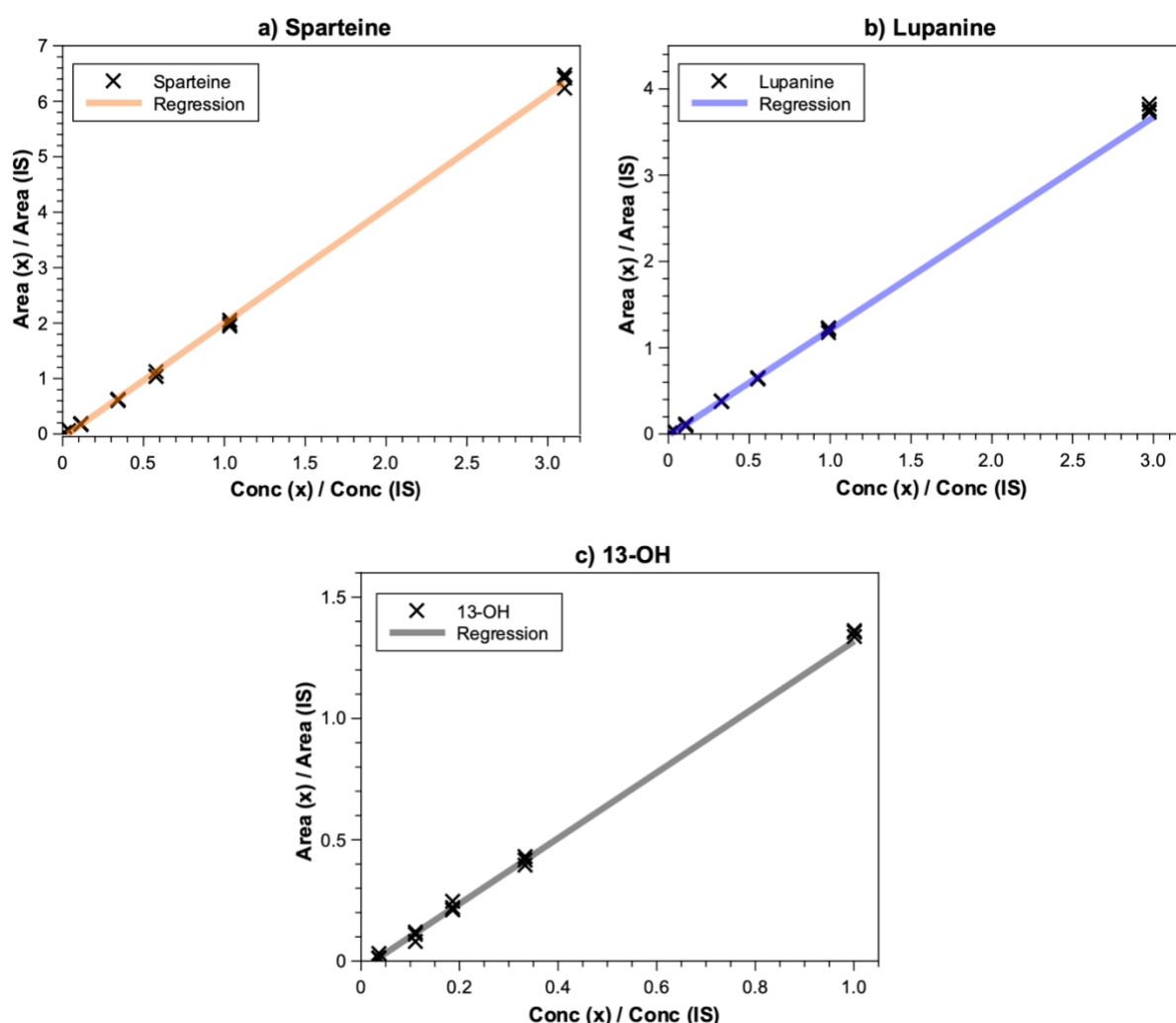


Figure 23: Example of plotted calibration curves.

Calibration curves are plotted for a) sparteine, b) lupanine and c) 13-OH. Standards were analyzed in triplicates and a linear regression analysis was applied (see Section 3.4.5).

For the Lisbon seed bank sample, first an overview analysis was conducted. This was done to know the rough alkaloid content of every sample and sort them from low to high alkaloid content for the final GC measurement. Since the samples total alkaloid content differs by several magnitudes this procedure avoids cross contamination and carry over effects. Furthermore, after every ten GC-analysis a blank run was initialized to crosscheck for contaminations. The standards were analyzed at least three times.

Identification with GC-MS: For the Identifications of alkaloids, 1 μ L alkaloid extract was injected at 290 °C with a split ratio of 1:8 with helium (5.0, Linde Schiedam, the Netherlands) at linear velocity mode 37 cm/sec into the GC-MS. The temperature program was identical to the one described for GC-FID (see above). The mass spectrometer transfer line was heated to 280 °C. The mass spectrometer was set in scan mode from 40 to 350 m/z with a solvent delay time of 3 min. The filaments operated at 230 °C with 70 eV and the quadrupole was continuously held at 150 °C. The identification was conducted by comparison of the spectra to the NIST database ⁸⁸.

Quantification with GC-MS: The quantification of alkaloids via GC-MS was only carried out for low alkaloid-containing samples. Although similar standards as shown for the GC-FID method (see Section 3.3.3) were used, the calibration curve was revised to only contain standards in a reasonable range. Similar GC and MS parameters were used as shown for the identification via GC-MS (see Section 3.3.3), except that the mass spectrometer was not in scan mode but in SIM mode. This SIM mode was divided into different retention time sections and each m/z value was measured for 50 ms. The following table shows the SIM and time values.

Table 9: SIM table for GC-MS quantification.

Component	Retention time	m/z value
Sparteine and caffeine	3.0 to 10.0 min	55, 67, 82, 97, 98, 109, 136, 137, 194, 234
Lupanine	10.1 to 13.9 min	55, 136, 149, 150, 248
13-OH	14.1 to 32.0 min	55, 134, 152, 246, 264

TLC: The separation of alkaloids via TLC remained difficult. Best results were obtained by using silica TLC plates (Silica 60, Merck, Darmstadt, Germany) with 5 % MeOH/DCM (v/v) and the addition of 1 % triethyl amine (v/v) as eluent with 2 μ L of the sample. After the solvent was evaporated, the TLC plate was heated to 150 °C, for at least 2 min. After cooling, the TLC plate was developed by dipping into a premixed Dragendorff reagent (Sigma-Aldrich, Missouri, USA) for 2 seconds and left to dry for 20 min on a glass plate.

Table 10: Retention factor of alkaloids in the TLC experiment.

	Sparteine	Lupanine	3b-OH	13-OH	Di-OH
Retention factor	0.04	0.20	0.19	0.17	0.04

3.3.4 Protein determination

For the protein determination of lupin samples Kjeldahl nitrogen determination was mostly chosen. However, some protein determinations were also carried out via bicinchoninic acid assay. Latter was only selected, when the relative protein content was in focus (only relevant for Section 4.5.7).

Nitrogen determination (Kjeldahl): 1 g of biomass was accurately measured (± 1 mg) into a Kjeldahl flask before one Kjeldahl tablet of 5 g (free of Hg and Se, Carl Roth, Karlsruhe, Germany) and 20 mL Kjeldahl grade sulfuric acid (Fisher science, New Hampshire, USA) were added. The Kjeldahl sample was destructed in a K-435 unit (Büchi, Flawil, Switzerland) at around 180 °C to 220 °C for 1 to 1.5 h. After the heating was stopped, the solution was allowed to cool, before the addition of 50 mL demineralized water took place. The highly acidic solution was then assembled into the distillation unit K-350 (Büchi, Flawil, Switzerland) and 90 mL of 32 % NaOH solution for Kjeldahl determination (Fisher Science, New Hampshire, USA) was added automatically from the distillation unit before a steam distillation was carried out. The distillate (water and NH₃) was captured by a 50 mL 4 % boric acid solution (w/w) before the boric acid solution was titrated via a dosimat 775 (Metrohm, Herisau, Switzerland) to the initial pH of the boric acid (pH 4.5) with 0.5 M HCl solution (VWR, Radnor USA) and methyl red as an indicator. The titer of the HCl solution was continuously monitored via titration of analytical-grade sodium carbonate.

Bicinchoninic acid assay (BCA): In this thesis the Pierce BCA test kit (Thermo fisher, Massachusetts, USA) was used in rare cases and only when the relative protein content was in focus. The methodical details can be found in the corresponding data sheet⁸⁹. Shortly, 2.5 mg protein extract was dissolved in 2 mL standard phosphate buffer saline with 0.9 % sodium dodecyl sulfate. 0.1 mL from the dissolved sample was mixed with 2.0 mL working solution. After an incubation time of 30 min at 37 °C, the absorption at 562 nm was measured (Shimadzu UV1800, Kyoto, Japan) and compared to the calibration curve.

3.3.5 Dietary fiber analysis

The determination of dietary fiber is based on the rapid integrated dietary fiber assay kit from Megazyme and simulates in-vivo human digestion. The details can be found in the corresponding datasheet⁹⁰. In the following a brief description is given:

1.0 g defatted sample was digested (4 h, 37 °C) by protease enzymes (*pancreatic α -Amylase* and *amyloglucosidase*). The suspension was then filtered through a glass filter and the filter cake was dried (oven, 110 °C, 24 h), corrected for protein content (Kjeldahl), and ash content. It contained the insoluble dietary fiber fraction. The gained filtrate was precipitated in a 78 % ethanol solution (v/v) and again filtrated, before drying and correction for protein (Kjeldahl) and ash content took place. This filter cake contained the so called small dietary fiber fraction, which precipitates with EtOH. The filtrate contained the soluble dietary fiber and was analyzed via HPLC Sugar-Pak column (Waters, 300 mm, 6 mm, 10 μ m) connected to a HPLC (Nexera-I, LC2040c, Shimadzu, Kyoto, Japan) at 40 °C equipped with a refractive index (RI) detector (Shimadzu RID20A, Kyoto, Japan). This fraction contained sugar monomers with a lower degree of polymerization (DP) than 10 units.

Table 11: Retention time of the components in the soluble dietary fiber fraction.

Component	Rt	Component	Rt
DP>5	6.1 min	DP=2 (Maltose)	9.0 min
DP=5 (Verbascose)	7.0 min	Glucose	10.9 min
DP=4 (Stachyose)	7.4 min	Fructose	12.5 min
DP=3 (Raffinose)	8.0 min	Glycerol	14.4 min

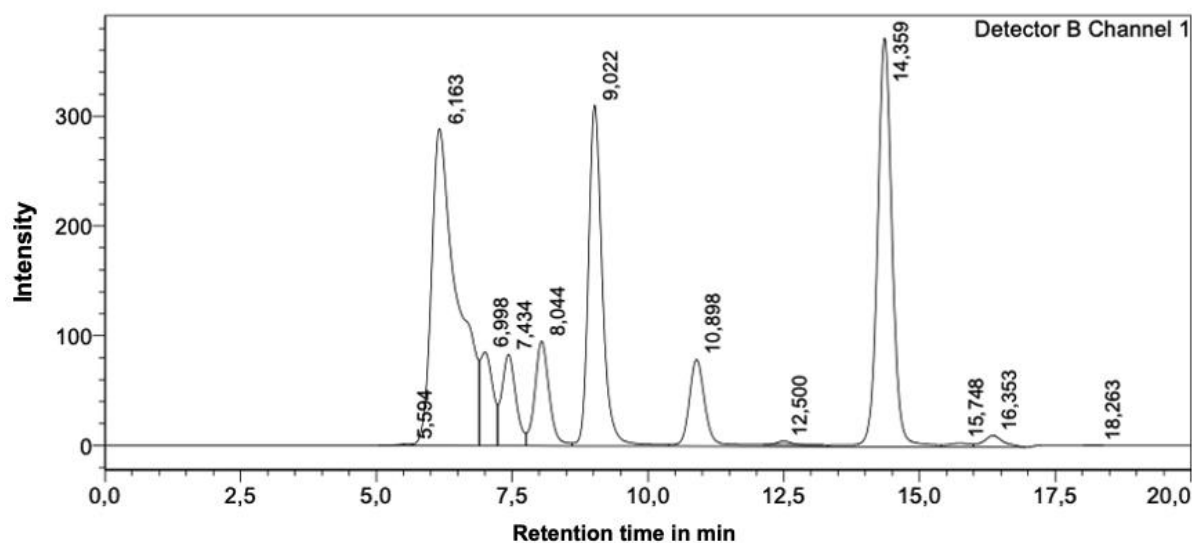


Figure 24: Chromatogram of the soluble dietary fiber fraction.

3.3.6 Lipid analysis

Total lipid content: The details regarding the total lipid content measurements can be found in Kniepkamp et al.⁵⁵. In summary, a weight determination was performed by accurately weighing the extracted lipid fraction (± 0.1 mg). Care was taken that all solvent was evaporated, by allowing the sample to equilibrate with ambient air for at least 24 h.

FAME analysis: The detailed FAME analysis can be found in Kniepkamp et al.⁵⁵ (see Section 7.6). Shortly, ca. 5 mg of a lipid sample was trans esterified via 4 mL of 5 % acetyl chloride solution in methanol (v/v). The solution was mixed and heated at 60 °C for 60 min, before adding 1 mL of 5 M NaCl solution. Next, 2.0 mL analytical grade n-hexane was added to the tube and rotated for 60 min, before the upper n-hexane layer was transferred into a GC-Vial and was ready for analysis. Quantification was performed by GC-FID with methyl palmitate, methyl stearate, methyl oleate, and methyl linoleate as standards and nonadecanoic acid as internal standards.

3.4 Calculations

3.4.1 Variance and standard deviation

The variance was calculated by the n-1 method.

$$S^2 = \frac{\sum_{i=1}^N (x_i - \bar{x})^2}{n - 1} \quad (15)$$

x_i : Result of experiment I,

\bar{x} : Average of an experiment set,

n : Number of experiments carried out in the dataset.

Standard deviations (SD) are shown for experiments which were carried out in triplicates and indicated by a \pm sign after the value and before the unit. The calculation of the standard deviation is based on the square root of the variance.

$$S = \sqrt{S^2} \quad (16)$$

S : standard deviation of a measurement,

S^2 : Variance of the experiment.

3.4.2 Student's t-test

Student's t-tests were applied when a group of experiments was compared with another group of experiments, i.e. for the comparison of total alkaloids via Soxhlet extraction vs. total alkaloids via Randall extraction. If not otherwise mentioned the two-sided independent t-test was used.

$$t = \frac{\bar{x}_1 - \bar{x}_2}{\sqrt{\frac{S_1^2}{n_1} + \frac{S_2^2}{n_2}}} \quad (17)$$

In this thesis, Excel 365 (Microsoft, Redmond, USA) was used for this calculation and led to a calculated p-value. A p-value below 0.05 indicates a probability of 95 % that the null

hypothesis (the data sets are similar) can be rejected, referred to as significance. A probability of 99 % (p-value < 0.01) refers to high significance.

3.4.3 Graphical processing

For the graphical processing Qti-plot in version 1.1.3 was used. Different regressions as limited growth, Gompertz-function, four-parameters logistic⁹¹ and the from Pasquet et al.⁹² suggested kinetic function were tested. Best results were obtained with the four-parameter logistic function and was therefore consequently applied.

The function is defined as following:

$$y(x) = p_4 + \frac{p_1 - p_4}{1 + \left(\frac{x}{p_3}\right)^{p_2}} \quad (18)$$

p_1 : response at 0,

p_2 : slope of the curve.

p_3 : inflection point,

p_4 : response at $\lim_{(x \rightarrow \infty)} y(x)$.

3.4.4 Recovery rate

The here-shown recovery rates are either based on the internal standard method (see Section 3.4.5) or calculated as shown here.

$$R = \frac{m_{exp}(x)}{m_{max}(x)} \quad (19)$$

R : recovery rate,

$m_{exp}(x)$: mass of the desired component x after the experiment,

$m_{max}(x)$: maximum possible mass of desired component x in this experiment.

$$m_{max}(x) = w_{biomass}(x) * m_{exp} \quad (20)$$

$w_{biomass}(x)$: weight distribution of desired component x in 100 g of DW biomass,

m_{exp} : Initial weight of biomass for this experiment.

For some methods the exact amount of $w_{biomass}(x)$ was not known (e.g. alkaloids), therefore the method that yielded in the highest mass was used.

3.4.5 Internal standard

In this thesis, the calculation of analyte concentration via internal standard was preferred over the calculation via external standard.

Concentration of a component in the extract: The plotted area of the internal standard divided by its concentration is proportional to the Area of the desired component x divided by its concentration. Mathematically it can be expressed as shown in Equation 21 (see also Figure 23).

$$\frac{A(IS)}{c(IS)} = Rf \frac{A(x)}{c(x)} \quad (21)$$

$A(IS)$: Area of internal standard,

$c(IS)$: concentration of internal standard,

Rf : Response factor (proportional factor),

$A(x)$: Area of component x,

$c(x)$: concentration component x.

This behavior allows the use of linear calibration line with following properties:

$$y = ax + b \quad (22)$$

$$\frac{A(x)}{A(IS)} = a \frac{c(x)}{c(IS)} + b \quad (23)$$

$$c(x) = \frac{\frac{A(x)}{A(IS)} - b}{a} * c(IS) \quad (24)$$

a : slope of the calibration curve,

b : x-intersection of the calibration curve.

Concentration of a internal standard in the extract: The concentration of the internal standard ($c(IS)$) is based on a one-point calibration curve (for validation see Figure 26), where the area of internal standard is plotted against its concentration. Therefore b for Equation 22 is 0 and following equation can be formed.

$$c(IS) = \frac{A(IS)}{a(IS)} \quad (25)$$

$a(IS)$: Slope of the internal standard one point calibration curve.

Mass concentration of components inside the biomatrix: For the calculation of the mass concentration of the desired component in the biomatrix, the exact knowledge of the volume is needed. In this thesis, the determination of volume was carried out by the internal standard as shown in the following:

$$V_{tot} = \frac{m(IS)}{M(IS) * c(IS)} \quad (26)$$

V_{tot} : Total volume of the extract,

$M(IS)$: Molar mass of internal standard.

Based on the volume, the mass concentration is calculated as follows:

$$w_{biomass}(x) = c(x) * M(x) * V_{tot} \frac{100}{m_{exp} - m_{H_2O}} \quad (27)$$

$M(x)$: Molecular mass of desired component x,

$m_{H_2O}(x)$: mass of water inside the sample.

Recovery rate for the internal standard calculation: The recovery rate of an experiment with an applied IS can be calculated by Equation 28.

$$R_{IS} = \frac{m_{end}(IS)}{m_0(IS)} \quad (28)$$

R_{IS} : Recovery rate of the internal standard,

$m_{end}(IS)$: Mass of internal standard at the end of an extraction as detected,

$m_0(IS)$: Mass of internal standard added at the beginning of the experiment.

3.4.6 Simple accumulated area calculation

For the preparation of some figures, a detailed concentration calculation was not necessary, therefore a simple calculation as shown below was used. This was only applicable, when the relative area of a component was of interest, i.e. the relative distribution of alkaloids over several fractions (see Figure 42).

$$A_{rel}(x) = \frac{A(x)}{A_{total}(x)} \quad (29)$$

$A_{rel}(x)$: Relative area/concentration of component x,

A_{total} : Sum of all areas.

3.4.7 Limit of detection (LOD) and limit of quantification (LOQ) determination

The LOD and LOQ values are important criteria to evaluate an analytical method. Several methods are known for their determination. In this thesis, the *European medical agency* suggested approach is applied⁹³. The following equations are used to determine the LOD and LOQ values.

$$LOD = \frac{3.3 * S}{a} \quad (30)$$

$$LOQ = \frac{10 * S}{a} \quad (31)$$

LOD : Limit of detection,

LOQ : Limit of quantification.

a was determined by the calibration curve of all samples. The standard deviation of response (S) can be either received by analysis of blank samples or analysis of standards around the detection limit. Unless not mentioned otherwise, the three lowest calibration standards were used to calculate the standard deviation. Hence, the LOD and LOQ values refer to the concentration of the extract. To compare methods to each other, LOD/LOQ values based on the raw mass were calculated according to Equation 32.

$$LOD(w(x)) = LOD * V_{tot} * \frac{100}{m_{exp}} \quad (32)$$

For the calculation of different alkaloid extraction methods, following parameters were applied.

Table 12: Applied parameters for the alkaloid LOD/LOQ values calculation.

	m_{exp}	V_{tot}		m_{exp}	V_{tot}
Soxhlet	1 g	10 ml	Randall	1 g	10 ml
LLE (high alk.)	0.1 g	1 ml	LLE (low alk.)	1 g	1 ml
Extrelut (high alk.)	0.1 g	1 ml	Extrelut (low alk.)	1 g	1 ml

3.4.8 Solvent-to-feed ratio

The solvent-to-feed ratio is used to compare the amount of used continuous solvent to the amount of used sample. It can be used to discuss the effectiveness and efficiency of different processes on different scales.

$$SF = \frac{\dot{m}}{m_{FW}(x)} \quad (33)$$

$$SF_{soxhlet} = \frac{70 \frac{ml}{cycle} * 0,66 \frac{g}{ml} * 25 cycle}{1 g} = 1155 \quad (34)$$

SF : Mass solvent-to-feed ratio,

\dot{m} : mass flow of solvent.

3.4.9 Moisture content

The moisture content of a sample was calculated automatically by the moisture analyzer and is defined as follows:

$$w_{H_2O}(x) = \frac{m_{H_2O}(x)}{m_{FW}(x)} \quad (35)$$

$w_{H_2O}(x)$: moisture content of the sample,

$m_{FW}(x)$: mass of fresh weight of the flour.

3.4.10 Ash content

The ash content was calculated by the weight of the remains after 600 °C treatment divided through the initial flour.

$$A(x) = \frac{m_{ash}(x)}{m_{FW}(x)} \quad (36)$$

$A(x)$: Ash content of the sample,

$m_{ash}(x)$: mass of remains after temperature treatment.

3.4.11 Proteins

The proteins inside a sample are calculated by the average nitrogen content.

$$\bar{N}(x) = \frac{\sum_{k=1}^n N_k(x)}{n} \quad (37)$$

$\bar{N}(x)$: Average nitrogen content of the sample x.

In case of defatted lupin flour (FW):

$$\bar{N}(Flour) = \frac{8.830 \% + 8.721 \% + 8.999 \%}{3} = 8.817 \% \quad (38)$$

Based on this, the protein content was calculated by multiplying with the Kjeldahl factor (as seen below).

$$P(x) = \bar{N}(x) * K_F \quad (39)$$

$P(x)$: Protein content of sample x,

K_F : Kjeldahl factor, here 6.25.

In example for defatted lupin flour FW:

$$P(flour) = 8.817 \% * 6.25 = 55.11 \% \quad (40)$$

In case of full fat flour (lipid content of 19 % see Section 7.5).

$$P(flour) = 55.11 \% * (1 - 0.19) = 44.64 \% \quad (41)$$

Weight distribution of a fraction: During the protein extraction, separation took place, in which one suspension is divided into two fractions (supernatant and precipitate). If not otherwise mentioned only one fraction was analyzed and the remaining fraction was calculated according to Equation 42.

$$m_{prec} = m_{exp} - m_{sup} \quad (42)$$

m_{prec} : Mass of precipitate,

m_{sup} : Mass of supernatant.

Nitrogen content of a fraction: The nitrogen content of a fraction was determined via Kjeldahl and calculated for the other fraction according to the following formula.

$$w_{prec}(N) = \frac{w_{exp}(N) * m_{exp} - w_{sup}(N) * m_{sup}}{m_{prec}} \quad (43)$$

$w_{prec}(N)$: Weight distribution of nitrogen inside the precipitate,

$w_{exp}(N)$: Weight distribution of nitrogen inside the biomass used for this experiment,

$w_{sup}(N)$: Weight distribution of nitrogen inside the supernatant.

As an example, the weight distribution of the precipitate at pH 4:

$$w_{prec}(N) = \frac{100 \text{ g} * 0.088 - 30.3 \text{ g} * 0.038}{69.7 \text{ g}} = 0,111 = 11.1 \% \quad (44)$$

Nitrogen to protein: Equation 45 shows the calculation of the weight distribution of proteins.

$$w_{exp}(P) = w_{exp}(N) * K_F \quad (45)$$

$w_{exp}(P)$: weight distribution of protein inside the biomass for this experiment,

$w_{exp}(N)$: weight distribution of nitrogen inside the biomass for this experiment.

Example nitrogen solubility at pH 4:

$$w_{prec}(N) = 0.111 * 6.25 = 0.694 = 69.4 \% \quad (46)$$

3.4.12 Carbohydrates

The calculation of total carbohydrate content was carried out as follows.

$$m_{\frac{carb}{DW}}(x) = 100 \frac{g}{100 \text{ g DW}} - m_{\frac{pro}{DW}}(x) - m_{\frac{lip}{DW}}(x) - m_{\frac{ash}{DW}}(x) \quad (47)$$

$m_{\frac{carb}{DW}}(x)$: Carbohydrates inside 100 g sample DW,

$m_{\frac{pro}{DW}}(x)$: Proteins inside 100 g sample DW,

$m_{\frac{lip}{DW}}(x)$: Lipids inside 100 g sample DW,

$m_{\frac{ash}{DW}}(x)$: Ash inside 100 g sample DW.

The example of *Lupinus mutabilis* is shown below.

$$m_{carbs} = (100 - 49.1 - 21.8 - 3.9) * \frac{g}{100 \text{ g DW}} \quad (48)$$

$$m_{carbs} = 24.7 \frac{g}{100 \text{ g DW}} \quad (49)$$

The standard deviation calculation is shown in Equation 50.

$$S_{carb} = \sqrt{S_{prot}^2 + S_{lip}^2 + S_{ash}^2} \quad (50)$$

4 Results and discussion

4.1 Overview

This thesis focuses on the extraction and analysis of valuable components from *Lupinus mutabilis branco* beans, a rather little-known crop. To highlight its use as a locally grown and high protein-yielding crop, several different extractions and determination methods for alkaloids, proteins, and lipids are introduced, tested, and analyzed. All methods were extensively examined, and their extraction parameters are discussed. Whenever suitable, the use of CO₂ was considered and compared to other methods. The lipid extraction was performed with lupin beans, but more extensively tested on cherry stones, since the latter matrix was more complex.

The following tables gives the reader a broad overview of the characterization of components in *Lupinus mutabilis* beans as found in this thesis (see Table 13), as well as a comparison of the different extraction methods (see Table 14).

Table 13: Overview of the components in *Lupinus mutabilis branco* beans.

Description	Value	Section
Moisture content	9.1 ± 0.8 %	4.2
Ash	3.9 ± 0.0 g/100 g DW	4.3
Protein (N × 6.25)	49.1 ± 0.8 g/100 g DW	4.5.2
Lipids	21.8 ± 0.8 g/100 g DW	7.5
C16:0	2.2 g/100 g DW	7.5
C18:0	1.3 g/100 g DW	7.5
C18:1	8.3 g/100 g DW	7.5
C18:2	6.3 g/100 g DW	7.5
Tocopherol	25.3 mg/100 g DW	7.5
Carbohydrates	24.7 ± 1.0 g/100 g DW	4.7
Total dietary fiber	23.2 ± 0.2 g/100 g DW	4.7
Insoluble dietary fiber	16.1 ± 0.2 g/100 g DW	4.7
Soluble fiber	0.6 ± 0.1 g/100 g DW	4.7
Oligosaccharides	6.5 g/100 g DW	4.7
Alkaloids	4.4 ± 0.2 g/100 g DW	4.4.7
Sparteine	612.8 ± 30.0 mg/100 g DW	4.4.7
Lupanine	2475.5 ± 137.7 mg/100 g DW	4.4.7
3β-Hydroxylupanine	621.8 ± 41.3 mg/100 g DW	4.4.7
13α-Hydroxylupanine	375.1 ± 26.0 mg/100 g DW	4.4.7
3β,13α-Dihydroxylupanine	339.8 ± 24.6 g/100 g DW	4.4.7

Table 14: Result-overview of extractions from *Lupinus mutabilis branco* beans.

Description	Method	Total yield	Rec. rate	Section
Alkaloids extraction ^a	Soxhlet	97 %	95 %	4.4.4
	Randall	100 %	95 %	4.4.5
	LLE	61 %	80 %	4.4.6
	SPE	88 %	98 %	4.4.6
Alkaloid purification	Mixed	-	8-15 %	4.4.12
Protein	IEPP	90 %	55 %	4.5.3
	IEPP-CO ₂	91 %	54 %	4.5.3
	Salting out	93 %	40 %	4.5.3
Lipids ^{a, b}	Soxhlet	100 %	98 %	7.6
	Randall	91 %	95 %	7.6
	scCO ₂	74 %	100 %	7.6
Carbohydrates	IEPP	58 %	97 %	4.7

a) is referring to normalized comparison and b) is calculated for cherry stones.

4.2 Moisture content

The moisture content of the biomatrices was determined via moisture analyzer (see Section 3.3.1). It is a critical parameter since it does not only allow the comparison to other laboratories but also hinders the extraction once a certain threshold is exceeded (as shown in Section 7.6). The moisture content for all here-tested lupin beans varied from 5-15 % and is therefore not suspected of decrease extraction efficiency. The moisture content of the *Lupinus mutabilis branco* beans which were used for most experiments, was analyzed multiple times, and determined with $9.1 \% \pm 0.8$ for the ground sample. The moisture content is also used to calculate the dry weight.

Table 15: Moisture content of the two tested lupin species.

	Moisture %
<i>Lup. mutabilis branco</i>	9.1 ± 0.8
<i>Lup. albus</i>	8.5 ± 1.0

4.3 Ash content

Lupinus mutabilis and *Lupinus albus* were tested for their ash content and the result is presented in the following table.

Table 16: Ash content of the two tested lupin species.

	Ash content
	<i>g/100 g DW</i>
<i>Lup. mutabilis branco</i>	3.93 ± 0.03
<i>Lup. albus</i>	3.88 ± 0.08

Both Lupin varieties contain around 3.9 g ash per 100 g DW of the flour. This result is also used to calculate the total carbohydrate content (see Section 3.4.12).

4.4 Quinolizidine alkaloids in lupin beans

Lupin beans have a high protein and lipid content (see Section 4.1), which puts them in a superior position to other legumes. However, most lupin varieties contain alkaloids, which can be a major drawback regarding human nutrition. Alkaloids can be harmful to the human body and hence do not allow the safe consumption of lupin beans and their products without knowing their specific alkaloid content. To avoid this problem, several measures can be taken. First, a lupin variety which has a low alkaloid content can be bred and then directly consumed. Another option is the extraction of individual components of the lupin bean and avoiding the coextraction of alkaloids. Lastly, the extraction of alkaloids themselves can be carried out. All three options involve the proper knowledge of the alkaloid concentration either from the beans or the final products. A safe limit of total alkaloid content is considered to be 200 mg/kg (see Section 2.2), which means that an adequate knowledge of alkaloid concentration is necessary. The determination of alkaloid concentration in lupin beans/products involves three steps: sample homogenization, extraction of alkaloids, and quantification.

In this thesis all three steps were carried out. After sample homogenization several different extraction methods were tested, namely Soxhlet, Randall, LLE, and SPE, before quantification via GC-FID or GC-MS took place. For this study, *Lupinus mutabilis branco* beans were chosen since they are available in high demand and contain a high concentration of alkaloids. As a result of the extraction method comparison, a new method for the extraction and quantification of alkaloids inside *Lupinus mutabilis branco* beans was developed which is not reported elsewhere and showed significant advantages to other methods. Furthermore, this method was applied to samples from the seed bank of Lisbon to find the lowest containing alkaloid species, which then can be bred and cultured in Europe. Lastly, the isolation of alkaloids was carried out.

4.4.1 Grinding of lupin samples

Although *Lupinus mutabilis* beans were available in high demand, the samples to quantify the alkaloids (seed bank of Lisbon) weren't. Since grinding has the highest loss ratio, a grinding process as described in Section 3.1.1 was developed. The yield was continuously monitored and can be reported with an average recovery rate of 93.8 %. The best method was found to manually grind the lupin beans in a coffee grinder, before using a knife mill at first in a 2 mm sieve and afterwards with a 1 mm sieve.

4.4.2 Identification of alkaloids

Before a quantification of alkaloids can take place, the alkaloids need to be extracted and identified. For this experiment, *Lupinus mutabilis branco* beans were ground and a 5 h Soxhlet extraction was carried out as described in Section 3.2.1. The extract was analyzed via GC-FID and GC-MS (see Section 3.3.3).

Sparteine (1), tetrahydrohombifoline (2), α -isolupanine (3), lupanine (4), 3β -hydroxylupanine (5), 13α -hydroxylupanine (6) and $3\beta,13\alpha$ -dihydroxylupanine (7) were identified by comparing the ions from the carried out GC-MS measurement with the national institute of standard library from 2012 database⁸⁸ and other published data^{27, 31} (see table Table 17). The GC-FID peaks were assigned by retention time comparison to the GC-MS measurement (see Figure 25).

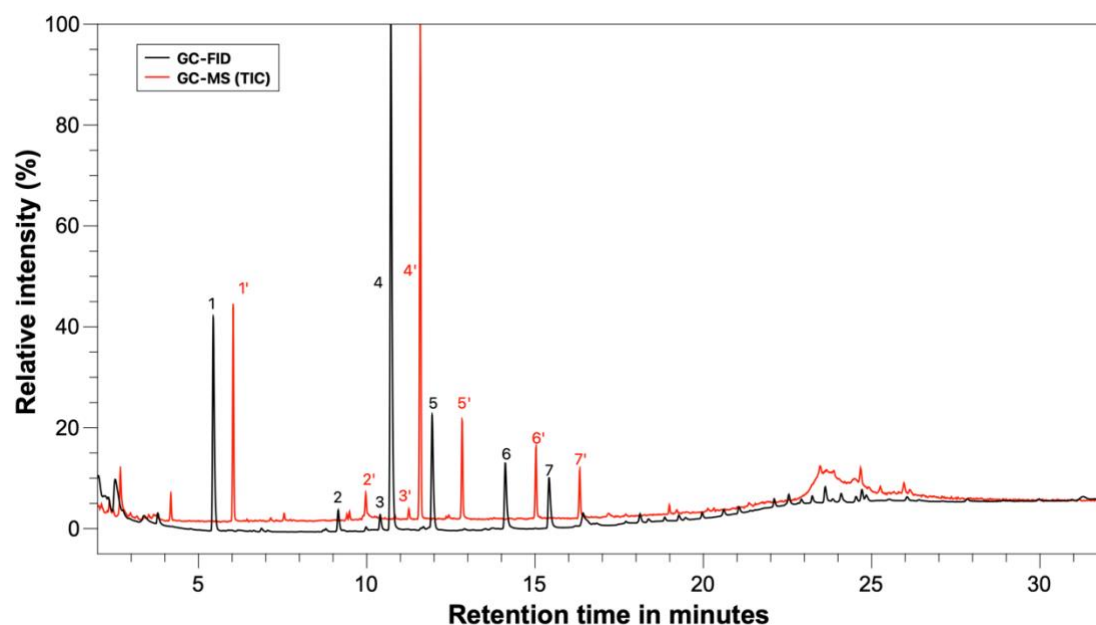
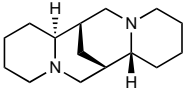
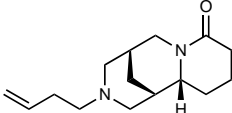
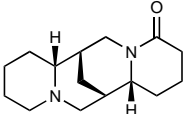
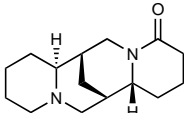
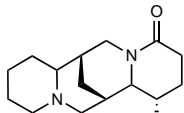
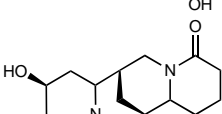
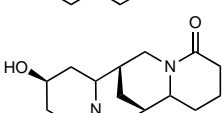


Figure 25: GC-FID and GC-MS chromatogram of *Lupinus mutabilis* Soxhlet extract.

GC-FID (black) and GC-MS total ion current chromatogram (TIC, red) of the same Soxhlet *Lupinus mutabilis branco* extract with a split ratio of 1:10. Peaks are identified as 1) sparteine, 2) tetrahydrohombifoline 3) α -isoupanine 4) lupanine 5) 13α -hydroxylupanine 6) 3β -hydroxylupanine 7) $3\beta,13\alpha$ -dihydroxylupanine.

Table 17: Detected alkaloid species in *Lup. mut. branco* samples.

	Name	Structure	Rt FID	Reference ions
			min	m/z (intensity)
1	Sparteine		5.4	137 (100), 98 (87), 36 (46), 97 (34), 234 (22).
2	Tetrahydro-rhombifoline		9.2	207 (100), 58 (78), 112 (27), 55 (17), 248 (1).
3	α -Isolupanine		9.9	136 (100), 248 (89), 149 (56), 247 (45), 98 (28).
4	Lupanine		10.7	136 (100), 149 (51), 248 (46), 150 (36), 55 (35).
5	3 β -Hydroxy-lupanine (3b-OH)		11.9	136 (100), 64 (83), 134 (51), 150 (40), 263 (35).
6	13 α -Hydroxy-lupanine (13-OH)		14.1	152 (100), 246 (55), 55 (50), 134 (45), 264 (37).
7	3 β ,13 α -Dihydroxy-lupanine (Di-OH)		15.5	152 (100), 280 (91), 165 (40), 134 (38), 150 (33).

The corresponding intensity is shown in brackets and was adapted from the national institute of standard library 2012⁸⁸.

4.4.3 Quantification of alkaloids

On closer inspection of the chromatograms of the Soxhlet extract from *Lupinus mutabilis branco* beans in Figure 25, the immensely large lupanine peak is noticeable. Since the response factor for the different alkaloids for the flame ionization detector (FID) is only slightly varying, the chromatograms indicate that lupanine is the main alkaloid, followed by the other major alkaloids, sparteine, 13-OH, 3b-OH, and Di-OH. All other alkaloids are only present in small quantities and therefore not further considered. This indication is consistent with other published data, which also name lupanine as the main alkaloid and sparteine, 13-OH, and 3b-OH as major alkaloids^{8,11}. From the major alkaloids, 3b-OH is less reported and Di-OH is accounted as a minor alkaloid^{8,9,94}.

To confirm the concentration, the use of a known standard is performed. In this work, the standard was prepared of the allegedly three main alkaloids, namely sparteine, lupanine, and 13-OH. Since no lupin bean reference sample is available, the total alkaloid content can only be evaluated in comparison to other methods. For this, the quantification was carried out via

internal standard calibration curves of those three alkaloids (see Section 3.3.3). The total alkaloid content was calculated by summarizing the content of single alkaloids.

The final concentration of the internal standard (250 µg/mL) was chosen, by evaluating different lupin bean extractions and choosing a concentration, which can be used for high and low alkaloid concentrations. All here-shown quantifications are based on the internal standard method, which assumes linearity in a range of 90 - 110 % (225 µg/ml to 275 µg/mL).

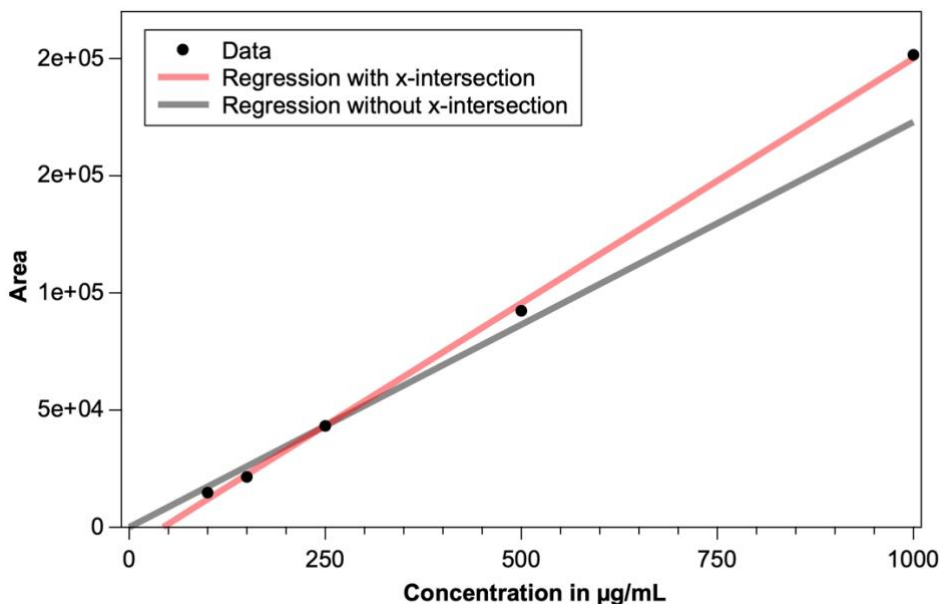


Figure 26: Linearity of the internal standard (caffeine).
Linear regression analyses were applied as shown in Section 3.4.5.

The linearity of caffeine was tested on a much larger scale (100 to 1000 µg/mL) to prove that the linearity and one-point calibration are valid. Figure 26 proves that the usage of an internal standard for concentration determination, without taking the value of the x-intersection into account, is valid in the desired range. An x-intersection can be caused for example by background noise or a coeluting peak in the solvent matrix. Based on the internal standard method and the results from the Soxhlet extraction of *Lupinus mutabilis branco* beans (see later in Table 19), an exact alkaloid distribution is calculated and shown in the following table.

Table 18: Alkaloid distribution in *Lupinus mutabilis branco* beans.

	Sparteine	Lupanine	3b-OH	13-OH	Di-OH	Total
<i>Lup. Mut.</i>	14%	56%	14%	9%	7%	100%

Results are based on GC-FID quantification of Soxhlet extracts.

The results confirm the above-mentioned hypothesis. Lupanine is the main alkaloid, which is responsible for more than half of the total alkaloid content (56 %). The lupanine concentration is followed by Sparteine and 3b-OH, both with a 14 % share and 13-OH with 9 %, respectively Di-OH with 7 % share.

4.4.4 Soxhlet extraction of alkaloids

Soxhlet extraction is one of the widely known extraction methods for secondary plant metabolites. It can be described as a multi-step extraction method (see more in Section 2.6.4). Methanol is suggested by other researchers as a suitable solvent for the extraction of quinolizidine alkaloids via Soxhlet ¹⁵. However, other extraction methods might be preferred concerning the reported coextraction of impurities ¹⁵.

Soxhlet cycles – Total alkaloid content: For a Soxhlet operation the number of extraction cycles is one of the major parameters among the choice of solvent. The number of cycles depends on the extraction time, the amount of used raw material, the sample size, the solvent's polarity, and the penetration rate of the solvent. To test for sufficient extraction cycles, *Lupinus mutabilis branco* beans were extracted via Soxhlet extraction and the concentration of alkaloids in the extract is plotted against the number of cycles as displayed in Figure 27 (see details in Section 3.2.1). One cycle is equivalent to 10-12 min.

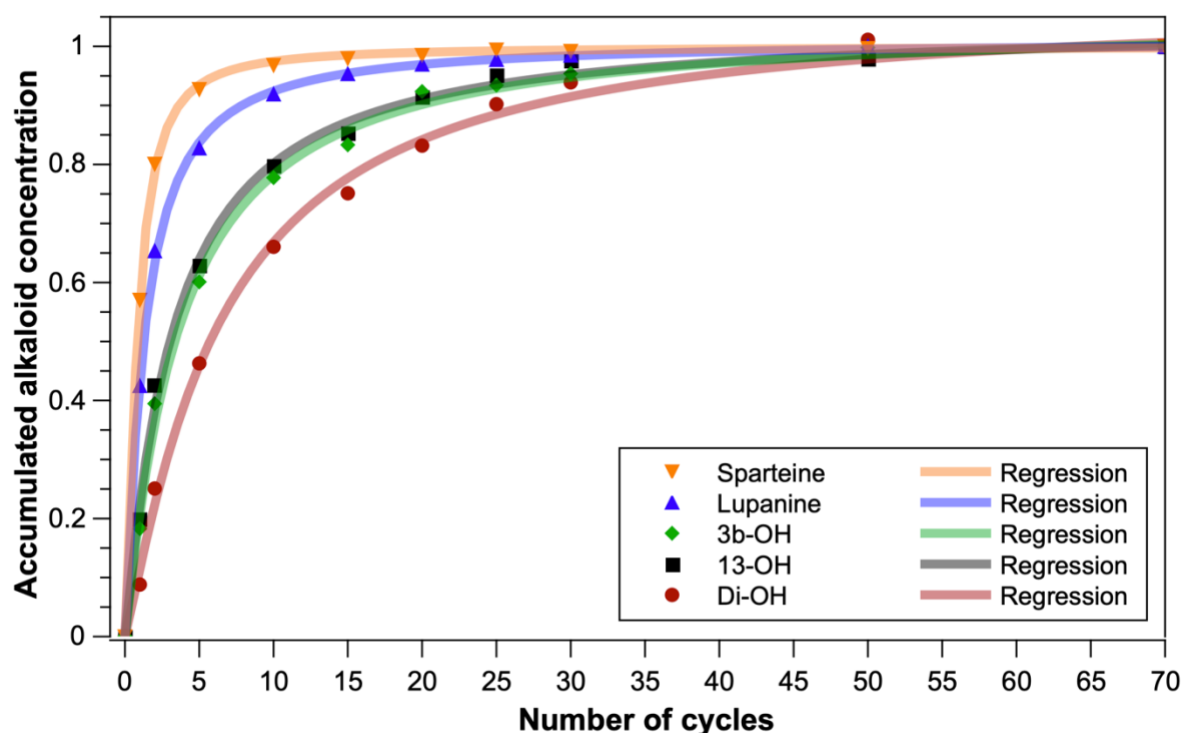


Figure 27: Soxhlet alkaloid extraction progress of *Lupinus mutabilis branco* beans.

The values are compensated for the alkaloid and internal standard taken out during the experiment and normalized to 100 % (70 cycles). Regressions were applied by four parameters logistic curve with the program Qtiplot and parameters can be found in Table 60.

Figure 27 shows the accumulated alkaloids inside the round bottom flask during Soxhlet extraction of *Lupinus mutabilis branco* bean flour and the regression via four parameter logistic curve (see details in Section 3.4.3). The extraction speeds of the alkaloids differ. More non-polar alkaloids like sparteine and lupanine (only one carboxyl group) are faster extracted than

more polar alkaloids like 13-OH and 3b-OH (one carbonyl and one hydroxy group). The slowest extraction seems to be found in Di-OH, which is the most polar alkaloid with two hydroxyl groups and one carbonyl group among two amine groups. Based on this experiment more than 95 % of Sparteine, Lupanine, 13-OH and 3b-OH possible alkaloid concentration at 70 cycles were achieved at 25-30 extraction cycles. Di-OH concentration was with 90 % slightly lower, but still reasonable. Hence, 25-30 cycles were chosen for further Soxhlet experiments, which is equivalent to 5 h and a solvent-to-feed ratio of 1155. Since the monitoring of Soxhlet cycles is rather time-consuming future experiments are only referring to the extraction time of 5 h.

Soxhlet alkaloid extraction – Validation and repeatability: In addition to the number of extraction cycles, the repeatability of Soxhlet operations was tested. For this purpose, ten Soxhlet extractions with one gram of *Lupinus mutabilis branco* sample were carried out (5 h, MeOH) and quantified via GC-FID internal standard method (see Section 3.2.1). The results are presented in Table 19.

Table 19: GC-FID quantification of *Lupinus mutabilis* Soxhlet extraction experiment.

N=10	Sparteine	Lupanine	3b-OH	13-OH	Di-OH	Total
	<i>mg per 100 g DW</i>	<i>mg per 100 g DW</i>	<i>mg per 100 g DW</i>	<i>mg per 100 g DW</i>	<i>mg per 100 g DW</i>	<i>mg per 100 g DW</i>
Mean	596.5	2407.6	589.9	373.3	314.8	4282.1
SD	15.9	89.1	23.7	16.4	17.4	152.7
SD (%)	3%	4%	4%	4%	6%	4%

More details can be found in Section 7.1.

Lupinus mutabilis branco beans are toxic for the direct consumption, which can be verified by the result of the total alkaloid concentration of 4282.1 ± 152.7 mg alkaloids per 100 g DW. The alkaloid content is therefore 214 times higher than the threshold (20 mg/100 g DW) for safe consumption.

The highest relative standard deviation of the 10 experiments was found for Di-OH with 6 %, followed by 4 % for the second highest. Furthermore, a recovery rate of 95 % was found for Soxhlet extraction. All in all, the high recovery rate, the low standard deviation, and the prove that most alkaloids are extracted within the first 25-30 cycles (see Section 4.4.4) indicate that Soxhlet is a robust and reliable method to quantify alkaloids in high alkaloid-containing lupin beans.

Problems with low alkaloid-containing species: Although the obtained alkaloid quantification results for *Lupinus mutabilis branco* beans showed sufficient results, a low alkaloid-containing sample was tested. This was done to prove that this method is not only suitable for high alkaloid-containing samples but also for low alkaloid-containing samples. It is of interest that

the tested method is also suitable for low alkaloid-containing since the method should allow a proper decision if a lupin product is considered as safe to consume (threshold of 20 mg/100 g). In this thesis, *Lupinus albus* was used as a low alkaloid-containing lupin bean. The results of the Soxhlet extraction and quantification via GC-FID can be found in Table 20.

Table 20: GC-FID quantification of *Lupinus albus* Soxhlet extraction experiment.

N=6	Sparteine	Lupanine	13-OH ^a	Total
	<i>mg per 100 g DW</i>	<i>mg per 100 g DW</i>	<i>mg per 100 g DW</i>	<i>mg per 100 g DW</i>
Mean	-	93.1	18.5	111.6
SD	-	5.7	1.9	6.5
SD (%)	-	6%	10%	6%

a) is referring to experiments where the reported LOD and LOQ values were ignored. More details can be found in Section 7.1.

Table 21: LOD and LOQ values for Soxhlet extraction and GC-FID quantification.

	LOD	LOQ
	<i>mg/100 g sample</i>	<i>mg/100 g sample</i>
Sparteine	1.57	4.75
Lupanine	2.14	6.50
13-OH	7.57	22.93

Results are also valid for Randall extraction.

Lupinus albus is a different species than *Lupinus mutabilis* and contains different forms and amounts of alkaloids in its beans. Since the focus in this thesis lies on *Lupinus mutabilis* beans, only the three alkaloids, where a known standard was present, are quantified, namely sparteine, lupanine, and 13-OH. The limit of detection (LOD) and limit of quantification (LOQ) of those three alkaloids were calculated for the GC-FID method (see Section 3.4.7) and are presented in Table 21. The concentrations of the three alkaloids were so low, that the LOQ values of 13-OH had to be ignored for the quantification. This means that at least for the quantification of 13-OH in low alkaloid-containing samples, the Soxhlet extraction with quantification via GC-FID is not suitable. Furthermore, increased standard deviations for alkaloids from *Lupinus albus* beans were detected. This is also related to the quantification at the LOD/LOQ area. In conclusion, it can be said that the LOD and LOQ values are sufficient to quantify medium to high amounts of alkaloids inside a sample but are not sufficient to quantify low alkaloid-containing samples. Especially when meeting the suggested requirement of a total alkaloid content smaller than 20 mg per 100 g sample. For example, the LOQ of 13-OH is already higher for the single alkaloid, than the required total threshold (see Table 21). Furthermore, it has to be noted, that the peaks could not be easily assigned. Figure 28 shows two GC chromatograms of the extraction obtained from *Lupinus albus* and *Lupinus mutabilis* with similar extraction and quantification methods.

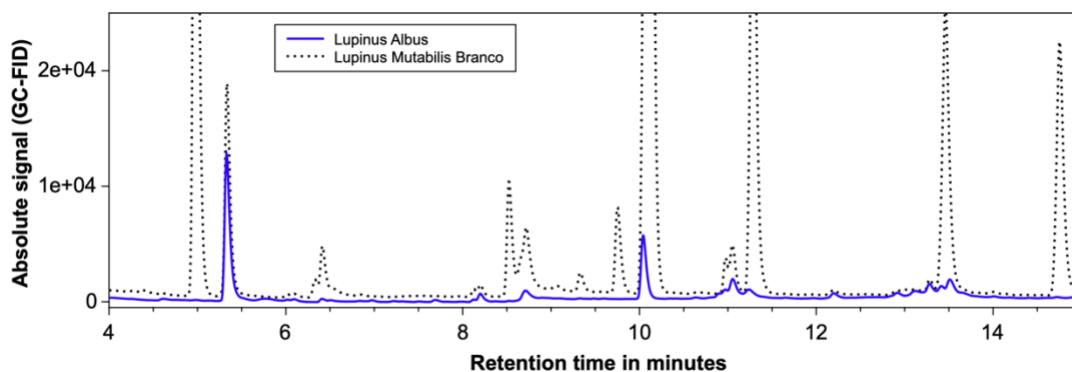


Figure 28: GC-FID chromatogram of Soxhlet extracts from two different species.

Similar extraction methods and quantification were applied for *Lupinus albus* (blue) and *Lupinus mutabilis branco* (black, dashed).

When comparing the size of the peaks in Figure 28, only the peak at around 5.5 min shows a similarity in area to the *Lupinus mutabilis* sample, which is caffeine (internal standard) and was expected. Among the three known alkaloids, only lupanine shows a clear peak (Rt: 10.2). Sparteine does not provide a sufficient signal and the 13-OH (Rt: 13.5) peak cannot be distinguished from other peaks, which occurred in the chromatogram (see Figure 29).

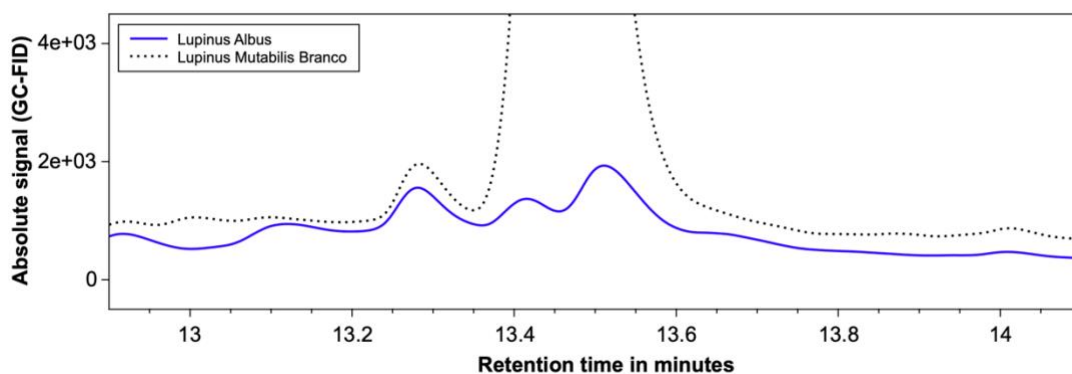


Figure 29: Detailed GC-FID chromatogram comparison of 13-OH from two lupin species.

Similar extraction methods and quantification were applied for *Lupinus albus* (blue) and *Lupinus mutabilis branco* (black, dashed).

To overcome those problems, the following strategies can be followed:

1) Changing the extraction procedure for low alkaloid samples: The extraction via Soxhlet seems to coextract a substance, which coelutes at the same retention time as 13-OH. A purification step, for example, a cleaning via flash column chromatography can be done to purify the sample and separate alkaloids from non-alkaloids. This costs extra time and would require a new Soxhlet extraction with an adjusted internal standard amount, to compensate for the low sensitivity, and was therefore not followed in this thesis. Another possibility offers the change from Soxhlet extraction to the often-used acid/base extraction followed by a cleaning step via diatomaceous earth (Extrelut). This method provides cleaner

chromatograms but deals with other drawbacks, like discrimination of polar alkaloids (as shown later).

2) Increase the signal of alkaloids at the detector: The low sensitivity can be changed by increasing the signal in the detector. For example, the split ratio of the GC can be adjusted from 1:8 (current) to splitless injection, increasing the signal by 8-fold. Furthermore, the injection volume could be increased from 0.5 μL to 1.0 μL (concerning the backpressure and the vapor capacity for the liner), doubling the signal. Both procedures will help to decrease the calculated LOD and LOQ values and increase the sensitivity. However, while the calculated LOD and LOQ values can be decreased, the problem with the 13-OH peak might not change, since it still cannot be identified which of the peaks is the 13-OH peak (see Figure 30).

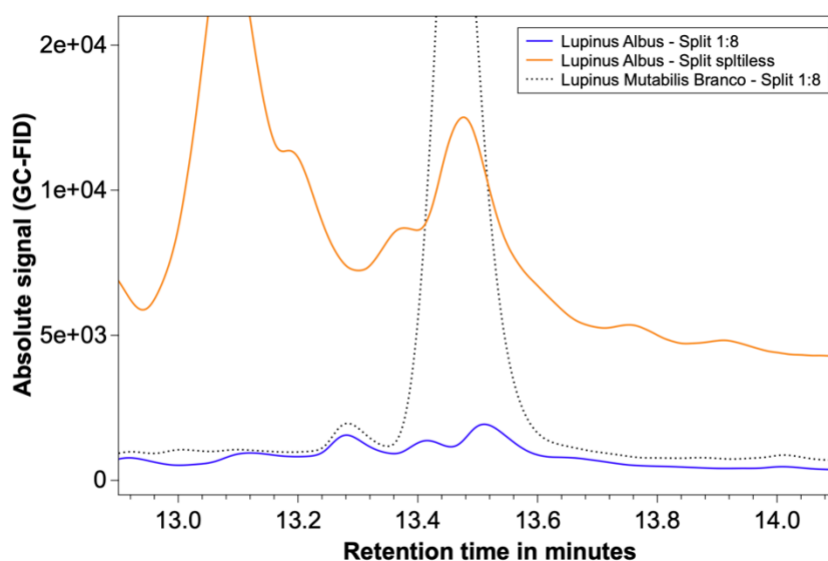


Figure 30: Detailed 13-OH chromatogram via splitless injection.

GC-FID chromatograms comparison between *Lupinus albus* in split (1:8), splitless (orange) and *Lupinus mutabilis branco* splitless (black, dashed). Similar extraction methods were applied.

The reason for this phenomenon lies in the background noise and noise-to-signal ratio. The here-used standard solution contains caffeine, sparteine, lupanine, and 13-OH in analytical grade MeOH. There is only a limited amount of background noises, which can disturb the 13-OH peak and therefore gives a clear peak also for a low 13-OH concentration, which then results in lower LOD, LOQ values, and increased sensitivity.

However, the increased sensitivity does not compensate for background noises inside a real sample, since other components that are not 13-OH, might elute at the same time. This can be seen in Figure 30, where the same sample as shown in Figure 29 was injected into a GC-FID with splitless mode. Also, the peak broadening through splitless injection and the lost adjustability for a pressure change in the injector part of the GC must be considered (see also discussion below).

As expected, the background noises and the peak broadening make the quantification of the 13-OH peak uncertain, hence another option should be followed.

3) Derivatization: For completeness, it should be mentioned that the derivatization of the alkaloids is also a suitable option. The derivatization could change the properties of the alkaloids, which then lead to a different retention time in the chromatogram. In this case, derivatization of 13-OH via trimethylsilyl chloride or trimethylsilyl iodide might be desired and would separate the 13-OH from the background peaks⁹⁵. Although this method would help to change retention time (despite the GC temperature program itself), it will not help to increase the concentration of the alkaloid. Furthermore, it introduces an additional step into the method, which requires an additional method development. This costs time, resources, and leads to errors, which is why this option is mentioned but not carried out.

4) Increasing the concentration of alkaloids inside the GC-vial: To deal with the increased background noise, the concentration of alkaloids inside the final GC-vial can be increased assuming that only the alkaloid concentration is increased, and the background concentration stays fixed. This can be done by increasing the amount of sample extracted in the Soxhlet extraction from 1 to 5 or even 10 g, or the final volume of 10 mL can be decreased. Since the method was developed to analyze samples, where only a limited amount of sample is available (<10 g, analyzed in triplicates), the increased amount of sample during extraction cannot be carried out for all samples. Also, the method would need another repeatability test (as shown in Section 4.4.4) and the amount of internal standard to alkaloid might not be sufficient for all samples. This makes this option also unsuitable for the desired purpose.

The other possibility of decreasing the final volume of 10 mL, was tested and showed insufficient repeatability because the decreased volume resulted in losses of alkaloids due to precipitation.

5) Standard addition: Another possibility to overcome the problem of measuring samples at the LOD/LOQ concentration is the so-called standard addition method. For this, a precise amount of standard will be added to the sample and the amounts will be lifted out of the LOD/LOQ range. This is mostly done via multiple concentrations, yielding a standard addition curve. Although this method has shown good results for a lot of different research topics, it is not further considered in this thesis. The reason lies in the high cost of the standard solution and the heavy workload. It also will only be applicable for available standards, which are only sparteine, lupanine, and 13-OH.

6) Change of detector: The lack of selectivity for alkaloids can be compensated by changing the GC-FID detector to a more selective detector. All tested alkaloids contain two nitrogen atoms, therefore the use of a nitrogen-phosphorous detector would increase the selectivity by identifying the correct peak as a nitrogen-containing peak, assuming that the coeluting peak has no nitrogen content.

Another detector option is the mass spectrometer (MS) detector. While the GC-MS can be used to identify peaks (as shown in Section 4.4.2), it can also be used to increase the

selectivity for specific alkaloid fragments. The identification of alkaloids was carried out by operating the mass spectrometer in scan modus. A quantification can be carried out in selected ion monitoring (SIM). During the scan mode, the MS uses the quadrupole to change the passing m/z value from a certain value in the selected increment continuously until the highest set m/z value is reached. In this case, a m/z ratio of from 50 to 500 with increments of 1 was used for the identification (see Section 3.3.3). With the SIM mode, the MS uses not all m/z values from 50 to 500 but only certain m/z values. In the example of 13-OH, the MS is adjusted so that after the retention time of 14 min only 55, 134, 152, 246, and 264 were used as m/z channels. This allows a longer time for the specific alkaloid fragment to be detected, which results in more mass fragments reaching the detector and therefore higher sensitivity. While an MS measurement in scan mode has already an increased sensitivity towards the GC-FID measurement, it will increase its sensitivity if the SIM mode is selected⁹⁶. The use of the MS with SIM mode allows therefore an increased sensitivity and selectivity towards the GC-FID method. This sensitivity can be even further increased, when a splitless injection is chosen and the volume of injection is increased, offering all the benefits as discussed above without their drawbacks. However, splitless injection has other difficulties, such as changing the pressure in linearity velocity mode or peak broadening and longer retention times, which will ultimately result in poor peak shapes. This is a consequence of the relatively broad injection band (in comparison with split injection), since the whole volume of the injector needs to be transferred into the capillary column.

In Figure 31 the comparison of the four chromatograms from the same *Lupinus albus* extract can be seen and how the peak broadening and shape have changed due to splitless injection. Nevertheless, the splitless injection in SIM mode does show a clear peak for 13-OH (orange), while the split of 1:8 in scan mode (blue) shows a lot of other peaks and in general an increased noise ratio. The SIM detection with a split ratio of 1:8 shows smaller but narrower peaks for Soxhlet (pink) and Randall method (purple), without the noise of the scan mode, while still being detectable and quantifiable. Therefore, a split ratio of 1:8 in SIM mode was also chosen for later analysis.

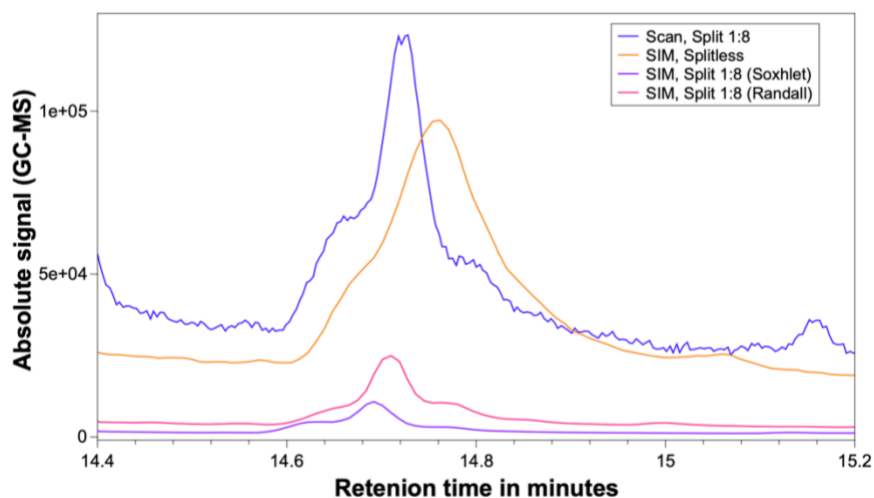


Figure 31: Detailed GC-MS chromatogram comparison of the 13-OH peak.

Soxhlet extracts of *Lupinus albus* were analyzed in scan and split 1:8 (blue), SIM and splitless (orange), SIM and split 1:8 (purple), and Randall extract with SIM and split 1:8 (pink).

Although the use of MS offers a huge benefit with respect to sensitivity and selectivity, it has a significant drawback for the quantification of alkaloids in lupin beans.

In FID measurements, the analyte is burned and yields into ions, which will then be measured between two electrodes. The ion yield is proportionally related to the number of carbon and its substitution. Similar structure yield therefore in similar signals and small changes in structure have only limited influence towards the signal. The calibration curve of 13-OH can therefore be used as a calibration curve for 3b-OH (isomers).

An MS measurement does not allow certain quantification of unknown peaks and requires therefore a standard. This is related to the difference in fragmentation. As it can be seen in Table 17, 13-OH and 3b-OH are isomers and have large similarities in structure but result in completely different fragments and intensities of those fragments. This makes the quantification of unknown peak uncertain. In the case of the here-shown alkaloid determination, 3b-OH and Di-OH were not commercially available and can therefore not be sufficiently analyzed via MS. A solution for this would be the purification of the desired alkaloids, as shown later (see Section 4.4.12).

Quantification of low alkaloid species via GC-MS: The combination of splitless, MS, and SIM mode offers an easy solution to decrease the method's LOD/LOQ values without changing the extraction method. It can therefore be seen as an extension to the already used and presented Soxhlet extraction procedure if a low alkaloid content is measured.

Although splitless injection increases the amount of alkaloids reaching the detector, it also affects the column efficiency and a broadening of the peaks as can be seen in Figure 31.

Therefore LOD/LOQ values are calculated in Table 22 with the GC-MS-SIM method with an injection volume of 1.0 mL and a split ratio of 1:8.

Table 22: LOD and LOQ values for Soxhlet and Randall extraction via GC-MS.

	LOD	LOQ
	mg/100 g sample	mg/100 g sample
Sparteine	0.24	0.74
Lupanine	0.60	1.82
13-OH	0.76	2.30

Quantification is based on SIM mode detection, with a split ratio of 1:8, and 1.0 mL injection volume.

In comparison to LOD/LOQ values from the GC-FID method (see Table 21), the LOD/LOQ values for the GC-MS method decreased to a reasonable value, now allowing the quantification within the desired threshold of 20 mg/100 g. As already discussed, even smaller LOD/LOQ values can be achieved by splitless injection. Since the threshold with a split ratio of 1:8 is sufficient further experiments were not necessary to carry out.

The new quantification results for the same low alkaloid-containing samples as shown for the GC-FID method (see Table 20) are shown in Table 23.

Table 23: GC-MS quantification of *Lupinus albus* Soxhlet extraction experiment.

N=6	Sparteine	Lupanine	13-OH	Total
	mg per 100 g DW	mg per 100 g DW	mg per 100 g DW	mg per 100 g DW
Mean	-	108.7	18.4	127.1
SD	-	8.4	2.6	10.1
SD (%)	-	8%	14%	8%
Soxhlet (%)^a	-	86%	101%	88%
p-value^a	-	0.005*	0.938	0.012*

SIM mode together with a split ratio of 1:8 and 1.0 mL injection volume were applied. a) is referring to the Soxhlet extraction and quantification of *Lupinus albus* by GC-FID. P-values were obtained by two-sided student's t-test and significant differences were marked by asterisk (*). More details can be found in Section 7.1.

The total determined alkaloid content was 127.1 ± 10.1 for the GC-MS method and 111.6 ± 6.5 mg/100 g DW for the GC-MS method. The LOD and LOQ values were on purpose ignored for the GC-FID method and showed unexpectedly smaller standard deviation. Moreover, there is a significant difference between the lupanine and total alkaloid quantification detected (see p-value), which seems to result in higher results for the GC-FID method than for the GC-MS method. The difference is 17 % does affect the total alkaloid content, which is therefore 14 % higher. The reason lies in the used calibration curve. While the GC-FID method applies a calibration curve reaching from LOD/LOQ values up to 4000 mg per 100 g, the GC-MS method uses a calibration curve, around the LOD/LOQ value from the GC-FID methods and is therefore more precise for lower alkaloid samples.

4.4.5 Randall extraction of alkaloids

Randall extraction is also a multi-step extraction procedure but is less frequently found in literature than Soxhlet operation. Randall offers the benefit of having a cooking/penetration step and rinsing step in a single extraction procedure (see details in Section 2.6.5). Together with the automatic solvent recovery, it can help to reduce the extraction and work-up time.

For Randall extractions, a similar amount of raw material (1 g) and final volume (10 mL) compared to Soxhlet were used. This results in analogous LOD/LOQ values and boundaries as shown for Soxhlet extraction (see Section 4.4.4).

Randall alkaloid extraction – Validation and repeatability: To test the Randall extraction as a potential extraction method for quinolizidine alkaloids, the *Lupinus mutabilis branco* flour was extracted via methanol. Each sample was extracted with a 40 min cooking and 80 min rinsing step before the quantification via the internal standard method took place (see Section 3.2.1 and 3.4.5). The results are presented in Table 24.

Table 24: GC-FID quantification of *Lupinus mutabilis* Randall extraction experiment.

N=10	Sparteine	Lupanine	3b-OH	13-OH	Di-OH	Total
	<i>mg per 100 g DW</i>	<i>mg per 100 g DW</i>	<i>mg per 100 g DW</i>	<i>mg per 100 g DW</i>	<i>mg per 100 g DW</i>	<i>mg per 100 g DW</i>
Mean	612.8	2475.5	621.8	375.1	339.8	4424.9
SD	31.6	145.2	43.6	27.4	26.0	271.3
SD (%)	5%	6%	7%	7%	8%	6%
Soxhlet (%)^a	103%	103%	105%	100%	108%	103%
p-value^a	0.164	0.224	0.057	0.860	0.021*	0.164

a) is referring to the Soxhlet extraction and quantification of Lupinus mutabilis by GC-FID. P-values were obtained by two-sided student's t-test and significant differences were marked by asterisk (). More details can be found in Section 7.1.*

While Soxhlet extraction resulted in 4282.1 ± 152.7 , Randall extraction resulted in 4424.9 ± 271.3 mg Alkaloids per 100 g DW flour, this means a total alkaloid content of 103 % compared to the Soxhlet results. By looking at the alkaloids individually, the Randall extraction gives similar or slightly higher yields for all alkaloids.

Although the standard deviations are higher than shown for Soxhlet, the highest standard of 8 % is still reasonable. There is a trend, in which higher retention times seem to generate higher standard deviation and vice versa. This trend is small but can be explained by increasing broadness and flattening of the peak during the chromatographic separation, leading to decreased slopes of the edges. This makes the proper integration more complicated and could lead to the observed increased standard deviation. This problem might be

addressed by increased temperature ramping. However, concerning the result, no further actions were taken.

For the student's t-test, the results from the extraction of *Lupinus mutabilis* beans via Soxhlet and Randall extractions were compared and showed only a significant difference in the case of Di-OH. As can be seen in Figure 27, Di-OH is the alkaloid with the slowest extraction rate via Soxhlet. Since Soxhlet extractions were carried out within 5 h, not all Di-OH might be extracted, which shows the advantage of the Randall extraction.

Quantification of low alkaloid samples via GC-MS: Soxhlet and Randall extraction have quite similar extraction parameters and are dealing with similar benefits and drawbacks. Low alkaloid determination suffers therefore for the same reasons as already stated for Soxhlet extraction, but the issue can be solved by using a GC-MS measurement in SIM mode, if the determination of low alkaloid content is desired and a standard is available.

Table 25: GC-MS quantification of *Lupinus albus* Randall extraction experiment.

N=6	Sparteine	Lupanine	13-OH	Total
	<i>mg per 100 g DW</i>	<i>mg per 100 g DW</i>	<i>mg per 100 g DW</i>	<i>mg per 100 g DW</i>
Mean	-	129.5	21.5	151.0
SD	-	11.6	2.5	13.8
SD (%)	-	9%	12%	9%
Soxhlet (%)^a	-	119%	117%	119%
p-value^a	-	0.005*	0.090	0.008*

Analyses were performed similarly to the already shown GC-MS method for low alkaloid samples via Soxhlet extraction. a) is referring to the GC-MS Soxhlet quantification experiment. P-values were obtained by two-sided student's t-test and significant differences were marked by asterisk (). More details can be found in Section 7.1.*

The difference between the Soxhlet and Randall extraction is significant, although they are applying the same determination method (GC-MS, SIM, Split 1:8). The Randall extraction showed higher alkaloid contents for lupanine, hence leading also to a significantly higher total alkaloid content, since lupanine has the highest contribution. The standard deviation is similar between both methods. In conclusion it can be said, that if a low alkaloid determination is conducted, Randall extraction should be favored over Soxhlet extraction.

4.4.6 Extraction of alkaloids via acid-base mechanism

The extraction of secondary plant metabolites via Soxhlet or Randall extraction is a common method but not often considered when it comes to the quantification of quinolizidine alkaloids in lupin beans. The reason for this lies in the coextraction of non-alkaloid molecules, which can elute at a similar retention time as the alkaloids and complicate the quantification (see Section 4.4.4).

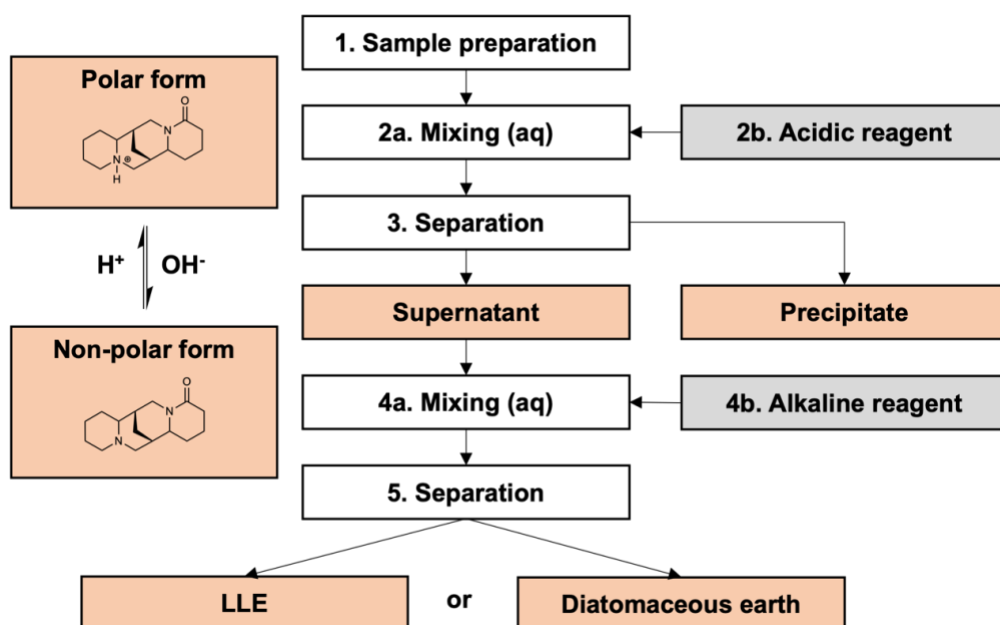


Figure 32: Process overview of the acid-base mechanism.

The most common extraction method is therefore based on the acid-base mechanism (see Section 2.2.2). An overview of the method is given in Figure 32. After the sample preparation (step 1), an acid (2b) is mixed with the sample (step 2a). The acid breaks/dissolves the sample matrix and converts the alkaloids into their polar form. This form is hydrophilic, and the alkaloid will be transported from the matrix into the aqueous (acidic) solution. In the following step (3), the remaining insoluble matrix is separated from the alkaloid-containing aqueous solution. Afterwards, the aqueous solution is alkalized (4b) and mixed (4a), which converts the alkaloids into their non-polar form, which is considered to be hydrophobic. Subsequently, the alkaloids are separated (step 5) from the aqueous phase by LLE or SPE (diatomaceous earth) and are transferred into an organic solvent.

Both methods (LLE and SPE) have in common that they offer improved LOD/LOQ values in comparison to the here-shown Soxhlet/Randall methods and could therefore be applied with GC-FID for quantification. This is related to the prevention of the coextraction of other non-alkaloid molecules. With the absence of non-alkaloid molecules, the final concentration of alkaloids can be a lot higher, since no precipitation effects occur. In the here-shown results, an extract of a 1 g lupin sample was used in 1.0 mL, respectively 0.5 g sample in 0.5 mL, allowing a decrease of LOD/LOQ values by 10 as seen in the following table.

Table 26: LOD and LOQ values for acid-base extraction via GC-FID quantification.

	LOD	LOQ
	mg/100 g sample	mg/100 g sample
Sparteine	0.16	0.48
Lupanine	0.21	0.65
13-OH	0.76	2.29

Liquid-liquid extraction (LLE): Liquid-liquid extraction is a common laboratory separation and purification method in which ideally the desired molecules are transported into one phase, while undesirable molecules remain in the other phase. To carry out an LLE, two immiscible phases are needed. In the case of alkaloids from lupin beans, Muzquiz et al. ³³ presented 1995 a method that applies 5 % TCA (3 x 5 mL) to separate the alkaloids from the insoluble matrix. The extracts were combined and alkalized by 10 M NaOH (1 mL) before LLE with DCM (3 x 5 mL) took place. About 20 years later Kamel et al. ²⁹ reported results for the quantification of lupin beans by using a similar method to the one described, showing the relevance of this technique. In this thesis, the LLE extractions were carried out based on the two literature resources (see details in Section 3.2.1). They were part of an internship project together with Sijze van der Meer and the results are presented in Table 27 and Table 28.

Table 27: GC-FID quantification of *Lupinus mutabilis* LLE experiment.

N=6	Sparteine	Lupanine	3b-OH	13-OH	Di-OH	Total
	mg per 100 g DW	mg per 100 g DW	mg per 100 g DW	mg per 100 g DW	mg per 100 g DW	mg per 100 g DW
Mean	339.2	1775.0	495.0	65.1	16.6	2690.8
SD	151.3	714.4	228.4	26.8	2.9	1114.7
SD (%)	45%	40%	46%	41%	17%	41%
Soxhlet (%) ^a	57%	74%	84%	17%	5%	63%
p-value ^a	0.006*	0.061	0.234	0.000*	0.000*	0.012*

a) is referring to the Soxhlet extraction and quantification of *Lupinus mutabilis* by GC-FID. P-values were obtained by two-sided student's t-test and significant differences were marked by asterisk (*). More details can be found in Section 7.1.

Table 28: GC-FID quantification of *Lupinus albus* LLE extraction experiment.

N=6	Sparteine	Lupanine	13-OH	Total
	mg per 100 g DW	mg per 100 g DW	mg per 100 g DW	mg per 100 g DW
Mean	-	162.6	5,2	167.9
SD	-	15.3	0.9	15.4
SD (%)	-	9%	17%	9%
Soxhlet (%) ^a	-	150%	28%	132%

a) is referring to the Soxhlet extraction and quantification of *Lupinus albus* by GC-FID. More details can be found in Section 7.1.



Figure 33:
Emulsion during
LLE of *Lupinus
mutabilis* beans.

For *Lupinus mutabilis*, the LLE recovery rate was determined at 80 % and the quantification resulted in 63 % of the total alkaloid content from Soxhlet extraction. Furthermore, all alkaloids individually showed a lower extraction yield than in the Soxhlet extraction. This is explicitly true for 13-OH (17 %) and Di-OH (5 %). The standard deviation of the method for every alkaloid is very high, which might be a result of the uncontrollable formation of an emulsion (see Figure 33), which made the accurate separation impossible.

The lower alkaloid-containing species *Lupinus albus* also showed emulsification. A recovery rate of 66 % (IS) and a total alkaloid extraction yield of 132 % compared to the Soxhlet results were found. The standard deviations were found to be smaller for the low alkaloid-containing sample, but still rather high in comparison to other methods, i.e. Soxhlet. The main alkaloid (lupanine) resulted in a 150 % yield compared to Soxhlet results, while 13-OH resulted in only 28 %. The higher result of lupanine can be explained by the use of GC-FID as a quantification method and the insufficient recovery rate.

The GC-FID and GC-MS methods require an internal standard recovery rate of 90 - 110 % (see Section 4.4.3). However, the recovery rate of 66 % is much lower and therefore far away from its designed concentration range for the calibration curve. Furthermore, the GC-FID method's calibration curve covers also a longer linearity which makes them uncertain for the determination of smaller concentration (see Section 4.4.4).

It was found that both tested species (*Lupinus mutabilis* and *Lupinus albus*) have shown much smaller extraction yields for 13-OH for LLE than reported for Soxhlet/Randall extraction. *Lupinus mutabilis* extractions have also shown, that not only 13-OH but also Di-OH showed very low extraction yields compared to the other alkaloids (sparteine, lupanine, and 3b-OH). Although *Lupinus mutabilis* contains 3b-OH and 13-OH, which differs only from the position of the hydroxyl group, they highly differ in extraction yields, 84 % for 3b-OH, respectively 17 % for 13-OH in comparison to the Soxhlet results. This means, that the behavior of 13-OH and Di-OH differs from sparteine, lupanine, and 3b-OH. If the acid-base extraction method is assumed to be an effective method to extract alkaloids from the matrix (as it will be shown later), the majority of 13-OH and Di-OH molecules stay in the aqueous phase and are not successfully transported into the organic layer.

Other parameters were tested, which included the change of acid and alkalization agent, as well as solvents for the LLE (hexane, cyclohexane, pentane, chloroform, diethyl ether, methyl tert-butyl ether, and ethyl acetate), but always resulted in the formation of emulsion, low recovery rates, and poor alkaloid quantity.

In summary, the acid-base extraction of lupin flour via LLE resulted in poor quantification of alkaloids in lupin beans and was therefore not further considered.

Diatomaceous earth - solid phase extraction (SPE): The SPE method is an alternative to the LLE-step during the acid-base extraction. It requires therefore a similar pre-treatment as discussed for the LLE (see Section 4.4.6) but differs in the last step (see Figure 32). In this step, the SPE method applies diatomaceous as a separation media, where the alkaline aqueous solution is soaked in. After a soaking time (here 15 min), the hydrophobic components are eluted by applying a non-polar solvent (here 3 × 20 mL DCM), while the aqueous solution stays adsorbed by the silica. The method is also called supported LLE and is often applied when a formation of emulsion hinders the extraction.

The recommended pH range of the most applied diatomaceous earth column (Extrelut) lies between pH 1 and pH 10⁸⁴. However, several reported methods apply a higher pH value of up to pH 12^{15, 27, 28}. Lee et al.³⁰ reported a method, which uses a pH of 9.5 to 10 and stayed therefore in the manufacturer pH range. Therefore, this method was chosen and tested for *Lupinus mutabilis branco* beans. The results are presented in the following table.

Table 29: GC-FID quantification of *Lupinus mutabilis* SPE extraction experiment.

N=10	Sparteine	Lupanine	3b-OH	13-OH	Di-OH	Total
	<i>mg per 100 g DW</i>	<i>mg per 100 g DW</i>	<i>mg per 100 g DW</i>	<i>mg per 100 g DW</i>	<i>mg per 100 g DW</i>	<i>mg per 100 g DW</i>
Mean	583.0	2418.4	632.7	190.3	51.0	3875.5
SD	29.8	95.5	26.1	13.6	4.4	160.4
SD (%)	5%	4%	4%	7%	9%	4%
Soxhlet (%)^a	98%	100%	107%	51%	16%	91%
p-value^a	0.224	0.796	0.001*	0.000*	0.000*	0.000*
Randall (%)^b	95%	98%	102%	51%	15%	88%
p-value^b	0.044*	0.313	0.505	0.000*	0.000*	0.000*

a) is referring to the Soxhlet extraction and quantification of *Lupinus mutabilis* by GC-FID, b) is referring to the Randall extraction and quantification of *Lupinus mutabilis* by GC-FID. P-values were obtained by two-sided student's t-test and significant differences were marked by asterisk (*). More details can be found in Section 7.1.

The SPE extraction achieves an internal standard recovery rate of 98 % for high and low alkaloid-containing samples. The chromatogram of the SPE shows clean peaks (see Figure 34) which is one of the reasons why it is preferred over methods like Soxhlet¹⁵. The results in Table 29 show that the standard deviation from the quantification of *Lupinus mutabilis branco* via SPE is comparable with the Soxhlet and Randall extractions. Further comparison reveals that the total alkaloid content is significant smaller for the SPE approach. By looking into the individual alkaloid quantification, it can be seen, that the 13-OH and Di-OH yields have a significantly lower extraction yield for SPE than for Soxhlet or Randall.

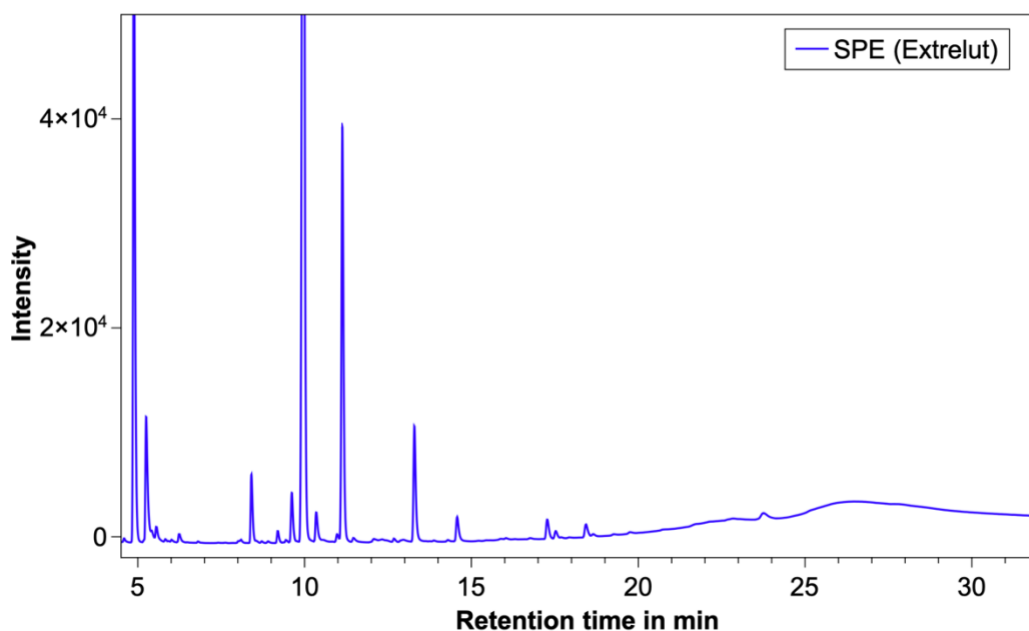


Figure 34: GC-FID chromatogram of *Lupinus mutabilis* extract via SPE (Extrelut).

In the case of 13-OH, only 51 % of the yield from Soxhlet and Randall can be found and in the case of Di-OH, only 16 % (respectively 15 % for Randall) can be found. Since the total alkaloid content is the sum of the individual alkaloid content, the difference in total alkaloid content between these methods can be explained by this finding. It reveals, that with the application of the SPE approach, some alkaloids are discriminated. This discrimination leads to a lower total alkaloid content of this method. This finding has a big impact because the most reported extraction method for lupin alkaloids is the extraction via an acid-base mechanism, followed by a separation via Extrelut column ⁹.

Since the lower yield for the 13-OH and Di-OH was also shown for the LLE (see Table 27), the acid-base mechanism was first suspected. During the acid-base extraction, a low and high pH was used, this could have induced side reactions of the alkaloids, which could potentially lead to alkaloid degradation or side products, which are then not detected as the initial alkaloid species anymore. The here-tested method did apply a pH of 10. Although it is not recommended by the supplier to exceed the pH of 10, many reported methods do. To test if one of the above-stated hypotheses is applicable, a new experiment was conducted.

The following Figure 35 and Figure 37 are based on calculations as shown in Section 3.4.6 and are only limited representable for actual percentages of the extraction. This allows an estimation of the concentration but is not accurate enough to give quantitative precise results for concentration analysis as can be seen by comparing this data with the quantified data from Table 29.

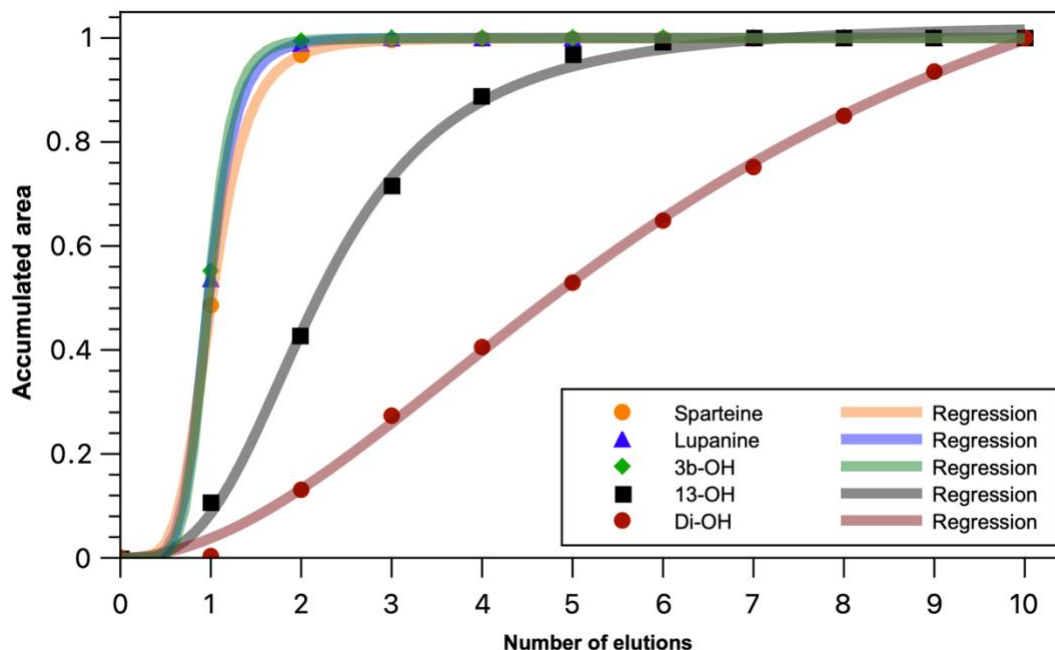


Figure 35: Extraction progress of SPE(Extrelut) from *Lupinus mutabilis branco* beans.

Each elution refers to 20 mL of DCM. Quantification was performed via GC-MS in scan mode. Regressions were applied by four parameters logistic curve with the program Qtiplot and parameters can be found in Table 61.

Sparteine, lupanine, 3b-OH, and caffeine (not shown) were completely eluted after applying 2 × 20 mL DCM. This is related to the lower polarity of those molecules and higher affinity towards the DCM. However, 13-OH and Di-OH were not sufficiently extracted within the recommended 3 × 20 mL DCM elution. For example, 13-OH was sufficiently eluted after ca. 6 × 20 mL DCM. Furthermore, Di-OH was even after applying 10 × 20 mL DCM not fully eluted, which can be seen by p_4 parameter value in Table 61 (see discussion below) and the slope in Figure 35. The chosen four parameter logistic regression curve does imply a slower slope in the beginning, followed by an increased slope, before again a slower slope emerges. The slope is related to the column size and affinity to transmit into the DCM phase, which is high for Sparteine, Lupanine, and 3b-OH but low for 13-OH and Di-OH. If the analyte has a low affinity towards the eluent in an open column chromatography, a longer retention time will be observed than an analyte with high affinity. However, in contrary to open column chromatography, the analyte is here distributed through the whole column bed. That means that the analyte from the bottom of the column starts to elute, while the majority of alkaloids remain in the column, which explains the reduced slope in the beginning. The slope increases when more eluent is applied because the maximum concentrated elution band is reaching the end of the column. Afterwards, the slope decreases again because most alkaloids are eluted before and are therefore no longer available for elution.

All in all, the results do indicate that the often and preferred method to extract alkaloids from lupin beans via the acid-base mechanism and elution via Extrelut column might result in discrimination of certain types of alkaloids, which is not due to the acid-base mechanism itself.

In summary, the previous results have shown that neither LLE, nor SPE lead to a successful quantification of the high alkaloid-containing species *Lupinus mutabilis branco* beans. However, the application of an SPE column might be still applicable for low alkaloid-containing samples. Subsequently, *Lupinus albus* was extracted via the Torres and Wink et al. proposed method ²⁷. The corresponding LOD/LOQ values can be found in the following table.

Figure 36: LOD and LOQ values for acid-base extraction via GC-MS quantification.

	LOD	LOQ
	<i>mg/100 g sample</i>	<i>mg/100 g sample</i>
Sparteine	0.02	0.07
Lupanine	0.06	0.18
13-OH	0.08	0.23

The results show that the combination of SPE and GC-MS quantification allows superb LOD/LOQ values (also true for LLE). But although the values allow the use of a GC-FID (see Table 26), GC-MS quantification was chosen, because it allows a better comparison between the methods.

Table 30: GC-MS quantification of *Lupinus albus* SPE (Extrelut) extraction experiment.

N=6	Sparteine	Lupanine	13-OH	Total
	<i>mg per 100 g DW</i>	<i>mg per 100 g DW</i>	<i>mg per 100 g DW</i>	<i>mg per 100 g DW</i>
Mean	-	115.1	15.7	130.8
SD	-	4.4	0.9	5.2
SD (%)	-	4%	5%	4%
Soxhlet (%) ^a	-	106%	85%	103%
p-value ^a	-	0.129	0.038*	0.442
Randall (%) ^b	-	89%	73%	87%
p-value ^b	-	0.018*	0.001*	0.010*

a) is referring to the Soxhlet extraction and quantification of *Lupinus albus* by GC-MS, b) is referring to the Soxhlet extraction and quantification of *Lupinus albus* by GC-MS. P-values were obtained by two-sided student's t-test and significant differences were marked by asterisk (*). More details can be found in Section 7.1.

The total alkaloid content of the SPE quantification shows comparable results in the case of Soxhlet (103 %) but significantly smaller results than Randall (87 %) extractions. In detail, Lupanine showed slightly higher concentrations for SPE than for Soxhlet, but lower concentration than determined by Randall. The p-value indicates that the difference in Lupanine concentration is insignificant between Soxhlet and SPE, but significant between Randall and SPE. However, this result is not given too much relevance, as this difference does not exist at higher concentrations, as shown for *Lupinus mutabilis*. In contrast to Lupanine, 13-OH did show for both Lupin varieties, significantly lower results. The 13-OH

concentration determined by SPE resulted in only 85 % of the determined concentration via Soxhlet and only 73 % via Randall extraction. The conducted t-test showed also a significant difference ($p < 0.01$) towards the Randall extraction and indicates that the issue with discrimination of the alkaloid also exists for low alkaloid-containing samples. Overall, Randall extraction seems to outperform SPE, which can be shown by the significantly higher results for all present alkaloids, namely lupanine, and 13-OH.

To avoid further speculation, the possibility of the difference in acidic and alkaline extraction agents was tested. Hence, *Lupinus albus* and *Lupinus mutabilis branco* beans were extracted and each elution was analyzed for its 13-OH and Di-OH content. The acidic extraction reagent was tested by using TCA and HCl. The alkaline extraction agent was tested by NH_3 (pH 10) and NaOH (pH 12). All quantifications were carried out by GC-MS and accumulated area calculations. A regression via the four parameter logistic curve were applied (see Section 3.4.3).

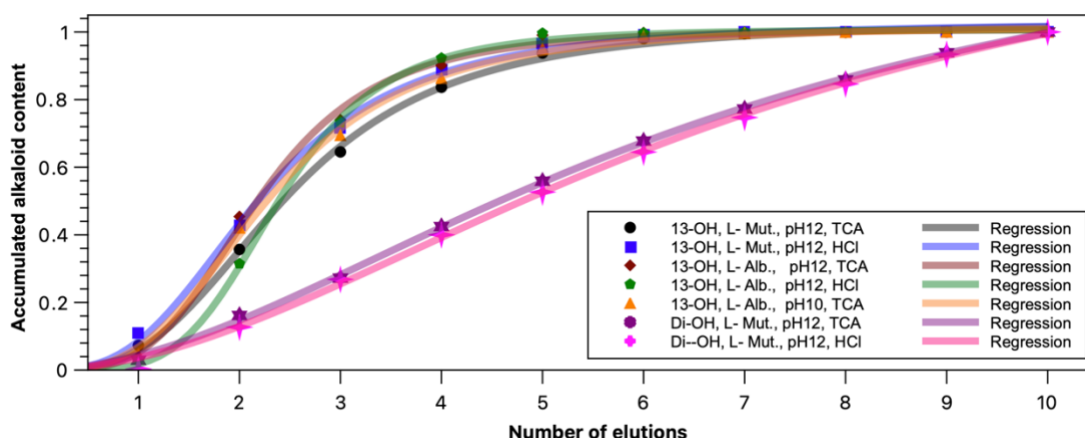


Figure 37: Effect of extraction parameter on the elution of 13-OH and Di-OH via SPE.

Regressions were applied by four parameters logistic curve with the program Qtiplot and parameters can be found in Table 62.

As shown in Figure 37, none of the applied conditions changed the elution behavior of 13-OH, the same is true for Di-OH. However, since the low alkaloid-containing species did not contain Di-OH it can only be shown for *Lupinus mutabilis branco* extractions. A closer look into the regression data (see Table 62) does show an increased p_4 parameter. This parameter indicates the highest reachable y-value. For 13-OH the p_4 parameter is around 1.0, which indicates that the chosen ten extractions are sufficient to show full extraction. However, the p_4 parameter is around 1.4-1.5 for the Di-OH extraction, indicating that ten extractions are not sufficient for the full Di-OH extraction.

In summary, it can be said that discrimination in alkaloid quantification takes place when the acid-base technique is applied. This is not due to the acid-base mechanism but to the following separation of alkaloids from the matrix via LLE or SPE. The here-shown method evaluation was purely focused on the quantification of alkaloids in *Lupinus mutabilis*, therefore the focus

was only on sparteine, lupanine, 3b-OH, 13-OH, and Di-OH. This means, that alkaloids in other species might also be affected by this method and the literature shown results are underestimating some alkaloids, which is not reported yet. In the case of *Lupinus mutabilis branco*, this underestimation can be demonstrated. Di-OH is reported as one of the minor alkaloids in *Lupinus mutabilis* beans^{8,9,31}, but it accounts for ca. 7 % in the here-tested species.

In summary, the extraction via acid-base mechanism and elution with an Extrelut column comes with improved LOD/LOQ values, good recovery rates, and cleaner chromatograms. However, this comes with the expense of an insufficient quantification of total alkaloid content through discrimination of polar alkaloids and should therefore not be used to determine thresholds of alkaloids in lupin products. Subsequently, other extraction methods like Soxhlet or Randall should be taken into consideration.

4.4.7 Method comparison

In this section the previously discussed analytical results from Soxhlet, Randall, LLE, and SPE extraction are summarized and compared to each other. Furthermore, non-analytical parameters such as investment costs, running costs, workload, and time are introduced and discussed.

Chromatogram:

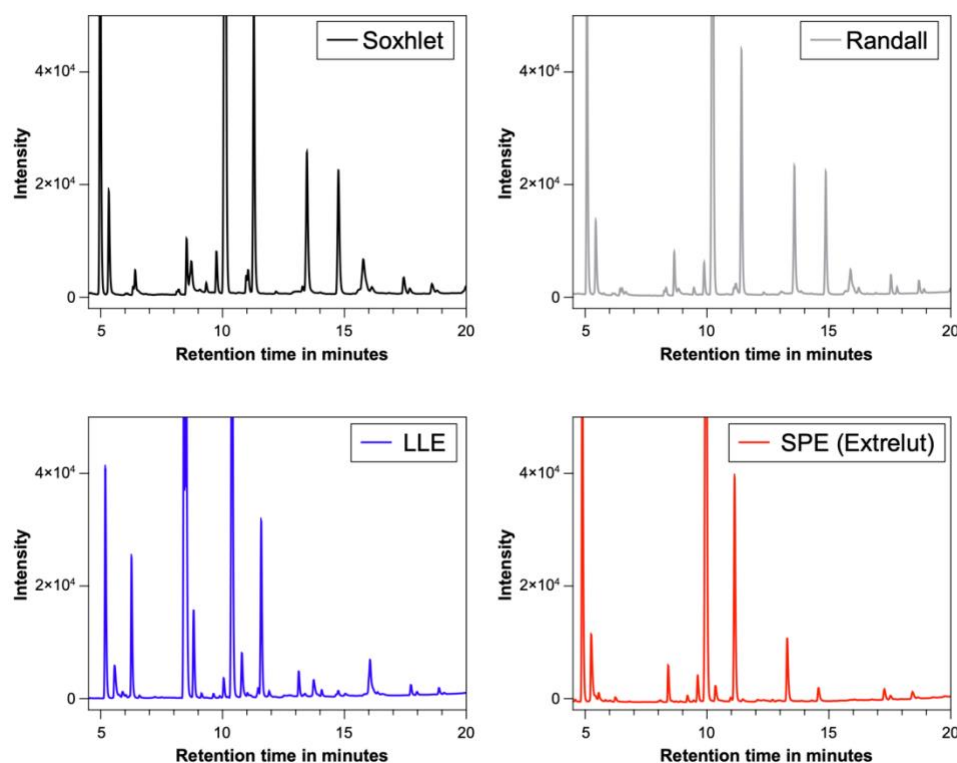


Figure 38: GC-FID chromatograms comparison of different extraction methods.

Soxhlet, Randall, and LLE show more peaks than the SPE (see Figure 38). GC-MS measurements have shown that the additional peaks are not alkaloids, but coextracted lipid components, which was also reported elsewhere ^{15, 22}. Hence, fewer peaks serve as a quality indicator for this comparison, suggesting that SPE should be preferred when aiming for a clean chromatogram

Recovery rate: The highest recovery rate can be found with SPE (98 %), followed by Randall and Soxhlet extraction. The LLE extraction showed a recovery rate of 80 %, respectively 66 % for low alkaloid-containing samples, which is not sufficient for a robust method. This means that Soxhlet, Randall and SPE have a sufficient recovery rate between 90 - 110 % for high and low alkaloid-containing samples.

Table 31: Recovery rate comparison of different alkaloid extraction methods.

	High Alkaloid content (<i>Lup. mut.</i>)	Low alkaloid content (<i>Lup. albus</i>)
Soxhlet	95 %	88 %
Randall	95 %	91 %
LLE	80 %	66 %
SPE	98 %	98 %

LOD/LOQ value: The LOD/LOQ values for measurements for Soxhlet and Randall extraction.

Table 32: LOD/LOQ value comparison for different methods.

	Sparteine <i>mg/100 g flour</i>	Lupanine <i>mg/100 g flour</i>	13-OH <i>mg/100 g flour</i>
Soxhlet	GC-FID:	GC-FID:	GC-FID:
Randall	LOD: 1.57	LOD: 2.14	LOD: 7.57
LLE (high alk.)	LOQ: 4.75	LOQ: 6.50	LOQ: 22.93
SPE (high alk.)	GC-MS:	GC-MS:	GC-MS:
	LOD: 0.24	LOD: 0.60	LOD: 0.76
	LOQ: 0.74	LOQ: 1.82	LOQ: 2.30
LLE (low alk.)	GC-FID:	GC-FID:	GC-FID:
SPE (low alk.)	LOD: 0.16	LOD: 0.21	LOD: 0.76
	LOQ: 0.48	LOQ: 0.65	LOQ: 2.29
	GC-MS:	GC-MS:	GC-MS:
	LOD: 0.02	LOD: 0.06	LOD: 0.08
	LOQ: 0.07	LOQ: 0.18	LOQ: 0.23

Table 32 shows that LOD/LOQ values for the GC-FID method with a Soxhlet or Randall extraction are not sufficient to quantify alkaloids in the threshold range of 20 mg/100 g. Therefore, a GC-MS method was developed, which helped to decrease the LOD/LOQ values

in those cases. However, the lowest LOD/LOQ values were still reached by acid-base extraction (LLE/SPE) and GC-MS determination.

Total alkaloid yield: The total alkaloid content of high and low alkaloid- containing species can be used to validate the trueness of the extraction method. The results of high alkaloid samples are summarized in Table 33. Based on these results the maximum obtained mass concentration was calculated for each alkaloid and presented in percentage in Table 34 (100 % is maximum).

Table 33: Average *Lupinus mutabilis* alkaloid extraction method yield.

N=10	Sparteine	Lupanine	3b-OH	13-OH	Di-OH	Total
	<i>mg per 100 g DW</i>	<i>mg per 100 g DW</i>	<i>mg per 100 g DW</i>	<i>mg per 100 g DW</i>	<i>mg per 100 g DW</i>	<i>mg per 100 g DW</i>
Soxhlet	596.5	2407.6	589.9	373.3	314.8	4282.1
Randall	612.8	2475.5	621.8	375.1	339.8	4424.9
LLE ^a	339.2	1775.0	495.0	65.1	16.6	2690.8
SPE	583.0	2418.4	632.7	190.3	51.0	3875.5

All shown results are quantified via GC-FID. a) is referring to the quantification of only six experiments.

Table 34: Maximum yield comparison between the methods for *Lupinus mutabilis branco* .

	Sparteine	Lupanine	3b-OH	13-OH	Di-OH	Total
Soxhlet	97%	97%	93%	100%	93%	97%
Randall	100%	100%	98%	100%	100%	100%
LLE	55%	72%	78%	17%	5%	61%
SPE	95%	98%	100%	51%	15%	88%

Results are normalized to the maximum obtained yield.

The highest total alkaloid content for high alkaloid-containing samples was determined for the Randall extraction (100 %). A similar extraction yield was shown by Soxhlet (97 %) and slightly smaller by SPE (88 %). Sparteine, lupanine, and 3b-OH are nearly similar extracted for the three methods, while 13-OH and Di-OH content is significantly smaller for the SPE method. As discussed earlier, this is related to a partial discrimination of more polar alkaloids during the elution. LLE shows the lowest result with a total alkaloid content of 61 % and is therefore not applicable for the here-tested *Lupinus mutabilis branco* species.

Table 35: *Lupinus albus* alkaloid extraction comparison quantified via GC-MS.

N=6	Sparteine	Lupanine	13-OH	Total
	<i>mg per 100 g DW</i>	<i>mg per 100 g DW</i>	<i>mg per 100 g DW</i>	<i>mg per 100 g DW</i>
Soxhlet	-	108.7	18.4	127.1
Randall	-	129.5	21.5	151.0
LLE^a	-	162.6	5.2	167.9
SPE	-	115.1	15.7	130.8

a) is referring to the quantification via GC-FID.

Table 36: Maximum mass concentration of *Lupinus albus* quantified via GC-MS.

	Sparteine	Lupanine	13-OH	Total
	<i>mg per 100 g DW</i>	<i>mg per 100 g DW</i>	<i>mg per 100 g DW</i>	<i>mg per 100 g DW</i>
Soxhlet	-	67%	85%	76%
Randall	-	80%	100%	90%
LLE^a	-	100%	24%	100%
SPE	-	71%	73%	78%

a) is referring to the quantification via GC-FID.

This trend can also be seen in the here-tested low alkaloid-containing species (*Lupinus albus*). The highest reported alkaloid content was carried out via LLE but was, contrary to all other measurements, carried out via GC-FID quantification and therefore not further considered in this comparison. For *Lupinus albus*, Soxhlet and SPE showed similar total alkaloid extraction, although the 13-OH discrimination was present. Hence, Randall extraction is also preferred for low alkaloid-containing samples.

Comprehensively, the results of the total alkaloid determination show, that LLE and SPE extractions are not suitable for a sufficient quantification of alkaloids, because of their discrimination of certain polar alkaloids.

Accuracy (Standard deviation): The accuracy is evaluated by the standard deviation of each method for low and high alkaloid-containing samples.

Table 37: Standard deviation for *Lupinus mutabilis* extractions via GC-FID.

N=10	Sparteine	Lupanine	3b-OH	13-OH	Di-OH	Total
Soxhlet	3%	4%	4%	4%	6%	4%
Randall	5%	6%	7%	7%	8%	6%
LLE^a	45%	40%	46%	41%	17%	41%
SPE	5%	4%	4%	7%	9%	4%

a) is referring to the quantification of only six experiments.

Table 38: Standard deviation for six *Lupinus albus* extractions via GC-MS.

N=6	Sparteine	Lupanine	13-OH	Total
Soxhlet	-	8%	14%	8%
Randall	-	9%	12%	9%
LLE^a	-	9%	17%	9%
SPE	-	4%	5%	4%

a) is referring to the quantification via GC-FID.

The high standard deviation for the *Lupinus mutabilis* LLE is a result of emulsion formation and a clear indication not to further consider this method. However, the three other methods are all within the same range, with the SPE providing slightly better results for the low alkaloid containing sample.

Other factors: The above-mentioned criteria can help to evaluate the method based on analytical criteria. However, other non-analytical criteria might be considered. The following table shows the evaluation of different cost-related criteria based on the experience during the preparation of this thesis.

Table 39: Summary of non-analytical extraction method comparison criteria.

	Investment costs	Running costs / Resources	Workload	Time
Soxhlet	Med.	Low	Low	Med.
Randall	High	Low	Low	Low
LLE	Low	Low-Med.	Med.	Low
SPE	Low	Med.	Med.	Low

The listing is sorted by appearance in the text and evaluated solely by the experience of the author.

The lowest investment costs are with LLE and SPE extraction, since only a few beakers and a Liquid-liquid separator respectively a column needs to be purchased and can all be found in common lab facilities. Soxhlet is also often a part of a lab facility, but comes with higher investment costs, since a Soxhlet extractor and a suitable condenser unit are required. Randall is less common and more expensive since it can operate a rinsing and cooking step simultaneously, which results in the highest investment cost in this comparison.

However, the running costs/resources are quite cheap for Soxhlet and Randall, they only require a solvent (here methanol), which also can be recycled after use. LLE and SPE require an acid, a base, and DCM. While the acid and the base cannot be recycled, DCM can be recycled, although not as good as methanol, with respect to its volatility. The SPE route also requires the use of an Extrelut column material, which is a specially treated diatomaceous earth from Merck, which should not be reused.

The workload for SPE and LLE extraction is higher than for Soxhlet and Randall. Soxhlet and Randall extraction have a weighing step, an evaporation step, and a re-dissolving step, but most of the process is performed automatically in the background and the operator's time can be spent on other tasks. LLE and SPE have more labor involved, and the operator is dedicated to this process.

For all extraction methods, the total required time is low, except for Soxhlet. The here-shown Soxhlet protocol requires at least 5 h (25 cycles).

4.4.8 Final evaluation

All in all, does the comparison of the four tested methods reveal, that Randall extraction is the most advantageous option. The only drawback is the relatively high LOD/LOQ values causing problems for the low alkaloid-containing species. However, it has been shown that this value can be reduced to reasonable levels by GC-MS operation, in which case the alkaloid must be present as a standard for quantification.

Randall extraction showed the highest total alkaloid content for high alkaloid-containing lupin beans. The tested individual alkaloid content was always the highest in the direct comparison, except 3b-OH which was insignificant smaller (98 %, see Table 29) in comparison to the maximum found yield with SPE. For low alkaloid-containing samples, LLE has a slightly higher total alkaloid content determined, which is related to the extremely low recovery rate (66 %, see Table 31) and to a different analysis method (GC-FID). This makes the result unreliable and therefore also for low alkaloid-containing lupin beans, Randall extraction is superior.

If Randall is not available, Soxhlet extraction should be still preferred over the currently most used extraction via acid-base mechanism and separation by LLE or SPE. With the here-tested samples, LLE showed emulsion properties, which decreased the accuracy and recovery rate. The SPE has the advantage of avoiding contamination of the chromatogram with non-alkaloid species, thus leading to very clean chromatograms and easy analysis. Also, the LOD/LOQ values are smaller (better) for this method. However, in this thesis, it was proven that the currently used protocol for this method shows discrimination of certain alkaloids and therefore shows significantly smaller alkaloid contents for the tested sample. It was shown that the 13-OH was insufficiently extracted and Di-OH was only poorly extracted. In the case of Di-OH, only 15 % of the Di-OH value was found in comparison to Randall. Because SPE is common and applied for years in literature it results in an underestimation of 13-OH and Di-OH for *Lupinus mutabilis*. Especially Di-OH is counted as a minor alkaloid^{8,9,31}, although its original concentration inside the here-tested lupin bean *mutabilis* species is with ca. 7 % nearly as high as 13-OH (9 %). Therefore, Di-OH should not be declared as minor alkaloid. This finding has a high chance of affecting also other lupin species since the currently used method

discriminates certain alkaloids, which would lead to a reevaluation of other lupin species and the currently used threshold of 20 mg/ 100 g DW.

4.4.9 Reasons for the insufficient alkaloid extraction via acid base extraction

The solvent extraction with methanol (Soxhlet, Randall) showed sufficient extraction effectiveness for sparteine, lupanine, 3b-OH, 13-OH, and Di-OH, while the acid-base extraction with SPE showed only sufficient results for sparteine, lupanine, and 3b-OH, but insufficient results for 13-OH and poor results for Di-OH. After soaking the alkaline solution into the Extrelut material, the SPE applies DCM as a non-polar eluent. This is probably the crucial step where the 13-OH and Di-OH are discriminated. As shown in later experiments, both alkaloids prefer the aqueous phase over the organic phase (see Section 4.4.12). This might also be the reason why an emulsion is formed via LLE (see Figure 33).

It could be speculated, that the higher water affinity is related to protonated nitrogen groups, however, since the pK_a of 13-OH is lower than the one of lupanine, this is probably not the case (see Table 2) ¹⁷.

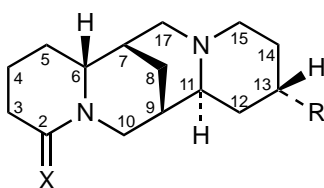


Figure 39: Schematic drawing of the lupanine family structure.
Figure was adapted according to Hemscheidt and Spenser ⁹⁷.

It is more conceivable that the hydroxyl group at position 13 (see Figure 39) is responsible for the higher water solubility of 13-OH and Di-OH. With the hydroxyl group on one side and the carbonyl group on the other end, the molecule might be polar enough to be water soluble, especially if there is a second hydroxyl group at the 3 position as shown in Di-OH.

Sparteine, 3b-OH, and lupanine have in common to be non-polar and do not have a hydroxyl group on the opposite side to the carbonyl group.

This finding might impact future alkaloid extraction strategies and official protocols to determine the alkaloid content of lupin products, since it was shown, that the most common method (SPE) gives lower results than traditional methods. It also needs to be evaluated, if an alkaloid which is more water-soluble changes the toxicity classification of the lupin bean, so this finding could have an even greater impact on the food and water safety.

4.4.10 Ranking unknown *Lupinus mutabilis* samples from Lisbon seed bank



Figure 40: Picture of the samples from the seed bank of Portugal.

In total 76 *Lupinus mutabilis* samples with a mass of around 15 g (depending on the sample) were obtained from the Lisbon seed bank. Randall extraction was proven to be superior to other extractions, which is the reason why it was chosen as the extraction method. The stability of the extraction method was continuously monitored and the Steward chart (see Figure 41), did not show any up or downwards trend.

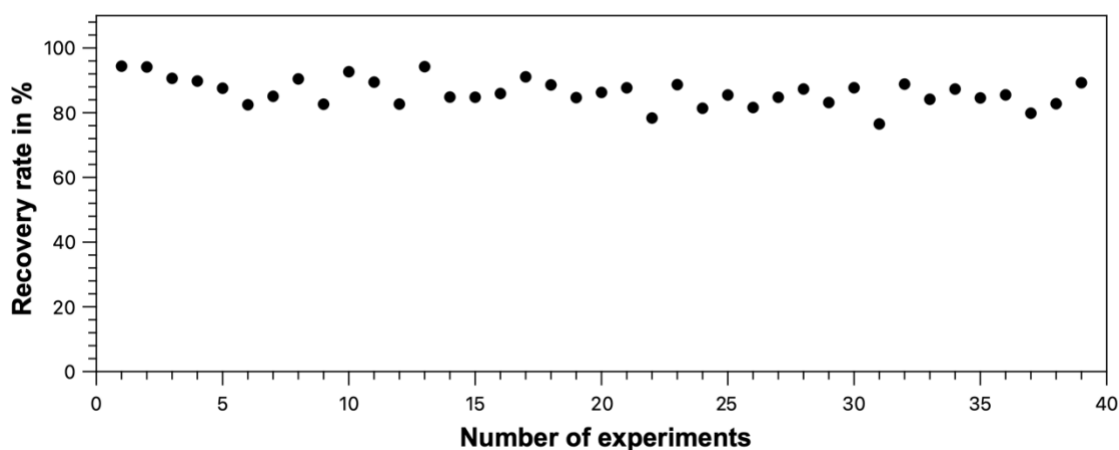


Figure 41: Steward chart of the average recovery rate.

One experiment refers to the average of six samples, which is the maximum the Randall unit can handle.

The detailed results regarding the concentration of the samples can be found in Section 7.2. In the following, the results are briefly summarized. The analysis of the seed bank samples via the GC-FID method showed that the lupin samples contained in the lowest detectable case

7.8 mg/100 g DW and in the highest case 4738.9 mg/100 g DW. Twelve samples did not show any quantifiable alkaloid content, since no peaks or only concentrations below LOD/LOQ values could be detected (see details in Section 7.2).

As discussed earlier, the extraction via Randall and analysis via GC-FID is preferred for a total scanning of alkaloid content. However, for small alkaloid content, the GC-FID determination is not sensitive enough, so the already introduced method of GC-MS via SIM was performed. With the lower LOD/LOQ values, it could be shown that 16 out of the 76 samples showed lower alkaloid content than 20 mg per 100 g DW and are therefore considered safe to consume.

Furthermore, it was found that the GC-MS results tend to show slightly higher results for the total alkaloid content than the GC-FID measurements. This is related to the calibration curve, which shows a slightly different slope for the GC-FID measurements than for the GC-MS measurement and was discussed earlier (see Section 4.4.6).

4.4.11 Chromatographic behavior of alkaloids from *Lupinus mutabilis branco*

To understand the chromatographic behavior of the alkaloids, many thin-layer chromatography (TLC) experiments were conducted. In general, it was found, that reasonable mixtures of ethylacetate/hexane were not strong enough to elute the alkaloids. Stronger two-component mixtures as MeOH/DCM, were able to elute the alkaloids but showed strong tailing effects. This tailing effect could be compensated by introducing triethylamine (TEA) into the mixture. TEA is an amine and helps to eliminate the acidic component of the silica gel. If not using TEA (or a similar alkaline additive), the acidic silica group will protonate the amine group of the alkaloid. This increases the polarity of the alkaloids and reduces the elution by an organic solvent. Good TLC Results were obtained by using 5 % MeOH/DCM (v/v) and the addition of 1 % TEA (v/v).

The detection of alkaloids on TLC plates was tested with ninhydrin solutions and Dragendorff reagent. Better results were obtained with the Dragendorff reagent and therefore chosen for all further experiments.

4.4.12 Isolation of quinolizidine alkaloids from *Lupinus mutabilis branco*

In the following, the purification of alkaloids as described in Section 3.2.2 is discussed and a few suggestions for future purifications are mentioned. It should be noted that this series of experiments was carried out once and no effort was taken to increase the recovery rate or to optimize single steps. The steps refer to the method overview presented in Figure 17.

Method: In the first step, the ground lupin beans were extracted via Soxhlet extraction. Although Randall extraction has several benefits (as discussed earlier), Soxhlet extraction

allows the easy upscaling of sample amount and was therefore chosen. After the cleaning and preparation (step 2-4), the first preparative column was carried out (step 5) and the fractions were analyzed with GC-FID. The results are presented in Figure 42 as an absolute (Figure 42 a) and relative (Figure 42 b) comparison of the alkaloid concentration in each fraction (see Section 3.4.6).

The elution of the 5 % MeOH/DCM + 1 % TEA-containing eluent was collected in fractions 1-34, before switching to the more polar eluent of 20 % MeOH/DCM + 1 % TEA, which elution was collected in fractions 35 to 47. As can be seen in both figures, the alkaloids are eluted in the following order: Lupanine, 3b-OH, 13-OH, Di-OH, sparteine. The order of elution fits with the increasing polarity of the molecule, except sparteine, which was due to polarity expected to elute first but represents in this experiment the last fraction.

The first eluent (5 % MeOH/DCM) does elute lupanine and 3b-OH from the column. However, the chromatography was not sufficient to separate them from each other. The relative elution profile shows that the majority of lupanine content is eluted before most of the 3b-OH content is eluted.

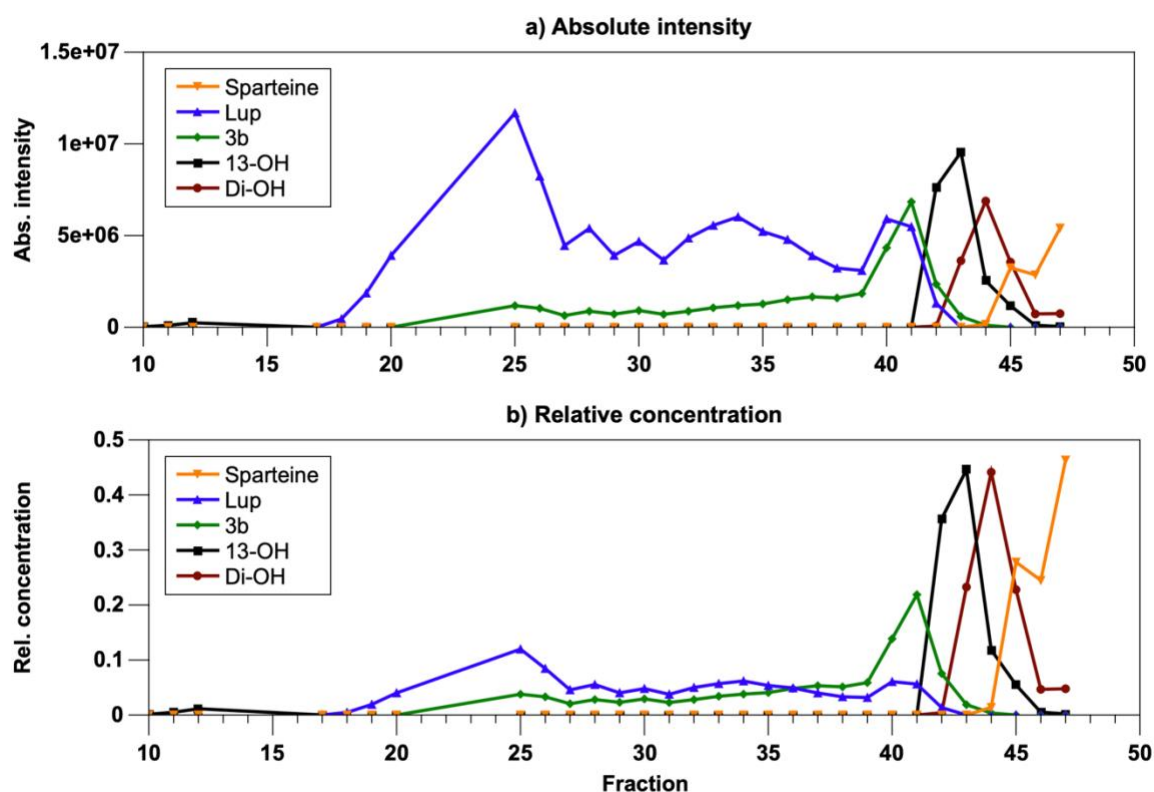


Figure 42: Alkaloid column elution profile for normal phase (NP).

a) Absolute Intensity (GC-FID) is based on the area of an alkaloid per fraction.

b) Relative concentration (GC-FID) is based on the abundance of a particular alkaloid in one fraction in relation to the abundance of this alkaloid in all fractions.

Despite this, the absolute lupanine content in fractions 39 to 43, where most 3b-OH can be found, is still nearly as high as the 3b-OH content (see Figure 42). This is related to the high initial lupanine concentration inside the lupin flour. On the one hand, it could be speculated that the use of more stationary phase and fewer sample would be beneficial for the separation and would allow a complete separation of lupanine and 3b-OH. On the other hand, the TLC (see Table 10) does also not show a good separation of those two alkaloids.

The increment of the eluent's polarity to 20 % MeOH elutes the above-discussed remains of the 3b-OH/lupanine fraction (fraction 39-43), followed by 13-OH (Fraction 42-45), Di-OH fraction (Fraction 43-47) and sparteine (Fraction 45-47).

Although the structure of 13-OH and 3b-OH only differ from the position of the hydroxyl group, the chromatographic behavior differs a lot. While 3b-OH behaves similarly to lupanine and elutes simultaneously, 13-OH behaves much more polar and elutes only, if a more polar eluent is applied. This behavior was also found for the analytical acid-base extraction as discussed in Section 4.4.11.

The order of the elution follows therefore the polarity of the alkaloid, with sparteine as an exception. Sparteine is the most non-polar alkaloid of this group and was therefore expected to elute first and not last during a normal phase chromatography. However, the alkaloid's chromatographic behavior is also linked to the acidity of the alkaloids, which differs in dependence on the substitution and ionization of the molecule. Sparteine is the ground structure for the here-discussed alkaloids, having two tertiary amine groups and an estimated pK_a value of ca. 12¹⁷ for the corresponding acid (see Table 2). This high pK_a results from the cyclic aliphatic ring stabilization of the potential ammonium ion via the +I effect. Ammonia (pK_a 9.2) and triethylamine (pK_a 10.7) are used to eliminate the acidic components of the silica gel but offer a pK_a value smaller than sparteine. This means it is highly likely, that at the described conditions at least one of sparteine's amine groups is protonated, which results in ionization and therefore in the reported higher retention.

Lupanine (pK_a 9.4¹⁷, 9.1¹⁸), 3b-OH, 13-OH (pK_a 8.8¹⁷), and Di-OH are considered as lupanine-type quinolizidine alkaloid⁹⁸. They contain two amine groups, but contrary to sparteine, the aliphatic cyclic rings are substituted with a carbonyl group. 3b-OH, 13-OH, and Di-OH do also contain an additional hydroxyl group, which also acts as an electron acceptor group and removes the electron density from the potential ammonium ion. This leads to a reduction of the stabilization effect of the ammonium ion. Furthermore, the carbonyl group is located next to the nitrogen atom and the combination is considered to be a N,N-dialkylamide, which is partly resonance stabilized (see the following figure).

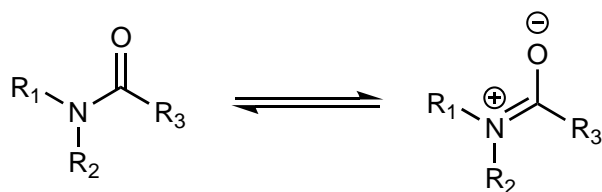


Figure 43: Resonance stability of an *N,N*-dialkylamide.

The resonance stability and the substitution with an electron acceptor functional group decrease the pK_a and allows easier deprotonation, which ultimately leads to a lower polarity and the experienced results⁹⁹. However, although sparteine was separate from the other alkaloids, no action was taken to purify sparteine, because sparteine can be bought in (for analytical chemistry) large quantities at reasonable prices (500 mg, 63.40 €, Merck, 05.02.2024).

In conclusion, it can be said that a rough separation of alkaloids took place but was not sufficient to have purified fractions. Therefore, another purification step was considered, and it was chosen to use preparative liquid chromatography (step 6).

The idea of using a reversed-phase separation lies in the completely changed order of elution. For this, some of the fractions from the preparative column (step 5) were combined and then separated via reversed-phase technology with 5 % MeOH in 10 mM Acetic acid. All newly obtained fractions were analyzed via GC-FID, before similar fractions were combined.

In the following step (step 7), the combined aqueous fractions were extracted via LLE and again analyzed via GC-FID. The measurement confirmed that for the combined lupanine and 3b-OH fraction, the extraction via LLE resulted in pure fractions. However, it was found that LLE was not applicable for Di-OH and very limited for 13-OH. It was found that Di-OH and 13-OH prefer the aqueous layer over the organic layer during the LLE and could therefore not be purified. This was a groundbreaking result since it proved the discrimination of Di-OH and 13-OH, that occurred during acid-base extraction. In Figure 44a, the aqueous fraction from the preparative column separation still contains 13-OH although it was extracted via LLE with 3×10 mL DCM. However, some of the 13-OH is transferred into the organic layer, where most of it is washed out during the second washing step of the organic layer via 3×15 mL water. This clearly shows the affinity of 13-OH towards the aqueous phase and explains also why 13-OH is only partially extracted via acid-base extraction in previous experiments. However, Di-OH has an even higher affinity towards the aqueous phase. Figure 44b reveals, that the DCM extract does not contain any reasonable amount of Di-OH after washing. Furthermore, it was found that the amount of Di-OH in the later gained washing fraction is lower than in the previously remaining aqueous fraction. This means that only a small amount of Di-OH was able to be dissolved inside the DCM layer but got later completely transferred into the aqueous phase again.

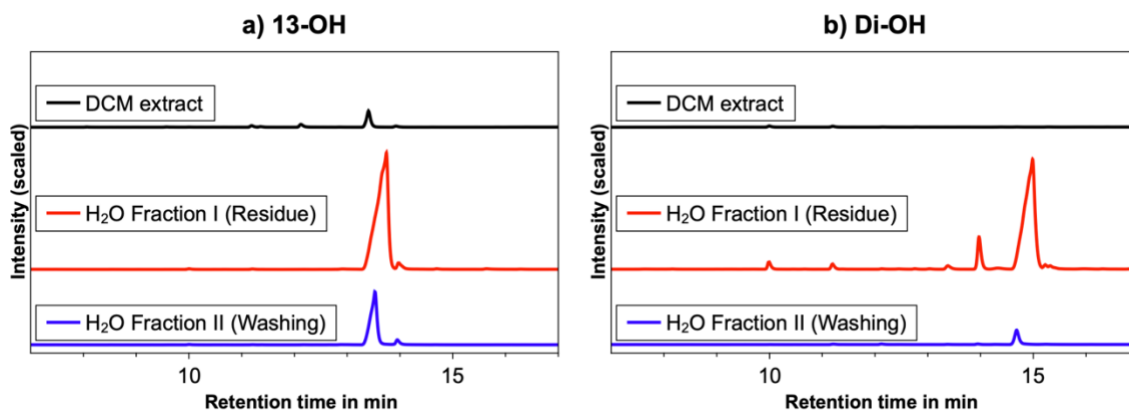


Figure 44: Solvation behavior of 13-OH and Di-OH during LLE.

Both, a) 13-OH, Rt: 13.5 min and b) Di-OH, Rt: 14.8 are in true intensity scale ratios. The previously gained aqueous fraction from the preparative column (see step 6 from Figure 17) was extracted via DCM by LLE. The DCM layer was further washed with water. The remaining aqueous fraction, which was extracted by DCM initially, is called H₂O fraction I (Residue, red), the washing fraction of the DCM extract is called H₂O fraction II (Washing, blue), and the DCM fraction after those extractions took place is called DCM extract (black). All samples were concentrated to 1 ml and analyzed via GC-FID.

The high affinity towards the aqueous phase was only found for 13-OH, respectively Di-OH. Lupanine and 3b-OH were fully extracted and could be found in yields greater than 90 % in the organic phase. This means, that LLE has the potential to separate the polar from apolar alkaloids and might have helped in the isolation of lupanine and 3b-OH. However, for the isolation of 13-OH and Di-OH another separation step needs to be carried out. This was done by applying the 3b-OH respectively Di-OH fraction onto a NP column (step 8).

Results:

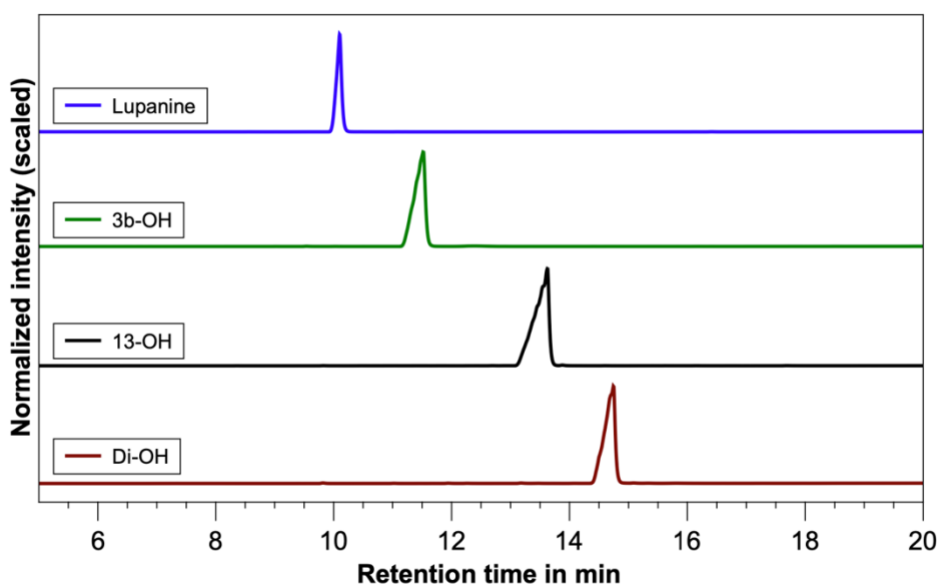


Figure 45: GC-FID analysis of purified alkaloid fractions in MeOH.

Tailing is due to extreme high concentration.

Table 40: Extracted mass and recovery rate for the purification.

	Lupanine	3b-OH	13-OH	Di-OH
Mass (mg)	40.26 mg	18.39 mg	23.94 mg	10.90 mg
Recovery rate (%)	8%	14%	31%	15%

The results are based on 22.98 g initial used lupine beans and a moisture content of 9.1 %.

The method resulted in purified fractions which were tested by GC-FID (see Figure 45) and showed a purity of over 95 % for all alkaloids. The recovery rates are determined to be between 8 and 31 %, which is quite low. The lowest yield (recovery rate) is given by lupanine. This is related to the fact, that not all lupanine-containing fractions from the normal phase separation (step 5) were used to purify lupanine. Secondly, were also not all fractions from the Prep-LC (step 6) used since during the elution of lupanine some coelution of other components took place. The fraction with the coeluting impurity was not further considered. The latter one is also true for 3b-OH. The low yield of 13-OH and Di-OH might be related that not all Di-OH and 13-OH are extracted fully from the normal phase column (step 5). However, the GC results show that clean fractions were obtained. This allows the use of the extraction method to produce a standard for calibration purposes, which was a previously bottleneck for GC-MS quantification (see Section 3.3.3).

Improvements for further alkaloid isolation experiments: For the purification of alkaloids, no optimization steps were conducted to increase the recovery rate. However, for carrying out another alkaloid isolation experiment, the following optimization steps are suggested.

The separation of lipids and alkaloids could be avoided by using a hexane Soxhlet extraction before the extraction of alkaloids via Soxhlet and methanol is carried out. Secondly, if a normal column chromatography is desired, it is recommended to always place the alkaloids on silica, since it helps to create a narrow band of eluting the alkaloids. In general, TEA showed better separation than NH₃(aq) and should therefore be applied in the MeOH/DCM mixture. The normal phase separation (step 5) should therefore be carried out with 10 % MeOH/DCM + 1 % TEA. Lastly, the column chromatography in step 5 showed overloading effects, which could be avoided by using a smaller amount of sample. If a normal phase column for a preparative LC system is available and can withstand high pH, it is advisable to replace the open column chromatography from steps 5 and 8.

4.4.13 Alkaloid extraction via scCO₂

Among all the here-shown extraction strategies, the application of scCO₂ is another suitable option to extract alkaloids or debitter the lupin products. However, the polar behavior of the alkaloids (see above) makes the use of CO₂ less applicable. Pure scCO₂ is a relatively nonpolar reagent and therefore often applied to extract lipids from a matrix (see Section 7.5

and Section 7.6). However, a modifier such as water, methanol or an alkaline agent might be introduced to increase the polarity which was also shown by Kim, Mae Cho, and Yoo¹⁰⁰. It seems that the extraction via scCO₂ and cosolvent is an option but might be less efficient than Soxhlet or Randall extraction. However, other options as the use of ionic liquid might be considerable but are beyond the scope of this thesis.

4.5 Protein extraction of lupin beans

Alkaloids are one of the challenges of lupin beans because no clear utilization has yet been found. However, in contrary to alkaloids, proteins are known to be utilized for food and feed purposes. One of the biggest advantages of lupin beans is the high protein content compared to other crops and is therefore researched in this thesis. Therefore, several different extraction methods were tested to extract proteins from the lupin bean matrix, which differed in applied extraction mechanism and sustainability. All applied methods involved wet processing, which means that all processes involved the application of aqueous solutions.

4.5.1 Choice of protein determination method

To evaluate the effectiveness of an extraction method, the protein content of the sample as well as the total protein content needs to be known, therefore the choice of an adequate protein determination method is crucial. Common protein determination methods are the Bradford protein assay, Lowry protein assay, Bicinchoninic acid assay (BCA), Amino acid determination, Dumas or Kjeldahl nitrogen determination. Bradford, Lowry, and BCA require the proteins of the sample to be dissolved in an aqueous solution and are affected through interference with the sample matrix. In preliminary tests with raw lupin protein, those methods showed solubility issues and interference, leading to inconsistent results. Therefore BCA, Bradford, and Lowry were not further considered.

Amino acid composition determination is a sufficient method to prove the actual protein content and does not interfere with other substances. This method involves hydrolyzation, derivatization (not always required), and analysis via HPLC¹⁰¹. Although this method allows a good quantification of the protein content, it is very labor-consuming and therefore inapplicable for the fast analysis of multiple extracts.

However, Dumas and Kjeldahl nitrogen determination are robust and fast methods. Both methods refer to the nitrogen content of the sample. This nitrogen content is related to the protein content via their amino acid composition. A nitrogen conversion factor of 6.25 is recommended for legumes (see Section 2.3.2). Most publications are using a conversion factor of 6.25 for lupin proteins, although it is known that this could lead to an overestimation

of the actual protein content ^{8, 102, 103} and a slightly lower nitrogen conversion factor of 5.8 ¹⁰⁴ might be more realistic.

In this thesis, protein content is mostly measured by Kjeldahl nitrogen determination, and a conversion factor of 6.25 is used for better comparability with other literature.

4.5.2 Protein content of *Lupinus mutabilis* beans

The protein content is calculated by Kjeldahl nitrogen determination of defatted *Lupinus mutabilis branco* beans (see Section 3.2.3). The experiments were carried out on different dates during a period of one year and used to calculate an average (see details in 3.4.11).

Table 41: Calculated protein content of *Lupinus mutabilis* flour with different properties.

Description	Value
Nitrogen content of defatted flour, FW	8.8 ± 0.1 %
Protein content (N × 6.25) of defatted flour, FW	55.1 ± 0.7 %
Protein content (N × 6.25) of full-fat flour, FW	44.6 ± 0.6 %
Protein content (N × 6.25) of full-fat flour, DW	49.1 ± 0.6 %

Based on these results, dry full-fat *Lupinus mutabilis branco* contains 49.1 ± 0.6 % protein, which means that half of the lupin material is protein. Although the actual protein content might be slightly lower, due to the overestimated Kjeldahl factor, the protein content is very high in comparison to other crops ⁴⁶.

4.5.3 Method comparison

Several different methods for protein extraction were tested and an abstract process overview was given in Figure 5. Most tested parameters are based on already reported experiments for other crops or other lupin varieties. The details are listed in Section 3.2.4 and a summary of the results is given in the following table. Since Lupin beans contain mostly globulins as the major Osborne fraction (see Table 4), extraction methods involving the ionic strength and pH were followed. The results presented in Table 42 are based on the final product, referring to *Precipitate II* in the process (see also Figure 5). The extraction via the CO₂-only process showed no successful extraction and is therefore purely listed as a method comparison. Salting out, IEPP, and IEPP-CO₂ have shown a protein concentration of 90 % or higher in their final product. These results indicate that all three methods can extract and concentrate proteins from the initial lupin flour matrix nearly to the same level. However, a difference can be seen by looking at the nitrogen recovery. While the salting out process results in a nitrogen recovery of 40 %, the nitrogen recovery values of both IEPPs (IEPP, IEPP-CO₂) outperform the salting out process with 54 %, respectively 55 % nitrogen recovery. Furthermore, this also

indicates, that the use of CO₂ instead of 1 M NaOH is a reasonable replacement, which can even lead to slightly higher yields than reported for the IEPP (as discussed later).

Table 42: Overview of protein extraction process parameters and results.

	Salting out	IEPP	IEPP-CO ₂	CO ₂ -only
1. Sample preparation	0.5 mm, defatted	0.5 mm, defatted	0.5 mm, defatted	0.5 mm, defatted
2a. Mixing	1:8 (w/w), 1 h, 30 °C,	1:10 (w/w), 1 h, pH 8.5, 20 °C	1:10 (w/w), 1 h, pH 8.5, 20 °C	60 bar, 1 h, 4 °C
2b. Reagent A	0.5 M NaCl	1 M NaOH	1 M NaOH	CO ₂
3. Separation	Centr. 10 min, 4000 RPM	Centr. 10 min, 4000 RPM	Centr. 10 min, 4000 RPM	Filtration 2 µm
4a. Mixing	1:3 (w/w), 16 h, 4 °C	pH 4.5, 1 h, 20 °C	60 bar, 1 h, 20 °C	60 bar, 1 h, 20 °C
4b. Reagent B	H ₂ O	1 M HCl	CO ₂	CO ₂
5. Separation	Centr. 10 min, 4000 RPM	Centr. 10 min, 4000 RPM	Centr. 10 min, 4000 RPM	Filtration 2 µm
Reference	53	50	52	-
Mechanism	Ionic strength	IEP	IEP	IEP
Nitrogen rec.	40 %	55 %	54 %	-
Protein conc.	93 %	90 %	91 %	-
Total alkaloid	249 mg/100 g	774 mg/100 g	2055 mg/100 g	-

The indicated numbering is referring to Figure 5. A more detailed process description can be found in Section 3.2.4.

The lower yield from the salting out process compared to the two IEPP-based processes is related to the two different extraction mechanisms. While the salting out process aims to separate the albumins and globulins via ionic strength from the remaining matrix, the IEPP precipitation aims to separate the globulins and glutelins from the matrix (see Table 4). This lower yield for the salting out process is contrary to the expectation since a bigger albumin than glutelin fraction was expected (see Table 5). However, the reported fractions in Table 5 might also depend on species, origin, and growing conditions and therefore differed from the here-tested *Lupinus mutabilis branco* sample.

Another important factor is the alkaloid content of the final product (*precipitate II*). The quantification is based on Randall extraction and GC-FID analysis. The comparison demonstrates that the three methods differ significantly in alkaloid content. The highest alkaloid content in the protein concentrate (*precipitate II*) was 2055 mg/100 g, found for the IEPP-CO₂ process. A smaller alkaloid content was shown by the IEP process with 774 mg/100 g. The lowest alkaloid content was 249 mg/100 g, which refers to the process of applying ionic strength as a separation mechanism (salting out).

This means, that the salting out process compensates its low nitrogen recovery with low alkaloid contaminated product. However, the desired 20 mg/100 g FW, which is considered as a safe threshold, has still not been reached. This goal could be reached, when a debittering step is carried out prior to protein extraction but was not further tested.

Furthermore, it could be speculated, that the low alkaloid content for the salting out extraction might be related to the high-water content applied to precipitate the fraction. For 100 g of sample ca. 3.2 L aqueous solution was applied. In comparison, for both IEPP processes were ca. 1.0 L aqueous solution used for 100 g initial flour. If considering the water solubility of the alkaloids as shown in Section 4.4.12, this is a reasonable explanation.

As already stated earlier, both IEPPs have higher alkaloid content inside the final product. However, although both IEPPs (IEPP and IEPP-CO₂) applied the same mechanism, applied the same amount of aqueous solution and resulted in the same nitrogen recovery, the alkaloid content in the final product differed by a factor of around 3. One reason might be that no stirring could be applied for the precipitation of *supernatant I* in the IEPP-CO₂ process. On the contrary, the IEPP was continuously stirred, because 1 M HCl (reagent B) was added, and a full distribution was needed to avoid formation of pH gradients. This is not the case for the IEPP-CO₂ process since dissolved CO₂ cannot reach a pH as low as 1 M HCl. This might have led to alkaloids attaching to the freshly precipitated protein and not being in equilibrium with the surrounding aqueous milieu, where they could have been dissolved. Another explanation could be, that the pH reduction exceeded the IEP and might led to lower than necessary pH values during the precipitation. The alkaloid solubility is at pH 3 lower than at pH 4 (see later in Figure 50), which could have resulted in the alkaloids being trapped in the precipitated protein and therefore not being in equilibrium with the surrounding media. After depressurization, the pH might have increased to the IEP, leading to more precipitated protein but reducing the chance of equilibration of the alkaloids with the aqueous media.

Lastly, the temperature was different. Although both precipitation processes are carried out at 20 °C (see Table 42). The final temperature of the IEPP-CO₂ suspension was cooler. This is related to the application of liquid CO₂ (60 bar, 20 °C), which will cool down during the depressurization step due to the expansion of CO₂ (Joule–Thomson effect).

Nevertheless, the salting out process also applied a cooling step for the precipitation, but leads in contrary to the IEPP-CO₂, to low alkaloid content inside the final product.

4.5.4 Influence of pH on the protein solvation

The above-shown IEPP and IEPP-CO₂ methods applied a pH of 8.5 to dissolve the proteins (see step 2 in Figure 5). To understand if this is the most optimized pH value, the influence of the pH on the protein solvation was tested. The below-discussed results are therefore referring to the intermediate after the first separation and not the final product.

The here-tested IEPP process uses 1 M NaOH as *Reagent A* and 1 M HCl as *Reagent B* (see Figure 5). To determine the pH-dependent weight and nitrogen solubility, the sample preparation (step 1) and mixing (step 2) were kept constant and only the amount of *reagent A* (1 M NaOH) was adjusted. The amount was changed to reach an integer pH range from 1 to 12 with an increment of 1 (see Section 3.3.4). After a separation step (step 3), the gained supernatant fractions (see Figure 46) were analyzed in terms of weight and nitrogen content. The results are presented as figures for mass fraction (Figure 47), nitrogen yield (Figure 48) and protein concentration (Figure 49) of the supernatant, and precipitate (see Section 3.4.11). The figures are prepared from the solvation data, which are presented in Section 7.3.

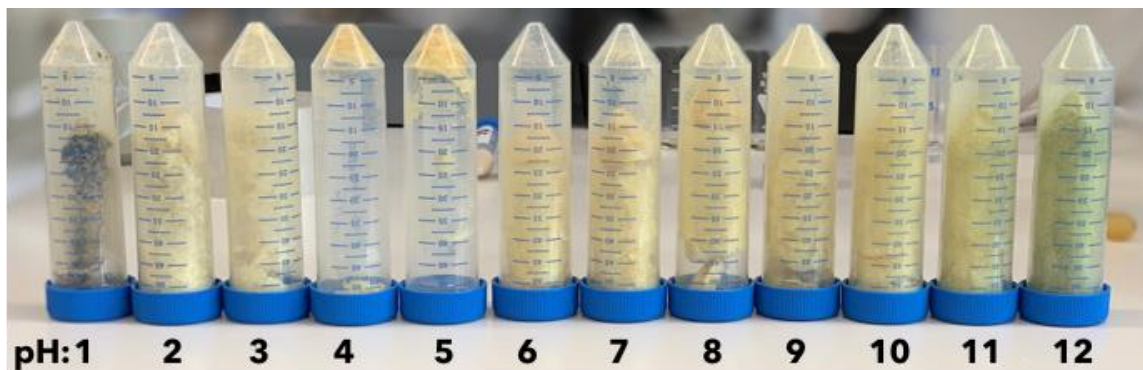


Figure 46: Picture of freeze-dried supernatant I fraction after pH treatment.

Figure 46 displays the 12 gained fractions. Most lyophilized supernatant fractions result in a yellow-colored residue. An exemption is shown by extremely low (pH 1) or high pH values (pH 12). Those samples showed a blackish (pH 1) and greenish color (pH12).

Weight distribution: The weight distribution between the two fractions (*supernatant I and precipitate I*) is shown in the following figure.

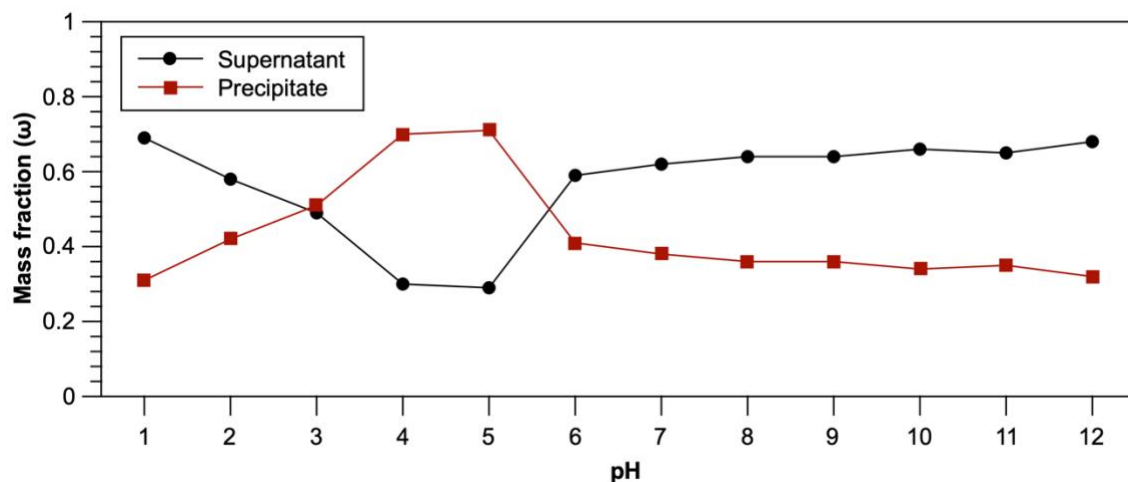


Figure 47: Influence of pH on the mass fraction (after drying).

It can be seen that the supernatant mass fraction decreases from pH 1 continually to pH 4/pH 5, where it reaches its minimum before it increases with higher pH values again. The biggest change can be found between pH 5 and pH 6. However, from pH 6 to higher pH values, the mass fraction of the supernatant did only slowly but gradually increase. The overall highest mass ratio of the supernatant was reached at pH 1 and the lowest at pH 5.

Nitrogen Concentration: Additionally, to the mass fraction, the nitrogen concentration of the supernatant was analyzed via Kjeldahl and presented in Figure 48.

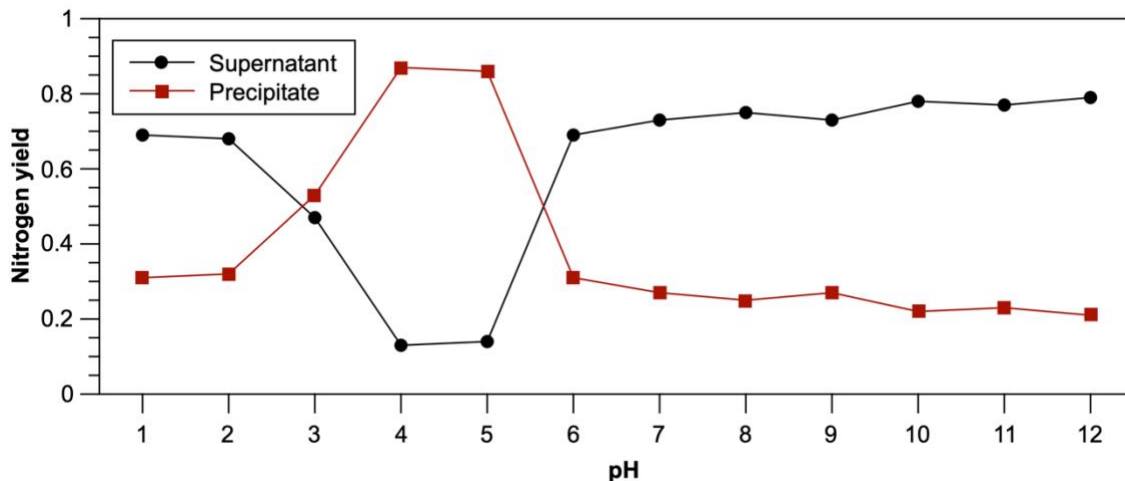


Figure 48: Influence of pH on the nitrogen concentration.

A high nitrogen solubility means, that a high nitrogen concentration is found in the supernatant. The results of the previously discussed weight distribution show that an extremely low pH does increase the mass fraction but, according to Figure 48, does not increase the nitrogen solubility. This indicates that at pH 1 compared to pH 2, other materials than protein were dissolved. The nitrogen concentration of the supernatant seems to be similar between pH 2 and pH 6-12 and shows a higher concentration of nitrogen in the supernatant than in the precipitate. At pH 3 similar concentrations in the supernatant and precipitate can be found, while pH 4 and 5 show a decreased nitrogen concentration for the supernatant and an increased nitrogen concentration for the precipitate.

To fulfill the goal of a highly effective protein extraction method, two strategies can be followed to isolate the protein fraction from the surrounding lupin matrix. One strategy is to aim for a high mass fraction and a low nitrogen concentration in the supernatant. This means that a lot of mass, which is not protein-related is separated from the lupin matrix by solvation. The remaining insoluble fraction is low in mass but high in nitrogen concentration (precipitate). This procedure could be applied at pH 4 and pH 5, where the supernatant contains a lower concentration of nitrogen than the precipitate. This process can be understood as a kind of washing step, where the matrix is separated by simply rinsing the non-protein related material.

However, the protein concentration of the precipitate cannot be further increased, which means that for a higher purity, another approach should be taken.

The alternative approach aims for a two-step process. In the first step, a low mass fraction with a high nitrogen concentration in the supernatant is required. This can be seen at high or low pH, where the supernatant contains a higher concentration of nitrogen than the precipitate. Although the results indicate a slightly lower protein concentration than the washing approach it has the advantage of applying another step after the solvation step for example another pH adjustment as shown for the IEPP process. In the second pH adjustment step in the IEPP process a pH around the isoelectric point value of the desired protein fraction is set (here pH 4 to 5). This approach allows to increase the nitrogen concentration in the final product from 11.0 % (69 % Protein) by washing at pH 4 to 14.5 % (90 % Protein) by applying the two-step process (see Table 42).

Nitrogen yield: But not only effectiveness but also sustainability and efficiency are important. Hence a closer look into the nitrogen yield is taken. The nitrogen yield determines how much nitrogen from the initial material can be found in the desired fraction. The higher the nitrogen yield, the lower the loss of protein/nitrogen in this process step. The nitrogen yield is displayed in following figure.

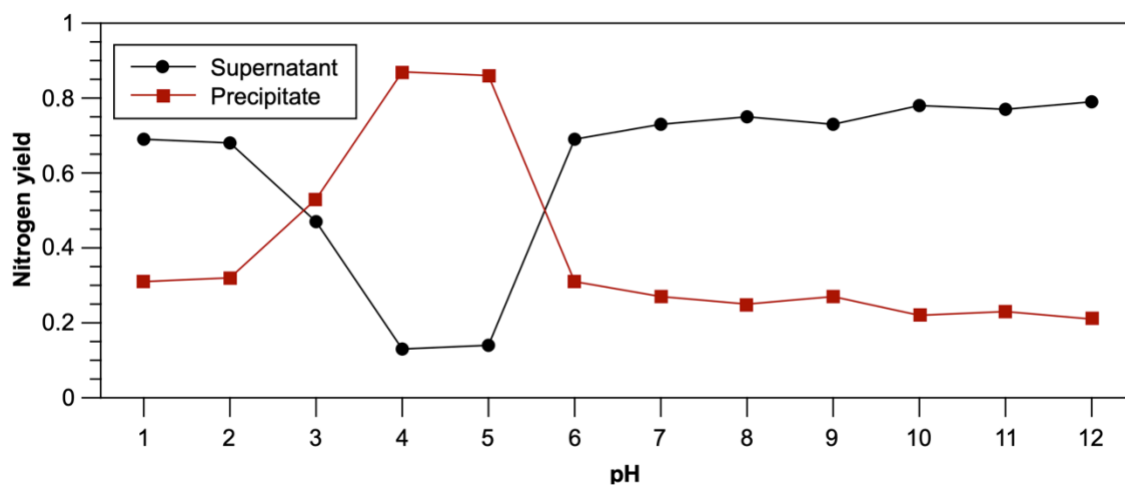


Figure 49: Influence of pH on the nitrogen yield.

According to Figure 49, the highest nitrogen yield can be found at pH 4. At this pH, the precipitate contains 87 % of the nitrogen content from the initial applied raw material. But as stated before, the proteins from *precipitate 1* at pH 4 cannot be further purified and still contains non-protein material, which leads to a protein concentration of 69 % (see Section 7.3). The IEPP applies two separation processes, from which the first separation takes place at pH 8.5. As can be seen from Figure 49, does the solvation of protein have the drawback of decreasing the nitrogen yield of around 20 % for the first separation. The following precipitation of proteins

at the IEP (pH 4 - 5) decrease the nitrogen yield further to 55 % in total but allows a protein concentration of 90 % (see Table 42). Therefore, only the two-separation process allows the isolation of proteins.

Coextraction of alkaloids: Furthermore, the influence of pH on the coextraction of alkaloids was observed. Therefore, the separated and dried *precipitate I* fraction (see Figure 5) was extracted via the Randall method and quantified via GC-FID analysis. The alkaloid recovery was calculated according to Section 3.4.4 presented in Figure 50.

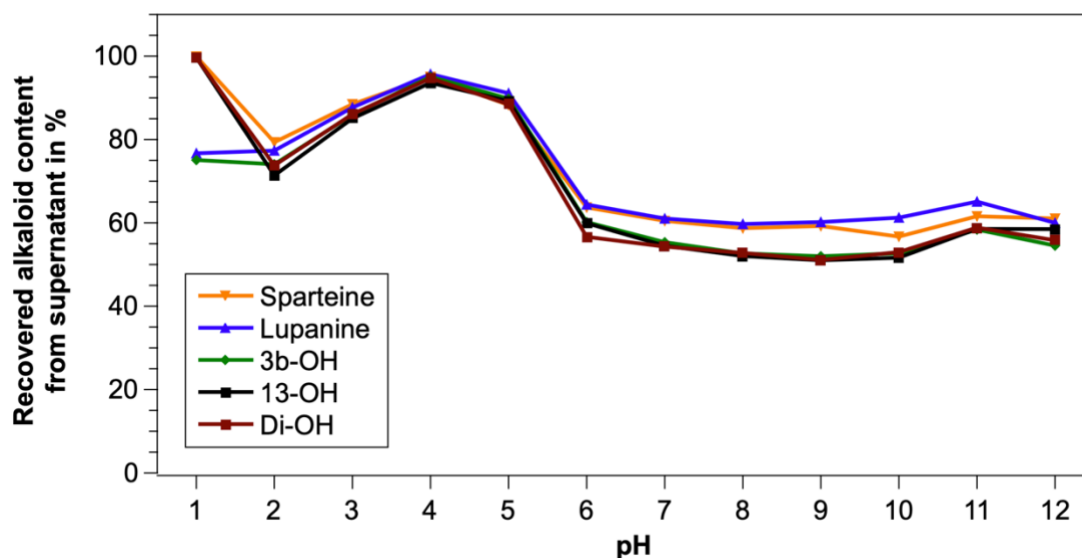


Figure 50: pH-dependent calculated recovery rate for individual alkaloids in supernatant.

Contrary to the extraction of alkaloids for analytical purposes, a high recovery of extracted alkaloids during the first step of an IEPP is not preferred, which means that a low alkaloid solubility is beneficial for the IEPP process.

During the IEPP process, a first separation between pH 8.5 is performed, in which the supernatant fraction undergoes a pH shift, and the protein gets precipitated at pH 4.5. The pH solubility should therefore be low in the first separation, and high in the second separation. This is the case with the alkaloid solubility and explains the alkaloid result from 700 mg /100 g lupin protein as can be seen in Table 42.

In general, the solubility of quinolizidine alkaloids is affected by the pH value. This result was expected since the pH does influence the alkaloid behavior. This phenomenon depends on the pK_a value, which allows a previously non-polar alkaloid to be converted into a polar alkaloid (see Section 2.2). The results show further that the smallest alkaloid recovery in the supernatant was 51 % (13-OH) at pH 10. This is relatively high and shows the overall hydrophilic nature of quinolizidine alkaloids as discussed earlier. During the acid-base extraction, a strong acid as 1 M HCl or 5 % TCA was used to reach pH values below pH 1. This corresponds with the shown recovered alkaloid content in the supernatant. Furthermore,

the data also show that sparteine, 13-OH, and Di-OH are completely dissolved in the supernatant at pH 1, but lupanine and 3b-OH are still presented in the *precipitate I* fraction. This observation might be related to their overall more nonpolar character.

The figure shows that, although lower pH values were applied, all alkaloids were nearly equally dissolved in the supernatant phase, except at pH 1. This behavior cannot be explained by destruction since the alkaloid extraction was carried out at a much lower pH value (see Section 3.2.1). Furthermore, the alkaloid solubility curves do show an unexpected behavior at pH 2, where the alkaloid solubility is smaller at pH 2 than at pH 3 and pH 1. From pH 3 towards pH 5 the alkaloid solubility increases to 80 %. It seems that with low protein solubility, the alkaloid extraction is increased (pH 4 - 5).

At pH 6 a drop in solubility can be observed, which can be explained by the acid-base polar/non-polar behavior of the alkaloids and the disruption of the N-glycosidic bonds, which break with respect to the added acid.

Conclusion: The extraction of protein via an IEPP involves the solvation and precipitation of the protein. The here-shown research regarding the solvation of protein/nitrogen showed high protein recoveries at pH 2 or lower and pH 6 or higher. The conducted analysis of alkaloids indicates that a higher pH allows less alkaloids to be present in the dissolved protein phase and could help to reduce alkaloid contamination inside the lupin product. However, the analysis could verify the already known hydrophilic behavior of quinolizidine alkaloids.

4.5.5 Influence of extraction time on the protein solvation

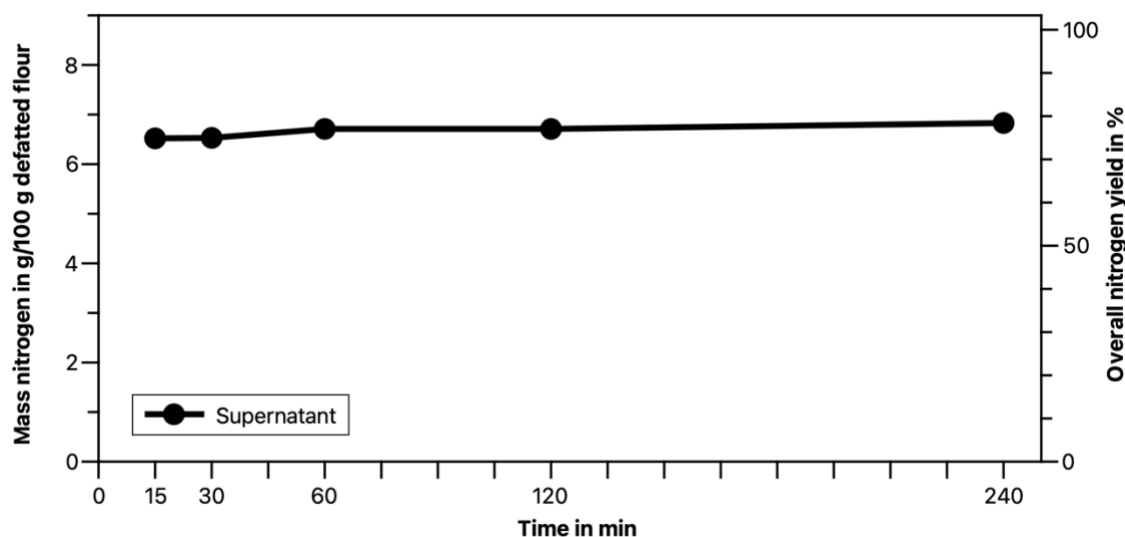


Figure 51: Influence of time on the nitrogen yield.

Most here-shown extractions were carried out by using 60 min for the solvation of proteins. To test if the 60 min are sufficient, the influence of time on the nitrogen content of the

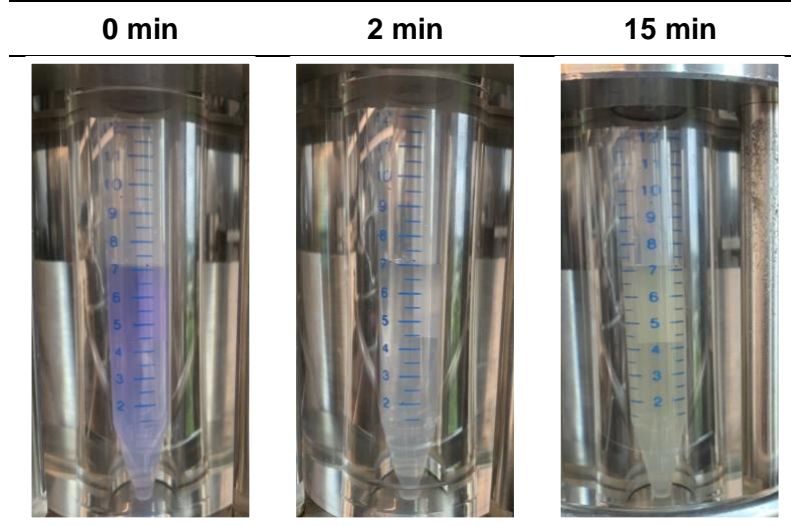
supernatant was analyzed at 15, 30, 60, 120, and 240 min (see Figure 51). The smallest yield was shown with 6.52 g N per 100 g flour at 15 min and the highest yield with 6.82 g N per 100 g flour at 240 min. The yield increased by less than 5 % although the time was increased by 16. In conclusion, it can be said that time did not have an apparent influence on the nitrogen solubility step of the IEPP. However, if time is valued higher than yield, the standard solvation time might be shortened from 60 to 15 min.

4.5.6 Parameters influencing the protein precipitation step in the IEPP-CO₂ process.

The optimization of the IEPP is not only the solvation of protein interesting (as shown above in Sections 4.5.4 and 4.5.5) but also the precipitation step in which the protein becomes concentrated. In the IEPP process, the solvation of nitrogen (see Figure 48) is at pH 4 to 5 the lowest. Therefore, a pH of 4.5 is applied for the standard IEPP to precipitate the proteins. For the IEPP-CO₂ process, HCl is substituted by CO₂, which works as a volatile acid (*reagent B*, see Figure 5). Since high pressures are required, direct pH measurements remain difficult, which is the reason why most parameters must be tested experimentally. Pressure and temperature have an influence on the solvation of CO₂ into the aqueous phase and therefore also on the pH (see details in Section 2.7).

View cell: To understand the behavior of CO₂ inside a closed vessel, a view cell experiment was conducted. Water with an indicator was used as a pH-sensitive solution and the color change was observed.

Table 43: Time-dependent optical change after pressurization at 60 bar.



The chamber was pressurized with 60 bar liquid CO₂ at room temperature. After 2 min the solution changed color (pH below 7) from blueish purple to colorless, before it started to become yellowish after 2 more min (not shown here). After 15 min a strong yellowish color

was developed (pH <6). The chamber was depressurized after 30 min and a pH of 3.9 was measured (1 atm, 20 °C).

This color change indicates that liquid CO₂ at 60 bar and 20 °C reached lower than necessary pH values for the precipitation step. However, tests with the flour mixture itself were also conducted, but did not show a clear color indication, due to the color of the solution itself.

Pressure and temperature: As the view cell experiment has indicated, a 30-min precipitation time seems to be enough to reach the optimum pH value of 4-5 for pure water. To understand the effect on a real sample, the protein solvation steps were carried out similarly to the IEPP process. Shortly, the flour was mixed with water at pH 8.5 and the dissolved protein solution was separated from the insoluble matrix. This aqueous solution was applied in another reactor, which can withstand higher pressure (see Section 2.3.6). The effect of pressure (60, 120, 240, and 480 bar) and temperature (20, 40, and 60 °C) on the protein precipitation was tested. Each experiment was carried out individually and the pressure was applied for 30 min, starting when the desired pressure was reached. The nitrogen yield results of the precipitation can be found in Figure 52 and the conjugated physical state of the CO₂ in Table 44.

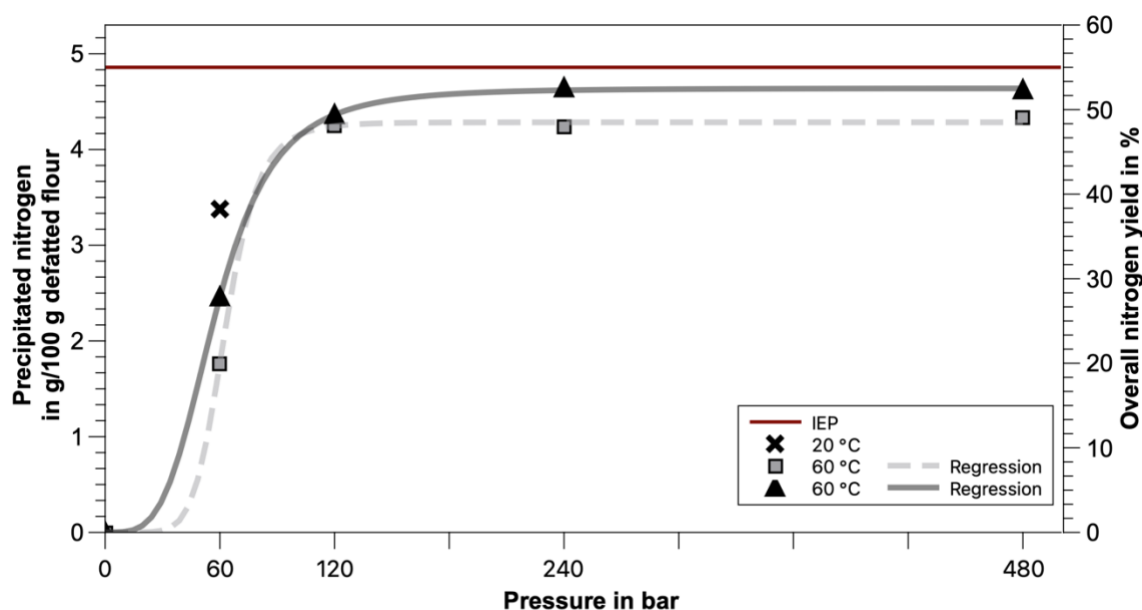


Figure 52: Precipitated nitrogen for different pressure and temperature values.

Experiments were carried out with 30 min equilibrium time and displayed as average from duplicate experiments. Regressions were applied by four parameters logistic curve with the program Qtiplot and parameters can be found in Table 63.

Table 44: Physical state of CO₂ for different temperature and pressure values.

T = 20 °C		T = 40 °C		T = 60 °C	
60 bar	liquid	60 bar	gaseous	60 bar	gaseous
120 bar	liquid	120 bar	supercritical	120 bar	supercritical
240 bar	liquid	240 bar	supercritical	240 bar	supercritical
480 bar	liquid	480 bar	supercritical	480 bar	supercritical

At 60 bar the lowest temperature (20 °C) resulted in a higher yield than experiments at 40 and 60 °C. In comparison to the two other temperatures (40 and 60 °C), the experiment at 20 °C applied liquid CO₂, while the experiments at 40 and 60 °C applied CO₂ in its gaseous state. An explanation for the higher yield at 20 °C might be, that liquid CO₂ has a higher mass transfer rate through higher density than gaseous CO₂. Furthermore, the solvation of CO₂ in water depends on temperature and pressure. The higher the pressure and the lower the temperature, the more CO₂ will be dissolved in the aqueous phase (see details in Figure 16). An isobaric experiment dissolves therefore more CO₂ at lower temperatures.

Although the experiment at 20 °C at 60 bar was promising, no further experiments with higher pressure values could be carried out. This was due to the depressurization step at the end of the experiment, where the experimental tube started to foam rapidly and sample loss was encountered, which ultimately led to non-reproducible results. This phenomenon is related to the high density of compressed liquid CO₂, which is released during the depressurization step. However, further increment of the pressure of the 40 and the 60 °C experiment was possible and showed an increase of precipitated nitrogen. At 120, 240, and 480 bar, nearly similar results were obtained from the 40 and 60 °C isotherms. In this region, the CO₂ is in its supercritical state. The results obtained are comparable to the standard IEPP with HCl as a precipitation agent (see red line in Figure 52).

Experiments at 60 °C resulted in all tested cases in higher yields than isobaric experiments at 40 °C. Although this difference is small, the result was not expected, since more CO₂ is dissolvable in the aqueous phase at lower temperatures. One explanation might be, that the optimum pH between 4 and 5 is better reached at 60 °C since the 40 °C experiment might exceed the optimum pH towards a lower value. Another explanation could be that at higher temperatures the viscosity of the water and scCO₂ phase become smaller allowing easier access for the CO₂ to enter the aqueous phase. This means that not enough time was given to reach a good equilibrium, which would explain why the higher pressure has such a high influence. In this experimental design, a higher pressure has automatically a longer contact time. Although the equilibration of each experiment was set to 30 min, the experiments at higher pressure were longer in contact with CO₂, due to the time it took to reach the pressure.

Influence of precipitation time: The view cell experiment has shown that a 30 min equilibration time is sufficient to reach a pH value below the IEP with pure water. To test, if this is also the case with a flour/water sample, three fixed temperature and pressure value experiments were conducted at different periods (15, 30, 60, 120, and 240 min). The three here-tested parameters are linked to different physical states of CO₂ (see Table 44). The supercritical state experiment (120 bar, 40 °C) showed higher yields than gaseous (60 bar, 40 °C) and liquid state experiments (60 bar 20 °C) at low time values. The results are presented in Figure 53 and carried out in triplicates.

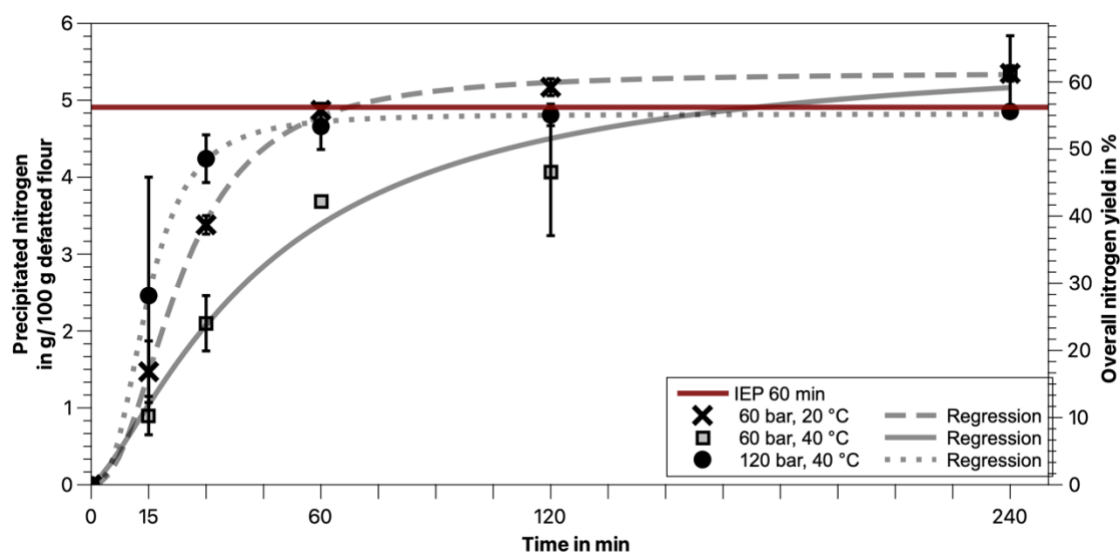


Figure 53: Influence of time on the nitrogen precipitation yield in the IEPP-CO₂ process.

Regressions were applied by four parameters logistic curve with the program Qtiplot and parameters can be found in Table 64.

In general, the precipitation of proteins via CO₂ shows high time dependency. Higher equilibration time leads to higher yields and vice versa. The results are therefore contrary to what was found for the solvation step in the IEPP, where only a minor influence of time was shown (see Section 4.5.6). A reason for this phenomenon might be the limited mass transport. While for the IEPP process, a magnetic stirrer bar was used to distribute the precipitation agent evenly, the distribution of CO₂ is based on its absorption rate and diffusion rate. This way of distribution is slower than conventional stirring and acts as a bottleneck for the CO₂ precipitation.

Furthermore, the previously discovered finding that higher pressure leads to higher yield, as seen in Section 4.5.6, is probably related to the longer contact time. This is caused by the difference in time to pressurize the system from 60 bar to 120 bar, which is not reflected in the equilibration time of 30 min. In the case of a 15-min experiment, the pressurization took an extra time of ca. 7 min for the 60-bar experiment, but ca. 15 min for the 120-bar. The real total contact time of CO₂ with the water was 22 min for the 60-bar experiment, respectively 30 min

for the 120-bar experiment. That result explains, why the 120-bar experiment does perform better at lower time values, since the time to reach the desired pressure is not reflected by the here-shown result. With longer contact time, the influence of this phenomenon becomes obsolete because the difference of adding 7 or 15 min to a total contact time of 240 min will only cause minor differences.

By comparing the liquid (60 bar, 20 °C) and gaseous state (60 bar, 40 °C) it can be found that the latter requires a longer equilibration time for similar results. This is related, to the behavior of CO₂, which at isobaric conditions allows to be dissolved in larger quantities at colder temperatures (see Figure 16). Another reason might be the lower mass transfer rate through its physical state. However, the 60 bar, 20 °C has a smaller p_4 parameter value for the regression than the 60 bar, 40 °C experiments (see Table 64). This means that although the experiments at 240 min showed similar yields, a further increment in time would lead to higher results for the 60 bar, 40 °C experiment. This is probably caused by a better suitable pH value for the 40 °C experiment, which is closer to the real IEP than the 60 bar, 20 °C experiment or the IEPP experiment. In conclusion does this mean, that a 60 bar, 20 °C experiment leads to high yields and fast precipitation, but if time is not a critical factor to consider, the 60 bar, 40 °C experiment may lead to slightly higher yields.

The 60 bar, 20 °C condition was also tested with the view cell and showed lower than necessary pH values after 15 min in demineralized water, this was not enough for the precipitation of lupin proteins. The experiment shows that, although the optimum pH is known, the best precipitation parameters are reached by applying CO₂ for much longer than 15 min. This phenomenon is most likely related to the buffer capacity and added NaOH solution to the lupin flour mixture. The CO₂ first needs to neutralize NaOH, before the carbonyl and amid groups in proteins act as a buffer (see Section 2.3.1). This is also the reason why the CO₂ view cell experiment with demineralized water reached relatively fast lower pH values and the CO₂ flour experiment did not.

However, if compared to the standard IEPP it can be said that with a precipitation time of 240 min, the standard IEPP can be slightly outperformed by applying liquid (60 bar and 20 °C) or gaseous CO₂ (60 bar, 40 °C).

In conclusion, it can be said that time is one of the most influencing factors for the precipitation with CO₂, which is contrary to the protein solvation experiment (see 4.5.5). However, the protein precipitation with CO₂ at longer equilibration times led to yields similar or in some cases higher than shown for the standard IEPP with HCl as a precipitation agent. The IEPP-CO₂ process can therefore be seen as an ecological alternative to the currently used standard IEPP, which comes with increased investment costs but reduced ecological impact.

4.5.7 Concept CO₂-only protein extraction

While all other shown processes require the use of either a basic solution and the followed neutralization (IEPP, IEPP-CO₂) or the excessive use of water and NaCl solution (Salting-out), the CO₂-only process can be designed to only consume CO₂ and water. It is also a two-separation process, which follows the general scheme of the wet protein separation as also shown in Figure 5.

In Section 4.5.6 it was proven that successful precipitation of proteins can be carried out with CO₂, however, the solvation of proteins was still carried out with a lye solution. But since the nitrogen solubility increases with higher and lower pH of the IEP, also low pH values can be used to dissolve proteins. In the case of CO₂, the view cell experiment with 60 bar and 20 °C has shown, that even after depressurization a pH value of 3.9 can be achieved (see Section 4.5.6). To further decrease the pH value lower temperatures and higher pressure can be applied. In the following the CO₂-only protein extraction process is introduced and its design is explained.

Experimental design: The whole process is designed to not depressurize the system between the solvation and precipitation steps because this would cost a lot of energy and resources. This means that the previously used separation method of centrifuging is replaced by filtration. In Figure 54 the concept of the CO₂-only process is shown. Three reactors (pressure vessels) are applied from which *reactor 1* and *reactor 2* are temperature regulated. The valve regulation is shown in Table 45 and a brief description of the different steps follows.

Step 1: Addition of flour/water solution. In this step, the flour/water mixture is introduced via V2 into R1.

Step 2: The CO₂ is introduced, and the temperature is adjusted. High pressure and low temperature values are recommended to reach low pH values, which increase the protein solubility and allow the transport into the aqueous phase.

Step 3: A counterpressure is applied in Reactor 2 to reduce the pressure difference between Reactor 1 and Reactor 2. This is done, because preliminary tests have shown, that the filtration fails if the pressure difference is too high. However, as an alternative a filter cascade can be used, in which each filter works also as a pressure barrier (see Figure 55).

Step 4: The dissolved proteins in the *supernatant 1* (filtrate) are transferred to Reactor 2 via adjustment (A) of V5, leaving the insoluble dietary fiber remaining in the filter F1. The temperature and pressure of Reactor 2 should be adjusted to meet the pH requirements of the IEP, which leads to precipitation of the previously dissolved proteins. It is expected that 60 bar, 20 °C and 60 min result in sufficient precipitation with respect to the parameters shown in Section 4.5.6.

Step 5: A counterpressure is applied in Reactor 3.

Step 6: The *supernatant II* (filtrate) is transferred into Reactor 3 and the precipitated proteins will be found in Filter F2.

Step 7: The *supernatant II* (filtrate) is removed via V8.

Step 8: The equipment is depressurized.

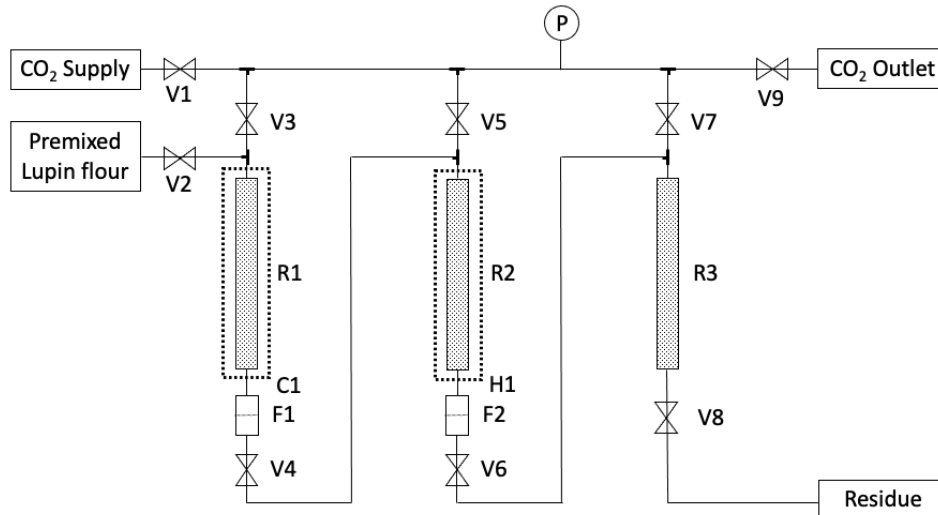


Figure 54: Process design for CO₂-only protein precipitation.
With cooler (C), filter (F), heater (H), reactor (R), and pressure gauge (P).

Table 45: Valve regulation during a CO₂-only protein extraction.

Step	V1	V2	V3	V4	V5	V6	V7	V8	V9	Description
1	0	1	1	0	0	0	0	0	1	Flour introduction
2	1	0	1	0	0	0	0	0	0	Pressurizing
3	1	0	0	0	1	0	0	0	0	Counterpressure F1
4	1	0	1	1	A	0	0	0	0	Transferring
5	1	0	0	0	0	0	1	0	0	Counterpressure F2
6	1	0	0	0	1	1	0	0	0	Transferring
7	0	0	0	0	0	0	0	1	0	Removal
8	0	0	1	1	1	1	1	1	1	Cleaning

Results solvation of proteins using CO₂: The separations in all previously shown protein extraction processes were carried out via centrifuging, which is due to the required continuously high pressure was not possible for the CO₂-only process. Therefore, an alternative was searched and found to be filtration. Different preliminary filtration tests were carried out. It was found that all tested filtration required a counterpressure to not break. However, with counterpressure, a clogging occurred. A filtration system that avoids clogging was designed by using a Tee-type Swagelok cascade design (see Figure 55) and contained a filter size from 60 µm to 7 µm to 2 µm.

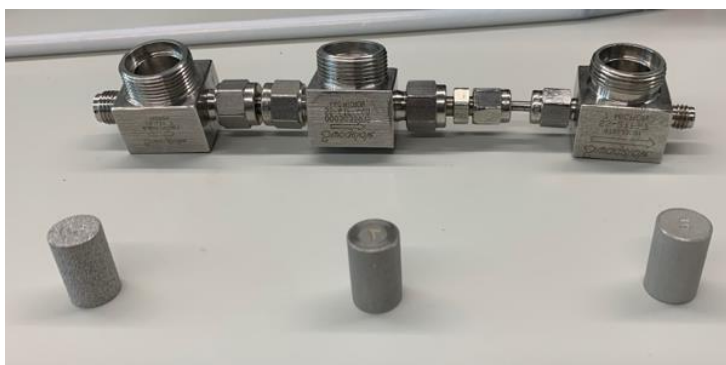


Figure 55: Filter cascade as used in protein solvation via CO₂ experiments.

High-pressure inlet on the left, followed by 60 µm (left), 7 µm (mid), and 2 µm (right) filtration.

Since the IEPP-CO₂ process has shown, that 60 bar and 20 °C is sufficient to precipitate the previously solved proteins, the research for the CO₂-only process was purely focused on the protein solvation step and its separation from the precipitate (filter cake). Different parallel trials were carried out and always compared with a centrifuge reference measurement (see Section 3.2.4). In the first trial, nitrogen and carbon dioxide were applied at 60 bar and two different temperatures (20 and 4 °C). The results are presented in the following table.

Table 46: Analysis of weight and protein content of the only-CO₂ process.

Reference (centrifuge)	Recovered dry weight		Recovered protein (BCA)	
	Total	70 %	Total	74 %
N₂, 4 °C, 60 bar	60 µm	17 %	60 µm	15 %
	7 µm	2 %	7 µm	2 %
	2 µm	2 %	2 µm	2 %
	Total	22 %	Total	19 %
N₂, 20 °C, 60 bar	60 µm	21 %	60 µm	20 %
	7 µm	7 %	7 µm	7 %
	2 µm	4 %	2 µm	4 %
	Total	32 %	Total	31 %
CO₂, 4 °C, 60 bar	60 µm	28 %	60 µm	31 %
	7 µm	11 %	7 µm	15 %
	2 µm	1 %	2 µm	1 %
	Total	40 %	Total	47 %
CO₂, 20 °C, 60 bar	60 µm	33 %	60 µm	38 %
	7 µm	14 %	7 µm	19 %
	2 µm	1 %	2 µm	1 %
	Total	48 %	Total	58 %

The analyses were carried out with the precipitate / fractions (filtrate) after protein solvation and filtration took place.

All shown results refer to the filter cake *precipitate I* (Figure 5), which is the unwanted fraction. A good protein solvation step should therefore show a low amount of protein inside the filter cake, but a high content of dry mass. The reference measurement resulted in 70 % of the initial used flour as recovered dry weight, which contained 74 % of the total protein content. As expected, the centrifuging experiment, which mixed the sample with water without the addition of pressure or reagent, was not sufficient to separate the proteins from the remaining matrix. In all other tests, where a pressure was applied, filtration was used as the separation method.

In general, the 60 μm filtration cake had the highest dry and protein recovery and the smallest mesh size (2 μm) led always to the smallest fraction. All experiments have in common, that smaller recovery rates than for the reference (centrifuge) experiment were shown. This indicates that filtration is less efficient than centrifuging, or smaller mesh sizes should be applied for the filtration.

Furthermore, it was expected that the nitrogen experiment would not affect the protein solvation since nitrogen will dissolve in water but not work as a volatile acid. The difference between protein and dry weight fraction is with a maximum difference of 3 % small and expected. On the contrary, it had been expected that the pressurization with CO_2 would lead to lower recovered protein since the recovered protein should be found in the filtrate (*supernatant I*). However, the opposite was the case, the application of CO_2 showed a higher amount of recovered protein in the filter cake than in the dry weight. This means that the application of CO_2 at 4 and 20 °C was indeed lowering the pH but could not exceed the IEP. This can have two reasons. First, the contact time (60 min) and the surface area were not sufficient. The surface area, which allows CO_2 to enter from above is rather small (\varnothing 1/4", 0.32 cm^2), while the tube filling is rather height (ca. 31 cm). Secondly, the buffer capacity of the flour might be too high and hinder the solution from reaching lower pH values.

Both hypotheses were tested. The former was tested by using a counter-flow to mix the water/flour mixture. Therefore, CO_2 was introduced at the bottom of the reactor and the flow of CO_2 was adjusted to reach 50-100 mL per min with a continual pressure of 60 bar (see picture). Furthermore, the hypothesis of a too-high buffer capacity was tested by decreasing the flour-to-water ratio from 1:10 to 1:20. However, no combination of parameters or process design showed a higher recovered dry weight than recovered protein content.

Another option is the increment of pressure to higher values. Higher pressure results in more dissolved CO_2 and ultimately lower pH values. Although this is a promising experimental design, it could not be carried out, due to the pressure limitation of single components.

In summary, no experiment proved the hypothesized solvation of protein via CO_2 . A lot of different parameters were tested, but none of them showed sufficient protein solvation power. Further experiments might focus therefore on reaching higher pressure values than the here-

tested 60 bar. Nevertheless, the research on new protein extraction processes revealed an interesting concept, which opens new opportunities to discover sustainable extraction methods.

4.5.8 Protein extraction evaluation

In this thesis, four aqueous protein extraction processes were tested and discussed, namely IEPP, IEPP-CO₂, salting-out and CO₂-only. The first three methods showed sufficient protein extraction ability for the *Lupinus mutabilis branco* beans with different properties. It was found that methods using the pH to dissolve and precipitate proteins from the matrix resulted in higher protein extraction yields than those using ionic strength. The parameters influencing the IEPP were analyzed and a successful substitution of 1 M NaOH (*reagent B*) was shown with the IEPP-CO₂ process, which applies CO₂ at 60 bar and 20 °C. Furthermore, it could be shown, that an optimized time window of 240 min could slightly outperform the yield of the standard IEPP. Nevertheless, this gained yield difference is small, and the economic potential is limited. This is due to the necessity of applying high-pressure equipment, food-grade CO₂, and longer waiting times than the standard IEPP. Therefore, it is considered that the standard IEPP still has the highest economic potential.

On the contrary, the theoretical concept of the CO₂-only process might have an advantage over the other here-shown processes, since it could allow the recycling of the volatile acid and therefore the reduction of costs. Although a lot of effort was taken, no sufficient protein solvation by purely using CO₂ was found, which is a requirement for a working protein extraction process. Future research might focus on developing a protein solvation process on purely CO₂ basic, but this might come with a drawback in lower yields since the acidic solvation allows less nitrogen solvation than the alkaline solvation as used for the standard IEPP. Furthermore, the use of CO₂ might influence the solubility of alkaloids inside the aqueous solution which was not beneficial for the IEPP-CO₂ process but could be beneficial for the CO₂-only process.

4.6 Lipids

Another valuable fraction of lupin beans are lipids, which have a wide range of applications. For example, lipids can serve as a sustainable fuel, whereas petrochemical analogues are being replaced by renewable resources. Furthermore, lipids can also be applied to the food and feed sector. The latter application is especially interesting when the extraction is coupled to a green and contamination-free process, such as scCO₂. Other lipid extraction uses mostly non-polar solvents such as hexane, which are harmful to the environment and not suitable as a food byproduct. Therefore, this thesis compares conventional solvent extraction with the

SFE technologies and evaluates critical parameters. This was not only done for lupin beans but also for cherry stones, which offered a more complex matrix and were therefore chosen for detailed parameter evaluation.

4.6.1 Lipid extraction and analysis of lupin beans

The detailed economic analyses of lipid extraction from lupin beans via Soxhlet and different scales of scCO₂ extraction can be found in Section 7.5 and are published in the Journal of Food Process Engineering (Wiley) with the title: *Supercritical carbon dioxide extraction of oils from Andean lupin beans: Lab-scale performance, process scale-up, and economic evaluation* (DOI: 10.1111/jfpe.14289).

The following normalized FAME composition was found in *Lupinus mutabilis* beans.

Table 47: Original reported normalized *Lupinus mutabilis* FAME composition.

	C16:0	C18:0	C18:1	C18:2	γ-tocopherol
	%	%	%	%	mg/100 g DW
Lup. Mut.	11.9	34.9	45.8	7.3	116.1

The results are reported in the supplementary material of Yu et al.⁵⁴ and based on a 6 h Soxhlet extraction of *Lupinus mutabilis* 0.5 mm flour.

However, the results are corrected with the recovery of 83.3 % to following results.

Table 48: FAME composition of *Lupinus mutabilis*.

	C16:0	C18:0	C18:1	C18:2	γ-tocopherol
	g /100 g DW	g /100 g DW	g /100 g DW	g /100 g DW	mg/100 g DW
Lup. Mut.	2.2	1.3	8.3	6.3	21.8

Results are based on Yu et al.⁵⁴ (see also Section 7.5) and adapted to 100 g DW.

The recovery rates are not based on the IS, because the IS was added after the extraction and is therefore not suitable for an extraction method comparison. Instead, the recovery rate is calculated by the summarized weight of the analyzed FAMES and divided by the total weight of the oil. Since the focus was put on the major four FAMES, the minor FAMES are not presented, which means that the real recovery rate is much higher.

The influence of the extraction method and various parameters were not tested with lupin beans but with cherry stones. This was done since all critical parameters of lipid extraction from lupin beans are also applicable to cherry stones. Furthermore, cherry stones offer optimization of moisture content, which is not necessary for lupin beans.

4.6.2 Lipid extraction and analysis of cherry stones

The details regarding the parameter influencing the lipid extraction can be found in Section 7.6 and are published in the Journal of Chemical Technology and Biotechnology with the title:

Lipid extraction of high-moisture sour cherry (*Prunus cerasus* L.) stones by supercritical carbon dioxide (DOI: 10.1002/jctb.7581).

For the shown overview of methods in Section 4.1, the results with the highest lipid yield (SK-RH20) were used and normalized. This was done since the reported recovery rate does not reflect the real recovery rate (see above).

Table 49: Lipid yield and recovery rate.

	Soxhlet	Randall	scCO ₂
Extraction yield	26.7 g/100 g DW	24.2 g/100 g DW	19.8 g/100 g DW
Recovery rate	86 %	83 %	88 %
Recovery rate (Normalized)	98 %	95 %	100 %

Results are based on the SK-RH20 extraction as reported in Section 7.6.

Furthermore, it was found that Randall extraction showed a better performance for more moisturized samples. However, the highest lipid yield was still gained with Soxhlet extraction and is therefore used for comparison.

4.7 Carbohydrates and dietary fiber in lupin beans

Among alkaloids, protein, and lipids, Carbohydrates are also an interesting fraction of lupin beans. Carbohydrates are the fuel of living (see Section 2.5) and can be gained from many sources. An often-used method to quantify the total amount of carbohydrates is a subtraction of all other fractions (see Section 3.4.12). *Lupinus mutabilis* has a mass of total calculated carbohydrates of 24.7 g/100 g DW.

Table 50: Total carbohydrates in *Lupinus mutabilis*.

	Total carbohydrates
<i>Lupinus mutabilis</i>	24.7 ± 1.0 g/100 g DW

Although the total carbohydrate fraction might take up one-quarter of the total dry lupin flour, the extraction of lupin plants for carbohydrates is not valuable, since high carbohydrate-containing plants are known (e.g. sugar cane and sugar beets) and used on a large industrial scale. Nevertheless, the analysis of carbohydrates is important, since a high carbohydrate fraction in the form of easily digestible sugars (e.g. saccharose, fructose, and glucose) is often linked to non-communicable diseases. The contrary is a high dietary fiber intake which is linked to a healthy diet (see Section 2.5) and could therefore increase the value of the lupin bean and its popularity in Europe. Since the standard IEPP is a suitable method to separate the proteins from carbohydrates, its fraction, as well as lupin beans themselves, are analyzed for dietary fiber content (see Section 3.3.5). For this, *Lupinus mutabilis*, *Lupinus albus*, and all fractions from the IEPP standard process were analyzed. The results are presented in the following tables.

Table 51: Total dietary fiber and its composition.

	Total dietary-fiber (TDF) g/100 g DW (% TDF)	Insoluble dietary fiber g/100 g DW (% TDF)	Soluble dietary fiber g/100 g DW (% TDF)	Total oligo-saccharides g/100 g DW (% TDF)
L. Mut. ^a	23.2 ± 0.2 (100 %)	16.1 ± 0.2 (69 %)	0.6 ± 0.1 (3 %)	6.5 (28 %)
L. mut. ^b	29.8 ± 0.2 (100 %)	20.6 ± 0.2 (69 %)	0.8 ± 0.1 (3 %)	8.3 (28 %)
L. albus ^b	41.3 ± 1.0 (100 %)	30.9 ± 1.0 (75 %)	2.8 ± 0.1 (7 %)	7.6 (18 %)
L. mut. Prec I	53.7 ± 1.9 (100 %)	45.2 ± 1.9 (84 %)	2.0 ± 0.2 (4 %)	6.6 (12 %)
L. mut. Sup II	25.0 ± 0.2 (100 %)	0.0 ± 0.0 (0 %)	0.1 ± 0.2 (0 %)	24.9 (100 %)
L. mut. Prec II	3.9 ± 0.7 (100 %)	1.3 ± 0.7 (33 %)	0.7 ± 0.1 (18 %)	1.9 (49 %)

Results were carried out in duplicates. For a) the results are calculated based on the determined lipid content. b) is referring to defatted samples.

Table 52: HPLC analysis of the total oligosaccharide fractions.

	DP=3 g/100 g DW (% Tot. Olig.)	DP=4 g/100 g DW (% Tot. Olig.)	DP=5 g/100 g DW (% Tot. Olig.)	DP>5 g/100 g DW (% Tot. Olig.)
L. Mut. ^a	2.6 (40 %)	3.3 (51 %)	0.3 (4 %)	0.3 (4 %)
L. mut. ^b	3.3 (40 %)	4.3 (51 %)	0.3 (4 %)	0.4 (5 %)
L. albus ^b	2.5 (33 %)	3.7 (49 %)	1.2 (15 %)	0.2 (3 %)
L. mut. Prec I	1.5 (22 %)	4.4 (67 %)	0.3 (5 %)	0.4 (7 %)
L. mut. Sup II	5.3 (21 %)	18.0 (72 %)	1.3 (5 %)	0.3 (1 %)
L. mut. Prec II	0.4 (21 %)	0.9 (44 %)	0.1 (5 %)	0.6 (29 %)

The oligosaccharide fractions describe the soluble dietary fiber fraction. Results were carried out in duplicates. For a) the results are calculated based on the determined lipid content. b) is referring to defatted samples.

Table 53: Total weight distribution of dietary fiber fraction.

	Total dietary-fiber	Insoluble dietary fiber	Soluble dietary fiber	Total oligo-saccharides
<i>L. mut. Sup I</i>	42%	3%	30%	85%
<i>L. mut. Prec I</i>	58%	97%	69%	15%
<i>L. mut. Sup II</i>	37%	0%	2%	79%
<i>L. mut. Prec II</i>	5%	3%	28%	6%

Sup I is calculated and consists of Sup II and Prec II.

It was found that *Lupinus mutabilis* beans have a total dietary fiber fraction of 29.8 g per 100 g DW for defatted, respectively 23.2 g per 100 g DW for full flour. This accounts for most of the calculated carbohydrate fraction and shows another advantage of the lupin beans. The other here-tested *Lupinus albus* (defatted) species contained 41.3 g per 100 g DW. In comparison: rice contains only between 3 and 10 g of total dietary fiber per 100 g DW and wheat 9 to 17 g per 100 g DW ¹⁰⁵. This means, from a nutritional point of view the value for total dietary fiber of both lupin bean varieties is high.

The main fraction of the dietary fiber of both lupin varieties consists of insoluble fiber and accounts for more than 2/3 of the total dietary fiber. The smallest fraction was in both cases the soluble dietary fiber which contributes less than 10 % to the total dietary fiber content. The total oligosaccharide fraction for both lupins seems to have a similar distribution with the DP=4 as the biggest fraction for ca. 50 %. The only major difference can be found for the DP=5 units, where *Lupinus albus* beans have a higher value.

The standard IEPP as shown in Section 4.5.3, separates the protein from the main lupin matrix via a two-step process. Shortly, In the first step, the insoluble part of the flour is separated from the dissolved proteins and other soluble parts by a high pH. The separated fraction is named *Prec I (Precipitate I)* and is considered to contain mostly insoluble dietary fiber.

The remaining *Sup I (supernatant I)* from this extraction undergoes a pH shift, where the proteins are precipitated (*Prec II*) and contain mostly proteins. The remaining supernatant *Sup II (supernatant II)* is another output fraction and is considered to contain mostly soluble carbohydrates. Since the *Sup I* fraction is divided into *Sup II* and *Prec II*, *Sup I* is calculated.

The data shows that *Prec I* consists of more than 50 % dietary fiber. Furthermore, 97 % of the total insoluble dietary fiber of lupin beans can be found back in this fraction (see Table 53). The high recovery rate and content of dietary fiber make this fraction valuable from an economic point of view, although it is mostly considered as a waste fraction from the protein extraction process.

Another valuable fraction is the extracted protein fraction (*precipitate II*). It has only a small fraction of dietary fiber, which is also in agreement with the high protein concentration of 90 % determined in previous experiments (N × 6.25, see Section 4.5.3).

The remaining fraction (*Sup II*) was assumed to contain mostly soluble oligosaccharides. This is also in accordance with the here-presented results since 79 % of the total oligosaccharides from *Lupinus mutabilis branco* can be found in this fraction.

A closer look into the details of the oligosaccharides weight distribution for those fractions shows that the protein fraction (*Prec II*) has a slightly different distribution than the two others. In *Prec II* the biggest oligosaccharide fraction is DP>5, which means that mostly large oligosaccharides can be found back. The *Sup II* has a DP=4 fraction of 18 g per 100 g DW and is therefore relatively higher. Nevertheless, the economic potential of this fraction is limited, since this fraction is gained in an aqueous state and would need to be dried.

In summary, the high dietary fiber composition in lupin beans puts the plant into a promising position in comparison to other legumes. The analysis of the single fractions of the standard IEPP showed that the often-considered waste fraction (*Prec I*) does contain mostly insoluble fiber. Therefore, the first step in the IEPP process can also be seen as an insoluble dietary fiber concentration step. Furthermore, the analysis does show that only a small amount of dietary fiber is found in the protein precipitate (*Prec II*), which verifies the successful protein extraction from Section 4.5.3.

5 Conclusion and outlook

Lupin beans offer an interesting matrix for the extraction of valuable components. Their benefit is the nutritional value and the Lupin's ability to grow in cold regions and on marginal lands. If lupin beans are grown locally, it can help to reduce the emission of greenhouse gases and reduce the impact of climate change.

A yet-considered drawback of lupin beans are the toxic quinolizidine alkaloids. In this thesis, several different extraction methods were introduced and tested. It was found that the extractions via SPE and LLE have the drawback of discriminating certain polar alkaloids, e.g. 13-OH and Di-OH for *Lupinus mutabilis*. This discrimination was avoided by using Randall or Soxhlet extraction and led to a successful quantification of alkaloids in unknown seeds. However, this result opens new research opportunities, because the discrimination might not be limited to *Lupinus mutabilis* and have therefore also affect other species since SPE and LLE are the most applied techniques. Furthermore, it needs to be evaluated, if with the knowledge of the higher polar alkaloid content, the toxicity classification of lupin beans changes.

Although alkaloids are harmful to human nutrition, they still have potential in other applications. For example, they could be applied as a natural insecticide or repellent for other crops¹² or for medical purposes, as an immunosuppressive, antiarrhythmic agent, or hypercholesterolemia medication^{8, 24, 98}. However, to evaluate alkaloid applications, further research needs to be conducted.

While all tested methods are based on the destruction of the lupin matrix for proper quantification, future research might also focus on the development of non-toxic debittering methods. This could be accomplished by the use of scCO₂ with basic modifiers¹⁰⁰, the modification of scCO₂ by ionic liquids¹⁰⁶, or other techniques such as advanced water-processing²⁰. Moreover, individual alkaloids were isolated and showed huge potential in the application as a standard. Nevertheless, the isolation method requires further optimization.

Because of their nutritional values, lupin beans offer a solution for the search for locally grown high-protein alternatives to meat¹. The here-tested *Lupinus mutabilis branco* beans contained 49.1 ± 0.8 g/100 g DW (N \times 6.25) protein. Different methods were tested, and it was shown, that each extraction has its benefit. The salting out process led to lower protein yields but offered the benefit of reduced alkaloid coextraction. All in all, the application of the IEPP process is recommended for its robustness, wide application, and highest protein yields. However, if a green process is desired, the HCl of the IEPP can be replaced by CO₂, which helps to reduce the environmental footprint of the process without reduced yield. A CO₂-only process was developed to reduce the environmental impact further but has not been successfully tested yet. Future research might therefore focus on the improvement of the CO₂-

only process. This can be done by the application of a better separation process, e.g. nanofiltration¹⁰⁷, or the application of higher pressure to reduce the pH.

Among proteins, the here-analyzed *Lupinus mutabilis branco* beans contained 23.2 ± 0.2 g dietary fiber. Successful extraction of the insoluble dietary fiber was shown by the standard IEPP, which can help to increase the value of the currently considered waste fraction.

The extraction of lipids was carried out with lupin beans and cherry stones. The former showed economic potential for the application of scCO₂ as an extraction agent on a large scale.

By putting all aspects in one picture a lupin biorefinery process is considerable. First, an unmodified scCO₂ extraction is conducted, where lipids are extracted via the introduced parameters. Next, a modifier is added to the scCO₂ stream, which extracts in a second step the alkaloids. The remains can be used directly, or a protein isolation step can be carried out with the parameter discussed for the CO₂-only process. This process design has the advantage that no depressurization step is necessary, hence increasing the sustainability of this process. Future work might therefore focus on the development of such a process, helping to increase the use of lupin beans and reducing its environmental impact.

Ultimately this thesis has shown several different methods to extract valuable components of lupin beans, and it offers a good starting point for an understanding of the applied extraction processes and the influence of its parameters.

6 Literature

1. World Health Organization, Climate Change 2022 - Mitigation of Climate Change, pp. 1-150 (2023).
2. United Nations, World population prospects 2019, pp. 1-39 (2019).
3. United Nations, Sustainable Development Goals, p. 4 (2019).
4. Stainforth DA and Calel R, New priorities for climate science and climate economics in the 2020s, *Nature Communications* **11**: 3864 (2020), DOI: 10.1038/s41467-020-16624-8.
5. European Union, EU imports of organic agri-food products, European Union, Brussels (2023).
6. Bebeli PJ, Lazaridi E, Chatzigeorgiou T, Suso M-J, Hein W, Alexopoulos AA, Canha G, van Haren RJF, Jóhannsson MH, Mateos C, Neves-Martins J, Prins U, Setas F, Simioniuc DP, Talhinhos P and van den Berg M, State and Progress of Andean Lupin Cultivation in Europe: A Review, *Agronomy* **10** (2020), DOI: 10.3390/agronomy10071038.
7. Gulisano A, Alves S, Martins JN and Trindade LM, Genetics and Breeding of *Lupinus mutabilis*: An Emerging Protein Crop, *Frontiers in Plant Science* **10**: 1385 (2019), DOI: 10.3389/fpls.2019.01385.
8. Carvajal-Larenas FE, Linnemann AR, Nout MJ, Koziol M and van Boekel MA, *Lupinus mutabilis*: Composition, Uses, Toxicology, and Debittering, *Critical Reviews in Food Science and Nutrition* **56**: 1454-1487 (2016), DOI: 10.1080/10408398.2013.772089.
9. Bundesinstitut für Risikobewertung, Risk assessment of the occurrence of alkaloids in lupin seeds (2017).
10. Aniszewski T, *Alkaloids - Secrets of Life*, Elsevier, Amsterdam, pp. 98-100 (2007).
11. Wink M, *Lupinus mutabilis* composition and potential applications of quinolizidine alkaloids, in *Insect-plant interactions*, ed by Bernays E, CRC Press, Boca Raton, pp. 47-62 (1992).
12. Boschin G and Resta D, Alkaloids Derived from Lysine: Quinolizidine a Focus on Lupin Alkaloids, in *Natural Products*, pp. 381-403 (2013).
13. Schrenk D, Bodin L, Chipman JK, Del Mazo J, Grasl-Kraupp B, Hogstrand C, Hoogenboom LR, Leblanc JC, Nebbia CS, Nielsen E, Ntzani E, Petersen A, Sand S, Schwerdtle T, Vleminckx C, Wallace H, Alexander J, Cottrill B, Dusemund B, Mulder P, Arcella D, Baert K, Cascio C, Steinkellner H and Bignami M, Scientific opinion on the risks for animal and human health related to the presence of quinolizidine alkaloids in feed and food, in particular in lupins and lupin-derived products, *EFSA Journal* **17**: e05860 (2019), DOI: 10.2903/j.efsa.2019.5860.
14. Cowling W, Huyghe C and Swiecicki W, Lupin breeding, in *Lupins as Crop Plants Biology, Production and Utilization*, ed by Gladstones JS, CAB International, Wallingford, pp. 93-120 (1998).
15. Wink M, Methoden zum Nachweis von Lupinen-Alkaloiden, in *Lupinen 1991*, University Heidelberg, Heidelberg (1992).
16. Hatzold T, Elmadfa I, Gross R, Wink M, Hartmann T and Witte L, Quinolizidine alkaloids in seeds of *Lupinus mutabilis*, *Journal of Agricultural and Food Chemistry* **31**: 934-938 (1983), DOI: 10.1021/jf00119a003.
17. Hama JR and Strobel BW, Natural alkaloids from narrow-leaf and yellow lupins transfer to soil and soil solution in agricultural fields, *Environmental Sciences Europe* **32** (2020), DOI: 10.1186/s12302-020-00405-7.
18. Mende P and Wink M, Uptake of the Quinolizidine Alkaloid Lupanine by Protoplasts and Isolated Vacuoles of Suspension-cultured *Lupinus polyphyllus* Cells. Diffusion or Carrier-mediated Transport?, *Journal of Plant Physiology* **129**: 229-242 (1987), DOI: 10.1016/s0176-1617(87)80082-2.
19. Birk Y, Dovrat A, Waldman M and Uzureau C, Lupin production and bio-processing for feed, food and other by products, European Communities, Brussels (1989).

20. Esteves T, Mota AT, Barbeitos C, Andrade K, Afonso CAM and Ferreira FC, A study on lupin beans process wastewater nanofiltration treatment and lupanine recovery, *Journal of Cleaner Production* **277** (2020), DOI: 10.1016/j.jclepro.2020.123349.
21. Carmali S, Alves VD, Coelho IM, Ferreira LM and Lourenço AM, Recovery of lupanine from *Lupinus albus* L. leaching waters, *Separation and Purification Technology* **74**: 38-43 (2010), DOI: 10.1016/j.seppur.2010.05.005.
22. Baer D, Reimerdes EH and Feldheim W, Methoden zur Bestimmung der Chinolizidinalkaloide in *Lupinus mutabilis*, *Zeitschrift für Lebensmittel-Untersuchung und -Forschung* **169**: 27-31 (1979), DOI: 10.1007/bf01353410.
23. Blaicher FM, Nolte R and Mukherjee KD, Lupin protein concentrates by extraction with aqueous alcohols, *Journal of the American Oil Chemists' Society* **58** (1981), DOI: 10.1007/bf02887317.
24. Cortes-Avendano P, Tarvainen M, Suomela JP, Glorio-Paulet P, Yang B and Repo-Carrasco-Valencia R, Profile and Content of Residual Alkaloids in Ten Ecotypes of *Lupinus mutabilis* Sweet after Aqueous Debittering Process, *Plant Foods for Human Nutrition* **75**: 184-191 (2020), DOI: 10.1007/s11130-020-00799-y.
25. Hwang IM, Lee HW, Lee HM, Yang JS, Seo HY, Chung YJ and Kim SH, Rapid and Simultaneous Quantification of Five Quinolizidine Alkaloids in *Lupinus angustifolius* L. and Its Processed Foods by UPLC-MS/MS, *ACS Omega* **5**: 20825-20830 (2020), DOI: 10.1021/acsomega.0c01929.
26. Gross R, von Baer E, Koch F, Marquard R, Trugo L and Wink M, Chemical composition of a new variety of the Andean lupin (*Lupinus mutabilis* cv. Inti) with low-alkaloid content, *Journal of Food Composition and Analysis* **1**: 353-361 (1988), DOI: 10.1016/0889-1575(88)90035-x.
27. Torres KB, Quintos NR, Necha LL and Wink M, Alkaloid profile of leaves and seeds of *Lupinus hintonii* C. P. Smith, *Zeitschrift für Naturforschung C* **57**: 243-247 (2002), DOI: 10.1515/znc-2002-3-408.
28. Resta D, Boschin G, D'Agostina A and Arnoldi A, Evaluation of total quinolizidine alkaloids content in lupin flours, lupin-based ingredients, and foods, *Molecular Nutrition and Food Research* **52**: 490-495 (2008), DOI: 10.1002/mnfr.200700206.
29. Kamel KA, Świącicki W, Kaczmarek Z and Barzyk P, Quantitative and qualitative content of alkaloids in seeds of a narrow-leaved lupin (*Lupinus angustifolius* L.) collection, *Genetic Resources and Crop Evolution* **63**: 711-719 (2015), DOI: 10.1007/s10722-015-0278-7.
30. Lee H-W, Hwang I-M, Lee HM, Yang J-S, Park EJ, Choi JW, Seo HY and Kim SH, Validation and Determination of Quinolizidine Alkaloids (QAs) in Lupin Products by Gas Chromatography with Flame Ionization Detection (GC-FID), *Analytical Letters* **53**: 606-613 (2019), DOI: 10.1080/00032719.2019.1661423.
31. Wink M, Meißner C and Witte L, Patterns of quinolizidine alkaloids in 56 species of the genus *Lupinus*, *Phytochemistry* **38**: 139-153 (1995), DOI: 10.1016/0031-9422(95)91890-d.
32. Wink M, Wounding-Induced Increase of Quinolizidine Alkaloid Accumulation in Lupin Leaves, *Zeitschrift für Naturforschung C* **38**: 905-909 (1983), DOI: 10.1515/znc-1983-11-1204.
33. Muzquiz M, Cuadrado C, Ayet G, de la Cuadra C, Burbano C and Osagie A, Variation of alkaloid components of lupin seeds in 49 genotypes of *Lupinus albus* from different countries and locations, *Journal of Agricultural and Food Chemistry* **42**: 1447-1450 (2002), DOI: 10.1021/jf00043a011.
34. Nossack AC, Vilegas JHY, Baer Dv and Lanças FM, Supercritical fluid extraction and chromatographic analysis (HRGC-FID and HRGC-MS) of *Lupinus* spp. alkaloids, *Journal of the Brazilian Chemical Society* **11** (2000), DOI: 10.1590/s0103-50532000000500011.
35. Buxbaum E, *Fundamentals of Protein Structure and Function*, Springer, Heidelberg, pp. 3-11 (2015).

36. Reece JB, Urry LA, Cain ML, Wasserman SA, Minorsky PV and Jackson RB, The Structure and Function of Large Biological Molecules, in Campbell Biology, ed by Wilbur B, Pearson Education, London, pp. 56-84 (2019).
37. Jeong Y, Kim HW, Ku J and Seo J, Breakdown of chiral recognition of amino acids in reduced dimensions, *Scientific Reports* **10**: 16166 (2020), DOI: 10.1038/s41598-020-73300-z.
38. Kjeldahl J, Neue Methode zur Bestimmung des Stickstoffs in organischen Körpern, *Fresenius' Zeitschrift für analytische Chemie* **22**: 366-382 (1883), DOI: 10.1007/bf01338151.
39. Mariotti F, Tome D and Mirand PP, Converting nitrogen into protein--beyond 6.25 and Jones' factors, *Critical Reviews in Food Science and Nutrition* **48**: 177-184 (2008), DOI: 10.1080/10408390701279749.
40. Lynch JM and Barbano DM, Kjeldahl Nitrogen Analysis as a Reference Method for Protein Determination in Dairy Products, *Journal of AOAC INTERNATIONAL* **82**: 1389-1398 (1999), DOI: 10.1093/jaoac/82.6.1389.
41. Smith P, Krohn R, Hermanson G, Mallia A, Gartner F, Provenzano M, Fujimoto E, Goeke N, Olson B and Klenk D, Measurement of protein using bicinchoninic acid, *Analytical Biochemistry* **150**: 76-85 (1985), DOI: 10.1016/0003-2697(85)90442-7.
42. Osborne TB and Harris IF, The Chemistry of the Protein-Bodies of the Wheat Kernel, *American Journal of Physiology-Legacy Content* **13**: 35-44 (1905), DOI: 10.1152/ajplegacy.1905.13.1.35.
43. Muranyi IS, PhD thesis: Properties of protein isolates from lupin (*Lupinus angustifolius* L.) as affected by the isolation method, Munich (2016).
44. Nadathur SR, Wanasundara JPD and Scanlin L, Sustainable Protein Sources, Elsevier, Amsterdam (2016).
45. Guerrieri N and Cavaletto M, Proteins in Food Processing, ed by Yada RY, Elsevier, Amsterdam, pp. 223-244 (2018).
46. Sanchez-Chino X, Jimenez-Martinez C, Davila-Ortiz G, Alvarez-Gonzalez I and Madrigal-Bujaidar E, Nutrient and nonnutrient components of legumes, and its chemopreventive activity: a review, *Nutrition and Cancer* **67**: 401-410 (2015), DOI: 10.1080/01635581.2015.1004729.
47. Berg J, Gatto jr GJ, Tymoczko JL and Stryer L, Stryer Biochemie, Springer, Berlin, pp. 34-77 (2015).
48. Duong-Ly KC and Gabelli SB, Salting out of proteins using ammonium sulfate precipitation, *Methods Enzymol* **541**: 85-94 (2014), DOI: 10.1016/B978-0-12-420119-4.00007-0.
49. Assatory A, Vitelli M, Rajabzadeh AR and Legge RL, Dry fractionation methods for plant protein, starch and fiber enrichment: A review, *Trends in Food Science & Technology* **86**: 340-351 (2019), DOI: 10.1016/j.tifs.2019.02.006.
50. Ruiz LP and Hove EL, Conditions affecting production of a protein isolate from lupin seed kernels, *Journal of the Science of Food and Agriculture* **27**: 667-674 (2006), DOI: 10.1002/jsfa.2740270713.
51. King J, Aguirre C and De Pablo S, Functional Properties of Lupin Protein Isolates (*Lupinus albus* cv Multolupa), *Journal of Food Science* **50**: 82-87 (2006), DOI: 10.1111/j.1365-2621.1985.tb13282.x.
52. Hofland GW, de Rijke A, Thiering R, van der Wielen LA and Witkamp GJ, Isoelectric precipitation of soybean protein using carbon dioxide as a volatile acid, *Journal of Chromatography B* **743**: 357-368 (2000), DOI: 10.1016/S0378-4347(00)00259-0.
53. Sussmann D, Pickardt C, Schweiggert UTE and Eisner P, Influence of Different Processing Parameters on the Isolation of Lupin (*Lupinus Angustifolius* L.) Protein Isolates: A Preliminary Study, *Journal of Food Process Engineering* **36**: 18-28 (2011), DOI: 10.1111/j.1745-4530.2011.00647.x.
54. Yu M, Kniepkamp K, Thie JP, Witkamp GJ and van Haren RJF, Supercritical carbon dioxide extraction of oils from Andean lupin beans: Lab - scale performance, process

- scale - up, and economic evaluation, *Journal of Food Process Engineering* **46** (2023), DOI: 10.1111/jfpe.14289.
55. Kniepkamp K, Errico M, Yu M, Roda - Serrat MC, Eilers JG, Wark M and van Haren R, Lipid extraction of high - moisture sour cherry (*Prunus cerasus* L.) stones by supercritical carbon dioxide, *Journal of Chemical Technology & Biotechnology* **99**: 810-819 (2024), DOI: 10.1002/jctb.7581.
 56. Thomas A, Fats and Fatty Oils, in Ullmann's Encyclopedia of Industrial Chemistry, Wiley, Weinheim, pp. 2-71 (2000).
 57. Menaa F, Menaa B, Kahn BA and Menaa A, Trans Fats and Risks of Cardiovascular Diseases, in Handbook of Lipids in Human Function, AOCS Press, Champaign, 21-38 (2016).
 58. Organization FaA, Fats and fatty acids in human nutrition, United Nations, Rom, pp. 1-166 (2010).
 59. Bhardwaj HL, Hamama AA and van Santen E, Fatty acids and oil content in white lupin seed as affected by production practices, *Journal of the American Oil Chemists' Society* **81**: 1035-1038 (2004), DOI: 10.1007/s11746-004-1018-0.
 60. Madeddu C, Roda-Serrat MC, Christensen KV, El-Houri RB and Errico M, A Biocascade Approach Towards the Recovery of High-Value Natural Products from Biowaste: State-of-Art and Future Trends, *Waste and Biomass Valorization* **12**: 1143-1166 (2020), DOI: 10.1007/s12649-020-01082-6.
 61. Krist S, White Lupin Seed Oil, in Vegetable Fats and Oils, pp. 789-793 (2020).
 62. Wu Z, Zhang Q, Li N, Pu Y, Wang B and Zhang T, Comparison of critical methods developed for fatty acid analysis: A review, *Journal of Separation Science* **40**: 288-298 (2017), DOI: 10.1002/jssc.201600707.
 63. Chiu HH and Kuo CH, Gas chromatography-mass spectrometry-based analytical strategies for fatty acid analysis in biological samples, *Journal of Food and Drug Analysis* **28**: 60-73 (2020), DOI: 10.1016/j.jfda.2019.10.003.
 64. Cummings JH and Stephen AM, Carbohydrate terminology and classification, *European Journal of Clinical Nutrition* **61**: S5-18 (2007), DOI: 10.1038/sj.ejcn.1602936.
 65. McCleary BV, McLoughlin C, Charmier LMJ and McGeough P, Measurement of available carbohydrates, digestible, and resistant starch in food ingredients and products, *Cereal Chemistry* **97**: 114-137 (2019), DOI: 10.1002/cche.10208.
 66. Dhingra D, Michael M, Rajput H and Patil RT, Dietary fibre in foods: a review, *Journal of Food Science and Technology* **49**: 255-266 (2012), DOI: 10.1007/s13197-011-0365-5.
 67. Medicine Io, Dietary Reference Intakes: Proposed Definition of Dietary Fiber, The National Academies Press, Washington, DC (2001).
 68. Santos F, Eichler P, Machado G, De Mattia J and De Souza G, By-products of the sugarcane industry, in Sugarcane Biorefinery, Technology and Perspectives, pp. 21-48 (2020).
 69. Chanioti S, Liadakis G and Tzia C, Solid-Liquid Extraction, in Food Engineering Handbook, CRC press, Boca Raton, pp. 253-286 (2014).
 70. Zhang QW, Lin LG and Ye WC, Techniques for extraction and isolation of natural products: a comprehensive review, *Chinese Medicine* **13**: 20 (2018), DOI: 10.1186/s13020-018-0177-x.
 71. Czeslik C, Seemann H and Winter R, Basiswissen Physikalische Chemie, Vieweg+Teubner, Wiesbaden, pp. 14-40 (2010).
 72. Kou D and Mitra S, Extraction of Semivolatile Organic Compounds from Solid Matrices, in Sample Preparation Techniques in Analytical Chemistry, ed by Mitra S, Wiley, Hoboken, 139-182 (2003).
 73. Furniss BS, Hannaford AJ, Smith PWG and Tatchell AR, Practical Organic Chemistry, Wiley, Hoboken, p. 165 (1989).

74. Zygler A, Słomińska M and Namieśnik J, 2.04 - Soxhlet Extraction and New Developments Such as Soxtec, in *Comprehensive Sampling and Sample Preparation*, ed by Pawliszyn J, Academic Press, Oxford, pp. 65-82 (2012).
75. Barthet VJ, Daun JK and Luthria DL, Oil Content Analysis: Myths and Reality, in *Oil Extraction and Analysis*, ed by Luthria DL, AOCS Press, Champaign, pp. 100-118 (2004).
76. Berthod A and Carda-Broch S, Determination of liquid-liquid partition coefficients by separation methods, *Journal of Chromatography A* **1037**: 3-14 (2004), DOI: 10.1016/j.chroma.2004.01.001.
77. Timothy FC, Holden BS and Seibert AF, Liquid-Liquid Extraction and Other Liquid-Liquid Operations and Equipment, in *Perry's Chemical Engineers' Handbook*, ed by Perry RH and Green DW, McGraw-Hill Education, New York City, pp. 1-94 (2019).
78. Witkowski A, Majkut M and Rulik S, Analysis of pipeline transportation systems for carbon dioxide sequestration, *Archives of Thermodynamics* **35**: 117-140 (2014), DOI: 10.2478/aoter-2014-0008.
79. Brunner G, Properties of Supercritical and Near-Critical Gases and of Mixtures with Sub- and Supercritical Components, in *Gas Extraction: An Introduction to Fundamentals of Supercritical Fluids and the Application to Separation Processes*, Steinkopff, Heidelberg (1994).
80. Hitchen SM and Dean JR, Properties of supercritical fluids, in *Applications of Supercritical Fluids in Industrial Analysis*, ed by Dean JR, Springer, Dordrecht, pp. 1-11 (1993).
81. Brunner G, Extraction of Substances with Supercritical Fluids from Solid Substrates, in *Gas Extraction: An Introduction to Fundamentals of Supercritical Fluids and the Application to Separation Processes*, Steinkopff, Heidelberg, pp. 179-250 (1994).
82. Skoog DA and Leary JJ, *Instrumentelle Analytik*, Springer, Heidelberg, pp. 623-649 (1996).
83. Malhotra P, *Analytical Chemistry*, Springer, Heidelberg, pp. 205-242 (2023).
84. Merck, Extrelut® NT working principle, Darmstadt, p. pp. 38-43.
85. Mitchell MJ, Jensen OE, Cliffe KA and Maroto-Valer MM, A model of carbon dioxide dissolution and mineral carbonation kinetics, *Proceedings of the Royal Society A* **466**: 1265-1290 (2009), DOI: 10.1098/rspa.2009.0349.
86. Diamond LW and Akinfiev NN, Solubility of CO₂ in water from -1.5 to 100 °C and from 0.1 to 100 MPa: evaluation of literature data and thermodynamic modelling, *Fluid Phase Equilibria* **208**: 265-290 (2003), DOI: 10.1016/s0378-3812(03)00041-4.
87. Murakoshi I, Yamashita Y, Ohmiya S and Otomasu H, (-)-3β-13α-dihydroxylupanine from *Cytisus scoparius*, *Phytochemistry* **25**: 521-524 (1986), DOI: 10.1016/s0031-9422(00)85514-4.
88. Shimadzu, NIST Mass Spectral Libraries. Nist, Gaithersburg (2012).
89. Thermoscientific, Pierce BCA Protein Assay Kit, Massachusetts, p. pp. 1-4 (2020).
90. Megazyme, Rapid integrated total dietary fiber assay procedure, Bray, p. pp. 1-23 (2020).
91. O'Connell MA, Belanger BA and Haaland PD, Calibration and assay development using the four-parameter logistic model, *Chemometrics and Intelligent Laboratory Systems* **20**: 97-114 (1993), DOI: 10.1016/0169-7439(93)80008-6.
92. Pasquet C, Monna F, van Oort F, Gunkel-Grillon P, Laporte-Magoni C, Losno R and Chateau C, Mobility of Ni, Co, and Mn in ultramafic mining soils of New Caledonia, assessed by kinetic EDTA extractions, *Environmental Monitoring and Assessment* **190** (2018), DOI: 10.1007/s10661-018-7029-0.
93. EMEA, *Validation of Analytical Procedures: Text and Methodology*, ed by EMEA, London, p. pp. 1-15 (2006).
94. Reinhard H, Rupp H, Sager F, Streule M and Zoller O, Quinolizidine alkaloids and phomopsins in lupin seeds and lupin containing food, *Journal of Chromatography A* **1112**: 353-360 (2006), DOI: 10.1016/j.chroma.2005.11.079.

95. Li SL, Chan SW, Li P, Lin G, Zhou GH, Ren YJ and Chiu FC, Pre-column derivatization and gas chromatographic determination of alkaloids in bulbs of *Fritillaria*, *Journal of Chromatography A* **859**: 183-192 (1999), DOI: 10.1016/S0021-9673(99)00867-5.
96. Harris DC, *Lehrbuch der Quantitativen Analyse*, Springer, Heidelberg (2014).
97. Hemscheidt T and Spenser ID, Biosynthesis of lupanine: incorporation of [3,3-2H₂]cadaverine, *Canadian Journal of Chemistry* **65**: 170-174 (1987), DOI: 10.1139/v87-026.
98. Cely-Veloza W, Kato MJ and Coy-Barrera E, Quinolizidine-Type Alkaloids: Chemodiversity, Occurrence, and Bioactivity, *ACS Omega* **8**: 27862-27893 (2023), DOI: 10.1021/acsomega.3c02179.
99. Ly T, Krout M, Pham DK, Tani K, Stoltz BM and Julian RR, Synthesis of 2-Quinuclidonium by Eliminating Water: Experimental Quantification of the High Basicity of Extremely Twisted Amides, *Journal of the American Chemical Society* **129**: 1864-1865 (2007), DOI: 10.1021/ja067703m.
100. Kim J, Mae Choi Y and Yoo K-P, Supercritical fluid extraction of alkaloids, in *Alkaloids: Chemical and Biological Perspectives*, ed by Pelletier SW, Pergamon, pp. 415-431 (2001).
101. Maehre HK, Dalheim L, Edvinsen GK, Elvevoll EO and Jensen IJ, Protein Determination-Method Matters, *Foods* **7** (2018), DOI: 10.3390/foods7010005.
102. Khanizadeh S, Buszard D and Zarkadas CG, Misuse of the Kjeldahl Method for Estimating Protein Content in Plant Tissue, *HortScience* **30**: 1341-1342 (1995), DOI: 10.21273/hortsci.30.7.1341.
103. Gorissen SHM, Crombag JJR, Senden JMG, Waterval WAH, Bierau J, Verdijk LB and van Loon LJC, Protein content and amino acid composition of commercially available plant-based protein isolates, *Amino Acids* **50**: 1685-1695 (2018), DOI: 10.1007/s00726-018-2640-5.
104. Lqari H, Vioque J, Pedroche J and Millán F, *Lupinus angustifolius* protein isolates: chemical composition, functional properties and protein characterization, *Food Chemistry* **76**: 349-356 (2002), DOI: 10.1016/S0308-8146(01)00285-0.
105. Prasadi NPV and Joye IJ, Dietary Fibre from Whole Grains and Their Benefits on Metabolic Health, *Nutrients* **12** (2020), DOI: 10.3390/nu12103045.
106. Keskin S, Kayrak-Talay D, Akman U and Hortaçsu Ö, A review of ionic liquids towards supercritical fluid applications, *The Journal of Supercritical Fluids* **43**: 150-180 (2007), DOI: 10.1016/j.supflu.2007.05.013.
107. Myronchuk VG, Grushevskaya IO, Kucheruk DD and Zmievskaia YG, Experimental study of the effect of high pressure on the efficiency of whey nanofiltration process using an OPMN-P membrane, *Petroleum Chemistry* **53**: 439-443 (2013), DOI: 10.1134/S0965544113070116.

7 Appendix

7.1 Detailed alkaloid quantification results

Table 54: Detailed GC-FID results of *Lupinus mutabilis* extraction experiments.

<u>Soxhlet</u>						
	Sparteine	Lupanine	3b-OH	13-OH	Di-OH	Total
	<i>mg per 100 g DW</i>	<i>mg per 100 g DW</i>	<i>mg per 100 g DW</i>	<i>mg per 100 g DW</i>	<i>mg per 100 g DW</i>	<i>mg per 100 g DW</i>
1	603.5	2474.7	618.2	390.0	336.1	4422.4
2	609.8	2474.6	591.9	373.1	300.9	4350.3
3	609.9	2518.4	621.5	391.1	336.4	4477.2
4	603.6	2459.7	609.0	379.8	333.8	4386.0
5	606.4	2433.7	593.6	396.0	328.0	4357.8
6	604.6	2403.2	592.7	372.0	307.6	4280.0
7	587.5	2376.7	584.4	364.0	314.4	4227.1
8	594.6	2370.4	581.6	363.2	300.8	4210.6
9	586.9	2363.1	553.4	361.5	289.0	4154.0
10	558.1	2201.6	552.3	342.4	301.5	3955.8
<u>Randall</u>						
1	663.8	2715.2	685.7	408.9	368.2	4841.8
2	614.8	2465.0	605.5	365.0	335.1	4385.3
3	647.0	2600.7	661.9	398.5	365.6	4673.7
4	621.4	2518.8	630.9	381.3	346.5	4498.9
5	631.4	2564.4	659.9	400.2	367.1	4622.9
6	599.5	2417.8	603.9	373.5	328.9	4323.6
7	603.3	2473.8	619.7	375.2	337.5	4409.5
8	548.3	2169.9	530.8	310.3	282.8	3842.1
9	600.1	2450.1	628.5	373.7	346.2	4398.6
10	598.0	2379.2	591.0	364.6	320.2	4253.1
<u>LLE</u>						
1	583.5	2855.3	831.4	117.5	19.9	4407.6
2	395.5	2148.2	643.6	66.7	14.4	3268.3
3	326.1	1850.1	536.6	48.2	12.1	2773.2
4	369.2	1818.7	463.9	61.2	17.6	2730.6
5	177.0	956.4	235.5	47.5	16.9	1433.3
6	183.7	1021.3	259.1	49.3	18.8	1532.2
<u>SPE</u>						
1	575.1	2377.4	623.8	193.6	53.8	3823.7
2	621.5	2500.8	661.2	212.2	55.7	4051.4
3	603.2	2474.1	655.3	195.2	54.0	3981.8
4	575.6	2430.0	633.0	190.9	53.0	3882.5
5	537.9	2250.4	587.5	183.2	49.2	3608.2
6	624.0	2572.3	672.9	205.6	53.8	4128.7
7	595.7	2479.6	640.0	186.5	50.8	3952.6
8	570.2	2380.2	624.9	190.9	51.5	3817.7
9	588.2	2416.0	626.3	161.8	40.6	3832.8
10	539.2	2303.5	602.3	183.5	47.5	3676.0

Table 55: Detailed GC-FID results of *Lupinus albus* extraction experiments.

<u>Soxhlet</u>				
	Sparteine	Lupanine	13-OH	Total
	<i>mg per 100 g DW</i>	<i>mg per 100 g DW</i>	<i>mg per 100 g DW</i>	<i>mg per 100 g DW</i>
1	-	91.1	18.2 ^a	109.3
2	-	98.6	18.7 ^a	117.3
3	-	100.2	21.0 ^a	121.2
4	-	94.4	15.5 ^a	109.9
5	-	85.2	18.0 ^a	103.2
6	-	89.1	19.8 ^a	108.9
<u>LLE</u>				
1	-	149.7	5.2	155.0
2	-	141.7	4.7	146.4
3	-	159.7	6.7	166.3
4	-	169.3	4.3	173.6
5	-	183.1	5.8	188.9
6	-	172.2	4.7	177.0
<u>SPE</u>				
1	-	109.4	14.9	124.3
2	-	120.6	17.1	137.7
3	-	116.3	15.9	132.1
4	-	111.6	15.4	126.9
5	-	119.3	16.3	135.6
6	-	113.2	14.9	128.1

a) results are quantified by ignoring the LOD/LOQ values.

Table 56: Detailed GC-MS results of *Lupinus albus* extraction experiment.

<u>Soxhlet</u>				
	Sparteine	Lupanine	13-OH	Total
	<i>mg per 100 g DW</i>	<i>mg per 100 g DW</i>	<i>mg per 100 g DW</i>	<i>mg per 100 g DW</i>
1	-	107.7	15.9	123.7
2	-	97.6	15.8	113.4
3	-	103.7	16.7	120.4
4	-	105.9	22.1	128.0
5	-	118.6	20.3	138.8
6	-	118.5	19.8	138.2
<u>Randall</u>				
1	-	118.50	18.01	136.51
2	-	125.64	19.97	145.61
3	-	119.80	19.56	139.36
4	-	128.59	22.66	151.26
5	-	134.36	22.24	156.61
6	-	150.01	26.80	176.81

7.2 Alkaloid analysis of seed bank samples

Table 57: Seed bank samples analyzed via GC-FID.

Sample	Sparteine	Lupanine	13-OH	3b-OH	Di-OH	Total	SD	SD	
<i>name</i>	<i>mg per</i> <i>100 g DW</i>	<i>mg per</i> <i>100 g DW</i>	<i>mg per</i> <i>100 g DW</i>	<i>mg per</i> <i>100 g DW</i>	<i>mg per</i> <i>100 g DW</i>	<i>mg per</i> <i>100 g DW</i>	<i>mg per</i> <i>100 g DW</i>	<i>%</i>	
1	12-1	LOD	LOD	LOQ	LOD	LOD	-	-	-
2	14-6	LOD	LOD	LOQ	LOQ	LOD	-	-	-
3	63-3	LOD	LOD	LOQ	LOQ	LOD	-	-	-
4	13-1	LOD	LOD	LOQ	LOQ	LOD	-	-	-
5	14-3	LOD	LOD	LOQ	LOQ	LOD	-	-	-
6	14-4	LOD	LOD	LOQ	LOQ	LOD	-	-	-
7	14-1	LOD	LOD	LOQ	LOQ	LOD	-	-	-
8	13-4	LOD	LOD	LOQ	LOQ	LOD	-	-	-
9	62-2	LOD	LOD	LOQ	LOD	LOQ	-	-	-
10	13-2	LOD	LOD	LOQ	LOQ	LOD	-	-	-
11	14-2	LOD	LOQ	LOQ	LOD	LOD	-	-	-
12	62-1	LOD	LOD	LOQ	LOD	LOD	-	-	-
13	14-9	LOD	7.8	LOQ	LOQ	LOD	7.8	0.2	3%
14	14-7	LOD	10.1	LOQ	LOQ	LOD	10.1	1.2	12%
15	Misak	LOD	12.0	LOQ	LOQ	LOD	12.0	0.8	7%
16	11	LOD	12.9	LOQ	LOD	LOD	12.9	0.5	4%
17	44-2	LOD	19.7	LOQ	LOQ	LOD	19.7	4.0	20%
18	12-p	LOD	25.9	LOQ	LOD	LOD	25.9	0.9	4%
19	15-1	LOD	35.6	LOQ	LOQ	LOD	35.6	0.5	2%
20	10-1	LOD	39.3	LOQ	LOQ	LOQ	39.3	3.5	9%
21	12-4	LOD	48.1	LOQ	LOQ	LOD	48.1	0.8	2%
22	15-2	LOD	51.0	LOQ	LOD	LOD	51.0	4.7	9%
23	13-3	LOD	65.5	LOQ	LOD	LOD	65.5	5.5	8%
24	20-1	19.9	51.8	LOQ	LOQ	LOD	71.7	4.3	6%
25	44-1	15.8	88.7	LOQ	LOQ	LOD	104.5	5.0	5%
26	Albus	LOD	129.5	21.5	LOD	LOD	151.0	13.0	9%
27	12-3	LOD	152.0	24.1	LOQ	LOD	176.2	7.9	4%
28	52-3c	14.8	146.3	22.9	LOQ	LOD	184.0	2.3	1%
29	8-3	15.7	147.3	27.4	LOQ	LOD	190.5	2.7	1%
30	52-1	26.4	176.9	LOQ	LOQ	LOD	203.3	9.3	5%
31	25-2	28.1	156.6	52.1	LOD	LOD	236.8	25.5	11%
32	14-5	16.8	222.4	35.8	LOD	LOD	275.0	11.6	4%
33	8-2	18.6	225.0	32.7	LOQ	LOD	276.2	10.4	4%
34	23-1	28.1	219.2	24.9	24.9	LOQ	297.1	8.9	3%
35	12ci	23.3	245.0	32.9	LOQ	LOD	301.3	11.6	4%
36	52-2	27.7	254.6	LOQ	25.1	LOQ	307.4	28.1	9%
37	26-2	33.0	194.4	61.8	31.7	LOQ	320.9	53.1	17%
38	6-2	12.9	262.5	26.3	27.4	LOQ	329.1	5.1	2%
39	2-3	28.3	262.7	29.4	30.9	LOQ	351.3	11.6	3%

Table is continued on the following page.

Table 57 continued.

Sample	Sparteine	Lupanine	13-OH	3b-OH	Di-OH	Total	SD	SD	
<i>name</i>	<i>mg per</i> <i>100 g DW</i>	<i>mg per</i> <i>100 g DW</i>	<i>mg per</i> <i>100 g DW</i>	<i>mg per</i> <i>100 g DW</i>	<i>mg per</i> <i>100 g DW</i>	<i>mg per</i> <i>100 g DW</i>	<i>mg per</i> <i>100 g DW</i>	%	
40	26-1	34.7	201.7	89.0	29.6	LOQ	355.1	6.1	2%
41	4-5	38.2	250.0	45.2	32.0	LOQ	365.3	32.9	9%
42	2-2	26.0	273.1	43.4	28.5	LOQ	371.0	18.4	5%
43	20-2	41.4	274.0	27.7	33.4	LOQ	376.6	33.9	9%
44	25-1	28.7	252.1	72.3	23.6	LOQ	376.7	14.9	4%
45	5-1	15.5	308.0	25.7	30.9	LOQ	380.1	36.2	10%
46	9-3	20.3	299.7	33.3	30.7	LOQ	383.9	13.2	3%
47	23-2	27.4	288.8	69.1	LOQ	LOQ	385.4	38.6	10%
48	3-1	16.4	329.7	25.7	29.7	LOQ	401.5	13.1	3%
49	2-1	28.5	318.6	30.5	34.5	LOQ	412.1	3.8	1%
50	9-2	25.5	330.3	32.3	30.0	LOQ	418.1	16.2	4%
51	64-4	33.2	320.2	23.7	41.8	LOQ	419.0	11.8	3%
52	12c	55.3	306.9	27.9	58.6	LOQ	448.7	18.5	4%
53	6-1	15.1	363.8	51.8	33.4	LOQ	464.0	18.9	4%
54	8-1	21.6	361.0	48.7	39.9	LOQ	471.2	30.2	6%
55	5-2	12.8	366.2	54.2	38.7	LOQ	471.8	31.4	7%
56	28	41.7	301.6	102.7	27.3	LOQ	473.3	9.0	2%
57	2-4	19.8	356.2	35.8	45.1	27.0	483.9	11.8	2%
58	63-2	47.0	270.6	88.6	45.5	39.0	490.7	25.4	5%
59	16-2	89.3	355.1	26.0	77.0	36.4	583.8	11.6	2%
60	21c	65.4	415.1	86.2	49.4	25.0	641.1	16.1	3%
61	9-1	44.2	459.6	51.6	59.5	30.0	644.8	31.5	5%
62	14-10	96.6	414.0	26.4	166.0	69.5	772.5	51.5	7%
63	12-2	11.9	623.5	131.8	37.4	24.7	829.3	25.7	3%
64	3-2	34.1	754.3	99.7	113.7	52.9	1054.8	38.0	4%
65	10-3	113.9	805.9	136.9	143.5	72.9	1273.0	4.9	0%
66	10-2	134.1	1266.1	156.3	102.6	37.7	1696.7	23.4	1%
67	63-1	171.6	1143.3	196.7	153.9	62.0	1727.5	44.8	3%
68	18	147.2	1122.7	234.8	140.2	84.4	1729.3	80.4	5%
69	21-1	150.5	1200.6	224.6	159.1	70.2	1805.0	58.0	3%
70	16-1	230.1	1236.6	161.7	263.6	112.9	2004.9	43.8	2%
71	14-8	147.6	1536.8	99.3	236.5	76.1	2096.4	11.9	1%
72	21-2	155.6	1606.8	255.0	135.1	65.5	2218.0	78.4	4%
73	17-1	192.6	1501.3	245.9	215.0	114.1	2268.9	44.6	2%
74	19-2	258.9	1438.3	274.2	200.0	116.0	2287.4	58.2	3%
75	17-2	155.5	1819.2	323.3	117.5	77.9	2493.4	32.6	1%
76	19-1	288.0	1733.8	245.1	150.2	83.8	2500.9	87.5	3%
77	27	350.1	1625.9	265.3	299.3	156.4	2697.1	58.5	2%
78	Mut.	612.8	2475.5	621.8	275.1	339.8	4424.9	257.4	6%
79	4-6	370.7	3049.6	358.9	757.9	201.8	4738.9	8.5	0%

Table 58: Low alkaloid-containing seed bank samples analyzed via GC-MS method.

	Sample	Sparteine	Lupanine	13-OH	Total	SD	SD
	<i>name</i>	<i>mg per</i>	<i>mg per</i>	<i>mg per</i>	<i>mg per</i>	<i>mg per</i>	%
		<i>100 g DW</i>	<i>100 g DW</i>	<i>100 g DW</i>	<i>100 g DW</i>	<i>100 g DW</i>	
1	12-1	LOD	2.8	LOQ	2.8	0.2	6%
2	14-6	LOD	2.0	LOQ	2.0	0.3	15%
3	63-3	LOQ	2.9	LOQ	2.9	0.4	13%
4	13-1	LOD	2.0	LOQ	2.0	0.3	14%
5	14-3	LOD	2.8	LOD	2.8	0.9	34%
6	14-4	LOD	2.5	LOQ	2.5	0.3	13%
7	14-1	LOD	3.1	LOQ	3.1	1.1	34%
8	13-4	LOD	2.2	LOQ	2.2	0.3	15%
9	62-2	LOQ	3.9	LOQ	3.9	1.0	25%
10	13-2	LOD	3.1	LOQ	3.1	0.1	3%
11	14-2	LOD	3.3	LOQ	3.3	2.0	61%
12	62-1	LOQ	3.0	LOQ	3.0	0.9	31%
13	14-9	LOD	4.2	2.7	6.9	1.8	25%
14	14-7	LOQ	6.9	3.4	10.2	2.2	21%
15	Misak	LOQ	10.0	6.5	16.5	1.6	10%
16	11	0.9	10.0	3.8	14.7	2.3	15%
17	44-2	1.5	20.8	7.1	29.4	5.9	20%
18	12p	0.8	30.5	6.3	37.5	2.1	5%
19	15-1	1.4	44.6	18.5	64.5	1.3	2%
20	10-1	LOQ	52.1	20.6	72.8	6.8	9%
21	12-4	LOQ	65.3	23.1	88.4	1.7	2%
22	15-2	1.3	71.1	23.1	95.6	2.0	2%
23	13-3	1.0	94.6	29.3	124.9	6.6	5%
24	20-1	14.6	70.7	16.5	101.8	6.9	7%
25	44-1	9.7	128.5	41.4	179.7	9.5	5%
26	Albus	LOD	129.5	21.5	151.0	13.8	9%

7.3 Results nitrogen solvation experiment

Table 59: Protein solvation experiment of *Lupinus mutabilis* beans at different pH values.

	Supernatant				Precipitate			
	ω_{sup}	N% _{sup}	P% _{sup} ^a	Y(N) _{sup}	ω_{prec}	N% _{prec}	P% _{prec} ^a	Y(N) _{prec}
pH 1	68.7%	8.9%	55.3%	69.0%	31.3%	8.7%	54.6%	31.0%
pH 2	58.1%	10.4%	65.0%	68.5%	41.9%	6.6%	41.4%	31.5%
pH 3	49.3%	8.5%	52.9%	47.3%	50.7%	9.2%	57.2%	52.7%
pH 4	30.3%	3.8%	23.9%	13.1%	69.7%	11.0%	68.7%	86.9%
pH 5	29.0%	4.4%	27.3%	14.3%	71.0%	10.6%	66.5%	85.7%
pH 6	59.4%	10.3%	64.3%	69.4%	40.6%	6.7%	41.6%	30.6%
pH 7	62.1%	10.4%	65.2%	73.5%	37.9%	6.2%	38.6%	26.5%
pH 8	63.7%	10.5%	65.3%	75.5%	36.3%	6.0%	37.2%	24.5%
pH 9	64.3%	10.0%	62.6%	73.1%	35.7%	6.6%	41.5%	26.9%
pH 10	66.3%	10.3%	64.5%	77.5%	33.7%	5.9%	36.7%	22.5%
pH 11	64.5%	10.6%	66.1%	77.4%	35.5%	5.6%	35.1%	22.6%
pH 12	67.8%	10.3%	64.4%	79.2%	32.2%	5.7%	35.6%	20.8%

a) is referring to the Kjeldahl determination methods ($N \times 6.25$).

7.4 Regression data

Table 60: Four parameter regression data for Figure 27.

	p_1	p_2	p_3	p_4	R^2
Sparteine	0	1.477	0.813	0.998	0.999
Lupanine	0	1.156	1.270	1.010	0.999
3b-OH	0	1.079	3.621	1.044	0.998
13-OH	0	1.086	3.225	1.037	0.998
Di-OH	0	1.141	6.439	1.073	0.998

Table 61: Four parameter regression data for Figure 35.

	p_1	p_2	p_3	p_4	R^2
Sparteine	0	5.009	1.011	0.999	0.999
Lupanine	0	6.266	0.977	1.000	0.999
3b-OH	0	7.230	9.713	1.000	1.000
13-OH	0	3.010	2.220	1.027	0.998
Di-OH	0	1.915	6.774	1.464	0.999

Table 62: Four parameter regression data for Figure 37.

	p_1	p_2	p_3	p_4	R^2
13-OH, L-Mut., pH 12, TCA	0	3.055	2.474	1.029	0.999
13-OH, L-Mut., pH 12, HCl	0	3.010	2.220	1.027	0.999
13-OH, L-Alb., pH 12, TCA	0	3.711	2.188	1.010	0.996
13-OH, L-Alb., pH 12, HCl	0	4.597	2.394	1.001	0.999
13-OH, L-Alb., pH 10, TCA	0	3.176	2.295	1.020	0.999
Di-OH, L-Mut., pH 12, TCA	0	1.865	6.368	1.428	0.999
Di-OH, L-Mut., pH 12, HCl	0	1.915	6.774	1.464	0.999

Table 63: Four parameter regression data for Figure 52.

	p_1	p_2	p_3	p_4	R^2
20 °C	-	-	-	-	-
40 °C	0	7.253	63.001	48.497	0.999
60 °C	0	3.813	58.185	52.520	0.999

Table 64: Four parameter regression data for Figure 53.

	p₁	p₂	p₃	p₄	R²
60 bar, 20 °C	0	2.257	23.311	5.275	0.999
60 bar, 40 °C	0	1.357	45.221	5.699	0.999
120 bar, 40 °C	0	2.745	14.755	4.820	0.999

7.5 Lupin oil extraction

Received: 21 September 2022 | Revised: 19 December 2022 | Accepted: 18 January 2023

DOI: 10.1111/jfpe.14289

ORIGINAL ARTICLE

Journal of
Food Process Engineering

WILEY

Supercritical carbon dioxide extraction of oils from Andean lupin beans: Lab-scale performance, process scale-up, and economic evaluation

Miao Yu¹  | Kai Kniepkamp¹ | Jan Pieter Thie¹ | Geert-Jan Witkamp²  | Rob J. F. van Haren¹ 

¹Research Centre Biobased Economy, Hanze University of Applied Sciences, Groningen, Netherlands

²Water Desalination and Reuse Center, Biological and Environmental Science and Engineering Division, King Abdullah University of Science and Technology (KAUST), Thuwal, Saudi Arabia

Correspondence

Miao Yu, Research Centre Biobased Economy, Hanze University of Applied Sciences, Zernikeplein 11, 9747 AS, Groningen, Netherlands.

Email: m.yu@pl.hanze.nl

Funding information

Bio-Based Industries Joint, Grant/Award Number: 720726.; European Regional Development Fund, Grant/Award Number: OPSNN0261

Abstract

Oil extraction from Andean lupin beans (*Lupinus mutabilis* SWEET) via supercritical carbon dioxide (scCO₂) was studied on both lab scale and pilot scale. On the lab scale, the effect of pressure, solvent-to-feed ratio (S/F), sample particle size and temperature on oil yield were evaluated. The oil quality (fatty acid [FA] composition and tocopherol content) were investigated. Five-hour scCO₂ extraction yielded about 86% oil of Soxhlet extraction (using hexane as solvent). The fraction of unsaturated FA rose with extraction pressure at specific time. High tocopherol contents were detected in oils extracted at low pressure. An increase in temperature was unfavorable to oil and tocopherol yield, thereby confirming the validity for preserving oil extract quality under a mild scCO₂ extraction condition. Oil quality and yield did not have identical optimum settings, opening up possibilities for producing different qualities of oils. Pilot-scale extraction offered comparable oil yield to lab-scale extraction at similar S/F ratio. Economic evaluation showed that it is promising to implement industrial scale scCO₂ process for lupin oil extraction. It was predicted that, at a specific industrial scale of extraction (2 × 1000 L, 550 bar, 40°C and S/F of 24), the manufacturing cost of oils got close to actual commercial production cost.

Practical Application

This study applied an environment-friendly high-pressure extraction method, supercritical carbon dioxide (scCO₂) extraction, to separate oils from Andean lupin beans (*Lupinus mutabilis* SWEET). ScCO₂ extraction can serve as an alternative oil extraction method to conventional ones that use fossil-derived organic solvents as the extractant. Up-scaled scCO₂ processing was estimated to be economically viable for commercial lupin oil production.

KEYWORDS

Andean lupin beans, economic evaluation, fatty acids, lab-scale, oil extraction, pilot-scale, supercritical carbon dioxide, tocopherol

This is an open access article under the terms of the [Creative Commons Attribution-NonCommercial License](https://creativecommons.org/licenses/by-nc/4.0/), which permits use, distribution and reproduction in any medium, provided the original work is properly cited and is not used for commercial purposes.

© 2023 Hanze University of Applied Sciences and The Authors. *Journal of Food Process Engineering* published by Wiley Periodicals LLC.

1 | INTRODUCTION

Lupin bean is the primary source of the commercial value of lupin that is of agronomic interest regarding its richness in protein, carbohydrate, oil and specific health-beneficial compounds such as polyphenols (Czubinski et al., 2019; Gulewicz et al., 2008; Sujak et al., 2006). Andean lupin (*Lupinus mutabilis* SWEET), one of the “lost crops of the Incas”, has gained increasing interest for the potential of growing on marginal land for soil enrichment and as fodder and food crop. Aside from the high protein and carbohydrate content (about 45% and 35% respectively), the Andean lupin beans contain about 20% oil (Borek et al., 2009a; Carvajal-Larenas et al., 2016a), which is comparable to mainstream sources of edible vegetable oils and proteins such as soybean. Andean lupin can grow, in contrast to soybean, in the northern agro-ecological zones in Europe and has the possibility to grow as a winter crop in the southern agro-ecological zones of Europe as well (Bebeli et al., 2020). This calls for attention to develop Andean lupin as a European crop for its oil and protein yield (Fleetwood & Hudson, 1982a).

A comparison of the oil content and fatty acid composition of Andean lupin bean with some other oilseeds is shown in Table 1. The Andean lupin bean and soybean are comparable in the content of oil, though lower than some other oilseeds. However, considering the oil and meal together, the high-protein content of the Andean lupin bean and soybean makes them more commercially competitive. The Andean lupin oil contains similar fatty acid components to other seed oils, especially argan oil, which are rich in unsaturated fatty acids and are desirable for human nutrition (Cowling et al., 1998). Compared with soybean oil, Andean lupin oil contains a relatively high fraction of

monounsaturated oleic acid (C18:1), which is considered better for cardiovascular health than polyunsaturated linoleic acid (C18:2) (Song et al., 2017a). Also, the reduction of linoleic acid improves oxidative stability without the production of trans-fatty acids (Clemente & Cahoon, 2009; Song et al., 2017a).

The stability of extracted oils under oxidative conditions depends on the level of natural antioxidants in the sample (Boekenoogen, 1964; Carpenter, 1979). One of the typical classes of natural antioxidants in plant oils is tocopherol, which is classified as α -, β -, γ - and δ -tocopherol. These natural antioxidants are not only involved in preventing oils from nonenzymatic oxidation, but also potentially in preventing and treating cardiovascular diseases, diabetes, neurodegenerative diseases, and even cancer (Bartoszińska et al., 2016; Bunea et al., 2012). The oil extracted from lupin beans was reported to have a tocopherol content of about 40–70 mg/100 g oil in literature (Feldheim et al., 1984). This tocopherol content is higher than some other conventional edible oils such as soybean oil (about 7–27 mg/100 g oil) and sunflower oil (about 9–43 mg/100 g oil) (Grilo et al., 2014).

Regarding the above aspects, the Andean lupin bean has a health-beneficial oil suitable for food and cosmetic applications.

The commonly applied methods for oil extraction from oilseeds are generalized and compared in Table S1 in the supplementary materials of this article. For oil extraction from lupin beans, mechanical extraction is scarcely applied, which might be due to their relatively low-oil content compared to other oilseeds. Instead, most of those studies focused on chemical extraction regarding the high-extraction efficiency. Both enzymatic extraction (Jung, 2009) and organic solvent extraction (Ortiz & Mukherjee, 1982) have been tested to extract

TABLE 1 Comparison of oil content and fatty acid composition of Andean lupin beans and some other oilseeds

Legume (species)	Oil content (%)	Component fatty acids (%)					References
		C16:0	C18:0	C18:1	C18:2	Other	
Andean lupin bean (<i>Lupinus mutabilis</i>)	20 ^a	11	6	47	31	5	(Borek et al., 2009a; Carvajal-Larenas et al., 2016a; Fleetwood & Hudson, 1982a)
Soybean (<i>Glycine max</i>)	20	9	4	26	51	9	(Fleetwood & Hudson, 1982a; Grela & Günter, 1995; Kostik, Memeti, & Bauer, 2013; Song et al., 2017a)
Rapeseed (<i>Brassica napus</i>)	44	5	2	63	20	10	(Fleetwood & Hudson, 1982a; Orsavova, Misurcova, Ambrozova, Vicha, & Mlcek, 2015)
Sunflower seed (<i>Helianthus annuus</i>)	44	5	4	28	61	2	(Akkaya, 2018; Kostik et al., 2013; Le Clef & Kemper, 2015; Orsavova et al., 2015)
Argan seed (<i>Argania spinosa</i>)	45	16	4	43	36	1	(Guillaume & Charrouf, 2011; Khallouki et al., 2003)
Peanut (<i>Arachis hypogea</i>)	52	8	3	65	19	5	(Kostik et al., 2013; Orsavova et al., 2015; Song et al., 2017a)
Pistacia khinjuk ^b	46	22	2	57	13	6	(Sodeifian, Ghorbandoost, Sajadian, & Ardestani, 2016)
Dracocephalum kotschy ^b	18	5	2	18	16	59	(Sodeifian, Sajadian, & Ardestani, 2017b)
Purslane seed (<i>Portulaca oleracea</i>) ^b	11	16	5	23	22	34	(Desta, Molla, & Yusuf, 2020; Sodeifian, Ardestani, Sajadian, & Moghadamian, 2018)

^aAll the numbers here are approximate values from the literature.

^bPlant materials with medical values.

lupin oils. In recent decades, the demand for sustainable chemical processes calls for extractions with little or no use of fossil-based solvents.

Supercritical fluid extraction is a powerful technique in separation processes, especially for the processing of natural materials. Supercritical carbon dioxide (scCO₂) has been used as an extractant for industrial production. It is advantageous to process thermal-labile materials such as proteins due to CO₂ mild critical conditions (critical temperature and pressure of 31°C and 74 bar respectively). Regarding this, scCO₂-defatted Andean lupin flour can be served for extraction of protein with well-preserved quality. The tuneable solvent properties such as density and viscosity (by changing operating temperature and pressure) allow optimized diffusion into source materials and dissolution of target compounds. Also, compared to conventional fossil-based organic solvents, scCO₂ is environment-friendly and does not cause any human health problems since it is nontoxic. Furthermore, scCO₂ possesses advantages such as cost-effectiveness, odourlessness, colourlessness, noncorrosivity and easy post-separation (Bozan & Temelli, 2003; Goto et al., 1993; Sahena et al., 2009; Gholamhossein Sodeifian & Ansari, 2011; GH Sodeifian et al., 2014; Gholamhossein Sodeifian & Sajadian, 2017; Gholamhossein Sodeifian, Sajadian, & Ardestani, 2016a, 2016b, 2016c; Sodeifian et al., 2017a; Sovilj, 2010).

scCO₂ has been extensively investigated as a novel solvent to process common oilseeds for oil extraction (J. Friedrich & Pryde, 1984; J. P. Friedrich & List, 1982; Herrero et al., 2010; Palmer & Ting, 1995; Stahl et al., 1980; Temelli, 2009). During the process, oils from the sample are dissolved into the supercritical phase. Dissolved oils are then separated from CO₂ by lowering the operating pressure (from supercritical state to subcritical state) (Anklam et al., 1998; Sahena et al., 2009), upon which the CO₂ can be recycled for another extraction. Relevant trials of applying scCO₂ for lupin oil extraction have been reported in the literature (Daković et al., 1989; Stahl et al., 1980). However, previous studies scarcely dealt with Andean lupin beans, and insufficient information was provided regarding the effectiveness of lupin oil extraction by scCO₂ and specific extraction conditions. The effect of factors such as extraction pressure, CO₂ flow rate and flour particle size on oil extraction remains to be clarified. Additionally, the correlation between extraction conditions and oil properties, such as fatty acid composition and tocopherol content, can provide insight into the characterization of the extraction process and production of high-quality oils for specific applications. This correlation has been scarcely studied for Andean lupin beans, though such oil properties were reported elsewhere to be affected by scCO₂ extraction conditions (Aladić et al., 2015; Birtigh et al., 1995; Corzini et al., 2017; Gustinelli et al., 2018; Leo et al., 2005; Merkle & Larick, 1995; Oliveira et al., 2002; Rombaut et al., 2017).

A step forward from lab-scale extraction to pilot-scale extraction opens up the potentiality of scCO₂ extraction for industrial oil production. However, the promotion of scCO₂ processing from the lab scale to the industrial scale (usually hundreds to thousands of liters) is usually hindered by the scarcity of relevant economic evaluations, especially when taking into account that the investment in scCO₂

extraction increases exponentially with the capacity (Carvalho et al., 2015). Experimentally, semi-industrial extraction set a feasibility limit of about tens of liters. The prediction on an upper-scale process requires extrapolation of down-scale performance and proper computational simulation, out of which the predicted commercial performance helps bridge the gap between lab research and industrial production (Ulrich, 1984; Zlokarnik, 2006).

This study aims to evaluate oil yield from Andean lupin beans via lab-scale scCO₂ process and the effects of scCO₂ processing conditions on oil quality in terms of fatty acid composition and tocopherol content. The extraction performance was also evaluated on a pilot scale. Moreover, it is aimed to employ the commercial simulator, SuperPro Designer[®] software, to conduct an economic evaluation and estimate the cost of manufacturing (COM) of oil from Andean lupin beans via up-scaled scCO₂ extraction.

2 | MATERIALS AND METHODS

2.1 | Materials and preparation of solutions

Beans of Andean lupin (*Lupinus mutabilis* SWEET, tarwi, chocho) were purchased from South America (Peru) and were used as raw material for oil extraction. Complete full-fat Andean lupin beans were pre-processed by using a lab-scale burr mill grinder (KitchenAid[®] Food Grinder with Jupiter Steel Cone Grinder Attachment) and sieved into different fractions by using mesh sizes of 0.5 mm, 1 mm and 2 mm, respectively. Particles in each fraction of the sieved flour have sizes that are smaller than or equal to the mesh size. CO₂ (99% purity) was purchased from Linde Group (Linde Gas Benelux BV, the Netherlands). Conventional Soxhlet oil extraction was performed using hexane (technical grade, Argos Organics, Geel, Belgium) as an extractant. Fatty acid components of the extracted oils were analyzed, in which acetyl chloride (Sigma-Aldrich, Zwijndrecht, the Netherlands), methanol (Sigma-Aldrich, Zwijndrecht, the Netherlands), sodium chloride (NaCl) (Sigma-Aldrich, Zwijndrecht, the Netherlands), hexane and ultrapure water (purified using a Milli-Q ultra-pure water system, Millipore[™], Molsheim, France) were used. Standard samples of methyl linoleate, methyl palmitate, methyl oleate and methyl stearate (Sigma-Aldrich, Zwijndrecht, the Netherlands) were used to build the calibration curve for concentration determination via gas chromatography analysis, in which hydrogen (99.9999% purity, Linde Gas Benelux BV, the Netherlands) was used as the carrier gas. Supelco 37 Component FAME mix (Supelco, Bellefonte, PA, USA) was used for peak identification in the chromatograph. For tocopherol content determination, NaOH (Fisher Scientific UK Ltd., Leicestershire, UK) dissolved in ethanol (HPLC-grade, Acros Organics, Geel, Belgium) was used for tocopherol extraction from the oils, and formic acid (99% purity, Acros Organics, Geel, Belgium) was used for neutralization. The α -, γ - and δ -tocopherol standards (Sigma-Aldrich, Zwijndrecht, the Netherlands) were used for concentration calibration. HPLC-grade acetonitrile (VWR, Strasbourg, France) containing 0.1% trifluoroacetic acid (Acros Organics, Geel, Belgium) and water were used as the mobile phase for liquid chromatography analysis.

2.2 | Soxhlet oil extraction

Extraction thimbles (Whatman, GE Healthcare, Den Bosch, the Netherlands) containing about 20 g ground lupin beans were transferred to a Soxhlet extractor. The extractor was filled with 300 mL of hexane and heated at the temperature of about 80 °C under reflux for 2 h, 5 h, 6 h, and 12 h, respectively. The 0.5 mm meshed particles were extracted under all these conditions. An extraction for 5 h from 2 mm meshed samples was also performed to check the effect of mesh size on the amount of obtainable oil. After the completion of each extraction, the thimbles filled with defatted flour were exposed to the air overnight for hexane evaporation. The mass difference of the flour before and after Soxhlet extraction was calculated as the mass of extracted oil. This mass difference was checked to be the same as the mass of the collected oil after separating from hexane using a rotary evaporator (IKA RV10, North Carolina, USA). Triplication of the thimbles under each condition was performed. In this report, the oil yield indicates the ratio of the mass of extracted oil to the mass of lupin flour for the extraction (see Equation 1).

$$\text{Extraction yield (\%)} = \frac{\text{Mass of extracted oil}}{\text{Mass of lupin flour}} \times 100\% \quad (1)$$

2.3 | Lab-scale supercritical carbon dioxide extraction set-up and processing

A schematic diagram of the lab-scale scCO₂ equipment (SFE 500, Separex, Champigneulle, France) is displayed in Figure 1. A picture of this equipment is shown in Figure S1 in the supplementary materials. For each extraction, 100 g of freshly ground and meshed lupin flour was placed in a 0.5 L extraction vessel. The moisture content of the milled full-fat flour was determined by a moisture analyzer (MB160, VWR, Italy). The moisture content of the flour was about 7% (w/w). According to the literature, this moisture level has little effect on the

extractability of oil from lupin beans (Snyder et al., 1984; Stahl et al., 1981). At both ends of the extractor, filter papers were placed to avoid the entrainment of the flour. The extractor was warmed up by an oven (France Etuves, XU058, Chelles, France). During the experiment, CO₂ from the storage cylinder (≈55 bar) was firstly cooled to a liquid state (≈5 °C) via the chiller (National Lab PCR P 13.02, Molln, Germany) and transported via a piston pump. The inline flow rate of CO₂ through the pump is monitored. Then the extraction vessel was pressurized (with CO₂) and heated to the desired supercritical state. Simultaneously, the separator, which is used to separate extract from CO₂, was adjusted to a subcritical state (about 60 bar at 30 °C). The oils which were miscible with scCO₂ in the extraction vessel were brought to the separator, in which the oils were separated from CO₂ and were retained in the vessel. The CO₂ was recycled during the extraction. The extracted oils were collected manually via the sample collection valve implemented at the bottom of the separator. The extraction lasted for 5 h with samples taken every hour. The extracted oils were weighed and stored at −20 °C for further analyses. Based on the weight, the extraction efficiency was calculated (see Equation 2). Since it is an exhaustive extraction technique for continuous oil separation, Soxhlet extraction using hexane as the solvent is usually employed to determine product oil quality. Therefore, the performance and potential of scCO₂ for lupin oil extraction, with reference to conventional Soxhlet extraction, can be elucidated via their comparison. After 5 h of extraction, the equipment was flushed with excessive CO₂ and then depressurised. The oil residues (mostly mixed with water) that were not collectable during the extraction were manually gathered from the separator.

$$\text{Extraction efficiency (\%)} = \frac{\text{Mass of oil extracted by scCO}_2}{\text{Mass of oil extracted by Soxhlet}} \times 100\% \quad (2)$$

The effects of three factors, that is, extraction pressure, scCO₂ flow rate, and particle mesh size, on the oil extraction were investigated via response surface methodology using a Box–Behnken Design

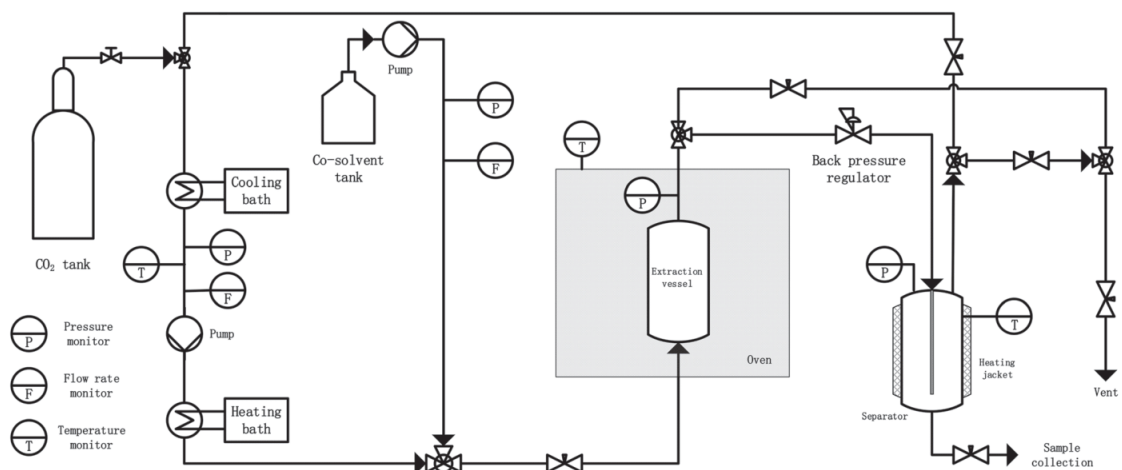


FIGURE 1 Schematic diagram of the lab-scale scCO₂ extraction equipment.

(BBD) (Sharif et al., 2014). Unlike Central Composite Design (CCD), which is another popular design for scCO_2 extraction, BBD has all the tested points in a safe operating zone based on predetermination, which is superior if out-of-range tests are hard to handle regarding physical or experimental constraints. CCD tends to have noninteresting test points or points that are beyond safe operating limits and improper to operate. Also, in contrast to CCD, BBD designs ensure that all factors are not set at their extremes simultaneously. Furthermore, BBD often has fewer design points than CCD and is easier to accomplish with the same number of factors (Montgomery, 2017; Gholamhossein Sodeifian, Sajadian, & Ardestani, 2016b). In this study, triplicated central point was used for BBD, and for the other design points, the responses were average of duplicates. The designed extractions were performed at a pressure range of 150 bar to 550 bar with a CO_2 flow rate of 10–25 g/min and particle mesh size of 0.5–2 mm. The detailed conditions are listed in Table S2 in the supplementary materials. The working temperature for the extraction was set at 40°C. One of those conditions that gave rise to a high oil yield was selected for a comparative study carried out at 60 and 80°C to investigate the effect of temperature on the extraction performance. Since different CO_2 flow rates were applied for extraction (10–25 g/min), indicating different amounts of CO_2 used, it is favorable to present the amount of extracted oil per mass of raw material versus the quantity of CO_2 per mass of raw material. This could help model the extraction kinetics or determine the solubility of oil in scCO_2 . For the later economic evaluation, the amount of consumed CO_2 per mass of extracted oil is basic information to calculate the energy consumption to compress the fluid. By having the criterion of oil yield against the solvent-to-feed ratio (S/F ratio), it is straightforward to evaluate and compare the efficiency of using scCO_2 to extract oils via operation at lab, pilot or even industrial installation. Therefore, the S/F ratio was used here and calculated as the ratio of the mass of consumed CO_2 to the mass of Andean lupin flour.

For the response surface analysis, a simple mathematical expression is used to approximate as closely as possible the real relationship between responses and factors (Mead & Pike, 1975). Here the experimental data and the independent variables were fitted by a second-order polynomial model. The response data were analyzed using the software Design-Expert (Design-Expert 11, State-Ease, Inc., Minneapolis MN, USA). Analysis of variance (ANOVA) was performed to evaluate the significance of quadratic models and coefficients. Based on the response surface model, optimal oil extraction efficiency was predicted and compared to experimental results.

2.4 | Determination of fatty acid composition

The oil samples were first esterified into fatty acid methyl esters (FAME) with acetyl chloride in methanol and then identified by Gas Chromatography - Flame Ionization Detector (GC-FID; Shimadzu, 's-Hertogenbosch, the Netherlands). Briefly, 5 mg oil was weighed accurately in a 25 mL glass tube, followed by adding 100 μl internal standard solution containing tetradecane, methyl nonanoate and

nonadecanoic acid (40 mg/50 ml hexane) as references for the state of sample injection, methyl ester standard sample and esterification reaction, respectively. After a one-hour reaction at 60°C with 3 ml 5% acetyl chloride in methanol with intensive mixing, 1 ml water, 0.3 g NaCl and 2 ml hexane were added and mixed, followed by 5 min centrifugation at 4000 rpm. The supernatant was then transferred to a 2 ml vial for GC-FID analysis.

The GC-FID was installed with an Rtx-5MS column (30.0 m length \times 0.25 mm diameter; 0.25 μm film thickness). The column oven temperature was set at 80°C, followed by an increase to 140°C at a rate of 20°C/min, then to 210°C at the rate of 3°C/min, and finally to 300°C at 20°C/min. During the GC measurement, a 0.5 μl sample was injected, and hydrogen was used as the carrier gas with a column flow rate of 1.2 ml/min out of a total flow rate of 10 ml/min. Standard samples of methyl linoleate, methyl palmitate, methyl oleate and methyl stearate were used to build the calibration curve for concentration determination. The calculation of fatty acid concentrations was based on the sample peak area relative to the internal standardization. The Soxhlet oil extracts and the scCO_2 oil extracts (in duplication) were measured.

2.5 | Determination of tocopherol content

A 10 mg oil sample was weighed in a 2 ml eppendorf tube, followed by adding 1 ml extractant (10% NaOH in ethanol) and vortex mixing. The mixture was rotated for 3 h for transfer of tocopherol into the ethanol phase, followed by centrifugation at 14000 rpm for 15 min. Fifty microlitres of formic acid were then added to the Eppendorf tube for neutralization. Afterwards, the mixture was again vortexed and rotated for 2 h, followed by centrifugation at 14000 rpm for 15 min. The supernatant was measured by liquid chromatography (LC) with an ultraviolet-visible detector (UV-Vis).

As there was no β -tocopherol detected in Andean lupin oil, only the standards of α -, γ - and δ -tocopherol were used as references. Stock tocopherol solution was prepared by dissolving the tocopherol standards in ethanol and stored at -20°C in the dark. The stock solution was diluted to different concentrations for calibration.

The LC analysis was performed using a Shimadzu LC-20AT (Shimadzu, 's-Hertogenbosch, The Netherlands) pump system with an XTerra MS C18 column (100 mm length \times 4.6 mm diameter; 3.5 μm particle size; Waters, Santry, Dublin, Ireland). A UV-Vis detector (SPD-20A) was used, and detection was performed at 295 nm, which was the optimum absorption wavelength determined by scanning the absorption spectra of tocopherols in quartz cuvettes using a Shimadzu UV-1800 spectrophotometer (Shimadzu, 's-Hertogenbosch, the Netherlands). During the LC analysis, a 20 μl sample was injected, and the eluent flow rate was 1 ml/min at binary gradient mode. Two mobile phases were used, that is, water and acetonitrile containing 0.1% trifluoroacetic acid. The fraction of the latter phase increased from 0% to 100% during the first 10 min and lasted until the end of the determination (15 mins in total). The column was at room temperature. Quantification was performed by comparing the sample peak

areas to those of references. Tocopherol content was expressed as mg per 100 g oil. The α - and δ -tocopherol concentrations were low and neglected for the data analysis. The γ -tocopherol content in the oils from Soxhlet extraction and $scCO_2$ extractions (in duplication) was reported.

2.6 | Pilot-scale $scCO_2$ oil extraction

$scCO_2$ extractions were also carried out on an upper scale by using a pilot scale supercritical fluid system (SFT-NPX-10, Supercritical Fluid Technologies Inc., Newark, DE, USA). The schematic diagram and pictures of this equipment are shown respectively in Figure 2 and Figure S2 (supplementary materials). The unit consisted of two stainless steel extraction vessels (volume ≈ 10 L; diameter ≈ 15.9 cm; length ≈ 54.5 cm; wall thickness ≈ 6 cm) and two stainless steel separators (volume ≈ 750 ml; diameter ≈ 7.6 cm; length ≈ 21.3 cm; wall thickness ≈ 2.5 cm). For extraction in this study, one of the extractors is used. Five kg ground lupin beans were loaded into a standard-steel basket, followed by being positioned into one 10 L extraction vessel. The extraction vessel and separators were respectively warmed up to 40 and 30°C via electrical heating jackets. Carbon dioxide was first cooled via the chiller (Emerson FFAP-017Z, St. Louis, MO, USA), followed by being transported via a pneumatic pump (Haskel, ASF-100-29,376-W, Burbank, CA, USA), and then warmed up by a heater (CAST-X 500, Batavia, IL, USA) before entering the extraction vessel.

The extraction started after pressurizing the extraction vessel to 350 bar. The extract passed the two separators consecutively with the respective pressure of 65 bar and 50 bar, controlled by an automatic back pressure control valve (shown as P-10 in Figure 2; RCV 755, Badger Meter, Milwaukee, WI, USA). The $scCO_2$ flow rate was adjusted to 500 g/min using a micro-metering regulating control valve (shown as P-8 in Figure 2; Butech, Erie, PA, USA). The extraction lasted for 5 h and the extracted oil samples were hourly collected. The extraction was performed in duplicate.

2.7 | Economic evaluation

For the economic evaluation of lupin oil extraction via $scCO_2$ processing, adapted methodology according to studies elsewhere (Carvalho et al., 2015; Prado et al., 2012) was used and the commercial simulation toolbox SuperPro Designer[®] v10.0 was employed. This toolbox is embedded with a databank of various equipment, unit operations and chemical materials that are usually used in the chemical industry. The toolbox solves all equations that are related to the involved processing units. Convergence of the model is achieved based on incorporated kinetic models, set iteration number and accuracy. The economic performance of four scales of the extraction equipment, that is, 10, 100, 500, and 1000 L, were evaluated. The oil yield of the modeled processes refers to the experimental pilot extraction result (10 L scale) and some lab-scale results. It is assumed that similar oil

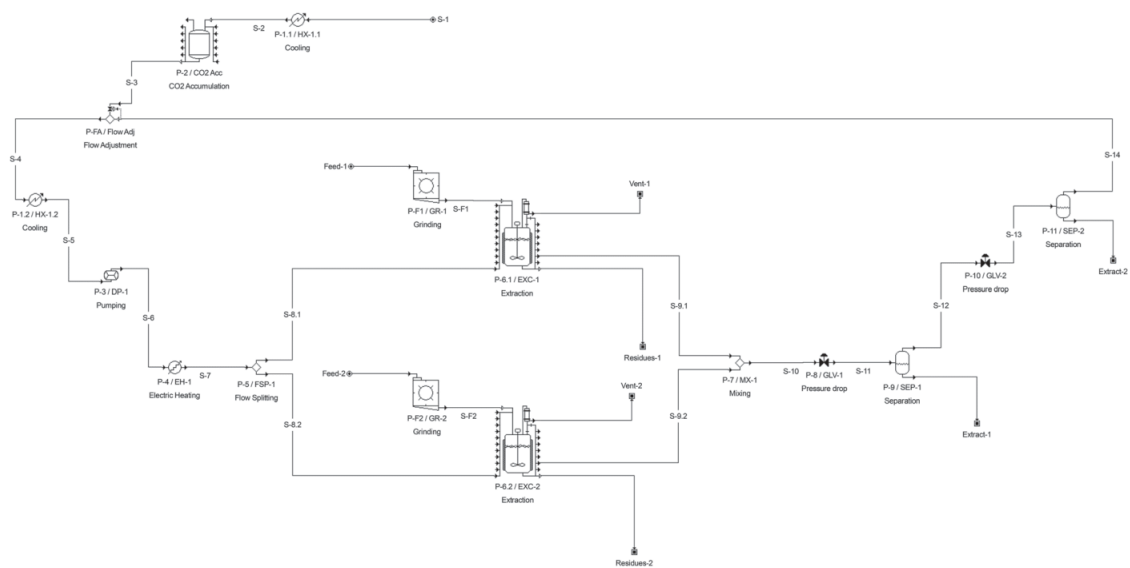


FIGURE 2 Schematic diagram of pilot-scale $scCO_2$ extraction equipment and $scCO_2$ process modeling via SuperPro Designer[®] for economical evaluation. In this process, S-4, S-5, S-6, S-7, S-8.1 and S-8.2 represent streams of CO_2 feeding; Feed-1 and Feed-2 the raw material feeding; S-F1 and S-F2 the preprocessed (ground) raw materials; S-9.1, S-9.2, S-10, S-11, S-12 and S-13 the streams containing CO_2 and extract; Residues-1 and Residues-2 the output of solid residues after the extraction; Vent-1 and Vent-2 represent CO_2 release for depressurization; Extract-1 and Extract-2 the output of extract that was separated from CO_2 ; S-14, S-1, S-2 and S-3, together with P-2 (accumulator) represent CO_2 recycling, accumulation and refilling to make up for CO_2 loss during the process.

extraction performance is achievable when maintaining the same S/F. This allows easy prediction of process performance at an industrial scale based on available experimental data.

The schematic diagram of the simulated process is illustrated in Figure 2. The extraction process includes the utilization of two high-pressure extractors and two separators for oil collection. During the production, CO₂ in a supercritical state in the extractor will separate the oil from the full-fat beans and brings it to the separators, in which CO₂ comes to a subcritical state and separates from the extracted oils. For semi-continuous production, the two extractors will operate alternately, that is, during the extraction in one extractor, sample collection and new raw material feeding can take place simultaneously in the other extractor. The separators work in a row. The schedule example of the extractors and other equipment is displayed in Figure S3 using a Gantt chart, which is a type of bar chart that illustrates activities (process steps, tasks or events) as a function of time. In the chart, the activities are usually listed on the left, with the time scale along the top. The position and length of a bar are used to demonstrate the start time, period and end time of each activity.

The input data for economic evaluation are listed in Table 2. The cost of extraction units can be approximated by considering both extractor capacity and inflation via Equation S1 by knowing the cost of equipment purchased on a different date and the cost index. In

addition to the cost of equipment predicted via Equation S1, the cost was also estimated according to specific commercial scCO₂ extractor costs ("Supercritical CO₂ extraction systems—Buffalo Extraction Systems: The Innovative Edge, www.buffaloextracts.com, 2023"). Linear regression was built for the machine cost as a function of the extractor volume. Based on this correlation, the modeled equipment cost is estimated. The approximate machine cost via the two above methods is listed in Table 2. The lower value was used for COM estimations.

The requirement for labour, which is shown in Table 3, depends on the operations and process scale. This is a rough approximation by considering vast labour work on process supervision, raw material grinding and feeding, extractor depressurization and residue collection. Assuming that most of the operations are automated, the labour time can be substantially shortened.

The cost of raw lupin beans of €0.4 is included in the COM calculation. Another cost of materials lies in the CO₂ venting for depressurization of the extractor. Additionally, the costs of utility are considered, consisting of electricity and cooling agents. The utilities are calculated based on the energy balance and the SuperPro Designer[®] databank.

Regarding the use of nontoxic CO₂ as the green solvent and the fully re-usable defatted lupin bean flour (containing mainly protein), the expenses on waste treatment will be excluded from the COM calculation.

The CO₂ physical-chemical properties were adjusted according to the literature (Duschek et al., 1990).

The cost of manufacturing, COM, can be determined when the fixed capital investment (FCI), cost of operating labor (COL), cost of utilities (CUT), cost of waste treatment (CWT), and cost of raw

TABLE 2 Economic parameters for economic evaluation

Cost of scCO ₂ extraction units	
2 × extractors of 10 L	€350,000 ^a (€260,000 ^b)
2 × extractors of 100 L	€1,500,000 (€660,000)
2 × extractors of 500 L	€3,800,000 (€2,200,000)
2 × extractors of 1000 L	€5,800,000 (€4,200,000)
Depreciation allowance	5%
Labour	
Labour cost	€15/labour hour ^c
Material cost	
Andean lupin bean	€0.4/kg
Carbon dioxide	€0.7/kg ^d
Utility cost	
Electricity	€0.14/kWh ^e
Cooling agent	€0.15/ton ^f

Note: Electricity price statistics. Retrieved from https://ec.europa.eu/eurostat/statistics-explained/index.php/Electricity_price_statistics.

Supercritical CO₂ extraction systems—Buffalo Extraction Systems: The Innovative Edge. Retrieved from www.buffaloextracts.com.

^aEstimated by Equation S1 according to CEPCI.

^bEstimated by the cost of commercial extractors at different scales ("Supercritical CO₂ extraction systems—Buffalo Extraction Systems: The Innovative Edge,"). Those data were used for COM estimation as they were lower than the machine cost predicated according to CEPCI.

^cThe labour cost refers to common salary standards in eastern Europe.

^dCalculated as €20/CO₂ tank (30 kg).

^eCalculated based on electricity prices in the Netherlands ("Electricity price statistics,").

^fRefers to the SuperPro Designer[®] databank.

TABLE 3 Labour (labour hours/hours) required for the scCO₂ extraction process of different scales. The process items refer to the schematic diagram in Figure 2

Process	Scale of scCO ₂ extractor			
	10 L	100 L	500 L	1000 L
P-F1	0.05	0.1	0.2	0.2
P-6.1				
Feed materials	0.2	0.2	0.5	0.5
Heat	0.05	0.05	0.05	0.05
Pressurize and feed solvent	0.05	0.05	0.05	0.05
Depressurize	0.05	0.05	0.05	0.05
Collect residues	0.2	0.2	0.5	0.5
P-F2	0.05	0.1	0.2	0.2
P-6.2				
Feed materials	0.2	0.2	0.5	0.5
Heat	0.05	0.05	0.05	0.05
Pressurize and feed solvent	0.05	0.05	0.05	0.05
Depressurize	0.05	0.05	0.05	0.05
Collect residues	0.2	0.2	0.5	0.5
P-8 and P-10	0.05	0.05	0.05	0.05

materials (CRM) are known or can be estimated (Turton et al., 2012). The COM is calculated via Equation 3.

$$\text{COM} = 0.180\text{FCI} + 2.73\text{COL} + 1.23(\text{CUT} + \text{CWT} + \text{CRM}) \quad (3)$$

in which the depreciation is not included.

It is arranged that the extraction will be running over a total of 7920 h (i.e., 330 days) per year.

3 | RESULTS

3.1 | Lab-scale oil extraction

3.1.1 | The oil yield of Soxhlet extraction

The oil yields of Soxhlet extractions are listed in Table 4. The two-hour extraction yielded about 16% oil, and this yield increased to about 19% when the extraction lasted for 5 h, followed by leveling off up to 12 h. According to a Student's *t*-test, the differences in the oil yields of the extractions for 5–12 h are not statistically significant ($p > 0.05$). Less oil yield was obtained from 2 mm meshed lupin particles.

3.1.2 | The oil yield of scCO₂ extraction at mild temperature (40°C)

Figure 3 exhibits the accumulated oil yield as a function of S/F ratios of scCO₂ extractions under different conditions. The amount of extracted oil increased with the consumption of CO₂, and the rate of extraction differed with pressure and particle size. The most rapid extraction occurred at 550 bar from 0.5 mm meshed particles with a CO₂ flow rate of 20 g/min (Figure 3b). The oil yield increased from 9.1% to 16.2% along with the S/F ratio from 12 to 60. For the slowest extraction, less than 2% oil was yielded over the extraction period (5 h). Similar trends occurred for the oil accumulation at 550 bar and 350 bar with high S/F ratios. A linear increase in oil production tended to occur first, followed by slower augmentation or even leveling off. For the rest of the extractions, quantities of yielded oil linearly increased at a slow rate over the extraction period.

TABLE 4 The oil yield from Andean lupin beans by Soxhlet extraction

Sample	Mesh size (mm)	Extraction duration (h)	Oil yield (%)
1	0.5	2	15.9 ± 2.0
2	0.5	5	18.8 ± 0.7
3	0.5	6	19.8 ± 0.7
4	0.5	12	18.3 ± 0.8
5	2	5	16.2 ± 0.7

Figure 4 shows response surfaces that illustrate the effect of pressure and particle size on the mass of extracted oil per mass of consumed CO₂, that is, the efficiency of CO₂ usage as the extractant, up to 1 h, 3 h and 5 h. In those plots, the third variable is set as constant on the middle level of the Box–Behnken design. The responses for the 1, 3, and 5 h models were transformed by log, square root and inverse square root, respectively. The fittings of those quadratic models to scCO₂ experimental data were evaluated by analysis of variance (ANOVA) (see Table S4 in the supplemental materials). The analysis revealed that the quadratic models were significant ($p < 0.05$) and fit the experimental data. The predicted R² (>0.76) of those models are in reasonable agreement with the adjusted R² (>0.95), which reflects that the quadratic models can explain more than 76% of corresponding response variability. The 1-h and 3-h models possess a nonsignificant lack of fit relative to the pure error ($p > 0.05$), indicating the adequacy of those models. For the 5-h model, the lack of fit was significant ($p < 0.05$), which is likely a result of less error in the experiments of the central points of the Box–Behnken Design than that of the other design points' experiments (Taheri, 2022).

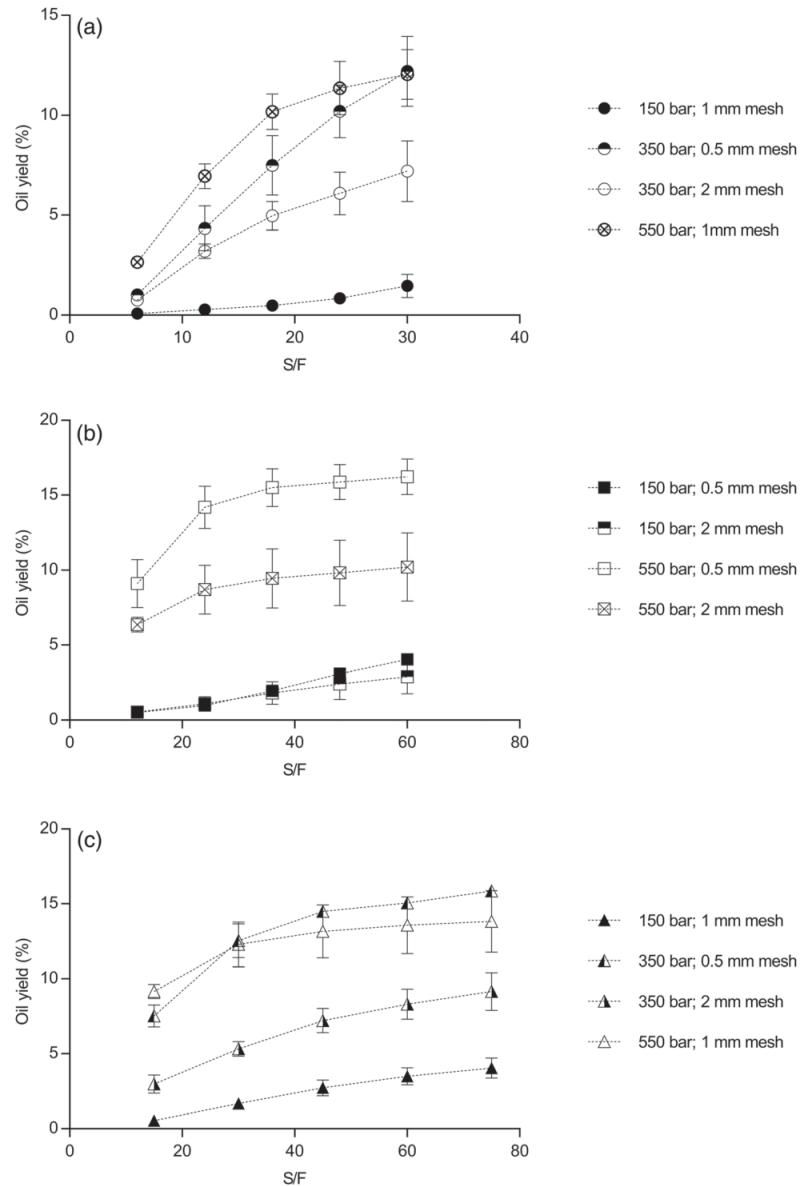
Extractions during the 1 h exhibit high efficiency of CO₂ usage, as indicated by the mass of extracted oil per mass of consumed CO₂. Up to 9×10^{-3} g oil could be extracted per gram of scCO₂ at 550 bar from 0.5 mm meshed particles. However, over all these five-hour extractions, each gram of CO₂ yielded an average of 2×10^{-3} g oil. As reflected by the interactive effects of pressure and particle size, slight changes to oil production occurred when varying particle sizes at low pressure, whereas at high pressure the yield increased with decreasing particle size. With either large or small particle sizes, the oil extraction tended to increase with pressure before flattening. When at high pressure, more oil was extracted per unit mass of CO₂ from small particles than from large ones.

The optimal oil yields were estimated by quadratic models, and two numerical optimisations were performed, with one prediction based on the targets of as low pressure and CO₂ flow rate whereas as high particle size as possible, and the other prediction using the upper limit of pressure and CO₂ flow rate, and lower limit of particle size of the Box–Behnken design. The predicted five-hour oil extraction efficiency was about 11% higher than those attained experimentally. The gap could be narrowed to about 8% by taking into account the residual oils that remained in the separator and were collected manually after depressurising the system.

3.1.3 | Effect of temperature on oil yield

Additional experiments were performed to study the effect of temperature on oil yield. The experiment was performed at 60 and 80 °C respectively, at 350 bar with 25 g/min CO₂ flow and 0.5 mm meshed particles. In Figure 5, the oil yield at 40, 60 and 80 °C are compared. Trends of oil yields against the S/F ratio were similar, with rapid oil extraction in the beginning, followed by slow oil accumulation. However, the overall oil yield decreased with temperature and about 1.5% and 2.5% of the oil was less extracted respectively at 60 °C and 80 °C than at 40 °C.

FIGURE 3 The oil yield of scCO_2 extraction at 40°C as a function of the S/F ratio. The error bars represent the range of measured values, from which the averages were calculated. The dashed lines are used to guide the eye.



3.1.4 | Fatty acid composition

This study focuses on the four most abundant fatty acids (amount to about 95% of total fatty acids) in the oils from lupin beans, that is, oleic acid (C18:1), linoleic acid (C18:2), palmitic acid (C16:0) and stearic acid (C18:0) (Fleetwood & Hudson, 1982a; Hatzold et al., 1983; Uzun et al., 2007).

The composition of fatty acids in the oils via scCO_2 extraction differed slightly from those via Soxhlet extraction, which is shown in Table S3 in the supplementary materials of this article. In the extracted oils, about half of the fatty acids were oleic acid, followed

by linoleic acid (about 35%) and saturated ones. This study addressed the effect of scCO_2 extraction parameters on the fatty acid components in terms of the ratio of unsaturated to saturated fatty acids and the ratio of mono-unsaturated to poly-unsaturated fatty acids. In the supplementary materials, Figure S4 illustrates those ratios in the oil samples that were collected every hour as a function of each operating factor, that is, the extraction pressure, CO_2 flow rate or particle size.

The unsaturated fatty acids tend to be dominant over the saturated ones in the oils extracted at high pressure from 1 mm particles with slow CO_2 flow (10 g/min). This effect of pressure disappeared

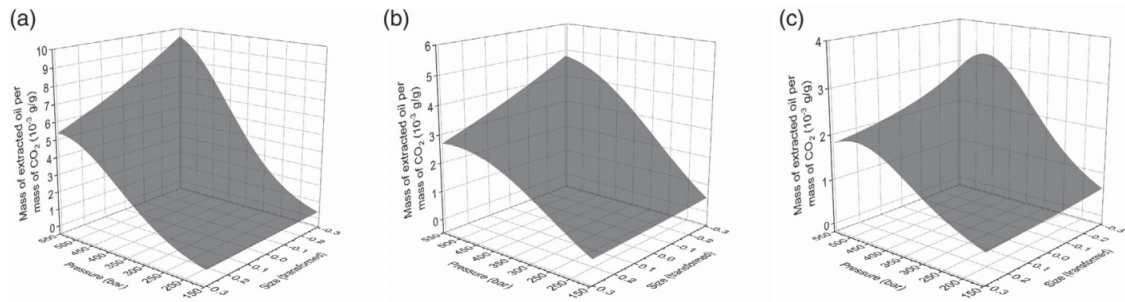


FIGURE 4 Response surfaces of the mass of extracted oil per mass of consumed CO_2 for the sCO_2 extraction as a function of pressure and particle size at 1 h (a), 3 h (b) and 5 h (c). The parameter of flow rate for those models was set on the middle level of the Box-Behnken design.

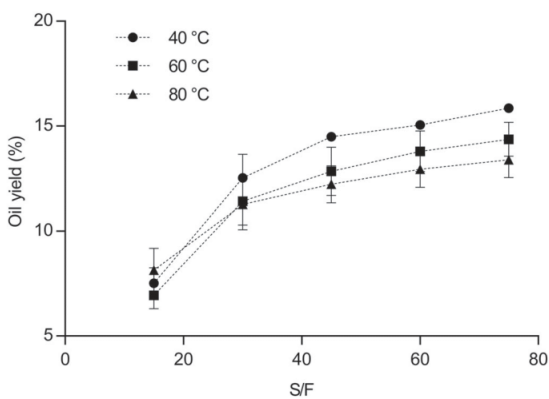


FIGURE 5 The oil yield as a function of S/F at 40, 60, and 80 °C, respectively. Those extractions were performed at 350 bar with a CO_2 flow rate of 25 g/min and a particle size of 0.5 mm. The error bars represent the range of measured values, from which the averages were calculated. The dashed lines are used to guide the eye.

when extracting with 25 g/min CO_2 flow. The oils extracted from 0.5 mm and 2 mm meshed flour with 20 g/min CO_2 flow contain a higher fraction of unsaturated fatty acids at higher pressure. The other two factors, that is, CO_2 flow rate and particle size, exerted less effect than the factor of pressure. The content of mono-unsaturated fatty acids tended to exceed the poly-unsaturated ones at the later stage of the extraction at high pressures (≥ 350 bar) from small particles (≤ 1 mm), especially when the CO_2 flow rate was low.

The ratio of unsaturated to saturated fatty acids has almost no correlation to the oil extraction efficiency, while the ratio of mono- to poly-unsaturated fatty acids has a very light correlation seemingly, as shown in Figure 6, in which the slopes of the linear regression of those values deviate slightly from zero in practice, though significantly in statistics ($p < 0.05$).

A comparison of the fatty acid composition in the oils extracted at 40 and 60 °C is shown in Figure S5 in the supplementary material. The differences in the ratio of unsaturated to saturated fatty acids,

and the ratio of monounsaturated to polyunsaturated fatty acids are not statistically significant ($p > 0.05$).

3.1.5 | Tocopherol content

The correlation of γ -tocopherol content in the oils to different sCO_2 extraction parameters was reflected in the graphs shown in Figure 7 (a). The tocopherol content varied in the range of 110 to 450 mg/100 g oil and was eminently affected by the extraction pressure.

The oils collected at 150 bar were tocopherol-richer than those collected at higher pressures. For the extractions carried out at 150 bar from small particles (≤ 1 mm) with a high CO_2 flow rate (≥ 20 g/min), the tocopherol content decreased with time. When extracting with 10 g/min CO_2 flow from 1 mm particles, an increase in the tocopherol content occurred before dropping down. Contrastingly, oils extracted at 150 bar from large particles (2 mm mesh) contained a relatively stable level of tocopherol over the extraction duration, and so do the oil samples extracted at higher pressure. A slight increase in the tocopherol content was observed for the extractions from large particles.

The accumulated mass of γ -tocopherols via sCO_2 extractions is shown in Figure 7 (b). Extractions at 550 bar and at lower pressures with CO_2 flow rate higher than 10 g/min from large particles (≥ 1 mm mesh size) yielded quick accumulation of tocopherols before leveling off. Those patterns are similar to the oil accumulation shown in Figure 3. For extractions at 150 bar, firstly a slow increase in the tocopherol quantity occurred, followed by acceleration.

Figure 8 displays tocopherol content and accumulated tocopherol mass as a function of oil extraction efficiency. Higher tocopherol content was observed in the samples with lower oil extraction efficiency, indicating somewhat of concentrating the solute. A quicker accumulation of tocopherol occurred in the extractions with low efficiency of oil extraction, corresponding to higher tocopherol content, though low oil yield. The rest of the extractions exhibited similar trends in the tocopherol augmentation. The total amount of extracted tocopherol was in proportion to the oil extraction efficiency. These above

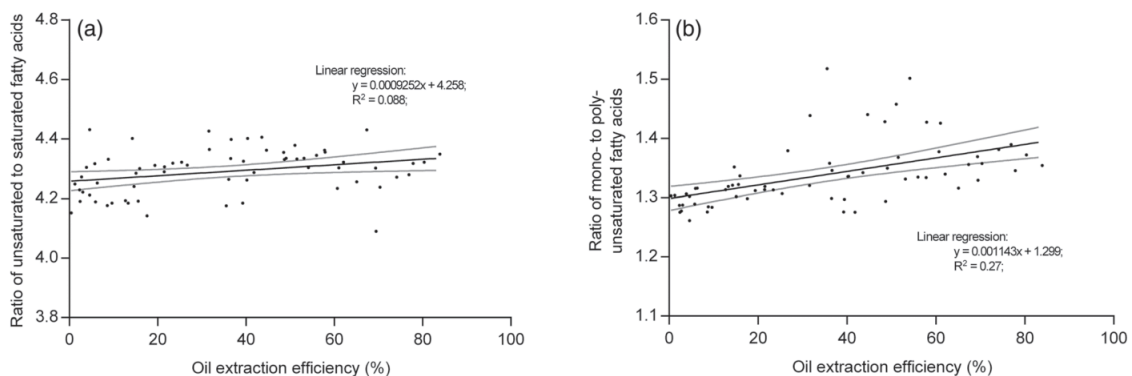


FIGURE 6 The ratio of unsaturated to saturated fatty acids (a) and the ratio of mono- to poly-unsaturated fatty acids (b) in the sCO_2 extracted lupin oils as a function of oil extraction efficiency. The experimental data were fitted by linear regression (the solid lines) with 95% confidence band (the gray curves).

findings were respectively reflected by the exponential decay curve of the nonlinear regression for the tocopherol content and the positive slope of the linear regression for the accumulated tocopherol mass.

The effect of a temperature of 60°C on the tocopherol content and the accumulated amount is displayed in Figure 9. Similar levels of tocopherol were observed in the oils collected at the early stage of extractions at 40°C and 60°C . However, the tocopherol content decreased by about 30% in the later oil samples extracted at 60°C . Also, there was about 10% less tocopherol collected in total over the five-hour extraction at 60°C than at 40°C . In the oils extracted by the Soxhlet method at about 80°C , the γ -tocopherol content was lower than in the sCO_2 extracts (see Table S3).

3.2 | Pilot-scale oil extraction

Oils from Andean lupin beans were also extracted via sCO_2 processing on a pilot-plant scale. The oil yield as a function of S/F is shown in Figure 10. The majority of oils (>80%) were collected from the first separator with a set pressure of 65 bar. The accumulated oil yield increased almost linearly with S/F from about 2.2% to 5.7% and from about 0.2% to 1.1% for the first and second separators, respectively. In total, about 6.5% yield was obtained over the extraction period (5 h). This yield was similar to that of the lab-scale sCO_2 oil extraction under comparable extraction conditions (see Figure 10b).

3.3 | Economic evaluation of sCO_2 extraction of Andean lupin oils

Based on the above pilot-scale oil yield data, the estimated cost of manufacturing (COM) of lupin oil via sCO_2 extraction is shown in Figure 11. When excluding the depreciation cost, a COM of as low as $\text{€ } 35/\text{kg}$ could be achieved when the extraction takes place at a 2×1000 L scale with an extraction duration of 5 h. When taking into

account the value of the defatted flour (assuming a selling price of about $\text{€ } 0.32/\text{kg}$), the manufacturing cost of oil can decrease to about $\text{€ } 30/\text{kg}$. The estimated COM decreased with time and plant scale. When it comes to the contribution of different terms of cost to COM, the cost of labour (COL) dominated the COM when the production scale was low (2×5 L), and this dominance was superseded by FCI when at an upper scale. The cost of materials (CRM) and cost of utility (CUT) increase with scale while decrease with extraction duration. The CRM became the second factor affecting the COM when at the industrial scale (2×1000 L).

The COM including 0.05FCI as the depreciation allowance is listed in Table 5. Together with those data, the annual oil production and corresponding COM based on the oil yield of optimal lab-scale extraction are exhibited. At different scales of production, the lowest COM occurred when the extraction lasts for 2–3 h, which is in correspondence to the maximum annual oil production. It is anticipated that the COM of extracted oil can drop to about $\text{€ } 13/\text{kg}$ when the extraction is conducted at 550 bar and 40°C at a plant scale of 2×1000 L with the extraction duration of 2 h (i.e., $S/F \approx 24$) from 0.5 mm meshed flour. When including the compensation for selling defatted flour, the COM can be cut to about $\text{€ } 11/\text{kg}$.

4 | DISCUSSION

This article describes an experimental study on the extraction of oils from Andean lupin beans using sCO_2 . Critical factors affecting oil yield and quality, and the potential for later process up-scaling are discussed in the following sections.

4.1 | sCO_2 oil extraction efficiency

The sCO_2 oil extraction tended to start with a high rate of oil production when processing with high pressure, high CO_2 flow rate, and

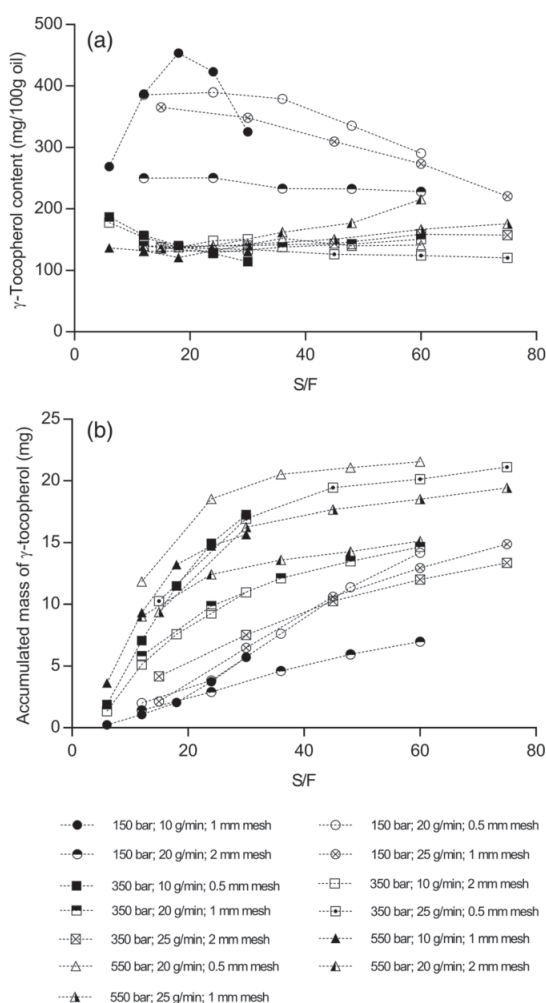


FIGURE 7 The content (a) and accumulated mass (b) of γ -tocopherol in oils via $scCO_2$ extractions as a function of S/F. The data shown in this figure are the average of duplicated measurements. The dashed lines are used to guide the eye. The data of each measurement are included in Table S5 and Table S6 in the supplementary materials of this article.

small particle size (see Figure 3). This quick oil accumulation lasted for 2–3 h and subsequently slowed down by reaching its plateau. This profile reflects the classical kinetics of extracting a compound from a solid matrix (Leo et al., 2005; Rocha-Urbe et al., 2014). When the dissolution rate of oil in $scCO_2$ dominated the extraction, the yield was characterized by a rapid and linear increase, usually at the beginning of the extraction. The mass of extracted oil per mass of consumed CO_2 in this phase was in the same order of magnitude as the solubility of triglyceride in $scCO_2$ reported elsewhere (Bamberger et al., 1988; Vasconcellos & Cabral, 2001). Afterwards, the extraction depended on the mass transfer from the seed matrix and thus diffusion-limiting. The extract accumulation decelerated or even ceased in this step.

When extracting from a large seed matrix with low pressure and low CO_2 flow rate, the amount of oil slowly and linearly increased over the studied period, representing the solubility-dependent extraction mechanism.

Oil yield tended to rise with pressure, which was probably the result of the increased solvation power of denser CO_2 . When extraction was carried out at a given CO_2 flow rate and particle size, the amount of collected oil tended to increase with pressure before leveling off. This might reflect the lessened CO_2 diffusivity due to the increase of viscosity with pressure, which consequently restrains the transfer of CO_2 in the seed matrix (Şanal et al., 2005; Wang et al., 2012; Zhao & Zhang, 2014). Oil production inversely correlated to particle size, which reflected the limited oil mass transfer in the seed matrix with the gradual depletion of oils. This limitation was more evident for large particles than for small ones.

Aside from the above three factors, this study also looked into the factor of temperature to compare the oil yield at 40, 60, and 80°C when keeping the other factors identical. The extraction at 60 and 80°C yielded moderately less oil. The temperature has different effects on oil extraction, as it influences oil solvation in $scCO_2$ and oil vapor evaporation differently (de Castro et al., 2012; Leo et al., 2005; Merkle & Larick, 1994). The ascending temperature impedes oil dissolution in $scCO_2$ in terms of reduced solvent density and solvation power. At the same time, oil vapor pressure increases and the viscosity of $scCO_2$ decreases with temperature. Under the studied circumstances, these two effects did not outweigh the abated solvation power of CO_2 .

The response surface methodology was used to evaluate the variables that give rise to the optimal oil extraction efficiency. Two predictions were compared by corresponding experiments, and there was about a 10% gap between the prediction and the measurement, which could be narrowed when including cleaned-out oil residues in the separator.

In this study, both water and oil were simultaneously extracted from the freshly ground lupin beans. The residual water in the separator introduced an additional source of variability. A previous study proposed little effect of moisture content on oil extractability as oil is more soluble than water in $scCO_2$ (Snyder et al., 1984). However, the collectability of the oil was found to be affected by the presence of water in the extract. Mixtures of water and oil tend to be viscous (Benayoune et al., 1998; Pal, 2001) and were difficult to collect from the separator during the experiments. This phenomenon has been scarcely reported in studies on $scCO_2$ oil extraction from seed materials. The $scCO_2$ oil extraction efficiency was evaluated by comparing it to the Soxhlet oil yield. On top of the distinctions in the solvating strength between $scCO_2$ and hexane, several postulations are proposed that might explain this gap in respect of the $scCO_2$ process. The low CO_2 shear force might toughly flush the remaining oils in the connectors or pipes to the separator, especially the part in which sub-critical CO_2 was transported. The $scCO_2$ extraction equipment was once flushed by hexane, and the recovered oil contributed to about a 3% increase in extraction efficiency. Nevertheless, this equipment was not frequently flushed by hexane regarding its corrosion to the plastic or rubber parts of the equipment. Apart from the above

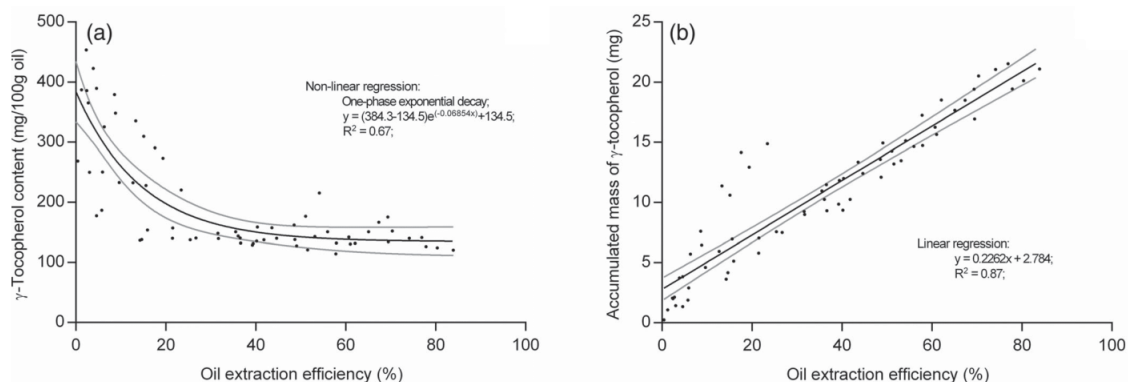


FIGURE 8 The γ -tocopherol content in the scCO_2 extracted lupin oils (a) and the accumulated mass of γ -tocopherol (b) as a function of oil extraction efficiency. The experimental data in (a) and (b) were respectively fitted by exponential regression and linear regression (the solid curve/line) with 95% confidence band (the gray curves).

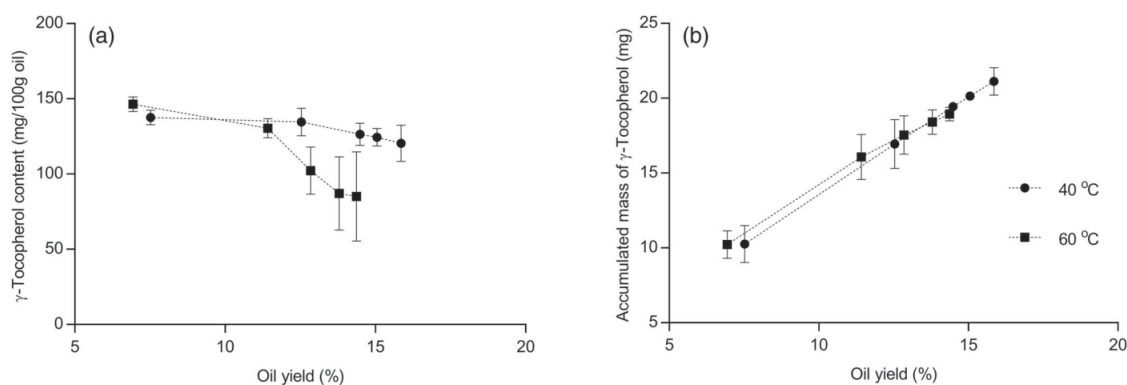


FIGURE 9 The content of γ -tocopherol (a) and the accumulated mass (b) as a function of oil yield of scCO_2 extractions at 40 and 60°C, respectively. The extractions were carried out at 350 bar with 25 g/min CO_2 flow and 0.5 mm meshed particles. The error bars represent the range of measured values, from which the averages were calculated. The dashed lines are used to guide the eye.

residues, the oil in the defatted flour after the scCO_2 extraction under the optimal condition was once extracted by the Soxhlet method, and it was found that about 5% oil remained in the defatted flour. Additionally, only one single separator was equipped for the scCO_2 extraction in this study. The compounds that were entrained by the subcritical CO_2 (at about 60 bar and 30°C) passing through the separator could not be counted as the collectable oil mass, especially when CO_2 was pumped fast through the separator. Those above hypotheses may partly explain the gap of the obtained extract mass between the scCO_2 extraction and the Soxhlet extraction.

4.2 | The quality of extracted oils

Two properties of the oils, that is, the fatty acid component and the tocopherol content, were analyzed and correlated to the extraction conditions, which are discussed in this section.

The fraction of unsaturated fatty acids in the extracted triglycerides, which is the major oil constituent, increased with pressure, especially in the beginning of the scCO_2 extraction with a low-solvent flow rate or in the later extraction from large particles with a high-solvent flow rate. A similar increase in the proportion of unsaturated fatty acids with pressure was also reported elsewhere (Merkle & Larick, 1995). The esters containing dominantly unsaturated fatty acids are superior to saturated ones in polarity and tend to be miscible to rather dense CO_2 with substantial quadrupole moment (DeSimone & Tumas, 2003). The effect of CO_2 flow rate and particle size was less evident. There was a high fraction of unsaturated fatty acids in oils extracted by CO_2 with a low-flow rate in the 1 h. In contrast to apolar saturated fatty acids with a high affinity to CO_2 and consequently stable dissolution in the solvent, the fraction of relative polar unsaturated fatty acids might increase in the scCO_2 when a low-flow rate was applied, as there was sufficient contact time between the CO_2 phase and the seed materials for mass transfer. This effect of

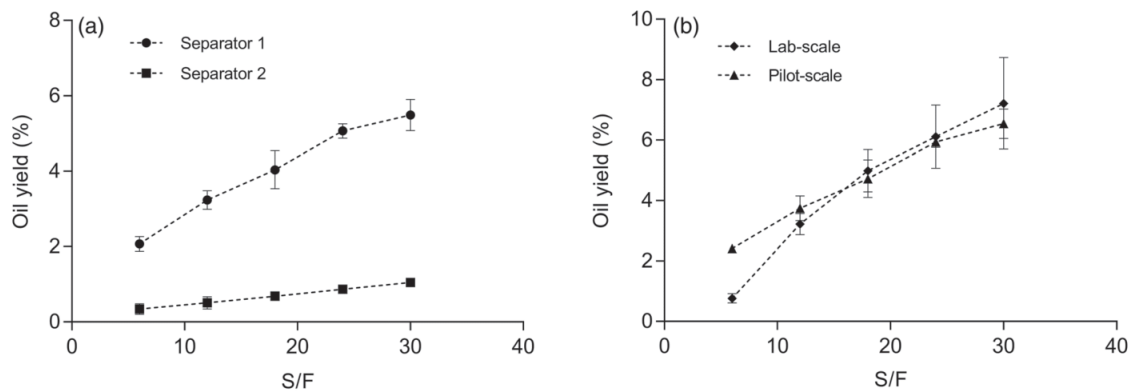


FIGURE 10 The accumulated oil yield of each separator (a) and the total (b) of pilot scCO_2 extraction as a function of S/F. The oil yield of lab-scale extraction under similar processing conditions is also shown for comparison. The error bars represent the range of duplicated measurements, from which the averages were calculated. The dashed lines are used to guide the eye.

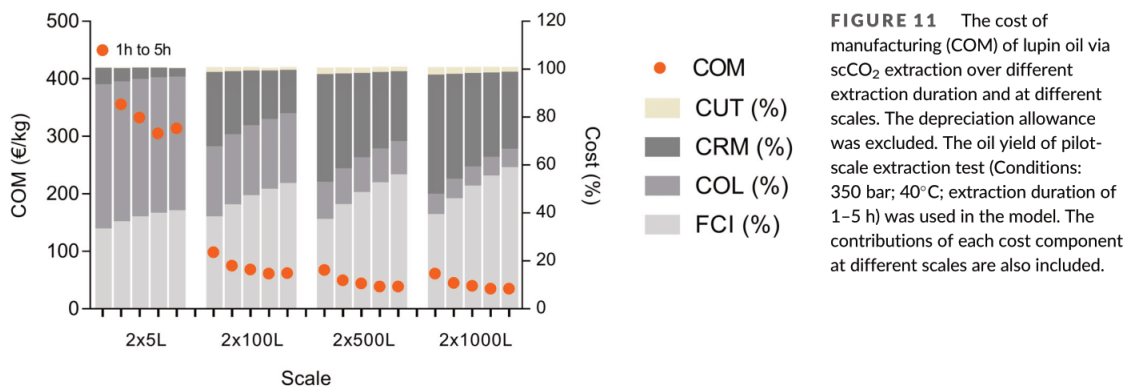


FIGURE 11 The cost of manufacturing (COM) of lupin oil via scCO_2 extraction over different extraction duration and at different scales. The depreciation allowance was excluded. The oil yield of pilot-scale extraction test (Conditions: 350 bar; 40°C; extraction duration of 1–5 h) was used in the model. The contributions of each cost component at different scales are also included.

flow rate vanished with the continuation of the extraction. With the evolving extraction, the effect of particle size on the proportion of the two types of fatty acids inferred a limitation in the diffusion of unsaturated fatty acids from the large seed matrix to the solvent.

The increase in pressure resulted in an increase in the fraction of monounsaturated fatty acids out of the unsaturated ones. This ratio was scarcely reported in previous studies, in which attention was paid to the concentration of mono- or poly-unsaturated fatty acids as a function of variables (Cheung, 1999; Taylor & Larick, 1995). It was hypothesized that this trend was contributed by the dissimilar polarity of those two fatty acids. The calculated dipole moment of linoleic acid was slightly higher than oleic acid ($\Delta \approx 0.13$ Debye; calculated via molecular modeling by Gaussian 16). Thus, the increase of oleic acid (relatively apolar) in the mobile phase outweighed linoleic acid when the pressure rose. This tiny difference in polarity may also account for the observation that the monounsaturated fatty acids were preferably extracted under the circumstance of low CO_2 flow and diffusion-limiting oil transfer from large seed matrix. Although the above fatty acid compositions differed per scCO_2 extractions with different

conditions, the ratio of unsaturated to saturated fatty acids and the ratio of mono- to poly-unsaturated fatty acids had practically no change with oil extraction efficiency, though significant statistically.

This study also investigated the content of tocopherol in the extracts, and γ -tocopherol was found to be the dominant form with the content ranging from 114 to 454 mg/100 g oil. The observed γ -tocopherol concentration in the scCO_2 -extracted oil exceeded those in the Soxhlet extract, which was in line with comparisons reported elsewhere (Feldheim et al., 1984; Oliveira et al., 2002).

The considerable effect of extraction conditions on tocopherol content is likely a consequence of the selectivity of scCO_2 in extracting targeted compounds (Bravi et al., 2007; Gustinelli et al., 2018; Reverchon & De Marco, 2006). Considering the competition between low-molecular weight tocopherols and long-chain triglycerides in affinity to scCO_2 , the detected difference in tocopherol concentration was probably due to the dilution by the oil phase. The tocopherol concentration was in reverse proportion to the oil yield, which was affected significantly by extraction pressure. This reveals the likelihood that the tocopherol extraction rate overrode the rate of oil

TABLE 5 The annual oil production and COM (including 0.05FCI depreciation allowance) via scCO₂ processing based on pilot-scale and lab-scale extraction results

Scale	Extraction duration (h)	Oil yield based on pilot extraction (350 bar; 40°C; S/F up to 30; 2 mm meshed flour)		Oil yield based on lab extraction (550 bar; 40°C; S/F up to 60; 2 mm meshed flour)		Oil yield based on lab extraction (550 bar; 40°C; S/F up to 60; 0.5 mm meshed flour)	
		Annual oil production (kg/year)	COM (€/kg)	Annual oil production (kg/year)	COM (€/kg)	Annual oil production (kg/year)	COM (€/kg)
2 × 10 L	1	319	490.5	841	186.1	1204	130.0
	2	370	390.7	860	168.0	1403	103.0
	3	373	367.7	747	183.7	1225	112.0
	4	391	338.4	648	204.5	1047	126.6
	5	370	349.2	577	223.6	916	140.8
2 × 100 L	1	3192	108.8	8412	41.3	12,042	28.8
	2	3699	83.9	8603	36.1	14,025	22.1
	3	3734	77.3	7471	38.6	12,254	23.5
	4	3915	69.9	6477	42.3	10,465	26.2
	5	3695	71.3	5771	45.6	9164	28.7
2 × 500 L	1	15,960	74.6	42,059	28.3	60,208	19.8
	2	18,495	55.8	43,016	24.0	70,126	14.7
	3	18,668	50.2	37,354	25.1	61,271	15.3
	4	19,573	44.6	32,384	27.0	52,325	16.7
	5	18,476	44.8	28,854	28.7	45,819	18.1
2 × 1000 L	1	31,920	68.0	84,119	25.8	120,416	18.0
	2	36,989	50.8	86,032	21.9	140,253	13.4
	3	37,335	45.7	74,708	22.9	122,542	13.9
	4	39,145	40.7	64,769	24.6	104,650	15.2
	5	36,951	40.9	57,708	26.2	91,637	16.5

extraction under specific conditions. It was also advised elsewhere to extract tocopherols at low pressure with low scCO₂ density as the intensified diffusion of CO₂ favors breakage of linkages of tocopherol in sample matrix (Dean, 2012; Harborne, 1973; Yunus et al., 2015). During extraction from large particles, there was slightly a later increase in the tocopherol content. As commented in the literature, the mass transfer of tocopherol is both associated with its solubility in the oil and its availability on the sample surface (Gustinelli et al., 2018; Leo et al., 2005). Followed by depletion of tocopherol from the surface, tocopherols from inner particles were extracted in the latter stage of the process, which is controlled by the diffusion of the solute and scCO₂ in the seed matrix (Güçlü-Üstündağ & Temelli, 2004; Gustinelli et al., 2018).

The profiles of accumulated tocopherol depend on both the tocopherol concentration and the quantity of extracted oils. The former applies to the cases in which the tocopherol extraction by scCO₂ was favored over the oil. This usually took place when extracting from small particles at low pressure. Under this condition, the tocopherol content became the dominant factor affecting the profile of tocopherol accumulation. Correspondingly, the profiles of tocopherol accumulation (see Figure 7) differed from the linear ones of oils (see Figure 3) and had an acceleration in the later phase of the extraction. When the rate of oil extraction exceeded tocopherol extraction,

tocopherol accumulation and oil accumulation shared similar trends, including both solubility-dependent and diffusion-limiting extraction curve patterns.

When scCO₂ extraction was carried out at 60°C, the tocopherol content stayed on a similar level as the processing at 40°C at the beginning and declined during the subsequent extraction phases. So did the quantity of accumulated tocopherol in the oils. This phenomenon was also observed elsewhere for scCO₂ tocopherol extraction (De Lucas, de la Ossa, Rincón, Blanco, & Gracia, 2002; Ixtaina et al., 2011; King et al., 1996; Leo et al., 2005). It was assumed as a result of the selectivity of CO₂ for tocopherols and competitive extraction of other compounds from the seed materials at higher temperatures. However, there were contrasting findings that the tocopherol concentration increased with extraction temperature, especially at low-extraction pressure (Bravi et al., 2007; Gustinelli et al., 2018). The drop in tocopherol content in our study might also be explained by other factors such as the thermal degradation of the antioxidant and the co-solvent effect of the oil, which were proposed in some previous research (Bruscatto et al., 2009; Ixtaina et al., 2011; Jachmanián et al., 2006; Steel et al., 2005).

The above knowledge on the fatty acid component and tocopherol content lays the foundation for the future development of fractionation processes to separate and concentrate specific components

out of the Andean lupin oils, which raise the biorefinery value of the lupin beans and require further investigation.

4.3 | Process scale-up and economic viability of scCO₂ process for Andean lupin oil extraction

Based on the results so far, it is promising to apply the scCO₂ technique to oil extraction from Andean lupin beans, the efficiency of which is close to conventional chemical extraction using fossil solvents and is higher than specific physical separation methods such as mechanical press, though the combination of scCO₂ extraction and mechanical press makes sense to produce oils with appropriate yield and quality (Aladić et al., 2014; Rombaut et al., 2014). The performance of up-scaled processes and anticipated economic viability are discussed in this section.

Pilot-scale scCO₂ extraction (10 L extractor) and lab-scale extraction (0.5 L extractor) yielded about 6%–7% oils from 2 mm meshed lupin flour over 5 h of extraction under similar conditions. This reflects somewhat the consistency in the performance of scCO₂ extraction via different equipment and at different scales. Thus, in this study, the findings on the lab-scale unit or pilot-scale unit were extrapolated to predict the performance of the industrial unit at the upper scale.

The COM (with depreciation allowance included) of industrial oil products tends to be sensitive to the cost of the facility and raw materials. Even with high investment, the industrial scCO₂ process (scale of 2 × 1000 L) is foreseen to be profitable based on estimation with the oil yield of 9%–16% over 1 h–5 h extraction. In this scenario, after subtracting the sales of defatted lupin flour from COM, oil production is profit-making as the manufacturing cost drops to lower than the B2B market price (about €12/kg), which is probably based on the classical extraction method. Even so, the economic feasibility and affordability of scCO₂ extraction are still highly scale-dependent. On a lower scale, the high investment restricts its application when compared with cheaper classical extraction methods.

The nonlinearity of oil yield as a function of extraction duration gives rise to a trade-off between the duration of each extraction batch and the number of annual operatable batches. By scheduling the extraction properly, optimal oil production and manufacturing costs can be achieved.

Commonly in literature, it is usual to predict the performance of up-scaled scCO₂ processes based on the solvent-to-feed ratio (S/F ratio) from down-scale studies. However, in practice, the situation is even more complicated regarding the integration of scaling-up factors and operating variables. The functionality of industrial scCO₂ oil extraction requires further investigation.

5 | CONCLUSIONS

This study used a lab-scale scCO₂ process to extract oils from Andean lupin beans and to evaluate various extraction factors that affect oil quality. Oil extraction efficiency and quality (in terms of fatty acids composition and tocopherol content) changed over time during the

extraction and were affected by pressure, CO₂ flow rate or particle size. More than 80% of oil from Andean lupin bean could be extracted by scCO₂ compared to conventional Soxhlet extraction. The oil extraction efficiency, the fatty acid components in the extracted oil and the γ -tocopherol content were pressure-dependent and somewhat affected by CO₂ flow rate and particle size. Additionally, extractions at higher temperatures yielded less oil and tocopherol. The extraction conditions for the maximum oil production were not consistent with those for the optimal oil quality, such as favorable ratios of unsaturated to saturated fatty acids and peak tocopherol content. The variation of fatty acid composition and tocopherol content as a function of extraction parameters provides information for future better control of the oil quality or selective refinery of specific components out of the Andean lupin oil for applications such as food or cosmetics. The lab-scale oil extraction performance was found to be in line with the pilot-scale extraction under similar extraction conditions with the same S/F ratio. The high oil yield made it promising to engineer the scCO₂ process into industrial oil production for Andean lupin beans. Economic evaluations indicated that it was economically feasible to establish scCO₂ processes for lupin oil extraction with proper control of the cost of labour, equipment (including depreciation allowance) and raw materials. The contribution of fixed capital investment (FCI) and cost of raw materials (CRM) to the manufacturing cost usually increased with the process scale, while the contribution of the cost of labour (COL) decreased with scale-up. It is anticipated that the cost of manufacturing (COM) can be further reduced with a further lifted oil yield and scaling up.

ACKNOWLEDGMENTS

This work was performed within the framework of project LIBBIO “*Lupinus mutabilis* for Increased Biomass from marginal lands and value for BIOrefineries” supported by the Bio-Based Industries Joint Undertaking under the European Union's Horizon 2020 research and innovation program under grant agreement NO. 720726. This research is also made possible by the “Industry 2030” project funded by the European Regional Development Fund (ERDF, OPSNNO261) from the European Union and the Province Groningen, the Netherlands.

CONFLICT OF INTEREST STATEMENT

The authors declare no potential conflict of interest.

DATA AVAILABILITY STATEMENT

The data that support the findings of this study are available upon reasonable request from the corresponding author.

ORCID

Miao Yu  <https://orcid.org/0000-0002-6435-0910>

Geert-Jan Witkamp  <https://orcid.org/0000-0002-4394-9713>

Rob J. F. van Haren  <https://orcid.org/0000-0002-5707-1120>

REFERENCES

- Akkaya, M. (2018). Fatty acid compositions of sunflowers (*Helianthus annuus* L.) grown in east Mediterranean region. *Rivista Italiana Delle Sostanze Grasse*, 95(4), 239–247.

- Aladić, K., Jarni, K., Barbir, T., Vidović, S., Vladić, J., Bilić, M., & Jokić, S. (2015). Supercritical CO₂ extraction of hemp (*Cannabis sativa* L.) seed oil. *Industrial Crops and Products*, 76, 472–478.
- Aladić, K., Jokić, S., Moslavac, T., Tomas, S., Vidović, S., Vladić, J., & Šubarić, D. (2014). Cold pressing and supercritical CO₂ extraction of hemp (*Cannabis sativa*) seed oil. *Chemical and Biochemical Engineering Quarterly*, 28(4), 481–490.
- Anklam, E., Berg, H., Mathiasson, L., Sharman, M., & Ulberth, F. (1998). Supercritical fluid extraction (SFE) in food analysis: A review. *Food Additives & Contaminants*, 15(6), 729–750.
- Bamberger, T., Erickson, J. C., Cooney, C. L., & Kumar, S. K. (1988). Measurement and model prediction of solubilities of pure fatty acids, pure triglycerides, and mixtures of triglycerides in supercritical carbon dioxide. *Journal of Chemical and Engineering Data*, 33(3), 327–333.
- Bartosińska, E., Buszewska-Forajta, M., & Siluk, D. (2016). GC–MS and LC–MS approaches for determination of tocopherols and tocotrienols in biological and food matrices. *Journal of Pharmaceutical and Biomedical Analysis*, 127, 156–169.
- Bebeli, P. J., Lazaridi, E., Chatzigeorgiou, T., Suso, M.-J., Hein, W., Alexopoulos, A. A., ... van den Berg, M. (2020). State and Progress of Andean lupin cultivation in Europe: A review. *Agronomy*, 10(7), 1038.
- Benayoune, M., Khezzer, L., & Al-Rumhy, M. (1998). Viscosity of water in oil emulsions. *Petroleum Science and Technology*, 16(7–8), 767–784.
- Birtigh, A., Johannsen, M., Brunner, G., & Nair, N. (1995). Supercritical-fluid extraction of oil-palm components. *The Journal of Supercritical Fluids*, 8(1), 46–50.
- Boekenoogen, H. A. (1964). *Analysis and characterization of oils, fats, and fat products*. Interscience.
- Borek, S., Pukacka, S., Michalski, K., & Ratajczak, L. (2009a). Lipid and protein accumulation in developing seeds of three lupine species: *Lupinus luteus* L., *Lupinus albus* L., and *Lupinus mutabilis* sweet. *Journal of Experimental Botany*, 60(12), 3453–3466.
- Bozan, B., & Temelli, F. (2003). Extraction of poppy seed oil using supercritical CO₂. *Journal of Food Science*, 68(2), 422–426.
- Bravi, M., Spinoglio, F., Verdone, N., Adami, M., Aliboni, A., d'Andrea, A., ... Ferri, D. (2007). Improving the extraction of α -tocopherol-enriched oil from grape seeds by supercritical CO₂. Optimisation of the extraction conditions. *Journal of Food Engineering*, 78(2), 488–493.
- Bruscatto, M., Zambiasi, R., Sganzerla, M., Pestana, V., Otero, D., Lima, R., & Paiva, F. (2009). Degradation of tocopherols in rice bran oil submitted to heating at different temperatures. *Journal of Chromatographic Science*, 47(9), 762–765.
- Bunea, A., Rugină, D., Pinte, A., Andrei, S., Bunea, C., Pop, R., & Bele, C. (2012). Carotenoid and fatty acid profiles of bilberries and cultivated blueberries from Romania. *Chemical Papers*, 66(10), 935–939.
- Carpenter, A. (1979). Determination of tocopherols in vegetable oils. *Journal of the American Oil Chemists' Society*, 56(7), 668–671.
- Carvajal-Larenas, F., Linnemann, A., Nout, M., Koziol, M., & Van Boekel, M. (2016a). *Lupinus mutabilis*: Composition, uses, toxicology, and debittering. *Critical Reviews in Food Science and Nutrition*, 56(9), 1454–1487.
- Carvalho, P. I., Osorio-Tobón, J. F., Rostagno, M. A., Petenate, A. J., & Meireles, M. A. A. (2015). Techno-economic evaluation of the extraction of turmeric (*Curcuma longa* L.) oil and ar-turmerone using supercritical carbon dioxide. *The Journal of Supercritical Fluids*, 105, 44–54.
- Cheung, P. C. (1999). Temperature and pressure effects on supercritical carbon dioxide extraction of n-3 fatty acids from red seaweed. *Food Chemistry*, 65(3), 399–403.
- Clemente, T. E., & Cahoon, E. B. (2009). Soybean oil: Genetic approaches for modification of functionality and total content. *Plant Physiology*, 151(3), 1030–1040.
- Corzzini, S. C., Barros, H. D., Grimaldi, R., & Cabral, F. A. (2017). Extraction of edible avocado oil using supercritical CO₂ and a CO₂/ethanol mixture as solvents. *Journal of Food Engineering*, 194, 40–45.
- Cowling, W., Buirchell, B., & Tapia, M. (1998). Lupin. *Lupinus* spp. promoting the conservation and use of underutilized and neglected crops. 23. Institute of Plant Genetics and Crop Plant Resources: Gatersleben/international plant genetic resources institute: Rome, Italy.
- Czubinski, J., Wroblewska, K., Czyżniewski, M., Górnaś, P., Kachlicki, P., & Siger, A. (2019). Bioaccessibility of defatted lupin seed phenolic compounds in a standardized static in vitro digestion system. *Food Research International*, 116, 1126–1134.
- Daković, S., Turkulov, J., & Dimić, E. (1989). The quality of vegetable oils got by extraction with CO₂. *European Journal of Lipid Science and Technology*, 91(3), 116–119.
- de Castro, M. D. L., Valcárcel, M., & Tena, M. T. (2012). *Analytical supercritical fluid extraction*. Springer Science & Business Media.
- de Lucas, A., de la Ossa, E. M., Rincón, J., Blanco, M., & Gracia, I. (2002). Supercritical fluid extraction of tocopherol concentrates from olive tree leaves. *The Journal of Supercritical Fluids*, 22(3), 221–228.
- Dean, J. R. (2012). *Applications of supercritical fluids in industrial analysis*. Springer Science & Business Media.
- DeSimone, J. M., & Tumas, W. (2003). *Green chemistry using liquid and supercritical carbon dioxide*. Oxford University Press.
- Destá, M., Molla, A., & Yusuf, Z. (2020). Characterization of physico-chemical properties and antioxidant activity of oil from seed, leaf and stem of purslane (*Portulaca oleracea* L.). *Biotechnology Reports*, 27, e00512.
- Duschek, W., Kleinrahn, R., & Wagner, W. (1990). Measurement and correlation of the (pressure, density, temperature) relation of carbon dioxide II. Saturated-liquid and saturated-vapour densities and the vapour pressure along the entire coexistence curve. *The Journal of Chemical Thermodynamics*, 22(9), 841–864.
- Feldheim, W., Schulz, H., & Katerberg, R. (1984). Untersuchungen zur Bestimmung des Tocopherolgehalts im unverseifbaren Anteil von Lupinöl (*L. mutabilis*). *Zeitschrift für Lebensmittel-Untersuchung Und Forschung*, 178(2), 115–117.
- Fleetwood, J., & Hudson, B. (1982a). Lupinseed—A new source of edible oil. *International Journal of Food Science & Technology*, 17(1), 11–17.
- Friedrich, J., & Pryde, E. (1984). Supercritical CO₂ extraction of lipid-bearing materials and characterization of the products. *Journal of the American Oil Chemists' Society*, 61(2), 223–228.
- Friedrich, J. P., & List, G. R. (1982). Characterization of soybean oil extracted by supercritical carbon dioxide and hexane. *Journal of Agricultural and Food Chemistry*, 30(1), 192–193.
- Goto, M., Sato, M., & Hirose, T. (1993). Extraction of peppermint oil by supercritical carbon dioxide. *Journal of Chemical Engineering of Japan*, 26(4), 401–407.
- Grela, E., & Günter, K. (1995). Fatty acid composition and tocopherol content of some legume seeds. *Animal Feed Science and Technology*, 52(3–4), 325–331.
- Grilo, E. C., Costa, P. N., Gurgel, C. S. S., Beserra, A. F., Almeida, F. N. D. S., & Dimenstein, R. (2014). Alpha-tocopherol and gamma-tocopherol concentration in vegetable oils. *Food Science and Technology*, 34(2), 379–385.
- Güçlü-Üstündağ, Ö., & Temelli, F. (2004). Correlating the solubility behavior of minor lipid components in supercritical carbon dioxide. *The Journal of Supercritical Fluids*, 31(3), 235–253.
- Guillaume, D., & Charrouf, Z. (2011). Argan oil and other argan products: Use in dermocosmetology. *European Journal of Lipid Science and Technology*, 113(4), 403–408.
- Gulewicz, P., Martínez-Villaluenga, C., Frias, J., Ciesiołka, D., Gulewicz, K., & Vidal-Valverde, C. (2008). Effect of germination on the protein fraction composition of different lupin seeds. *Food Chemistry*, 107(2), 830–844.
- Gustinelli, G., Eliasson, L., Svelander, C., Alming, M., & Ahm, L. (2018). Supercritical CO₂ extraction of bilberry (*Vaccinium myrtillus* L.) seed oil: Fatty acid composition and antioxidant activity. *The Journal of Supercritical Fluids*, 135, 91–97.
- Harborne, J. B. (1973). *A guide to modern techniques of plant analysis*. Chapman and Hall.

- Hatzold, T., Elmadfa, I., & Gross, R. (1983). Edible oil and protein concentrate from *Lupinus mutabilis*. *Plant Foods for Human Nutrition*, 32(2), 125–132.
- Herrero, M., Mendiola, J. A., Cifuentes, A., & Ibáñez, E. (2010). Supercritical fluid extraction: Recent advances and applications. *Journal of Chromatography A*, 1217(16), 2495–2511.
- Ixtaina, V. Y., Mattea, F., Cardarelli, D. A., Mattea, M. A., Nolasco, S. M., & Tomás, M. C. (2011). Supercritical carbon dioxide extraction and characterization of Argentinean chia seed oil. *Journal of the American Oil Chemists' Society*, 88(2), 289–298.
- Jachmanián, I., Margenat, L., Torres, A. I., & Grompone, M. A. (2006). Estabilidad oxidativa y contenido de tocoferoles en el aceite de canola extraído con CO₂ supercrítico. *Grasas Y Aceites*, 57(2), 155–159.
- Jung, S. (2009). Aqueous extraction of oil and protein from soybean and lupin: A comparative study. *Journal of Food Processing and Preservation*, 33(4), 547–559.
- Khallouki, F., Younos, C., Soulimani, R., Oster, T., Charrouf, Z., Spiegelhalter, B., ... Owen, R. (2003). Consumption of argan oil (Morocco) with its unique profile of fatty acids, tocopherols, squalene, sterols and phenolic compounds should confer valuable cancer chemopreventive effects. *European Journal Of Cancer Prevention*, 12(1), 67–75.
- King, J. W., Favati, F., & Taylor, S. L. (1996). Production of tocopherol concentrates by supercritical fluid extraction and chromatography. *Separation Science and Technology*, 31(13), 1843–1857.
- Kostik, V., Memeti, S., & Bauer, B. (2013). Fatty acid composition of edible oils and fats. *Journal of Hygienic Engineering and Design*, 4, 112–116.
- Le Clef, E., & Kemper, T. (2015). Sunflower seed preparation and oil extraction. In *Sunflower* (pp. 187–226). AOCS Press.
- Leo, L., Rescio, L., Ciurlia, L., & Zacheo, G. (2005). Supercritical carbon dioxide extraction of oil and α -tocopherol from almond seeds. *Journal of the Science of Food and Agriculture*, 85(13), 2167–2174.
- Mead, R., & Pike, D. (1975). A biometrics invited paper. A review of response surface methodology from a biometric viewpoint. *Biometrics*, 31(4), 803–851.
- Merkle, J., & Larick, D. (1994). Conditions for extraction and concentration of beef fat volatiles with supercritical carbon dioxide. *Journal of Food Science*, 59(3), 478–483.
- Merkle, J., & Larick, D. (1995). Fatty acid content of supercritical carbon dioxide extracted fractions of beef fat. *Journal of Food Science*, 60(5), 959–962.
- Montgomery, D. C. (2017). *Design and analysis of experiments*. John Wiley & sons.
- Oliveira, R., Fátima Rodrigues, M., & Gabriela Bernardo-Gil, M. (2002). Characterization and supercritical carbon dioxide extraction of walnut oil. *Journal of the American Oil Chemists' Society*, 79(3), 225–230.
- Orsavova, J., Misurcova, L., Ambrozova, J., Vicha, R., & Mlcek, J. (2015). Fatty acids composition of vegetable oils and its contribution to dietary energy intake and dependence of cardiovascular mortality on dietary intake of fatty acids. *International Journal Of Molecular Sciences*, 16(6), 12,871–12,890.
- Ortiz, J., & Mukherjee, K. (1982). Extraction of alkaloids and oil from bitter lupin seed. *Journal of the American Oil Chemists' Society*, 59(5), 241–244.
- Pal, R. (2001). Novel viscosity equations for emulsions of two immiscible liquids. *Journal of Rheology*, 45(2), 509–520.
- Palmer, M., & Ting, S. (1995). Applications for supercritical fluid technology in food processing. *Food Chemistry*, 52(4), 345–352.
- Prado, J. M., Dalmolin, I., Carareto, N. D., Basso, R. C., Meireles, A. J., Oliveira, J. V., Batista, E. A., & Meireles, M. A. A. (2012). Supercritical fluid extraction of grape seed: Process scale-up, extract chemical composition and economic evaluation. *Journal of Food Engineering*, 109(2), 249–257.
- Reverchon, E., & De Marco, I. (2006). Supercritical fluid extraction and fractionation of natural matter. *The Journal of Supercritical Fluids*, 38(2), 146–166.
- Rocha-Uribe, J. A., Novelo-Pérez, J. I., & Ruiz-Mercado, C. A. (2014). Cost estimation for CO₂ supercritical extraction systems and manufacturing cost for habanero chili. *The Journal of Supercritical Fluids*, 93, 38–41.
- Rombaut, N., Savoie, R., Thomasset, B., Bélliard, T., Castello, J., Van Hecke, É., & Lanoisellé, J.-L. (2014). Grape seed oil extraction: Interest of supercritical fluid extraction and gas-assisted mechanical extraction for enhancing polyphenol co-extraction in oil. *Comptes Rendus Chimie*, 17(3), 284–292.
- Rombaut, N., Savoie, R., Van Hecke, E., & Thomasset, B. (2017). Supercritical CO₂ extraction of linseed: Optimization by experimental design with regards to oil yield and composition. *European Journal of Lipid Science and Technology*, 119(9), 1600078.
- Sahena, F., Zaidul, I., Jinap, S., Karim, A., Abbas, K., Norulaini, N., & Omar, A. (2009). Application of supercritical CO₂ in lipid extraction—a review. *Journal of Food Engineering*, 95(2), 240–253.
- Şanal, İ., Bayraktar, E., Mehmetoğlu, Ü., & Çalimli, A. (2005). Determination of optimum conditions for SC-(CO₂+ ethanol) extraction of β -carotene from apricot pomace using response surface methodology. *The Journal of Supercritical Fluids*, 34(3), 331–338.
- Sharif, K., Rahman, M., Azmir, J., Mohamed, A., Jahurul, M., Sahena, F., & Zaidul, I. (2014). Experimental design of supercritical fluid extraction—a review. *Journal of Food Engineering*, 124, 105–116.
- Snyder, J., Friedrich, J., & Christianson, D. (1984). Effect of moisture and particle size on the extractability of oils from seeds with supercritical CO₂. *Journal of the American Oil Chemists' Society*, 61(12), 1851–1856.
- Sodeifian, G., & Ansari, K. (2011). Optimization of *Ferulago Angulata* oil extraction with supercritical carbon dioxide. *The Journal of Supercritical Fluids*, 57(1), 38–43.
- Sodeifian, G., Ardestani, N. S., Sajadian, S. A., & Moghadamian, K. (2018). Properties of *Portulaca oleracea* seed oil via supercritical fluid extraction: Experimental and optimization. *The Journal of Supercritical Fluids*, 135, 34–44.
- Sodeifian, G., Azizi, J., & Ghoreishi, S. (2014). Response surface optimization of *Smyrniun cordifolium* Boiss (SCB) oil extraction via supercritical carbon dioxide. *The Journal of Supercritical Fluids*, 95, 1–7.
- Sodeifian, G., Ghorbandoost, S., Sajadian, S. A., & Ardestani, N. S. (2016). Extraction of oil from *Pistacia khinjuk* using supercritical carbon dioxide: Experimental and modeling. *The Journal of Supercritical Fluids*, 110, 265–274.
- Sodeifian, G., & Sajadian, S. A. (2017). Investigation of essential oil extraction and antioxidant activity of *Echinophora platyloba* DC. Using supercritical carbon dioxide. *The Journal of Supercritical Fluids*, 121, 52–62.
- Sodeifian, G., Sajadian, S. A., & Ardestani, N. S. (2016a). Evaluation of the response surface and hybrid artificial neural network-genetic algorithm methodologies to determine extraction yield of *Ferulago angulata* through supercritical fluid. *Journal of the Taiwan Institute of Chemical Engineers*, 60, 165–173.
- Sodeifian, G., Sajadian, S. A., & Ardestani, N. S. (2016b). Extraction of *Dracocephalum kotschy* Boiss using supercritical carbon dioxide: Experimental and optimization. *The Journal of Supercritical Fluids*, 107, 137–144.
- Sodeifian, G., Sajadian, S. A., & Ardestani, N. S. (2016c). Optimization of essential oil extraction from *Launaea acanthodes* Boiss: Utilization of supercritical carbon dioxide and cosolvent. *The Journal of Supercritical Fluids*, 116, 46–56.
- Sodeifian, G., Sajadian, S. A., & Ardestani, N. S. (2017a). Experimental optimization and mathematical modeling of the supercritical fluid extraction of essential oil from *Eryngium billardieri*: Application of simulated annealing (SA) algorithm. *The Journal of Supercritical Fluids*, 127, 146–157.
- Sodeifian, G., Sajadian, S. A., & Ardestani, N. S. (2017b). Supercritical fluid extraction of omega-3 from *Dracocephalum kotschy* seed oil: Process

- optimization and oil properties. *The Journal of Supercritical Fluids*, 119, 139–149.
- Song, Y., Wang, X.-D., & Rose, R. J. (2017a). Oil body biogenesis and biotechnology in legume seeds. *Plant Cell Reports*, 36(10), 1519–1532.
- Sovilji, M. N. (2010). Critical review of supercritical carbon dioxide extraction of selected oil seeds. *Acta Periodica Technologica*, 2010(41), 105–120.
- Stahl, E., Quirin, K. W., & Mangold, H. K. (1981). Extraktion von Lupinenöl mit überkritischem Kohlendioxid. *Fette, Seifen, Anstrichmittel*, 83(12), 472–474.
- Stahl, E., Schuetz, E., & Mangold, H. K. (1980). Extraction of seed oils with liquid and supercritical carbon dioxide. *Journal of Agricultural and Food Chemistry*, 28(6), 1153–1157.
- Steel, C. J., Dobarganes, M. C., & Barrera-Arellano, D. (2005). The influence of natural tocopherols during thermal oxidation of refined and partially hydrogenated soybean oils. *Grasas y Aceites*, 56(1), 46–52.
- Sujak, A., Kotlarz, A., & Strobel, W. (2006). Compositional and nutritional evaluation of several lupin seeds. *Food Chemistry*, 98(4), 711–719.
- Supercritical CO₂ extraction systems—Buffalo Extraction Systems: The Innovative Edge. 2023. www.buffaloextracts.com
- Taheri, M. (2022). Techno-economical aspects of electrocoagulation optimization in three acid azo dyes' removal comparison. *Cleaner Chemical Engineering*, 2, 100007.
- Taylor, D. L., & Larick, D. K. (1995). Investigations into the effect of supercritical carbon dioxide extraction on the fatty acid and volatile profiles of cooked chicken. *Journal of Agricultural and Food Chemistry*, 43(9), 2369–2374.
- Temelli, F. (2009). Perspectives on supercritical fluid processing of fats and oils. *The Journal of Supercritical Fluids*, 47(3), 583–590.
- Turton, R., Bailie, R. C., Whiting, W. B., Shaeiwitz, J. A., & Bhattacharyya, D. (2012). *Analysis synthesis and design of chemical processes*. (Fourth edition International). Pearson Education International.
- Ulrich, G. D. (1984). *A guide to chemical engineering process design and economics*. Wiley.
- Uzun, B., Arslan, C., Karhan, M., & Toker, C. (2007). Fat and fatty acids of white lupin (*Lupinus albus* L.) in comparison to sesame (*Sesamum indicum* L.). *Food Chemistry*, 102(1), 45–49.
- Vasconcellos, V. R., & Cabral, F. A. (2001). A new method for estimating solubility of fatty acids, esters, and triglycerides in supercritical carbon dioxide. *Journal of the American Oil Chemists' Society*, 78(8), 827–829.
- Wang, H., Liu, Y., Wei, S., & Yan, Z. (2012). Application of response surface methodology to optimise supercritical carbon dioxide extraction of essential oil from *Cyperus rotundus* Linn. *Food Chemistry*, 132(1), 582–587.
- Yunus, M. A. C., Zhari, S., Haron, S., Arsad, N. H., Idham, Z., & Ruslan, M. S. H. (2015). Extraction and identification of vitamin E from *Pithecellobium jiringan* seeds using supercritical carbon dioxide. *Jurnal Teknologi*, 74(7), 29–33.
- Zhao, S., & Zhang, D. (2014). Supercritical CO₂ extraction of eucalyptus leaves oil and comparison with Soxhlet extraction and hydro-distillation methods. *Separation and Purification Technology*, 133, 443–451.
- Zlokarnik, M. (2006). *Scale-up in chemical engineering*. John Wiley & Sons.

SUPPORTING INFORMATION

Additional supporting information can be found online in the Supporting Information section at the end of this article.

How to cite this article: Yu, M., Kniepkamp, K., Thie, J. P., Witkamp, G.-J., & van Haren, R. J. F. (2023). Supercritical carbon dioxide extraction of oils from Andean lupin beans: Lab-scale performance, process scale-up, and economic evaluation. *Journal of Food Process Engineering*, 46(4), e14289. <https://doi.org/10.1111/jfpe.14289>

7.6 Lipid extraction from cherry stones



Research Article

Received: 10 August 2023

Revised: 13 December 2023

Accepted article published: 31 December 2023

Published online in Wiley Online Library:

(wileyonlinelibrary.com) DOI 10.1002/jctb.7581

Lipid extraction of high-moisture sour cherry (*Prunus cerasus* L.) stones by supercritical carbon dioxide

Kai Kniepkamp,^{a,b*}  Massimiliano Errico,^c Miao Yu,^a Maria Cinta Roda-Serrat,^c Jelle-Geert Eilers,^a Michael Wark^b and Rob van Haren^a

Abstract

BACKGROUND: Sour cherry (*Prunus cerasus* L.) stones are the major byproduct of the cherry industry and the efficient management of this biowaste can lead to achieving the food processing sustainability aimed at by the modern food industry. Despite its significant content of lipids, the valorization of cherry stone waste as feedstock for lipid extraction appears to be limited due to the high moisture content. This study explores the primary factors that affect the yield of lipid extraction using Soxhlet, Randall and supercritical carbon dioxide (scCO₂) extraction methods, with a particular emphasis on yield optimization for green extraction technologies (scCO₂).

RESULTS: The investigation revealed an increased lipid extraction yield for scCO₂ from 7.4 for dry crushed stones to 20.6 g per 100 g dry weight when the cherry kernels are separated. The high initial moisture content affected all three extraction methods, but mostly impacted the scCO₂ extraction, resulting in the co-extraction of an aqueous phase. Lipid and aqueous yield could be manipulated by time, temperature and pressure. However, no observable influence on the composition of fatty acid methyl esters was detected.

CONCLUSION: Numerous approaches are shown to enhance the lipid yield from cherry stone waste, depending on the desired outcome. When dealing with wet samples, Randall extraction proves to be the most effective method. On the other hand, scCO₂ extraction presents distinct advantages, such as the extraction of food-grade lipids and the co-extraction of a unique aqueous phase, which comes at the expense of a reduced lipid yield.

© 2024 The Authors. *Journal of Chemical Technology and Biotechnology* published by John Wiley & Sons Ltd on behalf of Society of Chemical Industry (SCI).

Supporting information may be found in the online version of this article.

Keywords: cherry pits; supercritical fluid extraction; extraction method comparison; water content; oil composition; biowaste valorization

INTRODUCTION

To tackle the ongoing issue of biowastes, byproducts and unused biomass, new ways for their recycling and valorization are continuing to be developed.^{1,2} In this context, residual streams like sour cherry stones might be valorized to reduce the environmental impact related to their disposal and simultaneously to diversify the market possibilities by applying the main principles of the circular economy related to waste minimization. Moreover, in the context of increasing uncertainty related to the global political situation and the emergence of new producers, sour cherry (*Prunus cerasus* L.) full exploitation, for example bio-cascading, is aimed.

Sour cherries can grow in cold regions and are commercially available. Although sour cherries can be safely consumed directly, it is common to find them in the market as processed food, like juice, jams, marmalades and toppings, or as alcoholic beverages

like cherry wine and cherry liqueur.^{3,4} Sour cherries contain polyphenols, like phenolic acids, flavonoids and anthocyanins,^{5,6} which are known for their antioxidative, anti-inflammatory and anticancer activities.^{4,7-9} Sour cherries consist of skin, flesh, a stone (shell

* Correspondence to: K Kniepkamp, Hanze University of Applied Sciences, Zernikeplein 11, 9747 AS Groningen, The Netherlands. E-mail: k.kniepkamp@pl.hanze.nl

a Hanze University of Applied Sciences, Groningen, The Netherlands

b Institute of Chemistry, Chemical Technology 1, Carl von Ossietzky Universität Oldenburg, Oldenburg, Germany

c Department of Green Technology, University of Southern Denmark, Odense, Denmark

© 2024 The Authors. *Journal of Chemical Technology and Biotechnology* published by John Wiley & Sons Ltd on behalf of Society of Chemical Industry (SCI).

This is an open access article under the terms of the [Creative Commons Attribution-NonCommercial-NoDerivs](https://creativecommons.org/licenses/by-nc-nd/4.0/) License, which permits use and distribution in any medium, provided the original work is properly cited, the use is non-commercial and no modifications or adaptations are made.

+ kernel) and a stem. For most sour cherry products, the juice of the cherries is the target. To obtain sour cherry juice, fresh sour cherries are pressed, and the desired liquid fraction is collected. The remains (skins, stems, flesh remains and stones) are considered as waste.^{10–12} One potentially valuable fraction can be the cherry stones, which account for *ca* 15% of sour cherries' fresh weight.¹³

The yearly worldwide production from 2006 to 2016 reached about 1.1–1.3 million tons, mainly from Europe, with a corresponding amount of biowaste from stones estimated at between 165 000 and 195 000 tons.¹⁴ Kandemir *et al.*¹⁵ more recently reported that the world production of sour cherries was estimated at 1.4 million tons. Considering that most of the production is related to juice production, its impact is clear in terms of biowastes generated.

Several investigations focused on the valorization of cherry stone waste. Pollard and Goldfarb¹⁶ proposed a conversion to biochar and activated biochar for soil amendments and heavy metal removal. Akalin *et al.*¹⁷ chose the production of bio-oil through hydrothermal processing as a valorization route. A completely different approach was proposed by Grubesa *et al.*¹⁸ considering cherry stones as aggregate in concrete. Despite these alternatives, the extraction of lipids remains the most consolidated and explored valorization method due to the high value of the fraction recovered.^{5,10,13,19–21}

Yilmaz and Gökmen reported that 23% of the stone weight is accounted for by the kernel fraction, while the remaining 77% is accounted for by the shell.¹³ Among the two, the kernel fraction is considered to have the highest lipid content; however, experimental data focusing on the comparison are lacking.

The most reported extraction strategies focus on classical extraction by nonpolar organic solvents^{5,19,20,22–25} or extraction via supercritical carbon dioxide (scCO₂)^{10,13,20,21} with and without the use of co-solvent. Although the application of classic organic solvent extraction is relatively simple, it has the disadvantage of a high environmental impact. Furthermore, difficulties in complete solvent recovery lead to contamination of the product and thus to reductions in quality and value of the product.^{26,27}

An alternative to the traditional organic solvent extraction approach is extraction via supercritical fluids, for example with carbon dioxide. Extraction via scCO₂ is a promising method to reduce the environmental impact and avoid any solvent contamination in the product, which makes this technique especially suitable for food-oriented compounds.^{28,29}

As with all unit operations, also the use of scCO₂ requires the optimization of the characteristic operating parameter of the process. In this way, the designer can target a specific objective function like the recovery of a target compound/class of compounds or the total yield.²¹

When comparing the lipid extraction yields from cherry stones or kernels corresponding to different extraction methods, only little data are given.¹⁰

The focus seems to be on the fatty acid methyl ester (FAME) composition of the transesterified extracts, which seems not to be significantly influenced by the choice of the extraction method.^{13,19} Oleic acid (C18:1) and linoleic acid (C18:2) are reported to be responsible for 70–90% of the total fatty acid composition,^{5,13,19,22,30} indicating a high unsaturated to saturated fatty acid proportion,¹³ giving another argument for the recovery of lipids from this feedstock.

While other publications focus on a particular extraction technique and one specific raw material, the study reported here took a new approach that focused on the comparison of different extraction techniques and the influence of the starting material

conditions. The primary objective of the study was therefore to explore the influence of parameters from the cherry feedstock and the choice of extraction method on the lipid yield and composition. Since scCO₂ is the most promising option in terms of sustainability and potential for optimization, its extraction parameters were additionally analyzed. Therefore, this paper provides a complete picture of the routes to be followed for high yield in lipid extraction.

EXPERIMENTS/MATERIALS AND METHODS

The cherry pomace used for the experiments was provided by cherry wine producer Frederiksdal located in the Danish region of Sjælland. The pomace was kept frozen at –22 °C until further use. For all samples the pomace was washed under running water to remove residues of flesh, sticks and stems from the stones. The stones were recovered in a sieve and dried using a paper towel.

During all experiments, the moisture content of the samples was continuously monitored and no change over time was observed.

Crushed cherry stones

After washing and drying, about 200 g of stones was ground in a GM 300 knife mill (Retsch, Haan, Germany) using 50 g of sample per batch. The grinding time was 2 min at a temperature of 22 °C. Afterward, all portions were mixed to ensure homogeneity and divided into four aliquots.

The first part constituted the sample called CS-Original and was used without any further treatment. The other parts were treated as follows: in a hot-air oven (UFE4000, Memmert, Schwabach, Germany) at 40 °C for 24 h (sample CS-D40); in a humidity chamber (HCP 108, Memmert, Schwabach, Germany) at 40 °C setting the relative humidity to 75% for 24 h (sample CS-RH75); or in a humidity chamber at 40 °C setting the relative humidity to 20% for 24 h (sample CS-RH20). All samples were stored at –20 °C in the dark until further use.

Separated cherry kernel

The kernel fraction was obtained by cracking the whole stone and sorting manually the kernels. This fraction was processed following the same procedure as for the crushed cherry stone samples. The untreated part was called SK-Original, while the others were designated SK-D40 (oven 40 °C, 24 h), SK-RH75 (humidity chamber 75%, 40 °C, 24 h) and SK-RH20 (humidity chamber 20%, 40 °C, 24 h) depending on the thermal treatment. All samples were stored at –20 °C in the dark, until further use.

Moisture analysis

For the dry weight determination, 2 g of cherry material was placed in a moisture balance (MB 160, VWR, Pennsylvania, USA). The balance recorded the initial weight and a halogen-infrared heat source set at 120 °C was used to evaporate the moisture from the sample. After the balance recorded no weight loss above 0.1% for 1 min, the remaining mass was used to calculate the loss of moisture. All measurements were carried out at least in triplicate.

Soxhlet extraction

An amount of 2 g of cherry material was accurately weighed into a lipid-free 22 mm × 80 mm thimble (Whatman, Maidstone, UK, pre-extracted with hexane) and closed with lipid-free cotton (Vernacare, Lancashire, UK, pre-extracted with hexane).

The sample was then extracted for 5 h with 100 mL of hexane (technical grade isomers, Fisher Sci, Massachusetts, USA) for 25–30 cycles in a 70 mL Soxhlet extractor.

The extract was filtered and evaporated with an RV10 rotation evaporator (IKA, Staufen im Breisgau, Germany) at 40 °C at reduced pressure. Lipids were transferred with analytical grade *n*-hexane (3 × 0.5 mL; Acros Organics, Geel, Belgium) into a glass vial and dried until weight equilibration was achieved. Measurements were carried out at least in duplicate.

Randall extraction

An amount of 2 g of cherry material was accurately weighed into a lipid-free 26 mm × 60 mm thimble (Whatman, Maidstone, UK, pre-extracted with hexane) and closed with lipid-free cotton.

The sample was extracted with 100 mL of hexane in a Soxtec Avanti 2055 apparatus (Foss, Hilleroed, Denmark). A cooking step at 170 °C for 40 min and a rinsing step for 80 min at 170 °C were performed before the extract was concentrated to around 10 mL. The extract from the extraction cup was then filtered and transferred into a round-bottom flask, evaporated and transferred into a vial, similar to the reported Soxhlet extraction method, before weight determination took place. Measurements were carried out in triplicate.

Supercritical fluid extraction

A supercritical fluid extraction 500 apparatus (Separex, Champigneulle, France) was used with carbon dioxide (99.7%; Linde, Schiedam, the Netherlands) for all experiments. An amount of 50 g of cherry material was measured and placed in the extraction vessel of the unit. After 30 min temperature equilibrium time, the experiments were carried out with a CO₂ flow rate of 25 g min⁻¹ for 6 h. Unless otherwise mentioned, the extraction was performed with a pressure of 350 bar and a temperature of 40 °C, which showed good performance in preliminary testing and other biomatrices.^{20,21,31} The extract was collected every 30 min from the collection vessel (60 bar, 40 °C) and the carbon dioxide was continuously recycled.

For cleaning purposes, the vessel was depressurized and disconnected. The remaining unit was then flushed with carbon dioxide (25 g min⁻¹, ca 200 bar, 40 °C) for 5 min. This fraction was collected, and its weight was added to the total yield calculations as a cleaning fraction. Afterward, a 1 mL min⁻¹ co-solvent stream of 96% ethanol (Arcos Organics, Geel, Belgium) was added to the scCO₂ for 10 min. This sample was collected independently and was not included in the weight determination. All experiments were carried out at least in duplicate.

Weight determination of lipid/water fraction

Most of the extracts recovered through scCO₂ consisted of two phases: a yellow lipid fraction and an aqueous fraction. Every sample was centrifuged for 3 min at 5000 rpm with a Universal 320 centrifuge (Hettich, Tuttlingen, Germany) at 22 °C.

After centrifuging, the test tube was weighed, then the upper oily fraction was carefully removed via Pasteur pipettes. The remaining aqueous fraction was weighed and the difference in weight before and after removing the lipid fraction was determined and used as lipid weight. After separation, all samples were stored at -20 °C in the dark until further use.

FAME determination

The FAME determination was based on transesterification as described by Lepage and Roy³² and adapted according to Yu *et al.*³¹ The internal standard (IS) solution was prepared by dissolving

40 mg of tetradecane (99%; Acros Organics, Geel, Belgium), 40 mg of methyl nonanoate (98%; Sigma Aldrich, St Louis, USA) and 40 mg of nonadecanoic acid (≥98%; Sigma Aldrich) in 10 mL of *n*-hexane (>99%; Acros Organics). Additionally, a FAME solution containing 20 mg of methyl palmitate (≥99%; Sigma Aldrich), 150 mg of methyl linoleate (≥99%; Sigma Aldrich), 120 mg of methyl oleate (Sigma Aldrich) and 10 mg of methyl stearate (99%; Sigma Aldrich) in 50 mL of *n*-hexane was prepared. Calibration standards were prepared by adding each of 0, 100, 250, 500 and 1000 µL of FAME solution to a vial before adjusting the total volume to 2.00 mL with *n*-hexane and adding 100 µL of the IS solution.

For the transesterification, about 5 mg of the lipid fraction sample was accurately measured in a glass sample tube, before 100 µL of IS solution was added. Then 4 mL of freshly prepared 5% acetyl chloride (98%; Acros Organics) in methanol (99.8%; Acros Organics) was added to each sample tube, before homogenization by vortexing. Afterward, the tubes were placed into a water bath at 60 °C and shaken every 15 min vigorously. After 60 min the tubes were cooled at ambient temperature and 1 mL of 5 mol L⁻¹ NaCl solution (97%; Fisher Sci, Massachusetts, USA) in Milli-Q® water (Merck, Darmstadt, Germany) was added. Additionally, 2.00 mL of *n*-hexane was added to each tube, before the tubes were rotated for 1 h. As a last step, the tubes were centrifuged for 5 min at 5000 rpm and the upper organic layer was transferred into a GC-Vial for analysis.

An amount of 0.5 µL of the prepared organic layer was injected into a GC-FID 2030 (Shimadzu, Kyoto, Japan), which was equipped with a 30 m × 0.25 mm × 0.25 µm film thickness HP-5MS column (Agilent, Santa Clara, USA). The injection temperature was set to 300 °C and the split was adjusted to 1.20 mL min⁻¹ column flow and 20 mL split flow. Hydrogen (6.0, Linde, Dublin, Ireland) was used as the carrier and detector gas. The detection temperature was adjusted to 325 °C.

The starting oven temperature was set to 80 °C and increased at 20 °C min⁻¹ until 140 °C. From here the temperature was increased at 3 °C min⁻¹ until 210 °C was reached followed by a temperature increment to 300 °C at 20 °C min⁻¹.

The quantification was performed by calculating the area of the desired FAME divided by the area of the IS methyl nonanoate and referring to the calibration curve with known concentrations.

Solvent-to-feed ratio

The solvent-to-feed ratio was calculated by dividing the mass of the solvent that came in contact with the sample by the sample mass, as reported in Eqn (1):

$$SF = \frac{m_{\text{Solvent}}}{m_{\text{Sample}}} \quad (1)$$

Method-specific normalized extraction efficiency

The method-specific normalized extraction efficiency was calculated for each method by dividing the yield per dry weight through the yield per dry weight of the driest sample of the chosen method (Soxhlet, Randall or scCO₂) and sample (crushed stone or separated kernel).

RESULTS AND DISCUSSION

Moisture content

Moisture content or moisture level is an important factor when it comes to extraction yield. To identify the influence of moisture

level on the yield of different extraction methods, stones and crushed kernels were obtained at four different moisture levels. The results from the moisture analysis expressed in terms of moisture level are reported in Table 1.

The highest moisture level was found in the raw material as obtained from the producer. The moisture content of the untreated material was 28.8% for stones and 50.0% for kernels.

The driest samples were achieved by using a humidity chamber with a relative humidity of 20% for 24 h. Moisture levels of about 4.7% for stones and about 3.6% for kernels were observed. Oven drying at 40 °C yielded a moisture content of *ca* 10.5% for stones and 11.5% for kernels. A bigger difference in dry weight for crushed stones and kernels was observed for the case of 75% relative humidity. The moisture level was 17.7% and 33.3% for stones and crushed kernels, respectively. This result might be explained by the difference between crushed stones and crushed kernels in terms of pores, lipid content and initial moisture content.

Extraction methods

The samples were extracted by Soxhlet, Randall and scCO_2 (350 bar, 40 °C) methods and analyzed in terms of lipid yield per dry weight. The results are reported in Fig. 1. As a general trend, it was observed that the amount of total lipids extracted from kernel samples is higher than that extracted from crushed stones. The highest lipid yield per dry weight was achieved by Soxhlet extraction of the driest kernel sample (SK-RH20, 3.6%). The lowest yield was observed for scCO_2 extraction of the most moisturized crushed stone sample (CS-Original, 33.3%). The Randall and Soxhlet extractions offered a comparable lipid yield for samples with a moisture content below 33%. An evident trend emerged, where higher-moisture samples led to higher extraction yields with Randall extraction than with Soxhlet operation. This trend can be marked by comparing the Randall and Soxhlet extraction yield from the most moisturized sample (SK-original, 50.0%), in which only two-thirds of the former extraction yield was collected via the latter method. The gap between Soxhlet and Randall lipid extraction yield for highly moisturized samples might be explained by the additional cooking step used in the Randall extraction. The boiling enhances not only the lipid but also the water solubility.³³ Furthermore boiling creates local shear stress due to the formation and cavitation of bubbles as well as an enhanced mass transfer. However, the highest lipid yield still corresponds to the Soxhlet extraction (SK-RH20, 3.6%).

When compared with Soxhlet and Randall extractions, the scCO_2 extraction showed a lower lipid yield in all tested cases. This might be due to the smaller solvent-to-feed ratio of 180 in comparison to *ca* 350 for Randall and 578 for Soxhlet (see supporting information). Besides this, Soxhlet and Randall extractions employ hexane as a solvent which has different solvation properties from carbon dioxide, for example density,

dielectric constant, dynamic viscosity, polarity and physical state, contributing to the differences observed for the extraction yield.³³⁻³⁵ Nevertheless, scCO_2 does offer a nontoxic and ready-to-consume product, absence of environmental contamination and easy downstream processing, which might compensate for the lower yield.^{26,28,29}

The absolute values reported in Fig. 1 show a decrease in lipid yield per dry weight for increasing moisture content for all methods and biomasses. To investigate the effect of moisture on the different methods and samples, method-specific normalized lipid extraction efficiencies are shown in Fig. 2. A moisture range of 4–12% yielded minimal losses (>80% yield) for all methods and sample matrices. The relatively strong decrease in the yield of the separated kernel sample by Soxhlet extraction (Fig. 2(e)) is due to the high value of the extraction yield from the lowest moisture content, which is the reference point and not shown in the crushed stone matrix (Fig. 2(b)).

Further increase of moisture content in the crushed stone matrix to 17.9% resulted in an apparent efficiency loss for scCO_2 , but not for Soxhlet and Randall extractions, indicating a higher sensitivity of the scCO_2 extraction process towards moisture than the other tested extraction processes. This trend was confirmed by the separated kernel matrix, which showed a similar trend for moisture content of 33.3%. The highest-moisture sample (SK-Original, 50%) was found to lead to only 29% of extraction efficiency, while Soxhlet extraction still resulted in 50% and Randall in 86% efficiency. Overall, Randall extraction was least affected by moisture content and always led to lipid yields of over 80%.

FAME composition

The lipid fraction obtained by Soxhlet, Randall and scCO_2 extractions from the separated kernel matrix was transesterified and analyzed for its FAME composition. The results are reported in Table 2. Methyl linoleate was found to be the most abundant FAME, accounting for around half of the total lipid fraction, followed by methyl oleate which accounted for roughly one-third of the total lipid fraction. The remaining fraction is mainly dominated by methyl palmitate and only a minor fraction by methyl stearate.

A conducted multivariate analysis of variance showed that the moisture level has no influence on the lipid composition (see supporting information). Furthermore, three of the four FAME components were also not significantly influenced by the choice of extraction method. The only significantly influenced component was methyl stearate, which showed a slightly higher average lipid yield for the Soxhlet extracts than for the other two methods. However, methyl stearate accounts only for 2% of the lipid content and its influence on the choice of extraction method is therefore limited.

Also investigated was whether the extraction process favors certain lipid compositions, which means that different FAME

Table 1. Moisture level of different cherry samples: crushed cherry stones (CS) and separated kernel fraction (SK)

Drying method	Crushed stones		Separated kernel	
	Name	Moisture level (\pm standard deviation) (%)	Name	Moisture level (\pm standard deviation) (%)
—	CS-Original	28.8 \pm 0.3	SK-Original	50.0 \pm 0.2
Humidity chamber 75%	CS-RH75	17.7 \pm 0.4	SK-RH75	33.3 \pm 0.5
Oven 40 °C	CS-D40	10.5 \pm 0.4	SK-D40	11.5 \pm 0.4
Humidity chamber 20%	CS-RH20	4.7 \pm 0.3	SK-RH20	3.6 \pm 0.2

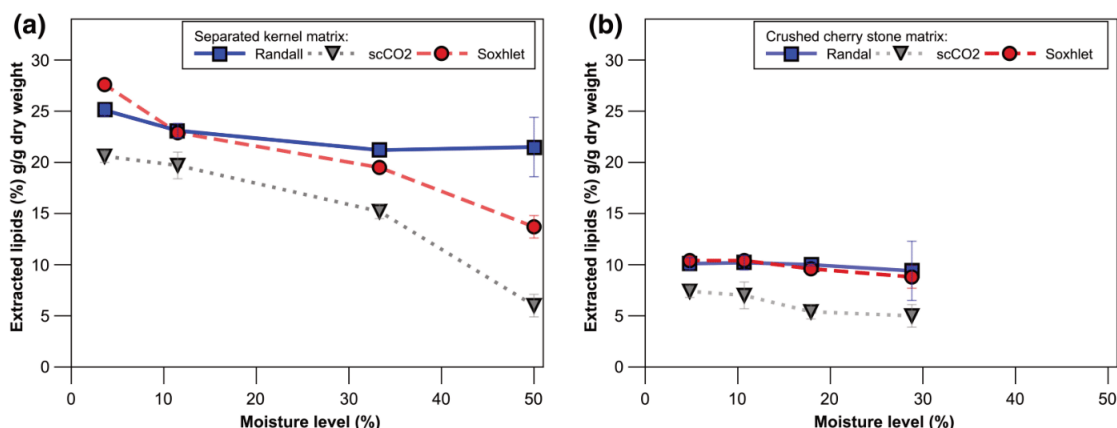


Figure 1. Lipid extraction yields from separated kernels (a) and cherry stones (b) obtained by Randall (blue, hexane 40 min cooking, 80 min rinsing), scCO₂ (grey, 350 bar, 40 °C, 6 h) and Soxhlet (red, hexane, 5 h) extractions as a function of sample moisture level. The results of yield are expressed in percentage of g g⁻¹ dry weight.

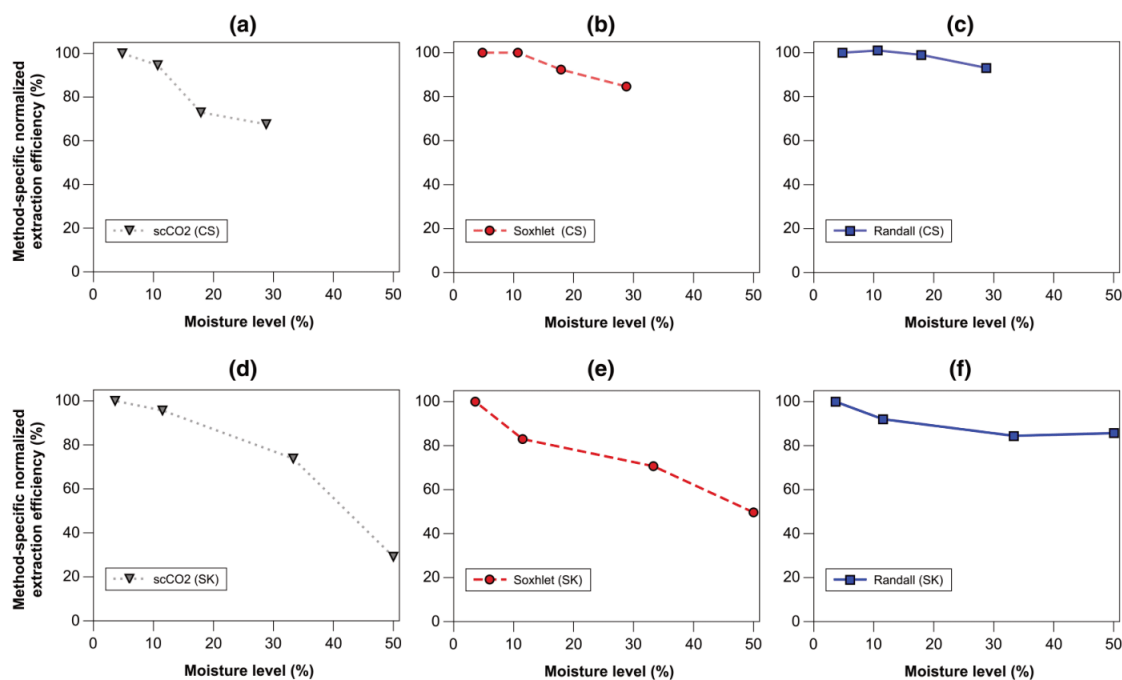


Figure 2. Method-specific normalized extraction efficiency against sample moisture level. Extraction efficiency of lipid yield per dry weight for crushed stones (CS) (a–c) and separated kernels (SK) (d–f) via scCO₂ (grey), Soxhlet (red) and Randall (blue) extractions.

compositions were observed at the beginning of the experiment from those at a later point of the experiment. However, such behavior was not found; in contrast to other matrices,^{31,36} the FAME composition kept the same proportions over the total extraction time (see supporting information, S1). Other FAMES were detected but were not quantified, due to their limited presence. The FAME composition obtained in this study indicates a

high unsaturated to saturated fatty acid proportion in agreement with the results reported by Bernardo-Gil *et al.*¹⁹

Co-extraction of an aqueous phase with scCO₂

It was discovered that, differently from the Soxhlet and Randall extractions, for most scCO₂ extractions it was possible to collect an aqueous phase. The proportion between the lipid and aqueous

Table 2. FAME composition of esterified kernel lipid fractions

Sample (moisture content)	Extraction process	Methyl palmitate (C16:0) (%)	Methyl stearate (C18:0) (%)	Methyl oleate (C18:1) (%)	Methyl linoleate (C18:2) (%)	Total (%)	USF/SFA
SK-Original (50.0%)	Soxhlet	6	2	30	41	79	9
	scCO ₂	5	2	33	47	87	11
	Randall	5	2	30	35	72	9
SK-RH75 (33.3%)	Soxhlet	5	2	30	44	81	10
	scCO ₂	5	2	32	49	98	11
	Randall	5	2	31	44	82	13
SK-D40 (11.5%)	Soxhlet	5	2	30	44	81	11
	scCO ₂	6	2	36	55	99	12
	Randall	5	2	33	47	87	11
SK-RH20 (3.6%)	Soxhlet	5	2	31	47	86	10
	scCO ₂	5	2	32	49	88	12
	Randall	5	2	32	51	89	12

Lipid fraction was obtained from Soxhlet (hexane, 5 h), scCO₂ (350 bar, 40 °C) and Randall (hexane, 40 min cooking, 80 min rinsing) extracted at different moisture levels and analyzed in duplicate. Percentages refer to the total lipid weight fraction (w/w). USF/SFA was calculated by dividing the unsaturated fatty acid (USF) by the saturated fatty acid (SFA) content.

Table 3. Aqueous and lipid yield of scCO₂ extractions

Sample (moisture content)	Lipid g g ⁻¹ FW (%)	Lipid g g ⁻¹ DW (%)	Aqueous g g ⁻¹ FW (%)	Sample (moisture content)	Lipid g g ⁻¹ FW (%)	Lipid g g ⁻¹ DW (%)	Aqueous g g ⁻¹ FW (%)
CS-Original (28.8%)	3.6	5.0	13.6	SK-Original (50.0%)	3.0	6.0	16.8
CS-RH75 (17.9%)	4.4	5.4	4.8	SK-RH75 (33.3%)	10.2	15.2	15.7
CS-D40 (10.7%)	6.3	7.0	4.6	SK-D40 (11.5%)	17.4	19.7	7.5
CS-RH20 (4.8%)	7.0	7.4	0.8	SK-RH20 (3.6%)	19.8	20.6	3.6

Yield of the obtained lipid and aqueous phase of scCO₂ extractions after 6 h (350 bar, 40 °C) expressed in percentage of extracted lipid mass divided by either fresh weight (FW) or dry weight (DW) at different moisture levels.

phases is reported in Table 3. To the best of our knowledge, there has been no study of the extraction or analysis of an aqueous phase recovered from cherry stones or kernels.

As expected, the highest aqueous phase yield was obtained by scCO₂ extraction of the sample with the highest moisture content (SK-Original, 50.0%). This sample also showed the lowest yield for lipid extraction. It was found that a high moisture content resulted in a high aqueous yield and low lipid yield and vice versa.

In addition to the reported total yield of lipids with scCO₂, the extraction progress was monitored in terms of lipid and aqueous yield over time for the cherry kernel extractions.

scCO₂ lipid and aqueous extraction yield over time

The curve shape of extracted lipid per fresh weight (Fig. 3(a)) and extracted lipid per dry weight (Fig. 3(b)) differs from that of the aqueous phase yield per fresh weight (Fig. 3(c)) over time. The lipid extraction curves (Fig. 3(a),(b)) of potentially high-lipid-yielding samples (SK-D40 and SK-RH20) seem to have a saturated shape which is shown by their potential high slope at the beginning, and their flat end. The saturated shape results probably through the limited mass transfer of lipids from the pores of the biomatrix to the scCO₂ phase, which was also reported elsewhere²⁰ and is in agreement with results for other lipid-containing matrices.³¹ While the yield limitation for the lipid extractions for drier samples might result from a limited diffusion process

(SK-RH20, SK-D40), the limitation for samples with higher moisture content (SK-RH75, SK-Original) might result from blockage of pores through water or inhibited partition of lipids of the scCO₂ phase. An increased moisture content showed therefore smaller lipid extraction rate per fresh and dry weight, which is not related to the maximum solubility of lipids inside the scCO₂ stream as shown in Fig. 3(a).

Differently from the lipid extraction yield, according to Fig. 3(c), the profiles of the aqueous phase yield have a more linear behavior, as described for zero-order kinetics. This behavior is also reported by Brown *et al.*³⁷ for the dehydration of carrots via scCO₂ in similar conditions as here shown and is mostly influenced by the temperature (as discussed later). Samples SK-RH75 and SK-Original show similar aqueous extraction yield curves per fresh weight despite the different moisture content. This might indicate a limit of water solubility in the scCO₂ phase at the tested conditions, which could reduce the lipid uptake inside the scCO₂-water stream and lead to the decreased lipid extraction. Although literature about the theoretical maximum solubility of the bi-phase water-scCO₂ system is available,³⁸⁻⁴⁰ a concrete value cannot be accurately determined, due to the co-interaction of cherry material and lipids, which might limit the water dissolution into the scCO₂ phase. This can be seen in sample SK-D40 (11.5%), where the water extraction trend emerged after around 150 min, corresponding to the

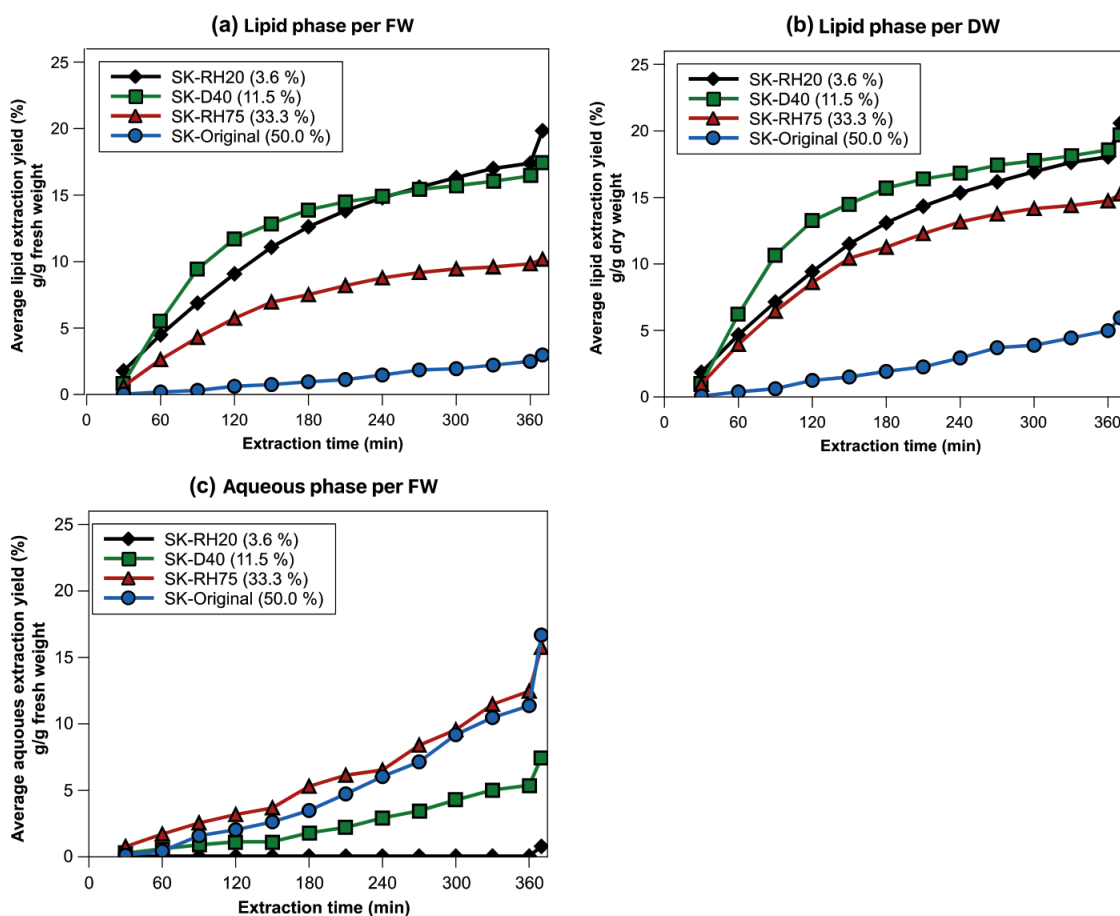


Figure 3. Lipid and aqueous extraction over time via scCO_2 extraction. (a) Accumulated yield of lipid phase per fresh weight (FW), (b) lipid phase per dry weight (DW) and (c) aqueous phase per fresh weight for separated cherry kernels at different moisture levels via scCO_2 extraction at 350 bar and 40 °C. The cleaning fraction, after 360 min of extraction, was considered and added as the data point at 370 min, which refers to the total yield as presented in Table 3.

point where around three-quarters of the lipids were extracted (Fig. 3(b)).

This behavior was not observed in the lower-moisture-containing samples. It could therefore be speculated that with longer extraction times the higher-moisture sample (SK-Original, 50.0%) could achieve a higher lipid extraction rate since most of the water is extracted, and the pores might be free to be accessed by the carbon dioxide.

During the extraction of the driest sample (SK-RH20), the highest lipid yield was achieved, and almost no aqueous phase was present and is therefore recommended for processes aimed at lipid yield, since it also avoids the need for another separation step.

Parameters influencing lipid or aqueous scCO_2 extraction

Due to the high lipid and medium aqueous yield, the crushed stone sample CS-D40 was chosen to be further analyzed for extraction at different conditions of pressure and temperature. Although the cherry kernel sample (SK-D40) resulted in a higher lipid fraction than the crushed stone sample (CS-D40), the latter

was chosen concerning the ease of handling and economic potential. Sample CS-D40 with a moisture content of 10.7% was extracted with similar time (6 h) and flow rate conditions ($25 \text{ g min}^{-1} \text{ CO}_2$) but for a pressure of 150, 350 and 550 bar and a temperature of 40, 60 and 80 °C. The influence of pressure and temperature was examined with respect to the accumulated lipid and aqueous extraction yield. The effect of temperature and pressure on the accumulated yield of aqueous and lipid phases for a 360 min scCO_2 extraction is shown in Fig. 4.

The highest pressure (550 bar) and highest temperature (80 °C) resulted in the highest measured lipid yield (7.0 g per 100 g of initial sample). This result would increase the extraction yield from 67% to 74% in comparison to the Soxhlet operation (Fig. 1) and shows that the co-extraction of an aqueous phase does not necessarily limit the extraction of the lipids.

The overall dominating effect for the extraction of lipids in the investigated parameter frame appears to be pressure. However, experiments at the lowest constant pressure (150 bar) showed a huge difference in lipid yield, although similar pressure was

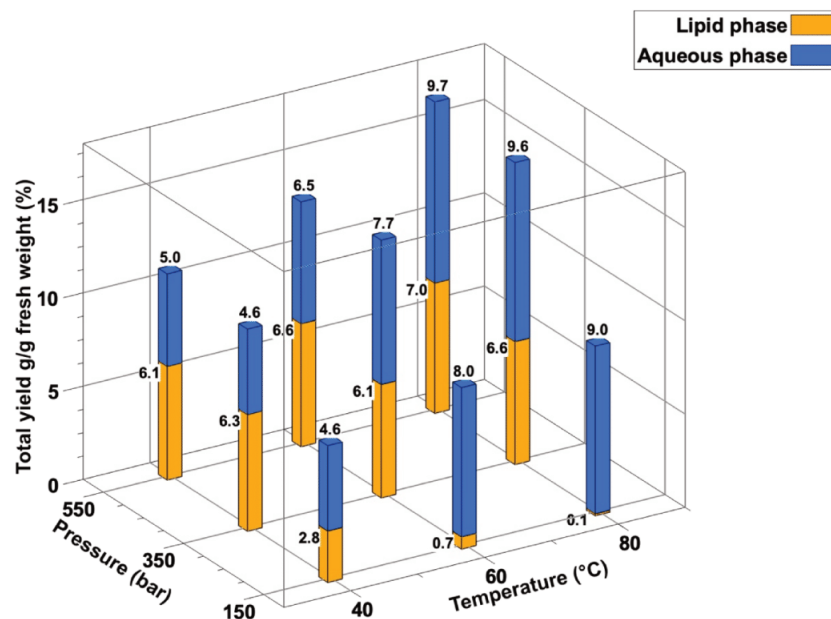


Figure 4. Influence of pressure and temperature on scCO_2 extraction yield. Accumulated yield of lipid (yellow) and aqueous phase (blue) after 6 h of extraction with scCO_2 at different temperature and pressure conditions.

applied. This can be explained by the density change of scCO_2 (see supporting information).⁴¹ This means that pressure becomes the dominating parameter for the extraction of lipids only after a certain threshold of density is reached.

The greatest aqueous yield was realized by 550 bar at 80 °C, followed by 350 bar at 80 °C and 150 bar at 80 °C. The data demonstrate a positive correlation between aqueous yield and temperature, meaning that the higher the temperature the more water can be extracted. It was found that a change in pressure has no significant effect on the extracted aqueous phase. This result is in agreement with binary solubility data of water and scCO_2 ^{38,39} and was also found for other biomatrices, for example carrots³⁷ and apples.⁴²

CONCLUSION

The study reported demonstrates the influence of the choice of extraction method, choice of raw material, raw material condition and extraction parameters on the lipid yield of cherry material, a previously considered waste product. While earlier studies have primarily focused on optimizing specific values or parameters of a chosen extraction method, the present study places a greater emphasis on the raw material.

The separation of kernels from cherry stones emerged as the most critical factor, leading to a doubling or even greater increase in terms of yield. This was followed by factors like moisture level and choice of extraction method. The findings reveal that the highest lipid yield can be achieved with the driest kernel samples using Soxhlet extraction, although the difference from Randall extraction was relatively small. However, Randall extraction was found to be rather unaffected by moisture level, due to the application of boiling hexane.

ScCO_2 extractions (350 bar, 40 °C) were inferior in lipid yield to the other two conventional extraction methods, and it was observed that scCO_2 extraction suffers the most due to increased moisture content. However, it offers a contamination-free and food-grade product, which might compensate for the potential lower yield.

The lipid yield of scCO_2 extraction was improved by elevated temperature (80 °C) and pressure (550 bar) values. The FAME composition was analyzed, and it could be shown that the composition is not or only to a limited extent influenced by the choice of extraction method, moisture content, pressure, temperature or time. The demonstrated high ratio of unsaturated to saturated FAMEs underlines the importance of the exploitation of cherry stones and green extraction techniques such as scCO_2 .

Among the contamination-free and food-grade lipid extracts, the scCO_2 extraction offers a great potential for the co-extraction of a novel aqueous phase, which could contain valuable phenolic components and is mostly influenced by temperature. Therefore, this work promotes the valorization of unused biomasses and helps to reduce waste.

ACKNOWLEDGEMENT

This research work was funded by the European Regional Development Fund as part of the Interreg North Sea Region project 38-2-4-17 BIOCAS, circular BIOMass CAScades to 100%, to whom the authors would like to express their gratitude. ME acknowledges the funding received from the European Union's Horizon 2020 research and innovation program under Marie Skłodowska-Curie grant agreement no. 778168. Open Access funding enabled and organized by Projekt DEAL.

DATA AVAILABILITY STATEMENT

The data that support the findings of this study are available from the corresponding author, upon reasonable request.

SUPPORTING INFORMATION

Supporting information may be found in the online version of this article.

REFERENCES

- Madeddu C, Roda-Serrat MC, Christensen KV, El-Houri RB and Errico M, A biocascade approach towards the recovery of high-value natural products from biowaste: state-of-art and future trends. *Waste Biomass Valorization* **12**:1143–1166 (2020). <https://doi.org/10.1007/s12649-020-01082-6>.
- Federici F, Fava F, Kalogerakis N and Mantzavinos D, Valorisation of agro-industrial by-products, effluents and waste: concept, opportunities and the case of olive mill wastewaters. *J Chem Technol Biotechnol* **84**:895–900 (2009). <https://doi.org/10.1002/jctb.2165>.
- Yilmaz FM, Gorguc A, Karaaslan M, Vardin H, Ersus Bilek S, Uygun O et al., Sour cherry by-products: compositions, functional properties and recovery potentials – a review. *Crit Rev Food Sci Nutr* **59**:3549–3563 (2019). <https://doi.org/10.1080/10408398.2018.1496901>.
- Grafe C and Schuster M, Physicochemical characterization of fruit quality traits in a German sour cherry collection. *Sci Hortic* **180**:24–31 (2014). <https://doi.org/10.1016/j.scienta.2014.09.047>.
- Bak I, Lekli I, Juhasz B, Varga E, Varga B, Gesztelyi R et al., Isolation and analysis of bioactive constituents of sour cherry (*Prunus cerasus*) seed kernel: an emerging functional food. *J Med Food* **13**:905–910 (2010). <https://doi.org/10.1089/jmf.2009.0188>.
- Nemes A, Szollosi E, Stundl L, Biro A, Homoki JR, Szarvas MM et al., Determination of flavonoid and proanthocyanidin profile of Hungarian sour cherry. *Molecules* **23**:3278 (2018). <https://doi.org/10.3390/molecules23123278>.
- Stryjecka M, Michalak M, Cymerman J and Kiełtyka-Dadasiewicz A, Comparative assessment of phytochemical compounds and antioxidant properties of kernel oil from eight sour cherry (*Prunus cerasus* L.) cultivars. *Molecules* **27**:696 (2022). <https://doi.org/10.3390/molecules27030696>.
- Blando F, Gerardi C and Nicoletti I, Sour cherry (*Prunus cerasus* L.) anthocyanins as ingredients for functional foods. *J Biomed Biotechnol* **2004**:253–258 (2004). <https://doi.org/10.1155/S1110724304404136>.
- Singh R, Dhanani T and Kumar S, Supercritical fluid extraction of bioactive compounds from fruits and vegetables, in *Fruit and Vegetable Phytochemicals*, ed. by Yahia EM. John Wiley & Sons, Inc., USA, pp. 749–762 (2017). <https://doi.org/10.1002/9781119158042.ch33>.
- Straccia MC, Siano F, Coppola R, La Cara F and Volpe MG, Extraction and characterization of vegetable oils from cherry seed by different extraction processes. *Chem Eng Trans* **27**:391–396 (2012). <https://doi.org/10.3303/CET1227066>.
- González-Domínguez JM, Fernández-González MC, Alexandre-Franco M and Gómez-Serrano V, How does phosphoric acid interact with cherry stones? A discussion on overlooked aspects of chemical activation. *Wood Sci Technol* **52**:1645–1669 (2018). <https://doi.org/10.1007/s00226-018-1047-5>.
- Ropelewska E, Classification of the pits of different sour cherry cultivars based on the surface textural features. *J Saudi Soc Agric Sci* **20**:52–57 (2021). <https://doi.org/10.1016/j.jssas.2020.11.003>.
- Yilmaz C and Gökmen V, Compositional characteristics of sour cherry kernel and its oil as influenced by different extraction and roasting conditions. *Ind Crops Prod* **49**:130–135 (2013). <https://doi.org/10.1016/j.indcrop.2013.04.048>.
- Blando F and Oomah BD, Sweet and sour cherries: origin, distribution, nutritional composition and health benefits. *Trends Food Sci Technol* **86**:517–529 (2019). <https://doi.org/10.1016/j.tifs.2019.02.052>.
- Kandemir K, Piskin E, Xiao J, Tomas M and Capanoglu E, Fruit juice industry wastes as a source of bioactives. *J Agric Food Chem* **70**:6805–6832 (2022). <https://doi.org/10.1021/acs.jafc.2c00756>.
- Pollard ZA and Goldfarb JL, Valorization of cherry pits: Great Lakes agro-industrial waste to mediate Great Lakes water quality. *Environ Pollut* **270**:116073 (2021). <https://doi.org/10.1016/j.envpol.2020.116073>.
- Akalin MK, Tekin K and Karagoz S, Hydrothermal liquefaction of corneal cherry stones for bio-oil production. *Bioresour Technol* **110**:682–687 (2012). <https://doi.org/10.1016/j.biortech.2012.01.136>.
- Grubeša IN, Marković B, Nyarko MH, Krstić H, Brdarić J, Filipović N et al., Potential of fruit pits as aggregate in concrete. *Construct Build Mater* **345**:128366 (2022). <https://doi.org/10.1016/j.conbuildmat.2022.128366>.
- Korlesky NM, Stolp LJ, Kodali DR, Goldschmidt R and Byrdwell WC, Extraction and characterization of Montmorency sour cherry (*Prunus cerasus* L.) pit oil. *J Am Oil Chem Soc* **93**:995–1005 (2016). <https://doi.org/10.1007/s11746-016-2835-4>.
- Bernardo-Gil G, Oneto C, Antunes P, Rodrigues MF and Empis JM, Extraction of lipids from cherry seed oil using supercritical carbon dioxide. *Eur Food Res Technol* **212**:170–174 (2001). <https://doi.org/10.1007/s002170000228>.
- Dimic I, Pezo L, Rakic D, Teslic N, Zekovic Z and Pavlic B, Supercritical fluid extraction kinetics of cherry seed oil: kinetics modeling and ANN optimization. *Foods* **10**:1513 (2021). <https://doi.org/10.3390/foods10071513>.
- Chandra A and Nair MG, Characterization of pit oil from Montmorency cherry (*Prunus cerasus* L.). *J Agric Food Chem* **41**:879–881 (2002). <https://doi.org/10.1021/jf00030a007>.
- Górnaś P, Rudzińska M, Raczek M, Mišina I, Soliven A and Segliņa D, Composition of bioactive compounds in kernel oils recovered from sour cherry (*Prunus cerasus* L.) by-products: impact of the cultivar on potential applications. *Ind Crops Prod* **82**:44–50 (2016). <https://doi.org/10.1016/j.indcrop.2015.12.010>.
- Shuang JIAC, Peng WU and Yang LIX, The research progress for extraction methods of effective ingredients from sour cherries. *Adv Food Sci Eng* **2**:68–80 (2018). <https://doi.org/10.22606/afse.2018.22002>.
- Al-Bachir M and Kouksi Y, Compositional characteristics of cherry kernel oil as influenced by gamma irradiation and storage periods. *Food Sci Technol Int* **27**:326–333 (2021). <https://doi.org/10.1177/1082013220956739>.
- Herrero M, Mendiola JA, Cifuentes A and Ibanez E, Supercritical fluid extraction: recent advances and applications. *J Chromatogr A* **1217**:2495–2511 (2010). <https://doi.org/10.1016/j.chroma.2009.12.019>.
- Al Juhaimi F, Ozcan MM, Ghafoor K, Babiker EE and Hussain S, Comparison of cold-pressing and Soxhlet extraction systems for bioactive compounds, antioxidant properties, polyphenols, fatty acids and tocopherols in eight nut oils. *J Food Sci Technol* **55**:3163–3173 (2018). <https://doi.org/10.1007/s13197-018-3244-5>.
- Sahena F, Zaidul ISM, Jinap S, Karim AA, Abbas KA, Norulaini NAN et al., Application of supercritical CO₂ in lipid extraction – a review. *J Food Eng* **95**:240–253 (2009). <https://doi.org/10.1016/j.jfoodeng.2009.06.026>.
- Švarc-Gajić J, Čerda V, Clavijo S, Suárez R, Mašković P, Cvetanović A et al., Bioactive compounds of sweet and sour cherry stems obtained by subcritical water extraction. *J Chem Technol Biotechnol* **93**:1627–1635 (2018). <https://doi.org/10.1002/jctb.5532>.
- Comes F, Farines M, Aumelas A and Soulier J, Fatty acids and triacylglycerols of cherry seed oil. *J Am Oil Chem Soc* **69**:1224–1227 (1992). <https://doi.org/10.1007/bf02637685>.
- Yu M, Kniepkamp K, Thie JP, Witkamp GJ and van Haren RJF, Supercritical carbon dioxide extraction of oils from Andean lupin beans: lab-scale performance, process scale-up, and economic evaluation. *J. Food Process Eng* **46**:e14289 (2023). <https://doi.org/10.1111/jfpe.14289>.
- Lepage G and Roy CC, Direct transesterification of all classes of lipids in a one-step reaction. *J Lipid Res* **27**:114–120 (1986). [https://doi.org/10.1016/s0022-2275\(20\)38861-1](https://doi.org/10.1016/s0022-2275(20)38861-1).
- Chang H, Zhong F, Cao R, Liu Y, Wang M and Pu X, Prediction of the solubilities of water in hydrocarbons with COSMO-RS and interpretation of the solubility characteristics. *J Solution Chem* **49**:365–382 (2020). <https://doi.org/10.1007/s10953-020-00966-4>.
- Span R and Wagner W, A new equation of state for carbon dioxide covering the fluid region from the triple-point temperature to 1100 K at pressures up to 800 MPa. *J Phys Chem Ref Data Monogr* **25**:1509–1596 (1996). <https://doi.org/10.1063/1.555991>.
- Phelps CL, Smart NG and Wai CM, Past, present, and possible future applications of supercritical fluid extraction technology. *J Chem Educ* **73**:1163 (1996). <https://doi.org/10.1021/ed073p1163>.

- 36 Merkle JA and Larick DK, Fatty acid content of supercritical carbon dioxide extracted fractions of beef fat. *J Food Sci* **60**:959–962 (1995). <https://doi.org/10.1111/j.1365-2621.1995.tb06270.x>.
- 37 Brown ZK, Fryer PJ, Norton IT, Bakalis S and Bridson RH, Drying of foods using supercritical carbon dioxide: investigations with carrot. *Innov Food Sci Emerg Technol* **9**:280–289 (2008). <https://doi.org/10.1016/j.ifset.2007.07.003>.
- 38 Sabirzyanov AN, Il'in AP, Akhunov AR and Gumerov FM, Solubility of water in supercritical carbon dioxide. *High Temp* **40**:203–206 (2002). <https://doi.org/10.1023/a:1015294905132>.
- 39 Wang Z, Zhou Q, Guo H, Yang P and Lu W, Determination of water solubility in supercritical CO₂ from 313.15 to 473.15 K and from 10 to 50 MPa by in-situ quantitative Raman spectroscopy. *Fluid Phase Equilibria* **476**:170–178 (2018). <https://doi.org/10.1016/j.fluid.2018.08.006>.
- 40 Wiebe R, The binary system carbon dioxide-water under pressure. *Chem Rev* **29**:475–481 (2002). <https://doi.org/10.1021/cr60094a004>.
- 41 Gupta R and Shim J, Solubility in supercritical carbon dioxide. *CRC Press* **1**:835–854 (2006). <https://doi.org/10.1201/9781420005998>.
- 42 Montañés F, Catchpole OJ, Tallon S, Mitchell KA, Scott D and Webby RF, Extraction of apple seed oil by supercritical carbon dioxide at pressures up to 1300 bar. *J Supercrit Fluids* **141**:128–136 (2018). <https://doi.org/10.1016/j.supflu.2018.02.002>.

8 List of publications

Publications:

Yu M, Kniepkamp K, Thie JP, Witkamp GJ and van Haren RJF, Supercritical carbon dioxide extraction of oils from Andean lupin beans: Lab - scale performance, process scale - up, and economic evaluation, *Journal of Food Process Engineering* **46** (2023), DOI: 10.1111/jfpe.14289.

Kniepkamp K, Errico M, Yu M, Roda - Serrat MC, Eilers JG, Wark M and van Haren R, Lipid extraction of high - moisture sour cherry (*Prunus cerasus* L.) stones by supercritical carbon dioxide, *Journal of Chemical Technology & Biotechnology* **99**: 810-819 (2024), DOI: 10.1002/jctb.7581.

Conference:

Kniepkamp K, Yu M, Kuipers M, Patternotte A, Martins JN, Wark M, van Haren RJF, *Analytica 2024*, München, Germany: Quinolizidine Alkaloid Quantification in Lupin Beans.

9 Erklärung

Ich versichere, dass ich die vorliegende Arbeit selbständig verfasst und keine anderen als die angegebenen Quellen und Hilfsmittel benutzt und die allgemeinen Prinzipien wissenschaftlicher Arbeit und Veröffentlichungen, wie sie in den Leitlinien guter wissenschaftlicher Praxis der Carl von Ossietzky Universität Oldenburg festgelegt sind, befolgt habe. Des Weiteren erkläre ich, dass die Dissertation weder in ihrer Gesamtheit noch in Teilen einer anderen wissenschaftlichen Hochschule zur Begutachtung in einem Promotionsverfahren vorliegt oder vorgelegen hat.

Kai Kniepkamp